Genetic architecture and molecular mechanisms underlying light entrainment of the *Drosophila* circadian clock

Thesis submitted for the degree of

Doctor of Philosophy

at the University of Leicester

by

Adeolu Badi Adewoye

Department of Genetics

University of Leicester

October 2010

Abstract

Genetic architecture and molecular mechanisms underlying light entrainment of the *Drosophila* circadian clock

Adeolu Badi Adewoye

Despite significant progress in the understanding of how the circadian clock is entrained by light, the genetic architecture and molecular basis of this process are still largely unknown. This study was undertaken to identify biological pathways underlying light entrainment in *Drosophila melanogaster*. Complementary approaches that combined quantitative trait loci (QTL) mapping, complementation tests, and genome-wide gene expression profiling were used.

One hundred and twenty-three recombinant inbred lines (RIL) were assayed for circadian photosensitivity. Composite interval mapping identified a single significant QTL. Quantitative deficiency complementation test refined this QTL interval into two smaller QTLs consisting of 140 candidate genes. Complementation tests with null mutant strains suggested segregating alleles of *timeless* and *cycle* may contribute to the variation in light response. In addition, two genes *CG9879* and *Lilliputian* located within the QTL showed a significant differential expression in two RIL that were analysed by microarrays. Interestingly, *Lilliputian* interacts with several genes such as *Shaggy* and *nejire* which have been previously implicated in the circadian clock.

Global profiling of gene expression following a light pulse at ZT15 revealed 209 differentially expressed genes in a laboratory strain (Canton-S). These genes are involved in several biological processes, however genes related to signal transduction, gene regulation, glutamate receptor activity, cellular communication and chromatin remodelling were statistically over-represented. RNA interference mediated knockdown further supported the role of these genes in the light response. Notable among these genes were *nrv1, Neurofibromin 1, still life* and *Thor*. In addition, the microarray experiments indicated that histone modifications may also play an important role in light entrainment of the clock. Consistently, an aberrant light response was found in various mutants and transgenic strains in which histone acetylation, de-acetylation, and methylation (of DNA and histones) are defective.

Acknowledgements

This work could not have been done without the support, ideas and patience of my supervisor Dr Eran Tauber, so thank you for making it possible. Our approaches could not be more different, but I have learnt to value your ideas and perspective.

I would also like to say thank you to Prof Bambos Kyriacou for his financial support, advice and sharing his professional experience. I will always remember your sense of humour and maturity. I greatly appreciate the support and assistance of all my colleagues in lab 124 Genetics department, University of Leicester. A special thanks to Dr Lin Zhang for her support, stimulating chats during lunch-breaks and on train journeys to Nottingham. I would also like to say thank you to Mobina Khericha, Dr Mirko Pegoraro and Dr Stephane Dissel for all their help.

I would like to thank our collaborator Prof Sergey Nuzhdin at the University of Southern California for providing the recombinant inbred lines used in chapter 3 study. In addition, I like to thank Dr Christopher Talbot for all his support on QTL studies and his insightful discussion.

Last but not least, this work could not have been completed without the support of my dearest wife Marguerite and my son Ayotunde. I have rewritten this short paragraph over and over trying to express my gratitude and love. I can't. I don't know of words that adequately express it. Maybe there are no words in the world to say how proud and lucky I am to be part of a loving and happy family. Big thank you.

Dedication

This thesis is dedicated to the loving memory of my parents

and my father-in-law Dr Fu'ad Sabour.

O my God! O Thou forgiver of sins, bestower of gifts, dispeller of afflictions! Verily, I beseech Thee to forgive the sins of such as have abandoned the physical garment and have ascended to the spiritual world. O my Lord! Purify them from trespasses, dispel their sorrows, and change their darkness into light. Cause them to enter the garden of happiness, cleanse them with the most pure water, and grant them to behold Thy splendours on the loftiest mount.

- `Abdu'l-Bahá

List of Abbreviations

Abbreviation	Definition
ANOVA	Analysis of Variance
CIM	Composite Interval Mapping
cM	centiMorgan
CT	Circadian Time
DD	Constant Dark conditions
DNA	Deoxyribonucleic Acid
HAT	Histone Acetyltransferase
HDAC	Histone Deacetylase
Hr	Hour
ICC	Immunocytochemistry
LD 12:12	12 hours of Light: 12 hours of Darkness
LL	Constant Light conditions
LOD	Logarithm of Odds
M	Molar
mg	Milligramme
MIM	Multiple Interval Mapping
min	Minute
ml	Milliliter
mM	millimolar
mRNA	Messenger Ribonucleic Acid
NaB	Sodium Butyrate
nChIP	Native chromatin immunoprecipation
ng	Nanogramme
PCR	Polymerase Chain Reaction
QTL	Quantitative Trait Loci
RIL	Recombinant Inbred Line
RNA	Ribonucleic Acid
RNAi	Ribonucleic Acid Interference
Rnase	Ribonuclease
rpm	Rotations per Minute
s	Second
SDS	Sodium Dodecyl Sulphate
timG4>dcr2	*timGal4-dicer2*
UAS-GOI-IR	Upstream Activation Sequence (gene of interest) inverted repeat
ZT	Zeitgeber Time
µg	Microgramme
µl	Microliter

Contents

Table of Figures

Table of Tables

Chapter 1: Introduction

1.1 Preface

The rotation of the Earth round its axis causes daily changes in illumination, humidity, and temperature. As a consequence, adaptive timekeeping mechanisms have evolved, allowing organisms to adjust to these environmental fluctuations. This often results in a preference for activity in a certain time of the day (phase), which is species-specific (Pittendrigh. 1993).The endogenous mechanisms that drive behavioural and physiological rhythms with a 24 hr periodicity are collectively referred to as the circadian clock (Latin: *circa* =around; *diem* = day) (Bell-Pedersen *et al*. 2005; Halberg. 1960).

Several studies have indicated that the universality of the circadian clock may reflect its importance for Darwinian fitness (Golden *et al*. 1998; Johnson *et al*. 1998; Kumar *et al*. 2005; Yerushalmi and Green. 2009). For instance, the survival of fruit flies (*D. melanogaster*) (Pittendrigh and Minis. 1972), blowflies (*Phormia terraenovae*)(von Saint Paul and Aschoff. 1978), Cyanobacteria (Ouyang *et al*. 1998) and mice (*Mus musculus*)(Wyse *et al*. 2010) was significantly enhanced when their endogenous period closely matched the environmental light-dark cycles. In *Arabidopsis* for example, strains cultured under photoperiods that were different from their endogenous circadian period, produced less chlorophyll, exhibited reduced growth and survival (Dodd *et al*. 2005). The circadian clock is also important for reproductive fitness as shown in

various organisms such as *Drosophila* and Cyanobacteria (Beaver *et al*. 2002; Johnson *et al*. 1998; Kumar *et al*. 2005; Ouyang *et al*. 1998). In mice, disruption of the circadian oscillations resulted in irregular oestrous cycles and high rate of pregnancy failure (Miller *et al*. 2004).

The numerous health problems associated with the disruption of the circadian clock and its role in hormonal balance and behavioural activity underpin its importance to human well-being. For example, the disruption of circadian rhythms has been linked to cancer (Kuo *et al*. 2009; Stevens and Rea. 2001), neurodegenerative disorders (Pallier *et al*. 2007; Pallier *et al*. 2007) and metabolic disorders (Englund *et al*. 2009; Sookoian *et al*. 2008). Similarly, dysfunction in circadian rhythms was implicated in depressions such as seasonal affective disorder (SAD) (Bunney and Bunney. 2000). In addition, chronic sleep disorders in humans such as *Advanced sleep phase syndrome* (ASPS) and *Delayed sleep phase syndrome* (DSPS) have also been linked to the disruption of the circadian clock (Jones *et al*. 1999). The major impact of the circadian clock on physiological processes is increasingly recognised and addressed in medical treatments (chronotherapy). For instance, the efficacy of some drugs can be greatly enhanced by adjusting the time of administration as shown in some cancer treatments (Hrushesky *et al*. 2009).

Studies over the past few decades have localised the clock in several organisms. In mammals, the central (master) pacemaker driving circadian

rhythms resides in the suprachiasmatic nucleus (SCN) located in the hypothalamus (Klein *et al*. 1991; Stephan and Zucker. 1972). In non-mammalian vertebrates such as birds the central pacemaker resides in the pineal gland (Headrick Zimmerman and Menaker. 1979). Studies in *Drosophila* have identified self-sustaining circadian rhythms in lateral, dorsal and ventral part of the brain. It has also been reported in some peripheral tissues, such as the ring gland and Malpighian tubules (Plautz *et al*. 1997). In mammals, the master clock seems to coordinate the rhythmic activities generated by the peripheral clock (Helfrich-Förster *et al*. 2007). In contrast, *Drosophila* central and peripheral clocks seem to rely on autonomous photoreceptors, as synchronisation of their molecular oscillations is seen in isolated organs (Giebultowicz *et al*. 2000; Plautz *et al*. 1997).

The current view of the circadian system is based on three fundamental components: the entrainment (input) pathways, the oscillators and the output pathways (reviewed by Tomioka and Matsumoto. 2010) (Fig 1.1). Genes are assigned roles in input, oscillator or output pathways if null mutations abolish entrainment (Eskin. 1979), result in complete arrhythmicity (Hardin. 2005) or eliminate output rhythms (Roenneberg and Merrow. 1999). The oscillator genes are important for generating and sustaining rhythms under constant conditions (reviewed in (Hardin. 2006). Many of these genes encode transcription factors or proteins that play a role in gene regulation supporting the idea that the 24 h-

rhythms rely on transcriptional/translational feedback loops (reviewed in Hardin. 2006; Tomioka and Matsumoto. 2010).

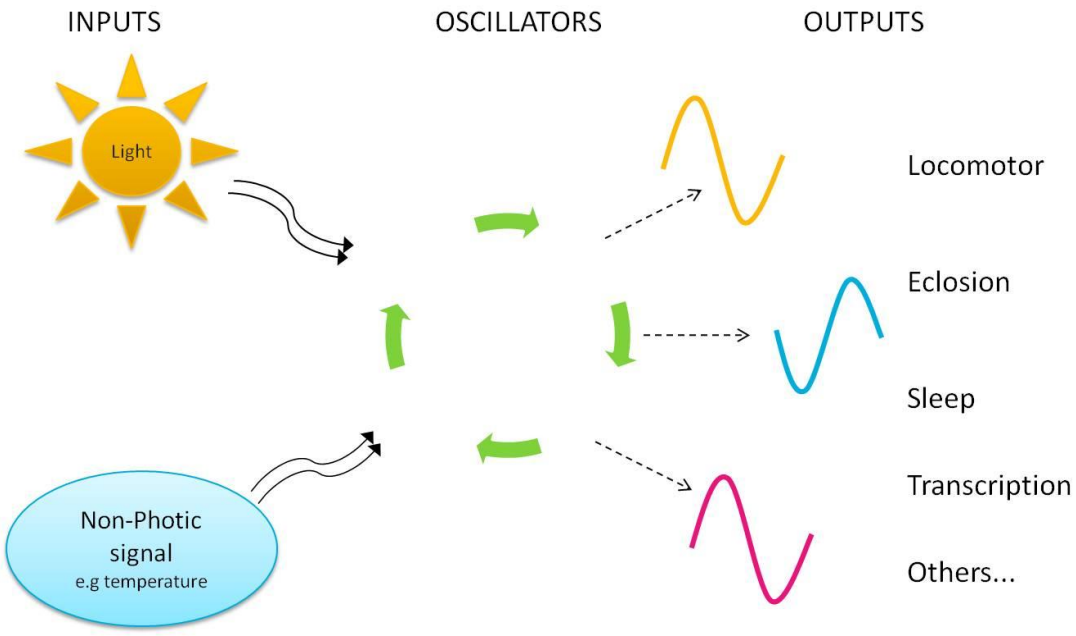

Figure 1.1: A schematic of circadian system showing the three conceptual components of the circadian clock

The entrainment pathways link the oscillators to the environmental time cues, known as the zeitgebers (literally translated as "time-givers"). In nature, the daily light –dark cycle (LD) is the primary zeitgeber (Helfrich-Förster and Engelmann. 2002) probably because it exhibits the most consistent and reliable rhythm (Johnsson and Engelmann. 2008). However, other zeitgebers such as: temperature (Pittendrigh *et al*. 1958), humidity (Halket. 1931), feeding (Stephan *et al*. 1979), and social interactions (Levine *et al*. 2002a) do exist. The information from the input pathways modulates the rhythm generated by the circadian

oscillators. The output pathways translate these oscillations into behavioural and physiological overt rhythms.

1.2 Fundamental properties of circadian oscillators

Circadian oscillators have three characteristic properties: an endogenous (free-running) rhythm, temperature compensation and entrainment (Pittendrigh. 1960). The free-running period (FRP) refers to the endogenous rhythm generated by the pacemaker when no entraining time-cues are present, usually manifested under laboratory conditions (Pittendrigh. 1954; Sehgal *et al*. 1992). Temperature compensation mechanisms allow organisms to maintain a fairly constant circadian period over a broad range of temperatures, in contrast to most other biochemical processes that are temperature-dependent (Pittendrigh. 1960; Roenneberg and Foster. 1997). Temperature changes may however alter the phase of the rhythm (Johnson *et al*. 2003), as well as its amplitude (Chen *et al*. 2006; Pittendrigh *et al*. 1991). Temperature compensation was first observed in the eclosion rhythm of *Drosophila pseudoobscura* (Pittendrigh. 1954), and subsequently shown to be a universal feature (Barrett and Takahashi. 1995; Ruby *et al*. 1999; Tosini and Menaker. 1998). It has also been demonstrated in mammalian cultured cells where the circadian oscillation of clock genes is fairly robust over temperature ranging from 33 – 42^0C (Tsuchiya *et al*. 2003).

The third hallmark of the circadian pacemaker is its ability to adjust (entrain) to environmental time cues (zeitgeber) such as temperature and light whose cycles mark the 24 hr solar day. The entrainment of the FRP to a zeitgeber cycle results in an overt rhythm whose period is equal to that of the zeitgeber, with a stable phase relationship (Johnson *et al*. 2003). The light -dark cycle is arguably the most important zeitgeber, capable of entraining almost all circadian rhythms (Johnson. 2001). Light entrainment of the circadian clock is the focus of this thesis and is described in more details in section 1.7 and 1.8.

1.3 *Drosophila:* a model organism for chronobiological research

Half a century ago, Pittendrigh demonstrated the existence of well-defined circadian outputs in *Drosophila pseudoobscura* (Pittendrigh. 1960). This marked the beginning of *Drosophila* chronobiology, which has since experienced a steady and rapid expansion. Many of the assays developed then remain useful in investigating how the circadian system works. Focus however, soon shifted to *Drosophila melanogaster*, utilising the advantage of the genetic resources available for this species.

Earlier genetic analyses of fruit flies relied heavily on two circadian rhythm outputs: the pupal eclosion (a population rhythm), and the locomotor activity of individual adults (Konopka and Benzer. 1971). Later, more circadian output rhythms such as the olfactory response (Krishnan *et al*. 1999), egg-laying

(McCabe and Birley. 1998), mating (Tauber *et al*. 2003), cuticle deposition (Ito *et al*. 2008) and many others have been documented.

The first circadian clock gene was discovered by Konopka and Benzer (1971) during a mutagenesis screen (induced by ethyl methane sulphonate, EMS) looking for flies with rhythm disruption in eclosion and locomotor activity. They identified three mutations, which were mapped to a single locus on the X chromosome named *period*. These mutations were termed: *per* short (per^{s}), *per* long (per^{L}) and null *per* (per^{01}), with each having a different effect on the circadian period (Konopka and Benzer. 1971).

Subsequently, *per* mutations have been shown to affect a range of clock outputs indicating its central role in the circadian clock (reviewed by Stanewsky. 2003). The success in isolating *per* prompted researchers to screen for other clock mutants/ genes. As a result, other clock genes have been identified through genetic and molecular approaches. Those genes include: *timeless (tim)* (Sehgal *et al*. 1994); *dClock* (*Clk*) (Allada *et al*. 1998); *cycle* (*cyc*) (Rutila *et al*. 1998); *doubletime* (dbt) (Kloss *et al*. 1998); *cryptochrome* (*cry*) (Emery *et al*. 1998); *shaggy* (*sgg*) (Martinek *et al*. 2001), *vrille (vri)* (Blau and Young. 1999), *Par domain protein 1ε (Pdp1ε)* (Cyran *et al*. 2003) and of recent *jetlag (jet)* (Koh *et al*. 2006) and *clockwork orange* (*cwo*) (Kadener *et al*. 2007; Lim *et al*. 2007b; Matsumoto *et al*. 2007).

1.4 The molecular mechanism of the clock in *Drosophila*

At the core of circadian clocks are the molecular feedback loops, which generate rhythmic molecular oscillations (Bell-Pedersen *et al*. 2005). Proteins encoded by some of the clock genes can activate or repress their own transcription (Young and Kay. 2001), alter their protein stability, or change their subcellular localisation (Johnsson and Engelmann. 2008). In *Drosophila*, the feedback loop consists of at least three interconnected loops: (i) *per*/*tim* loop, (ii) *Clk* and (iii) *cwo* (Fig 1.2) which together constitute a robust pacemaker (Glossop *et al*. 1999; Tomioka and Matsumoto. 2010; Young and Kay. 2001). The positive factors (dCLK, CYC and PDP1ε) activate the expression of the negative factors (PER, TIM and VRILLE), which then feed back to suppress the expression of *per* and *tim*. Once the negative factors are reduced, the positive factors can then start the next cycle of transcription. Each of the feedback loops is discussed in further detail in the following paragraphs.

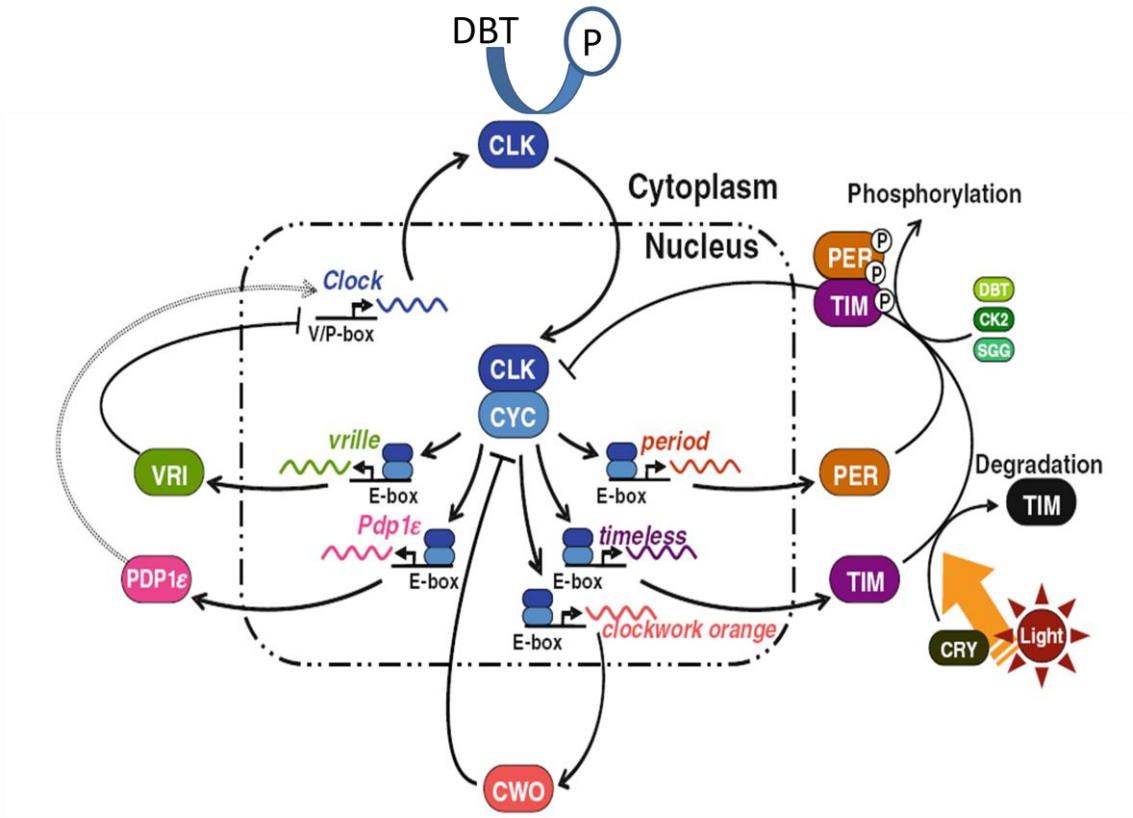

Figure 1.2: The Drosophila molecular clock showing the three feedback loops

per/tim(right hand side); *dClk* and *vri/Pdp1ε* (left hand side) and *cwo*(bottom) that are interlocked to generate 24-h rhythms. Note cwo binds E-box to complete at DNA level with CLK-CYC. The figure was adapted from (Tomioka and Matsumoto. 2010).

1.4.1 The *per–tim* negative feedback loop

The transcription of *per* and *tim* is activated by the CLK-CYC heterodimer from the middle of the day through early night by binding to their E-box elements within the promoter regions (Fig 1.2) (Darlington *et al*. 1998; Hao *et al*. 1997; McDonald and Rosbash. 2001). The translated PER is phosphorylated by DBT and *casein kinase 2* (CK2) leading to its degradation, but becomes stable once it binds to TIM (Hardin. 2005). In addition, PER is also

stabilised by PROTEIN PHOSPHATASE 2A (PP2A) which removes the phosphates added by DBT and CK2 (Sathyanarayanan *et al*. 2004). TIM is phosphorylated by SGG which in turn promotes the translocation of PER-TIM into the nucleus (Kloss *et al*. 2001) see Fig 1.2. The complex then binds to CLK-CYC heterodimer and blocks its binding to *per* and *tim* E-boxes, thereby inhibiting *per* and *tim* transcription (Rutila *et al*. 1998; Scully and Kay. 2000). PER and CLK are once again destabilised via DBT phosphorylation, resulting in their degradation, while TIM is degraded by light via CRY (Hardin. 2006). The accumulation of hypophosphorylated CLK results in its dimerisation with CYC, thus beginning a new round of *per* and *tim* transcription (Fig 1.2) (Bae and Edery. 2006).

1.4.2 *dClk* transcriptional feedback loop

d*Clk* exhibits a rhythmic oscillation of its mRNA while the protein is relatively constant throughout the day with temporal change to its state of phosphorylation (Allada *et al*. 1998; Bae and Edery. 2006; Hardin *et al*. 1990; Sehgal *et al*. 1994). While the levels of *per* and *tim* mRNA peak in early evening (ZT 13 –16), *Clk* mRNA level cycles in antiphase at late night/ early morning (ZT 23 –4) see Fig 1.3 (Allada *et al*. 1998; Hardin *et al*. 1990), suggesting the involvement of a different transcriptional regulator (Bae *et al*. 1998). The continuous oscillation of *dClk* mRNA in constant darkness (DD) suggests circadian regulation (Bae *et al*. 1998). This oscillation is abolished in mutants

lacking PER (per^{01}) or TIM (tim^{01}), indicating that the two proteins are linked to *dClk* transcription (Bae *et al*. 1998; Glossop *et al*. 1999).

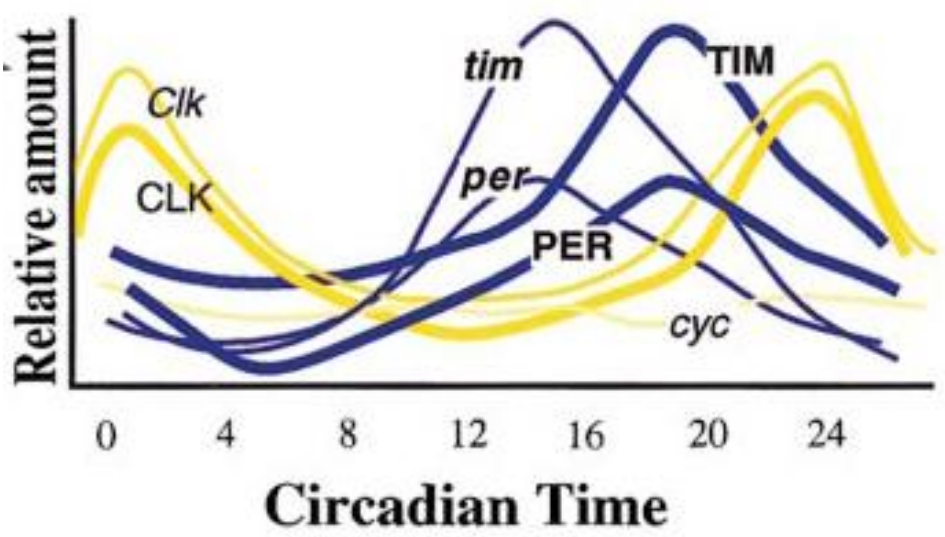

Figure 1.3: Profile of clock transcripts and their protein expression in LD
Adapted from (Dunlap. 1999).

In addition, the *dClk* mRNA expression level in these two arrhythmic mutant flies was similar to or lower than the trough values seen in wild-type flies, a further indication that PER and TIM can also function as transcriptional activators (Bae *et al*. 1998). Further studies with double mutants: per^{01}; $dClk^{Jrk}$ and per^{01}; *cyc0* under LD or DD showed a level of *Clk* mRNA peak similar to the wild-type flies indicating that PER and TIM activate *dClk* transcription via de-repression (Glossop *et al*. 1999). On the basis of these observations, a second transcriptional feedback loop was proposed. This loop interlocks with the *per–tim* feedback loop (Fig 1.2) and involves the oscillation of *dClk* mRNA or both *Clk* and *Bmal1* in mammals (Cyran *et al*. 2003; Glossop *et al*. 1999). Two basic leucine zipper (b-ZIP) transcription factors VRI and PAR DOMAIN PROTEIN

1ε (PDP1ε) are shown as essential components of this second feedback loop in addition to *dClk* (Cyran *et al*. 2003; Glossop *et al*. 2003). The requirement of PDP1ε for *Clk* expression was thought not essential but it may function in regulating oscillator output as is required for behavioural rhythmicity (Benito *et al*. 2007).

vrille mRNA oscillation parallels that of *per* and *tim*, suggesting regulation by common transcription factors (Blau and Young. 1999). Flies carrying a functional copy of *vri* exhibit a shorter period of locomotor activity, and when *vri* is expressed constitutively, rhythmicity is abolished or the period becomes longer (Blau and Young. 1999). Interestingly, VRI accumulation coincides with the expected phase of *dClk* repression. This suggests that *vrille* acts in repressing *dClk* transcription (Glossop *et al*. 2003).

vri and *Pdp1ε* have highly conserved basic DNA binding domains suggesting they bind the same set of target genes (Cyran *et al*. 2003). Blau (1999) identified a functional E-box within the *vri* promoter and demonstrated that the nucleotides flanking this E-box are similar to those flanking the *per* E-box. Further findings have shown that *per* and *vri* E-box elements are more strongly activated by dCLK than those of the *tim* E-box in cell culture (Blau and Young. 1999). A similar E-box occurs upstream of *Pdp1ε* - a possible site for dCLK-CYC binding (Cyran *et al*. 2003).

Several lines of evidence have shown that when CLK levels are high, shortly after dawn, VRI levels increase and inhibit further transcription of *dClk* by binding to VRI/PDP1ε (V/P) promoter element in the *Clk* promoter(Cyran *et al*. 2003). Since VRI levels peak 3-6 h before PDP1ε, the repression of *dClk* by VRI is separated from its activation by PDP1ε. Further studies of *vri* and *Pdp1ε* expression in null mutants of *Clk* and *cyc* show a reduced level of *vri* and *Pdp1ε* mRNAs, supporting dCLK-CYC role in their regulation (Blau and Young. 1999; Cyran *et al*. 2003).

In summary, the current model for the second feedback loop entails: dCLK/CYC binds *vri* and *Pdp 1* E-box elements during the early night to activate their transcription (Cyran *et al*. 2003). Subsequently, VRI accumulates in phase with its mRNA and binds V/P box enhancer elements to repress *Clk* transcription (see Fig 1.2). On the other hand, PDP1ε accumulation peaks during mid to late night and activates *Clk* transcription (Hardin. 2005). Because of VRI and PDP1ε affinity to the same regulatory element within the *dClk* promoter, the V/P ratio is thought to regulate the level of *dClk* transcription. (Cyran *et al*. 2003). In addition, the replacement of VRI homodimer by free PDP1ε homodimer may result in non-functional VRI: PDP1ε heterodimers (Lim *et al*. 2007a). Overall, the *dClk* loop is thought to confer stability and robustness to the *per–tim* loop. It also regulates the rhythmic expression of *cryptochrome* - the dedicated clock photoreceptor (Glossop *et al*. 2003).

1.4.3 *cwo* loop

The third loop includes *cwo* a transcriptional repressor which belongs to the basic helix loop-helix ORANGE family (Kadener *et al*. 2007). The expression of *cwo* is rhythmic (Lin *et al*. 2002b; Ueda *et al*. 2002) and is regulated by CLK (Kadener *et al*. 2007; Lim *et al*. 2007b; Matsumoto *et al*. 2007; McDonald and Rosbash. 2001; Richier *et al*. 2008). *cwo* is thought to inhibit its own expression as well as the expression of other clock genes such as *per* and *tim* via E-box elements (Tomioka and Matsumoto. 2010). A null mutation of *cwo* lengthens rhythmic activity in flies. In contrast, increases *cwo* mRNA level reduces the transcript peak levels of *per*, *tim*, *vri* and *pdp1ε* and leads to their loss of oscillation (Richier *et al*. 2008). On the basis of these observations, CWO was suggested to regulate the expression of clock genes (Richier *et al*. 2008).

1.5 Post-translational regulation of PER and TIM

In recent years, there is increasing evidence that post-translational modifications also play a vital role in the clock, by regulating protein stability, localisation and protein-protein interactions (Kloss *et al*. 1998; Lin *et al*. 2002a; Martinek *et al*. 2001; Yu *et al*. 2006). Post-translational modifications are thought to maintain the daily oscillation of clock proteins by imposing a delay between the activation and repression of clock transcripts (reviewed by Gallego and Virshup. 2007). Rhythmic post-translational modifications may underlie circadian oscillations even when mRNA or protein level does not cycle (Fan *et*

al. 2007; reviewed byGallego and Virshup. 2007). Modifications such as sumolyation, ubiquitylation, glycosylation, methylation, phosphorylation and histone acetylation have been implicated in the circadian clock (Cardone *et al*. 2005; Duguay and Cermakian. 2009; Edery *et al*. 1994; Hirayama *et al*. 2007; Taylor and Hardin. 2008; Weber. 2009).

In the context of the clock, phosphorylation is probably the most studied modification. In the cytoplasm, phosphorylation is thought to affect the timekeeping mechanism in two ways. It regulates PER stability and the timing of PER-TIM complexes nuclear entry (Fang *et al*. 2007; Harms *et al*. 2004; Price *et al*. 1998). In *Drosophila,* phosphorylation of PER by the activity of DOUBLE-TIME (DBT) - the homolog of mammalian *casein kinase Iε* (CKIε) is thought to start in the cytoplasm and proceeds in the nucleus (Kloss *et al*. 1998; Price *et al*. 1998). Though *dbt* protein does not oscillate, its pivotal role in clock functions is well documented (Price *et al*. 1998). For instance, mutations in *dbt* gene were reported to either abolish rhythmicity dbt^{ar} or alter period length as seen in short dbt^{s} and long dbt^{L} mutants (Bao *et al*. 2001; Price *et al*. 1998). Furthermore, dbt^{s} has been shown to accelerate both the accumulation of PER in the cytoplasm and the disappearance of nuclear PER (Bao *et al*. 2001). However, in a severe long-period mutation, PER stays much longer during the declining phase of the cycle than in wild-type flies (Price *et al*. 1998). Hence, the period

length is due to prolonged block of CLK-CYC activity. Thus, DBT seems to modulate the stability of PER in flies.

Three proteins: DBT, SHAGGY and CLK II are reported to influence the timing of PER -TIM complex entry into the nucleus (Harms *et al*. 2004). TIM is a continuous target for degradation during the daytime through the activity of a photoreceptor: CRYPTOCHROME (CRY) (Emery *et al*. 1998). SHAGGY (SGG) - the ortholog of mammalian GSK-3 phosphorylates TIM *in vivo* hence regulating its nuclear entry (Martinek *et al*. 2001). Furthermore, over-expression of SGG was shown to enhance TIM nuclear translocation and shortened the period of activity in the flies (Martinek *et al*. 2001). Although TIM is phosphorylated by SGG, its stability is not affected, which may suggest the involvement of other kinases/phosphatases in TIM degradation (Martinek *et al*. 2001). A recent study reported that PROTEIN PHOSPHATASE 1 (PPI) dephosphylates and stabilises TIM - a requirement for rhythmic abundance of PER/TIM in molecular oscillator (Fan *et al*. 2007).

PER-DBT and TIM translocate into the nucleus either separately or as a complex (Meyar *et al*. 2006; Vosshall *et al*. 1994) and subsequently interact with CLK to repress CLK-CYC transcription pathways thus inhibiting E-box transcription (Lee *et al*. 1998). DBT, possibly from the PER-DBT complex, enters the nucleus (Kloss *et al*. 2001) to phosphorylate and destabilize CLK resulting in a further regulation of the *per*/*tim* loop (Kim and Edery. 2006). However, the

stability of PER is stabilised by PROTEIN PHOSPHATASE 2A (PP2A), which dephosphorylates CLK and PER (Kim and Edery. 2006; Sathyanarayanan *et al*. 2004). The dephosphorylation of PER by PP2A facilitates its nuclear translocation (Sathyanarayanan *et al*. 2004) and enhances TIM nuclear expression which seems to depend on PER (Meyar *et al*. 2006). Although, PP1 plays a vital role in stabilising and regulating TIM/ PER rhythmic abundance, the nuclear entry timing of PER-TIM complex or as an individual protein is thought to be regulated by PP2A (Fan *et al*. 2007; Meyar *et al*. 2006). In addition, PER has been shown to form a functional homodimer. This homodimer is thought to be essential for both behavioural and molecular rhythmicity, which suggests a role in the clock machinery (Landskron *et al*. 2009). For more review see (Gallego and Virshup. 2007).

1.6 The neural basis of the clock in Drosophila

Drosophila's master clock is located in the brain where about 100,000 neurons are present, of which approximately 150 control the circadian clock (Helfrich-Förster *et al*. 2007; Kaneko and Hall. 2000). The clock neurons are classified according to their spatial location in the brain into two main groups: the lateral neurons (LNs) and the dorsal neurons (DNs) (Fig 1.4). Recent studies indicate that the LNs are the main clock neurons required for generating a robust free-running rhythm, while the DNs seem to be less essential and

probably play a role in other functions (Helfrich-Förster *et al*. 2007; Taghert and Shafer. 2006).

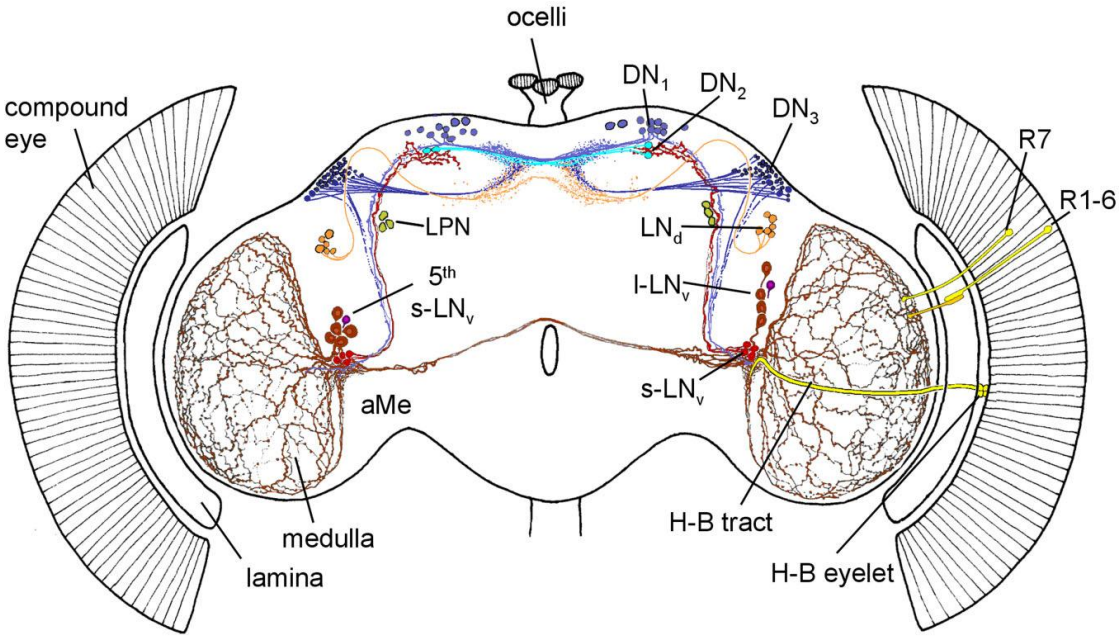

Figure 1.4: Clock neurons in adult fly brain

showing s-LNv = small ventral lateral neurons; l-LNv = large ventral lateral neurons; DN = dorsal neurons; LPN = lateral posterior neurons; LNd = lateral dorsal neuron and the H-B tract connecting the Hofbauer – Buchner (H-B) eyelets (adapted from (Helfrich-Förster *et al*. 2007)). See section 1.6 for detail.

1.6.1 The lateral neurons (LNs)

This group of neurons consists of 15 – 18 neurons in each brain hemisphere, and is further divided into three subgroups: the small ventrolateral neurons (s-LNvs), the large ventrolateral neurons (l-LNvs) and the dorsalateral neurons (LNds) (reviewed in (Helfrich-Förster. 2003) as illustrated in Fig 1.4. In each brain hemisphere, four s-LNvs, about five l-LNvs, six LNds and the recently identified fifth s-LNvs have been characterised. All the LNvs and a subset of three LNds express the blue light-sensitive protein CRY. The LN neurons are

further characterised by their expression of the neuropeptide pigment-dispersing factor (PDF) (Renn *et al*. 1999). PDF is expressed in both the s-LNvs and the l-LNvs with the exception of the fifth s-LNvs (Kaneko *et al*. 1997; Renn *et al*. 1999). It has also been shown that the four PDF-positive s-LNvs and the fifth PDF-negative s-LNvs response to light differently (Helfrich-Förster *et al*. 2007). The PDF staining of the l-LNvs extends through the distal medulla and connects the accessory medulla of the brain hemisphere via the posterior optic tract (reviewed in Helfrich-Förster *et al*. 2007) (Fig 1.4).

In LD condition, the PDF neurons control the morning activity bouts, whereas the PDF- neurons control the evening activity (Cusumano *et al*. 2009). In constant light (LL), the period of the PDF s-LNvs is shortened, while the period of the PDF s-LNvs (5th) is lengthened (Rieger *et al*. 2006).

1.6.2 The dorsal neurons

The dorsal region of *Drosophila*'s brain has about 80 neurons of which none is known to express PDF (reviewed byHelfrich-Förster *et al*. 2007). These are classified into three groups: the DN1, DN2, and DN3 neurons (Fig 1.4). The DN1 are approximately 14 to 16 neurons and have been recently divided into two subgroups: the DN1 anterior and the DN1 posterior (Shafer *et al*. 2006). This classification was based on the expression of GLASS (Klarsfeld *et al*. 2004; Shafer *et al*. 2006), a transcription factor essential for photoreceptor differentiation (Moses *et al*. 1989).

GLASS is expressed in DN1p, but not in DN1a (Shafer *et al*. 2006). The DN1p is thought to contribute to the light sensitivity of the pacemaker cells (Klarsfeld *et al*. 2004) . Subsets of DN1p are thought to drive rhythmic activity in LL conditions (Stoleru *et al*. 2007). The DN1a are two GLASS-negative DN1, identifiable by their anterior position, survival in *glass* mutant background, and the expression of the neuropeptide IPNamide (IPNa)(Shafer *et al*. 2006).

DN2s consist of two cells located near the central anterior terminals of the small LNvs (Fig 1.4) but their function is unknown. The expression of clock genes in DN2 are in anti-phase to other clock cells in larval stages (Kaneko and Hall. 2000), but become synchronised at the adult stage in LD and first few days in DD (Blanchardon *et al*. 2001).

DN3 consist of approximately 40 neurons in each adult fly brain hemisphere (Fig 1. 4). They are reported to consist of a circadian oscillator, which is independent of LNs, but not sufficient to drive rhythmic activity in DD (Veleri *et al*. 2003).

1.7 Light entrainment of the circadian clock

In mammals, the light signal is perceived by the retina and transmitted to the master oscillator via the retinohypothalmic tract (RHT) (Morse and Sassone-Corsi. 2002). In *Drosophila*, the circadian clock perceives light through photoreceptor cells in the eye, or by the deep-brain photoreceptor proteins,

which then transmit the signal to the central oscillators. Under natural conditions, the phase and the period of the circadian clock are thought to be entrained by the appearance of light at dawn and its disappearance at dusk. This can be simulated in the laboratory by brief light pulses administered to flies during the subjective night (Pittendrigh. 1993). In general, two models have been proposed to explain how light entrains the clock: the discrete model (non-parametric /phasic) and the continuous model (parametric / tonic) (Johnson *et al*. 2003; Johnson. 1999).

The continuous model implies that a parameter in the circadian system is continuously responding to light, while the discrete (non-parametric model) posits that the light impacts the pacemaker at specific phases only (Daan. 2000). The continuous model was based on the observation that the FRP (in LL) depends on light intensity, and suggests that light has a continuous effect on clock entrainment to the LD cycle (reviewed by Johnson *et al*. 2003). One of the mechanisms proposed for how this model works is based on modulation of the oscillation's velocity by ongoing acceleration at some phases and decelerating at others.

In the discrete model, entrainment results from daily discrete phase shifts equal in magnitude to the difference between the endogenous period (τ) and the period of the LD cycle (T). The abrupt phase-shifting of the oscillators

results in either advancing or delaying it by an amount equal to τ – T (Johnson *et al*. 2003; Pittendrigh. 1981).

1.7.1 Phase response curve

The phase response curve (PRC) is a useful plot for analysing the phase–dependent light response (in DD). A PRC shows the relationship between the phase shifts of a circadian rhythm and the circadian phase in which the zeitgeber was introduced (Johnson. 1999; Pittendrigh and Minis. 1964). According to the discrete model, the response of the circadian oscillator to a given light intensity depends on the time (phase) of the stimulus. PRC of different organisms invariably show that during the subjective day, light stimuli have little effect on the ongoing activity (the so called 'dead-zone) (Johnson. 2001; Pittendrigh. 1960) (Fig 1.5). On the other hand, light pulses during the subjective night typically shift the phase ($\Delta\phi$) of the free- running rhythm. It delays the phase of onset of activity rhythm **(-$\Delta\phi$)**, when administered at early night (CT 12- 18) and advances the phase **(+$\Delta\phi$)** during the second half of the night (CT 18- 2) (Johnson. 2001; Pittendrigh. 1960) (Fig 1.5).

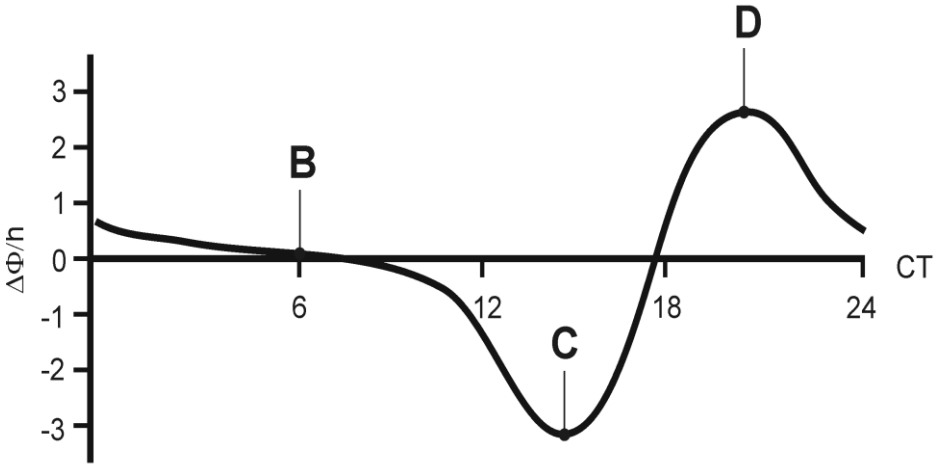

Figure 1.5: A light-induced phase response curve (PRC)

showing three different zones based on light response to light stimulus at different phases. Light-pulses during the subjective day have no or little phase shift shown in point B, while at early and late subjective night it delays (point C) and advances (point D) the phase of activity respectively.

In general, two different PRC profiles have been proposed for light-induced PRC: *Type 1* (weak response) and *Type 0* (strong response) (Johnson *et al*. 2003; Winfree. 1970) (Fig 1.6). The shapes of these PRCs depend on the strength of the entraining stimulus, the duration, the phase when it was administered, and the photo-sensitivity of the organism (Johnson *et al*. 2003). A weak light intensity produces a Type 1 PRC with a low amplitude and phase shift of a few hours (usually less than 6 h). Type1 PRC shows a continuous transition between the delay phase and the advance phase shift in the subjective night. In contrast, a strong light intensity produces Type 0 PRCs with a high amplitude and phase shift as large as 12 h (Johnson *et al*. 2003; Winfree. 1980). Type 0 PRCs have a distinct break point in transition between the delays and the advances in the mid-subjective night (Johnson *et al*. 2003).

A light pulse towards the middle of the subjective night in systems with Type 1, does not phase shift the clock, but does in systems with Type 0 (Johnson. 1999). In addition, a single light pulse of intermediate intensity presented close to the middle of the subjective night could produce arrhythmicity (Johnson *et al*. 2003; Winfree. 1970), which is referred to as the point of singularity (Winfree. 1980). For a given light intensity, the observed PRC (type 1 or type 0) is species-specific. However, organisms may exhibit both PRCs at different light intensities (Fig1.6).

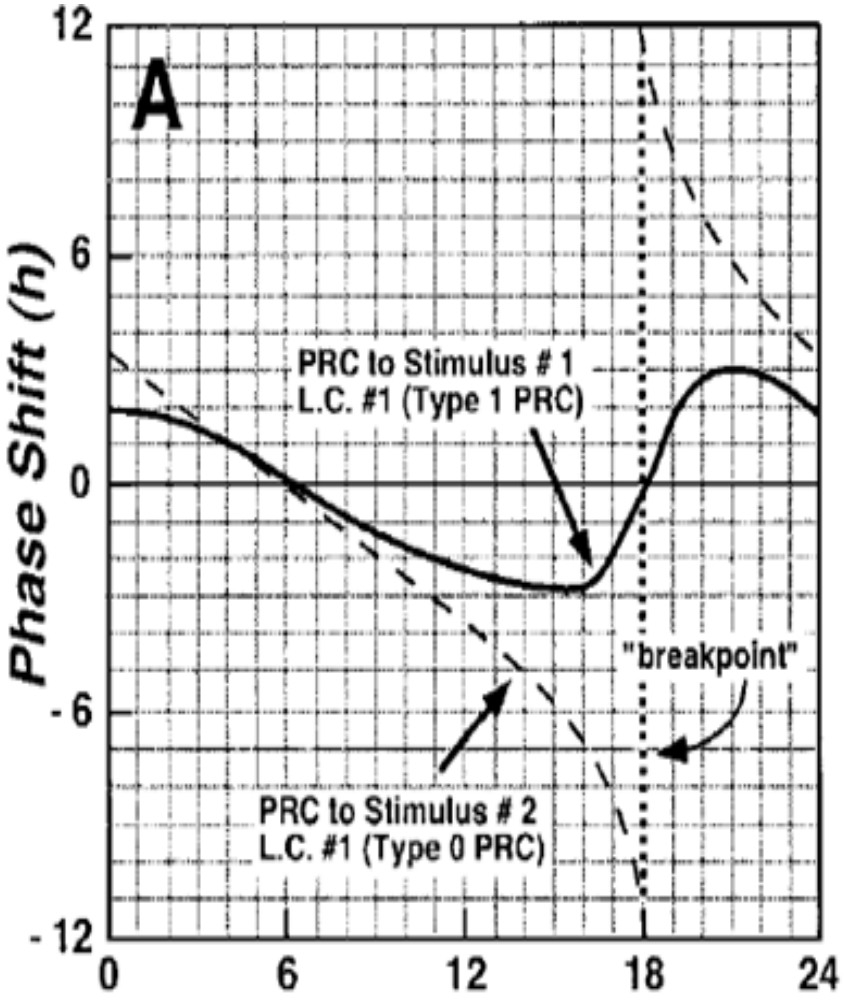

Figure 1.6: Type 1 and Type 0 phase response curves

Type 1 (lower amplitude) and Type 0 (higher amplitude), the PRC was generated by light of different intensities in *Drosophila*. The breakpoint is the transition between delay and advance, when phase shifts of a Type 0 PCR are plotted as advances and delays (adapted from Johnson *et al*. 2003).

1.8 The molecular basis of light entrainment

1.8.1 Circadian photoreception

In general, animals possess two distinct groups of photosensory organs: ocular and extraocular photoreceptors (Helfrich-Fӧrster *et al*. 2002). The ocular photoreceptor provides light input to the neural networks largely for image

detection but may also have a possible role in entrainment of the clock. The extraocular photoreceptors are incapable of complex image detection but are thought to be involved in the entrainment of the clock and the timing of photoperiodic (seasonal) responses (Cronin. 1986; Helfrich-Förster and Engelmann. 2002).

Extraocular photoreceptors are found in both vertebrates and invertebrates (Cronin. 1986; Menaker and Underwood. 1976; Rieger *et al*. 2003). For instance, light entrainment in humans is thought to be mediated mainly by melanopsin-based retinal ganglion cells and not via rods or cones (Gooley *et al*. 2010). Evidence from two blind subjects lacking functional rods and cones confirmed the presence of a non-visual ocular photoreceptive mechanism, as these subjects exhibited normal rhythmic activities, phase resetting and melatonin suppression in response to light stimulation (Gooley *et al*. 2010; Zaidi *et al*. 2007). This is thought to be driven by short-wavelength (480nm) -sensitive photosensitive retinal ganglion cells (Zaidi *et al*. 2007).

In *Drosophila*, the visual system consists of three classes of photosensory organs: the HB eyelets, the ocelli (cup-like simple eye) and the compound eyes see Fig 1.4 (Pollock and Benzer. 1988). Each of the three ocelli located on the fly head has a single light-collecting lens and about 90 photoreceptor cells (Pollock and Benzer. 1988). The spectral sensitivity of the photoreceptor cells within these ocelli (peaks in violet 420 nm) (Hu *et al*. 1978) differ from the spectral

sensitivity seen in the photoreceptors within the compound eyes (peaks 500 nm) (Goldsmith. 1990) suggesting a different photopigment (Pollock and Benzer. 1988).

In addition to the presence of ocular photoreceptors, *Drosophila* also possesses extraretinal photoreceptors called Hofbauer – Buchner (H-B) eyelets. These are located at the posterior margin of the compound eye and project directly to the accessory medulla (aMe) (Hofbauer, Buchner 1989) see Fig 1.4. The H-B eyelet contains specialised pigment cells with numerous microvilli, which are arranged into coherent rhabdomeres (Helfrich-Förster and Engelmann. 2002; Yasuyama and Meinertzhagen. 1999). The presence of well-organised rhabdomeric microvilli - a defining feature of photoreceptors, further supports the photoreceptive role of the H-B eyelet (Yasuyama and Meinertzhagen. 1999).

1.8.2 Circadian photopigments

Studies in *Drosophila* have contributed to the identification of different photopigments involved in circadian clock entrainment (Emery *et al*. 1998; Helfrich-Förster *et al*. 2002; Hofbauer and Buchner. 1989). Based on genetic and molecular approaches, several candidate genes have been proposed such as *arrestin*, and *cryptochrome* (Emery *et al*. 1998; Hardie and Raghu. 2001; Lee *et al*. 2003). These genes can be grouped into two broad classes based on whether

opsin- or flavin–based pigments are encoded (reviewed in Green. 2004; reviewed in Shichida and Matsuyama. 2009).

Rhodopsins are members of the G protein couple receptors (GPCR) family and play a vital role in the visual signal transduction pathway (Hardie and Raghu. 2001; Montell. 1999). They display different spectral sensitivities as shown in Fig 1.7. The visual signalling pathway captures incidental light and converts it to neural signals that can be processed by the brain. This pathway involves several factors encoded by many genes; hence disruption of any of these genes could inhibit the cascade. The light incidence is absorbed by rhodopsin in all the ocular photoreceptors and transduced into electrical charge in the plasma membrane by a G-protein-coupled signalling pathway (Hardie. 2001). Rhodopsin is activated when light is absorbed by the 11 *cis* to *all –trans* photoisomerisation of chromophore (*3*-hyroxyl retinal or retinal in non-dipteran) (Vogt and Kirschfeld. 1984). In contrast, majority of the other G-protein-coupled receptors are activated by chemical messengers (Hardie. 2001).

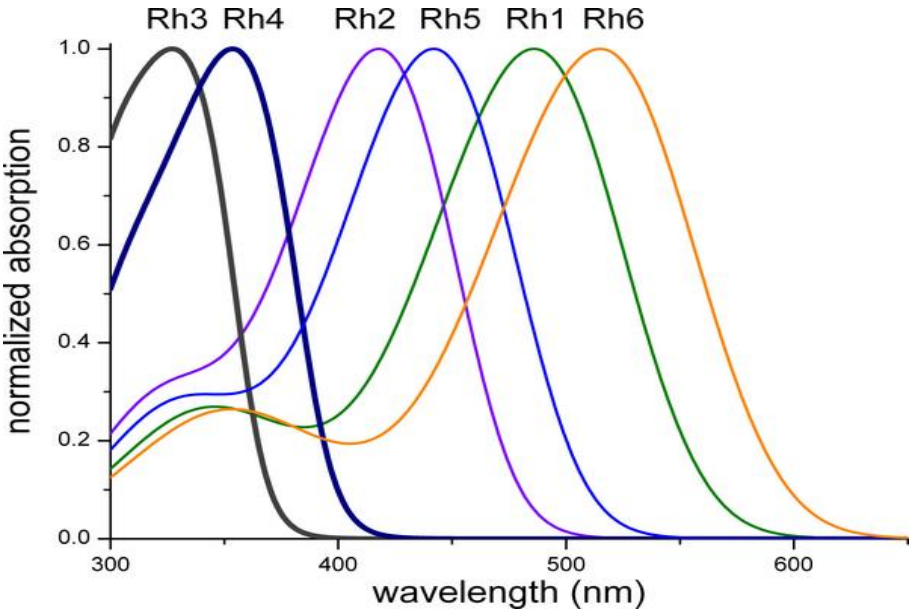

Figure 1.7: The absorption spectra of Rhodopsins expressed in *Drosophila*

Figure was adapted from (Stavenga and Arikawa. 2008).

The resulting photoisomerisation triggers the conversion of rhodopsin into an active metarhodopsin state. The metarhodopsin catalyses the activation of a G-protein nucleotide exchange of GTP for GDP and dissociates a Gα subunit which remains active until the bound GTP is hydrolysed (Hardie. 2001). The activated G –protein (transducin) binds and activates the effector enzyme, phosphoionsitide-specific phospholipase C (PLC), encoded by the *norpA* gene in *Drosophila* (Tweedie *et al*. 2009). The PLC produces a soluble inositol-1 4, 5-trisphophate and membrane bound diacylglycerol (DAG) from the hydrolysis of the minor membrane phospholid phosphatidylinositol-4, 5-bisphosphate (Hardie and Raghu. 2001). This causes the opening of two classes of Ca^{2+} permeable photosensitive channels: the transient receptor potential (TRP) and the TRP-like (TRPL) with 40% sequence identity (reviewed in Hardie

and Raghu. 2001). However, the mechanism involved in the opening of these light sensitive channels by the activation of PLC still remains unknown.

Cryptochromes (CRY) are members of a large family of blue-light sensitive flavo-proteins originally identified in *Arabidopsis* (Ahmad and Cashmore. 1993). They have also been identified in many organisms including bacteria and insects. They are now known to be involved in light entrainment of circadian clocks, as well as in magneto-reception (Cashmore. 2003; Gegear *et al*. 2008). In mammals and some insects (but not *Drosophila*), two paralogs CRY1 and CRY2 are expressed, both of which function in clock machinery (Harmer *et al*. 2000; Zhu *et al*. 2008). In *Drosophila,* a single CRY is present, which serves as the circadian photoreceptor (Emery *et al*. 1998; Ito *et al*. 2008) and in other functions. For instance, it serves as a clock core component in peripheral clocks (Krishnan *et al*. 2001) . This is shown in cry^{b} and cry^{0} flies, where molecular oscillations of PER and TIM were abolished in peripheral tissues (the legs, compound eyes, antennae and Malpighian tubules) (Levine *et al*. 2002b). CRY has been shown to act as a repressor of the CLK-CYC transcriptional activity in the compound eyes (Collins *et al*. 2006).

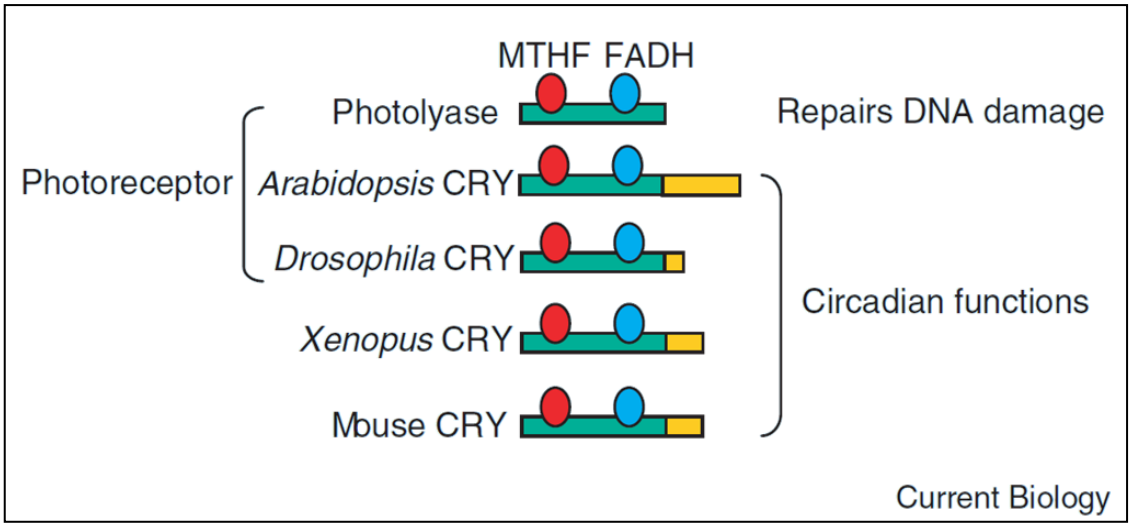

Figure 1.8: Cryptochrome structures in various organisms

showing a core domain (green) with high sequence similarity to DNA photolyases. This domain consists of two co-factors: a flavin (FADH,blue) and a pterin (MTHF,red) binding sites, adapted from (Green. 2004).

Drosophila's CRY shows an overall structural similarity to bacterial light-activated DNA repair enzyme photolyase (in particular the 6-4 photolyase) (Fig 1.8) but lacks DNA repair activity (Ahmad and Cashmore. 1993; Lin and Todo. 2005). Based on *cry* action spectra and the homology to photolyase, it was classified as a blue-light receptor (Cashmore. 2003). Like photolyase, cryptochromes also contain two chromophores: a pterin (methenyltetrahydrofolate, MTHF) and flavin adenine dinucleotide (FAD) (Lin and Todo. 2005; Zordan *et al*. 2001) (Fig 1.8). The pterin region functions as a light harvesting chromophore by absorbing photons and transferring the excitation to flavin via a series of redox reactions. In addition, *Drosophila* and plants' CRY absorbs photons and transduces the signal in a similar way to the photolyase. They use the energy generated in changing their conformation thus

enhancing protein-protein interactions as opposed to DNA repair in photolyases (Green. 2004).

Further insights into the role of CRY in circadian photoreception were provided by the isolation of *cry* mutations, cry^{baby} (cry^{b}) and cry^{m} (Busza *et al*. 2004; Stanewsky *et al*. 1998). These mutations affect a highly conserved amino acid in the chromophore –binding site of FAD necessary for CRY and photolyase functions (Stanewsky *et al*. 1998). cry^{b} mutants do not respond to short light stimuli that normally would phase shift the rhythm in wild-type flies (Stanewsky *et al*. 1998) and are behaviourally hypersensitive to light pulses when CRY^{+} is over-expressed (Emery *et al*. 1998). In addition, cry^{b} flies displayed a rhythmic locomotor activity under constant light, a condition that turns wild-type flies arrhythmic (Emery *et al*. 2000). In a nutshell, *cry* mutant flies exhibit profound molecular and behavioural light response defects.

Interestingly, cry^{b} flies still entrain behaviourally to a new phase of an adjusted LD cycle ('jet-lag' experiment) but takes longer than in wild type flies. In addition, the molecular clock in LN neurons still responds to light entrainment in cry^{b} flies (Stanewsky *et al*. 1998). These observations suggest the presence of a CRY-independent light input pathway. This pathway was thought to involve the compound eyes, the ocelli and H-B eyelet, which all express opsin-based photopigment (Helfrich-Förster *et al*. 2001). In addition, these structures have also been shown to contribute to circadian light

sensitivity (Emery *et al*. 2000; Stanewsky *et al*. 1998). Flies lacking compound eyes and ocellar function owing to null mutation of *no receptor potential A (norpA)*, entrain to LD cycles in a similar way as cry^{b} mutants but are less sensitive to lower light intensities when compared to the wild-type flies (Emery *et al*. 2000; Stanewsky *et al*. 1998). Moreover, double mutant flies $norpA^{p41}$; cry^{b} are still capable of entrainment, suggesting a possible photoreceptor role for H-B eyelets (Stanewsky *et al*. 1998).

In 2001, Helfrich-Forster and colleagues studied a *glass* (*gl*) null mutation to investigate the role of (visual) photoreceptors in entrainment. *gl* encodes a DNA –binding Zinc –finger protein necessary for the development of all fly photoreceptor cells (Moses *et al*. 1989). In gl^{60j} (*n*ull mutation) flies, all known internal and external eye structures, including the H-B eyelets, are eliminated (Helfrich-Förster *et al*. 2001; Moses *et al*. 1989). In addition, the dorsally located clock neurons are also absent (Helfrich-Förster *et al*. 2001). Similar to the observation in *norpA* mutant, *gl* mutant flies entrain to a shifted LD cycle but at a slower rate compared with the wild-type flies (Helfrich-Förster *et al*. 2001). However, gl^{60j} cry^{b} double mutants appeared to be completely blind to LD cycles (unlike the *norpA;* cry^{b} double mutants which are still capable of entrainment). This sheds more light on role of extraretinal photoreceptor H- B eyelets in LD entrainment and supports a CRY-independent pathway for clock light entrainment.

1.8.3 TIM is a key component of light entrainment

The light degradation of TIM is thought to play a central role in *Drosophila*'s circadian light entrainment. It has been shown to correlate with the delay and advance phase shifts in flies (Hunter-Ensor *et al*. 1996). However, the specific signals that mediate TIM response to light are largely unknown, though the roles of a few genes have been proposed (Koh *et al*. 2006; Stanewsky *et al*. 1998). Light stimulation changes the conformation of CRY allowing it to bind to TIM resulting in its degradation (Busza *et al*. 2004; Dissel *et al*. 2004). However, in CRYΔ flies (deletion of 20 amino acids within the C-terminus) this light-dependent interaction of CRY with TIM-PER was abolished and rhythmic activity in LL over short period was observed (Dissel *et al*. 2004; Rosato *et al*. 2001). In addition, CRYΔ reduces the level of TIM and inhibits the nuclear accumulation of PER-TIM in the lateral neurons under DD condition (Dissel *et al*. 2004). This latter observation displays a similar phenotype to wild-type flies under constant light. These observations suggest that CRYΔ flies are less sensitive to light and play a role in TIM stability.

Another important component of *Drosophila* light entrainment is JETLAG (JET), which is thought to transmit light signals from CRY to TIM for degradation (Koh *et al*. 2006). JET is an F-box protein with leucine-rich repeats encoded by *jetlag* gene in *Drosophila*. A single amino acid substitution in JET causes molecular and behavioural defects in flies' photic entrainment (Koh *et al*.

2006). *Jet* mutant flies exhibit a high percentage of rhythmic behaviour in constant light and a reduced phase shift in response to light pulses in the subjective night (Koh *et al*. 2006). Furthermore, by co-expressing JET and CRY in *tim* expressing S2R *Drosophila* cells, the level of TIM drops rapidly upon light treatment but remains stable in dark conditions (Koh *et al*. 2006). Interestingly, *jet* mutant phenotype is only observed in fly strains carrying (*ls-tim*)-a natural variant of *tim,* this will be discussed in more detail in chapter 3.

Recently, null mutations of COP9 complex homolog subunits (*CSN4* and*CSN5*) have been shown to inhibit normal light-induced TIM degradation in fly larval pacemaker cells (LNs) (Knowles *et al*. 2009). When the expression of *CSN5* was down-regulated in *pdf*-positive LNs, light-induced phase shifts were reduced. Interestingly, overexpression of *jet* rescued this behavioural defect in flies suggesting that CSN and JET function in a common light-dependent TIM degradation pathway (Knowles *et al*. 2009).

A light pulse in the early subjective night delays the phase of rhythmic activity by 2- 6 hours while stimulation at late subjective night advances the phase by about 2 hours (Johnsson and Engelmann. 2008; Myers *et al*. 1996; Saunders *et al*. 1994). In the early subjective night, light signal degrades TIM but TIM is thought to re-accumulate rapidly owing to its high level of cytoplasmic mRNA (Myers *et al*. 1996). Thus, the phase of clock is delayed by the duration it takes TIM to re-accumulate. In contrast, premature degradation of TIM in

response to light stimulation during the late subjective night is not compensated hence advances the phase of the clock as CLK-CYC inhibition is released.

1.9 Study aims and objectives

Despite extensive progress in understanding of the circadian clock, the molecular basis of light entrainment still remains unclear. Previous studies revealed that wild populations of *Drosophila* vary significantly in their circadian photic sensitivity, and that this trait co-varies with latitude (Pittendrigh and Takamura. 1989; Sandrelli *et al*. 2007). This phenotypic variation presumably reflects local adaptation of the clock to the seasonal change of day-length. Yet, the genetic variation underlying this phenotypic variation is largely unknown.

One of the objectives of this study was to identify candidate loci contributing to natural phenotypic variation in light response using quantitative trait loci (QTL) approach. This QTL experiment, which is described in chapter 3, was further examined by complementation tests and microarray profiling in an attempt to narrow down the QTL and identify candidate genes underlying the variation.

Global expression profiling using microarrays was another approach taken in this study to identify genes which are involved in light entrainment of the clock. Several studies have already shown that light-induced phase shifts are accompanied by changes in gene expression (Porterfield and Mintz. 2009; Rusak *et al*. 1990). For instance, the expression of an array of immediate early genes, transcription factors and some circadian clock genes in the SCN in response to light stimulation have been reported in several organisms

(Porterfield and Mintz. 2009; Rusak *et al*. 1990). However, little is known about the transcriptional changes associated with light-induced phase shifts in *Drosophila*. Chapter 4 of this thesis describes the experiments aimed at understanding these transcriptional changes at a genome-wide level. The objective was to identify differentially expressed genes in response to light stimulation and investigate the biological pathways involved.

Since one of the interesting findings that emerged from the microarray experiment (chapter 4) was the enrichment of genes involved in covalent histone modifications, the role of these genes in light entrainment of the clock was further studied. The results of these experiments are summarised in chapter 5. Growing evidence indicates that histone modifications play an important regulatory role in the mammalian clock (reviewed in chapter 5) and the current study suggests that these modifications may play a similar role in *Drosophila.*

Chapter 2: Materials and methods

This chapter describes general procedures and reagents used in this study. Additional information will be provided in the material and methods sections in each of the following results chapters.

2.1 Chemicals and reagents

All stock solutions and buffers used were prepared as outlined in (Sambrook and Rusell. 2001) unless stated otherwise. Solutions were sterilised by autoclaving at 120^{0}C for 20 min or by filtration through an acrodisc syringe filter 0.2µM (Life sciences). All chemicals were analytical grade from Fischer Scientific (Loughborough, UK) or Sigma-Aldrich Company Ltd (Poole, UK) unless stated otherwise.

2.2 Genomic DNA extraction and purification

2.2.1 Extraction from a single fly

Genomic DNA was isolated from a single fly following Gloor's protocol (Gloor and Engels. 1992). In brief, a single fly was placed in a 1.5 ml tube and crushed for 5- 10 s using a P20 pipette tip containing 50 µl Squishing buffer (SB: 10 mM Tris-HCl pH 8.2; 1 mM EDTA; 25 mM NaCl and 200 µg/ml of proteinase K). The remaining SB was expelled from the pipette tip and the sample incubated for 20 -30 min at room temperature. The proteinase K was heat

inactivated at 95^{0}C for 2 min. 1 µl of this extract was subsequently used for PCR of a reaction volume between 10 - 20 µl.

2.2.2 Extraction from multiple flies

For extraction of DNA from more than one fly, the samples were ground in liquid nitrogen using a mortar and pestle. 1ml of tail lysis buffer (100mM EDTA, 100mM NaCl, 50mM Tris-HCl pH 8.0, 1% SDS and proteinase K to a final concentration of 200µg/ml) was added and incubated at 37^{0}C overnight or for 4-5 h at 55^{0}C with shaking. The cell lysate was purified with 1ml (phenol, chloroform and Isoamyl-alcohol (IAA) of ratio of 25:24:1 respectively). The mixture was centrifuged at 3000 rpm for 15min at room temperature (RT) each time. The supernatant was then extracted with 1ml Chloroform and IAA in a ratio of 24:1 and spun for 3000 rpm for 15min at RT. The supernatant was transferred to a new tube and precipitated by adding 100 µl of 4M NaCl, 500 µl of water (to dilute SDS) and twice the starting volume of 100% ethanol. The solution was then inverted several times and the precipitated DNA was transferred into a 1.5ml tube containing 500µl 70% ethanol. The solution was centrifuged at 13,000 rpm for 10 min at 4^{0}C. In cases where a small quantity of DNA was present in the solution, the suspension was left overnight at -20^{0}C and centrifuged at 3000 rpm for 30min at 4^{0}C. The supernatant was discarded and the pellet washed with 70% ethanol. The pellet was air-dried and re-suspended in the appropriate volume of TE (10mM Tris-HCl pH 7.5, 0.1mM

EDTA pH 8.0) overnight at RT. DNA concentration and 260/208 purity ratio were determined by measuring its absorbance at 260nm using NanoDrop 2000 (Thermo Scientific).

2.3 DNA amplification and analysis

2.3.1 Polymerase chain reaction (PCR)

PCRs were primarily performed using a standard Taq polymerase (Kappa Taq polymerase, Biosystem) and 11.1x AJJ buffer [2M Tris pH 8.8, 1M Ammonium sulphate, 1M $MgCl_2$, β-mercaptoethanol (Sigma), 1/10 dilution of 100mM EDTA pH 8.8, 100mM dNTPs (Amersham) and 10mg/ml BSA (Amersham)] was used unless stated otherwise. The standard PCR components and cycling conditions used in this study are listed in Table 2.1 and Table 2.2.

Table 2.1: Standard PCR components used in this study

PCR reagent	**Volume (µl)**
DNA	Up to 50 ng
11.1x buffer	0.9
Tris (2 M)	0.06
Forward primer (10 µM)	0.5
Reverse primer (10 µM)	0.5
Taq DNA polymerase	0.1
Nuclease-free water	Make up to final volume of 10 µl

Table 2.2: Standard PCR cycling parameters used in this study

PCR step	Temperature	Duration (min : sec)
Initial Denaturation	94^{0}C	2:00
Denaturation*	94^{0}C	0:30
Annealing	50^{0}C to 70^{0}C depending on primers used	0:30
Extension	72^{0}C	0:30 – 2:00 (depending on the amplicon size)

*Repeat step 2, 3 and 4 for 40 cycles

Final extension	72^{0}C	10:00
Hold	10^{0}C	Forever

All PCR assays were performed using DYAD™ DNA Engine Peltier Thermal Cycler. For each set of primers, the annealing temperatures were first determined using a gradient of temperatures in the annealing step.

2.3.2 Agarose gel electrophoresis

Amplified DNA products were mixed with loading dye (0.25% bromophenol Blue; 0.25% cyanole) and loaded on 1 – 2% (w/v) agarose gels alongside appropriate DNA molecular marker. Agarose gels were melted in 1x TBE(109g/L Tris, 55g/L Boric Acid, 9.3g/L EDTA in de-ionised water) and 1µg/ml of ethidium bromide was added. Gels were run between 100 – 150 volts for 25- 50 min and the DNA visualised under UV light. The signals were detected and captured by Gene Genius (Bio-imaging System Inc, UK). The size of the DNA fragments was inferred from the molecular marker.

2.4 Total RNA extraction and analysis

RNA work was carried out in RNase treated surface and solutions were prepared following Sambrook and Russel (Sambrook and Rusell. 2001) precautions on RNase contamination.

2.4.1 Total RNA extraction

Male flies were entrained to 12h: 12h light cycles for 4 days at 25^0C and given 30 min of light stimulation at ZT 15 (on the 4^{th} day). The treated and control flies were collected 1hr (ZT 16.5) after the light pulse in darkness by snap freezing in liquid nitrogen and stored in -80^0C until ready for further processing. Fly heads were collected in microcentifuge tubes kept on dry ice by vigorously vortexing the fly samples and using a sieve to separate the heads from the bodies.

Frozen fly heads were ground with a pestle in a mortar containing liquid nitrogen. The total RNA was extracted using Tri-reagent (Invitrogen) following the protocol recommended by Invitrogen. In brief, fly heads were homogenised in 2 ml Tri-reagent and incubated at RT for 5 min. 400 µl chloroform (0.2ml per 1 ml of TRI Reagent) was added and vigorously shaken for 15 s. The mixture was incubated at RT for 10 min and centrifuged at 4,000 rpm for 15 min at 4^0C. The upper phase was transferred into a new RNase-free 15 ml falcon tube and 1 ml (0.5 ml/ 1ml of TRI reagent starting volume) of isopropanol was added to

precipitate the RNA. The mixture was incubated for 10 min at RT and centrifuged at 4000 rpm for 10 min at 4^0C. The supernatant was carefully removed leaving behind RNA pellet. This was washed with 1 ml 75 % ethanol (by vortexing) and centrifuged at 3000 rpm for 5 min at 4^0C. The supernatant was aspirated and the pellet was centrifuged for 1 min. The remaining solution was removed and the pellet air-dried from 10 min. The pellet was then re-suspended in 100 µl RNase-free water, subsequently purified and quantified as described in section 2.4.2.

2.4.2 Total RNA purification and quantification

Total RNA samples were cleaned using the RNeasy® MinElute™ Cleanup kit (Qiagen). RNA concentration and 260/208 purity ratio were determined using NanoDrop 2000 (Thermo Scientific) and sample quality was assessed by the Agilent 2100 Bioanalyzer (Agilent Technologies, Santa Clara, CA, USA) according to the manufacturers' protocols.

2.4.3 Complementary DNA (cDNA) synthesis

Total RNA for cDNA synthesis was treated with DNase (Ambion) to remove any contaminating DNA (Table 2.3), which was performed in an RNase-free microcentrifuge tube.

Table 2.3: DNase treatment reagents

Reagents	Volume (µl)
Total RNA	Up 1 µg
10X DNaseI reaction Buffer	5
rDNase I (2U/µl)	1
DEPC-treated water	Up 50*

*The tube was incubated for 30 min at 37°C

The reaction was terminated by adding 5 µl of the DNase Inactivation Reagent. The mixture was incubated for 2 min at RT with occasional mixing and centrifuged at 13,000 rpm for 1.5min. The supernatant was carefully transferred into a new RNase-free 1.5 microcentrifuge tube. This was then used for cDNA synthesis as described below:

cDNA synthesis was performed using AffinityScript™ Multiple Temperature Reserve Transcriptase (Stratagene). DNase-treated RNA (1µg) was mixed with 3µl of random primer (0.1µg/µl) and RNase-free water to total volume of 15.7 µl. The mixture was incubated at 65°C for 5 min and then chilled on ice for 10 min. Table 2.4 lists the components that were added to the mixture to a final volume of 20 µl.

Table 2.4: cDNA synthesis: reagents and volume used

Reagents	Volume (µl)
10× AffinityScript RT Buffer	2
dNTP mix (25 mM each dNTP)	0.8
RNase Block Ribonuclease Inhibitor (40 U/µl)	0.5
AffinityScript Multiple Temperature RT	1

The reaction was then incubated at 25°C for 10 min, followed by 50°C for 1 h and then the reaction was terminated by heat inactivation at 70°C for 15 min on a thermocycler. The product was used directly for PCR amplification or stored at -20^{0}C until needed.

2.5 Immunocytochemistry (ICC) and fluorescence imaging

2.5.1 Brain dissection

Adult male flies were collected at the appropriate time points and quickly fixed in 4% paraformaldehyde containing 0.1% Triton X-100 for 30 min on ice and for a further 2 hr at room temperature. Samples were washed three times for 15 min each in 1x Phosphate Buffer Saline (PBS) containing 0.5% Triton X- 100 (PBST) at RT and 1x PBS added after the last wash. Brains were dissected in a disc containing 1x PBS solution under a microscope with two pairs of fine forceps. The fly was held facing up with one pair of forceps on the left hand, and the proboscis was removed with the other pair of forceps. The right pair of forceps was gently inserted into the cavity just below the eye to grip the eye and discharged the head from the body. The left pair of forceps was used to grip the other eye and gently pull the two pairs of forceps away from each other to open the head cuticle. After removing the brain from the head, the surrounding trachea and the air-sacs were carefully removed. The brains were kept in 1x PBS on ice or 4^{0}C until used.

2.5.2 Whole- mount immunocytochemistry

Whole mount ICC of adult brains was performed as described by Helfrich-Förster (Helfrich-Förster. 2007) with a few modifications. Brains were blocked in PBST containing 5% heat inactivated normal goat serum (NGS) for 1 hr at RT. Immunolabelling was performed by incubating the brains and the required primary antibodies at 4°C for a week in blocking solution containing 0.1% Sodium azide with gentle agitation. The antibodies were removed and the brains washed three times for 20 min each time with 1ml PBST at RT. Secondary antibodies were then added and incubated for 1h at RT. The brains were washed as described above, mounted onto microscope slide (VWR) with a drop of Prolong antifade (Invitrogen) and cured in the dark for 24 h at RT. The slides were stored at 4^0C until needed and after imaging. The samples were viewed on FV1000 Olympus confocal microscope mostly at 20x objective. The optimal settings for the laser intensities, laser gain, amplifier gain and offset were adjusted on an experimental basis to enhance the quality of the images.

2.6 Fly stocks and maintenance

All experiments in this study were done using *D. melanogaster* adult flies grown in vials containing standard sucrose-yeast medium: add 46.3 g sucrose; 46.3 g deactivated dry yeast; 10 g agar in 1L of water and boiled. Cold nipagin (20%, 2g of methyl 4-hydroxybenzoate dissolved in 10 ml ethanol) was added when the mix temperature was between 50 -55°C. Vials were tightly bunged

with cotton wool balls and kept in temperature controlled rooms (either at 18˚C or at 25˚C) under 24 h-cycles of 12 h of light and dark (LD 12:12). Flies were handled using CO_2 anaesthesia as recommended in Greenspan (Ashburner *et al*. 2005), or on ice when setting up behavioural experiments. Crosses were performed using appropriate balancers and designed in accordance with recommendations in Ashburner (2005). The specific fly strains used in each experiment are described in the Methods section of each Results chapter.

2.7 Locomotor activity experiments

Glass tubes (10cm x 0.5cm) were filled with approximately 2 cm deep of sugar/agar medium and sealed with a black rubber cap. Tubes containing food were left overnight at 25^0C to dry excess water. A single male fly was placed in each tube and loaded into DAM2 Drosophila activity monitor (Trikinetics Inc, Waltham,USA), which holds thirty-two tubes. The activity monitors were then placed in an incubator set at 25^0C with ~70 % humidity. As a fly moves back and forth within its tube, it interrupts an infrared beam that crosses the tube at its midpoint. This interruption is detected and recorded as the measure of fly activity. The number of counts recorded over a 30 min period is the locomotor activity for that time bin.

For the light pulse experiments, flies were entrained at 25^0C in LD cycle for 4 days and allowed to free-run for 3 days in constant dark(DD). In the following week, this entrainment regime was repeated with the same set of flies

but with 20 min light pulse at ZT15 on the last dark phase of the LD cycle (Fig 2.1). The timing of the activity bout on the second day in DD (the offset of activity) was used as a reference point for phase measurements. The phase of the first week (no pulse) was used as reference phase and the phase in the second week (light pulse) was used as response phase. The phase shift was calculated as the difference between the reference phase and the response phase, with negative value representing a delay phase shift ($-\Delta\Phi$, see Introduction). This was analysed manually by looking at each fly activity profile to determine the reference phase and the experimental phase. Note that all the analyses were done blindly (i.e the genotype was unknown during the analysis). The light pulse data in chapter 3 (QTL studies) was analysed based on this method. In subsequent chapters (4 and 5), the analyses were done using BeFly software (Kyriacou and Green unpublished).

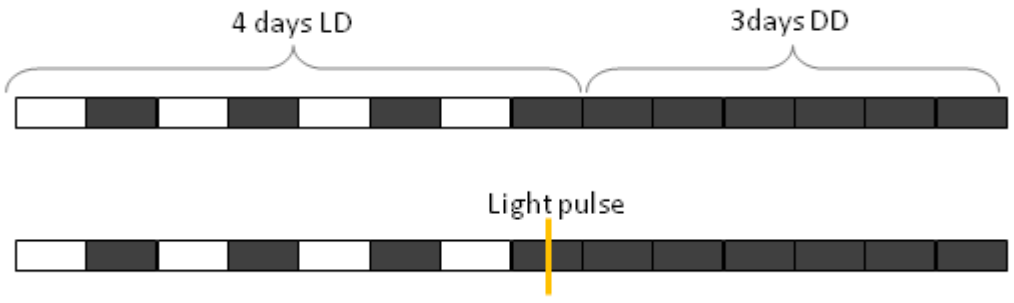

Figure 2.1: Light pulse experiment protocol used in this study

Genotypes were randomly mixed in the activity monitors and all analyses done blindly.

To determine the endogenous circadian period, flies were entrained in LD 12:12 cycle for 4 days and then allowed to free-run for 7 days in constant

dark (DD) or in constant light (LL) at 25^0C. The free-run data was analysed using autocorrelation analysis and by spectral analysis using the CLEAN algorithm (Rosato and Kyriacou. 2006). Post CLEAN data was assembled and further processed using a collection of macros in the BeFly package (Kyriacou and Green unpublished). The activity of a fly was considered rhythmic when it showed a significant autocorrelation and spectral analysis. A single detectable peak above the 99% confidence limit (CL) in the CLEAN analysis was taken as the endogenous period. Individuals with multiple peaks above the 99% CL were considered to be displaying multiple rhythms, while any other pattern below 99% CL was regarded arrhythmic.

2.8 RNA interference (RNAi) knockdown

The expression of candidate genes was down-regulated using Gal4/UAS binary system (Brand and Perrimon. 1993) and as described by (Dietzl *et al*. 2007) . In this study, two drivers (*timGal4* and *timGal4-dicer2)* were separately used to drive the expression of UAS-IR construct targeting gene of interest. All RNAi stocks used in this study were obtained from Vienna Drosophila RNAi Centre (VDRC). The specific strains and the details of each experiment are described in the methods section of each results chapter.

2.8.1 RNAi crossing scheme

Flies carrying UAS-IR construct targeting candidate genes described in chapter 4 and 5 were crossed to *tim*Gal4 or *tim*Gal4-*dicer2* as presented in Fig 2.2.

$$w^{118};\frac{timGal4}{Cyo};+ \;\; x \;\; w^{1118};\frac{UAS-GOI\ RNAi}{UAS-GOI\ RNAi};+ \;\; \Rightarrow \;\; w^{1118};\frac{timGal4}{\Downarrow UAS-GOI\ RNAi};+$$

$$w^{118};\frac{timGal4}{Cyo};+ \;\; x \;\; w^{1118} \qquad \Rightarrow \;\; w^{1118};\frac{timGal4}{+};+$$

$$w^{118} \;\; x \;\; w^{1118};\frac{UAS-GOI\ RNAi}{UAS-GOI\ RNAi};+ \qquad \Rightarrow \;\; w^{1118};\frac{UAS-GOI\ RNAi}{+};+$$

Figure 2.2: Crossing scheme used in this study: for both drivers

The text in blue represents the knockdown of gene of interest (GOI) and those in black text are the controls for both the driver and UAS construct. The red arrow indicates down-regulation of GOI. Note that the w1118 flies used in this study do not carry per^{SLIH} mutation known to show circadian rhythm defects.

2.9 Statistical analysis

Parametric and non-parametric statistical tests were used depending on the normality of data set. Normality test for the each data set was performed using Kolmogorov-Smirnov and Shapiro-Wilk tests. All statistical analyses were performed using the Statistical Package for the Social Sciences (SPSS), version 16.0. Further statistical procedures are described in the relevant chapters.

Chapter 3: Mapping quantitative trait loci (QTL) underlying circadian light sensitivity in Drosophila

3.1 Introduction

While many of the core components of the circadian system for various model organisms have been identified (chapter 1: Introduction), the extent of natural genetic variation associated with the circadian clock is largely unknown. This variation is however expected to be substantial, reflecting different molecular adaptations that have been evolved in wild populations responding to different environmental cues. Furthermore, these molecular variations in clock genes may exhibit geographical clines, following the latitudinal change of photoperiod and temperature (Kyriacou *et al*. 2008). Identifying and elucidating these variations is important for better understanding of the clock and its evolution.

Early studies (Pittendrigh *et al*. 1991) have shown that light sensitivity in natural populations of *Drosophila auraria* follows a latitudinal cline with an apparently reduced light sensitivity (the entraining power of light) in northern populations. This was explained as an adaptive response to the extremely long days of the summer. Recently, Tauber and colleagues (2007) identified a natural polymorphism in *tim* that involves a single-base insertion/deletion, situated between two alternative translation starts. The *ls-tim* allele (the insertion) produces both long and short isoforms of the protein whilst the *s-tim* allele (the

deletion) generates only the shorter isoform as translation from the first ATG codon is truncated via a premature stop codon. This polymorphism follows a robust latitudinal cline and is maintained by directional selection (Tauber *et al*. 2007). Light pulse experiments, have indicated that *ls-tim* flies are generally less light responsive than flies carrying *s-tim* (Sandrelli *et al*. 2007).

The recently discovered protein JETLAG (JET) has been identified as being involved in promoting the light-induced degradation of TIM (Koh *et al*. 2006). JET is an F-box protein, which physically associates with TIM and induces TIM's ubiquitinisation. Interestingly, the phenotype of *jet* mutants (being rhythmic in continuous light) is only expressed in strains carrying the *ls-tim* allele but not those with *s-tim* (Peschel *et al*. 2006). These discoveries have demonstrated how natural genetic variation modulates light sensitivity of the circadian clock. It also underscores how characterisation of natural variations in clock genes may lead to a better understanding of the circadian-clock mechanism.

Quantitative trait loci (QTL) mapping is a popular approach for identifying genes that underlie phenotypic variation (Box 1). Attempts to map circadian traits by QTL mapping have been made previously in plants (Darrah *et al*. 2006; Michael *et al*. 2003; Swarup *et al*. 1999), mice (Yoshimura *et al*. 2002) and recently in fungi (Kim *et al*. 2007) but in most cases did not result in the identification of the actual polymorphism that accounts for the phenotypic

variation. *Drosophila*, with its compact genome and the available powerful genetic tools provides a quick way to go from an identified QTL to a specific gene and polymorphism within a gene (Mackay. 2001). Curiously, *Drosophila* has been used in QTL screens of numerous traits (Mackay. 2001) but circadian-clock QTL have not been mapped yet. Hence the current study is aimed at identifying QTL for circadian photo-sensitivity and candidate genes underlying these QTL.

Box 3.1. QTL mapping

Quantitative traits are influenced by polygenes, gene interactions, and environmental factors (Falconer and Mackay. 1996; Lynch and Walsh. 1998). Genes underlying polygenic traits are difficult to identify directly from the phenotype as their alleles segregate at multiple loci. However, through indirect inference from linked marker loci, significant progress has been made in understanding complex traits. QTL mapping identifies the genomic regions associated with the trait of interest, the effect of the QTL on the trait and epistatic interaction if any. The likelihood of detecting QTL depends on various factors such as the heritability of the trait, experimental design, statistical analysis used, genome size and number of individuals in the experimental population (Darvasi *et al*. 1993; Lander and Botstein. 1989).

(Box 3.1. continued)

QTL mapping consists of two important stages: the construction of a linkage map of the markers (fragment of DNA with an identifiable physical location in a chromosome and traceable inheritance often microsatellites and single nucleotide polymorphisms {SNPs}) and the correlation of the trait with the markers. Successful QTL mapping relies on a well constructed genetic (linkage) map spanning the genome of interest. In constructing a linkage map, genetic markers are assembled in a linear order within linkage groups based on the proportion of recombination events between any two markers (map units are measured in centiMorgans).

The various experimental designs for QTL mapping usually rely on an inbred population (although designs based on outbred or natural populations also exist), which are generated by mating two inbred parents, whose alleles are homozygous at most loci as a result of self pollination (in plants), or mating among close relatives over several generations. From the F1 generation, several populations can be derived such as backcross (BC), selfed (F_{n+1}) population or recombinant inbred (RI) strains generated by sib mating for several generations (Fig 3.1). The RI lines are particularly useful for traits with a low heritability, since a single genotype can be tested many times (multiple replicates per line) (Falconer and Mackay. 1996).

(Box 3.1. continued)

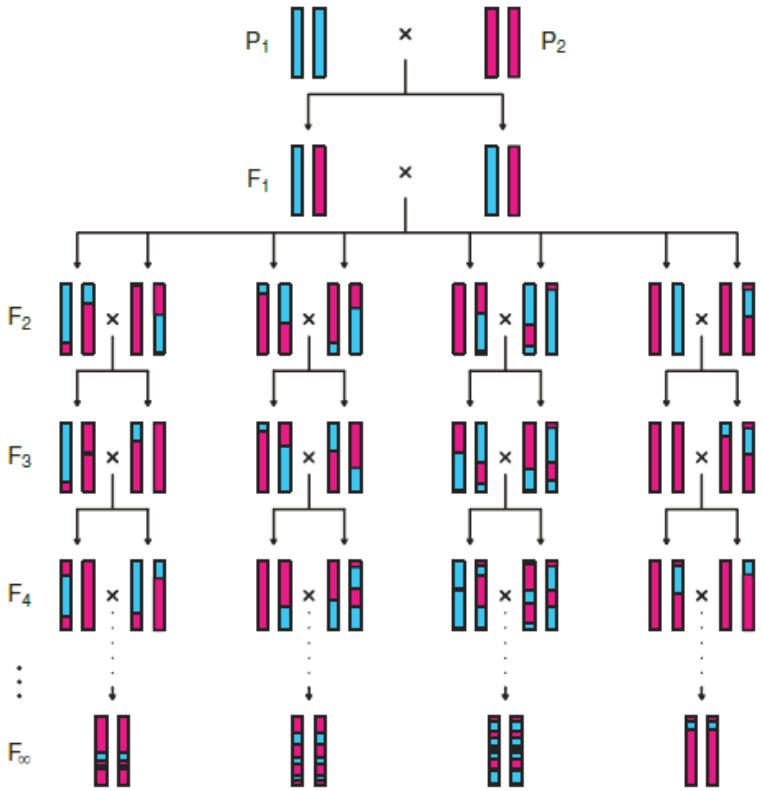

Figure 3.1: Generating recombinant inbred (RI) strains

Two isogenic parental lines are mated and the F1 are intercrossed (only autosomes are shown). In the following generation's sibling are repeatedly mated. After 10-20 generations, the resulting nearly isogenic RI lines represent each a unique mosaic of the parental lines (Broman 2005).

Single marker analysis is the simplest statistical method for QTL analysis. For each marker, individuals are grouped based on their marker genotypes and the trait means are compared. The process is repeated one marker at a time, hence named single marker analysis. One of the main shortcomings of this technique is that the outcome is confounded by the QTL effect and the distance from the marker (Falconer and Mackay. 1996).

(Box3.1. continued)

This problem was solved by the Interval mapping (IM) algorithm, which scans whether a QTL lies between two adjacent markers. The genotype of the QTL is modelled at different QTL sizes and locations between the flanking markers and the maximum likelihood estimator (MLE) that best explains the phenotype data is selected. The MLE is compared to a null model (no QTL present between markers) via a likelihood ratio test and usually is expressed as the log of Odds (LOD) (e.g. LOD 3 implies that the presence of QTL is 1000 times more likely than H_0). The significance threshold is often calculated by a permutation approach where the LODs are recalculated for permutated datasets. The LOD drop-off rule (Lander and Botstein. 1989) may be used to estimate confidence interval for the QTL. The location corresponding to a drop in the LOD score of 1 or 2 units from a peak in the LOD score amounts to 96.8 or 99.8 % confidence intervals respectively (Mangin *et al*. 1994).

Composite interval mapping (CIM) has more power to detect QTL (Zeng. 1994). This technique examines an interval between two markers for QTL. It is similar to IM but has the ability to simultaneously control for the effects of QTL outside the interval, treating markers also as covariates (this reduces residual variation and helps identify further QTLs).

(Box3.1. continued)

Multiple interval mapping (MIM) is a recent extension of IM, which operates in a similar manner to CIM but models multiple QTL and all possible epistatic interactions (Kao *et al*. 1999; Zeng *et al*. 1999). A more in-depth description of these algorithms and the statistics of QTL mapping can be found in (Broman and Sen. 2009).

3.2 Materials and methods

3.2.1 Mapping population

The recombinant inbred (RI) strains were generated by Sergey Nuzhdin at the University of Southern California. The lines were generated from two isofemale strains sampled from an orchard population in Winters (California), and were made isogenic by 40 generations of inbreeding. The lines were maintained in vials of yeast-sucrose-agar medium (as described in chapter 2) under (~70 % relative humidity, at either 18°C or 25 °C and 12h: 12h light cycle). Only male flies were used in the experiments.

3.2.2 Molecular markers and the linkage map

The original set of 102 single nucleotide polymorphism (SNP) markers spanning the three chromosomes of the RI strains (Bergland *et al*. 2008) was reduced to 44, as the segregation pattern of many of the markers did not follow the expected ratio. Linkage maps were constructed on MapMaker/Exp 3.0b program (Lander *et al*. 1987; Lincoln *et al*. 1993) using the Kosambi mapping function. The marker order on each of the chromosomes was established using the default setting of MapMaker (minimum LOD of 3.0, maximum distance of 37.2 cM, informativeness criteria of a minimum 44 individuals and a minimum distance of 4 cM). The linkage map was subsequently used in QTL analyses in Windows QTL cartographer (WinQTLCart) version 2.5 (Wang *et al*. 2007).

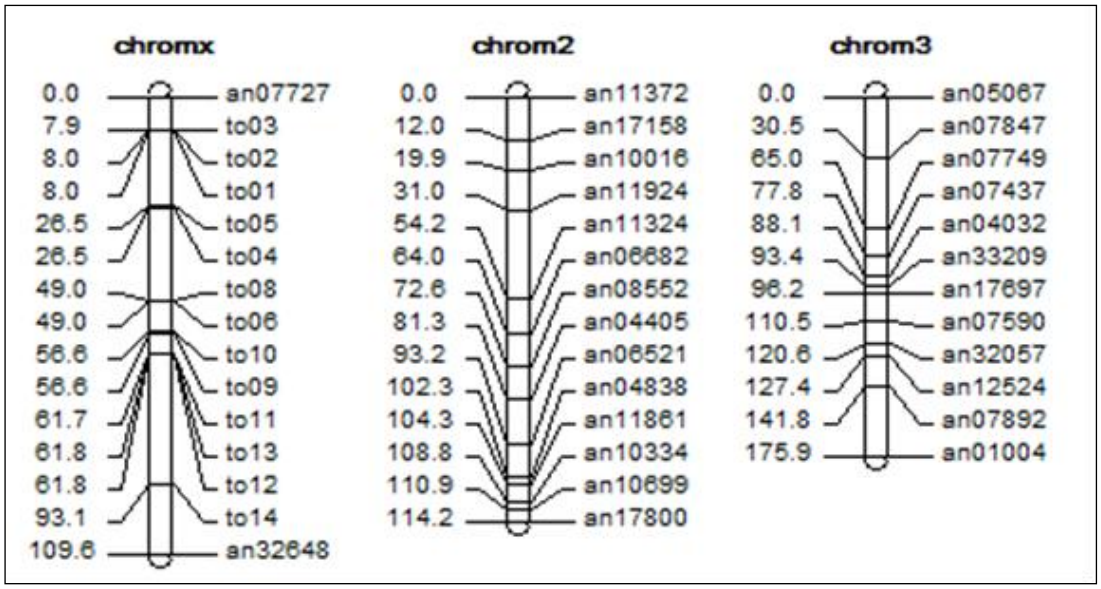

Figure 3.2: The genetic linkage map of the Winter RI strains

Based on 44 SNP intergenic markers that show expected segregation rate. Total map size is 355 cM.

3.2.3 Statistical analyses and QTL analysis

The phase shift of 20 males from each RIL was measured, and their mean was used in subsequent analysis. Using the Statistical Package for the Social Sciences (SPSS) version 16.0, Kolmogorov-Smirnov test indicated that the distribution of the means were normal. The genome scans for QTL were performed using composite interval mapping (CIM) (Zeng *et al*. 1999). This was then followed by multiple interval mapping (MIM, Kao *et al*. 1999; Zeng *et al*. 1999), which tends to have more statistical power and precision for detecting QTL (Kao *et al*. 1999). Both analyses were performed in Windows QTL Cartographer version 2.5 program (WinQTLCart) (Wang *et al*. 2007).

For CIM analysis, the parameters for background control were set to five markers and a 10 cM window size (in model 6), such that only markers 10 cM away from the test interval were included in the model, using a forward and backward regression method. The genome-wide significance threshold scores were determined at 5% level by running 1000 permutations (Churchill and Doerge. 1994). MIM analyses were performed using forward and backward regression selection on all markers with partial r^2 probability set to = 0.01 as the initial model. The Bayesian information criterion (BIC) model selection, the penalty function set to $c(n) = In(n)$ and performed at 1-cM walk speed. MIM was used to refine QTL positions, search for new QTL, search for epistatic interactions among the detected QTL, to estimate the individual QTL effects and the proportion of phenotypic variance explained by the QTL. The confidence intervals (95%) for the QTL were determined by extending the QTL for 1-LOD from the highest peak according to (Lander and Botstein. 1989; Mangin *et al*. 1994). When this was impractical, the markers spanning the QTL as determined from the map were used. The cytological positions and the putative genes were estimated using the markers's physical location from Ensembl release 56 and the FlyMine database (Lyne *et al*. 2007). In addition, the whole genome was scanned using MIM method for any epistatic interaction between the QTL.

3.2.4 Complementation tests

The deficiency stocks used for complementation tests are listed in Table 3.1. All the stocks were obtained from the Bloomington *Drosophila* Stock Centre (BDSC). A total of 11 deficiency stocks spanning QTL 2 (22B1 – 25B1) and QTL 3 (71E1 – 79A1) (Table 3.1) were used to fine-map the QTL intervals. Two RI lines with RIL 104 and low RIL 58, which showed high and low light response respectively, were chosen for further analysis of the QTL as the parental lines were not available. In addition to their light response, these lines showed close resembled to the parental genotypes along the QTL regions. Males from RIL58 and RIL104 were crossed with virgin females from each of the deficiency lines, resulting in four F1 genotypes: *58*/*Df*, *58*/*Bal*, *104*/*Df* and *104*/*Bal*, where *Df* and *Bal* refer to deficiency and the balancer chromosomes respectively.

Quantitative failure to complement the QTL alleles is inferred, when the difference in mean light response between the genotypes *58*/*Df* *104*/*Df* was significantly greater than that between *58*/*Bal* 104/*Bal.* In a two-way ANOVA, failure to complement is indicated by a significant interaction term. Analyses were performed in SPSS (v16) software.

Complementation tests were also carried out using null mutant strains of candidate genes within the QTL. Crosses were performed as described above, but using the mutant strain and w^{1118} instead of the Df and the balancer chromosome. The mutant stocks are listed in Table 3.2

Table 3.1: List of deficiency stocks used for complementation tests

Stock number	Deficiency Chromosome	Balancer Chromosome	Cytological Breakpoints
	QTL 2		
3133	Df(2L)dp-79b, dpDA cn^{1}	In(2LR)bwV1, b1 bwV1	22A3 - 22E1
6648	Df(2L)dppd14	In(2LR)Gla, wgGla-1	22E4-F2;22F3-23A1
90	Df(2L)C144, dpp^{d_ho} ed^{1}	In(2LR)Gla, $^{wgGla-1}$ Bc1 Egfr^{E1}	23A1-23A2;23C3-23C5
6875	Df(2L)BSC28	SM6a, bw^{k1}	23C5-D1;23E2
6507	y1 w*; Df(2L)drm-P2, P{lacW}Pdsw^{k10101}	SM6b	23F3--24A2
5330	Df(2L)ed^{1}	CyO; P{ftz/lacC}^{1}	24A2;24D4
	QTL 3		
2993	Df(3L)st-f13, Ki^{1} $^{rnroe-1}$ p^{p}	TM6B, Tb^{1}	72C1-D1;73A3-4
6411	Df(3L)BSC8	TM3, Ser^{1}	74D3-75A1;75B2-5
8082	w^{1118}; Df(3L)ED4782, P{3'.RS5+3.3'}ED4782	TM6C, cu^{1} Sb^{1}	75F2;76A1
6646	Df(3L)BSC20, st^{1} ca^{1}	TM6B, Tb^{1}	76A7-B1;76B4-5
5126	Df(3L)XS533	TM6B, Sb^{1} Tb^{1} ca^{1}	76B4;77B

Table 3.2: Mutant stocks used for complementation tests (null mutants)

Gene	Mutant genotype	Chr	Cytological Breakpoints
	QTL 2		
Thor	*y^{1} w; Thor^{2}*	2	23F3 - 23F3
tim	*w; tim^{01}*	2	23F6 – 23F6
	QTL 3		
cycle	*w;cyc^{01}*	3	76C6 – 76C6
	QTL 4		
Clock	*Clk ^{jrk}*	3	66A12 – 66A12

3.2.5 cDNA microarrays

3.2.5.1 Sample collection

Males (1- 5 days old) from RIL58 and RIL104 were entrained as described in Chapter 2. Flies were split into two groups, one presented with a light pulse for 30 minutes at ZT 15 and a control group kept at the same conditions without the pulse. Flies were collected at ZT 16.5. Two independent replicates were prepared per condition, totalling 8 samples: 2x lines (L) x treatments (T) x 2 replicates. Preparation of total RNA (from fly heads) and quality control were performed as described in section 4.2.2 of chapter 4.

3.2.5.2 Probe preparation, hybridisation and processing

Invitrogen superscript plus indirect cDNA kit was used to generate fluorescently labelled cDNA from 35 μg total RNA according to the manufacturer's protocol (Invitrogen). The purification and quantification were done as recommended by the Invitrogen protocol. The purified Alexa 555 and Alexa 647 labelled cDNA were hybridised to *Drosophila* Oligo 14Kv1 array (Canadian Drosophila Microarray Centre) according to University Health Network (UHN) Microarray Centre amino-allyl (indirect) labelling protocol. All other steps were performed as recommended by UHN microarray centre. The array slides were scanned on Molecular Devices' GENEPIX 4000 microarray scanner.

3.2.5.3 Data processing and statistical analysis

The raw data (.gpr file) was **processed using the GeneChip Robust Multi-array Average (GC-RMA)** method (Wu *et al*. 2004) on R package (http://www.r-project.org/) and the Graphical User Interface of the *limma* package (affylmGUI) (http://bioinf.wehi.edu.au/affylmGUI/) (Wettenhall and Simpson. 2010). To identify transcripts whose expression may account for the difference between the RI strains, a two-way ANOVA with treatment (T) and line (L) as factors was performed. Transcripts that show a significant interaction (T x L) were considered as quantitative trait transcripts.

3.3 Results

3.3.1 Quantitative genetic variation

Delay phase shifts ($-\Delta\Phi$) were measured 20- 30 males from each of the 123 RI lines. An extensive variation was observed among the RI lines ranging from -1.9 to -5.5 hr delays (Fig 3.3). The mean values for each of the RIL are presented in appendix 7.1. This variation was statistically significant as shown by ANOVA (F (122, 1968) =3.050, p <.001). The broad-sense heritability was h^2 = 0.3, suggesting that the genetic component of the phenotypic variation of this trait is significant.

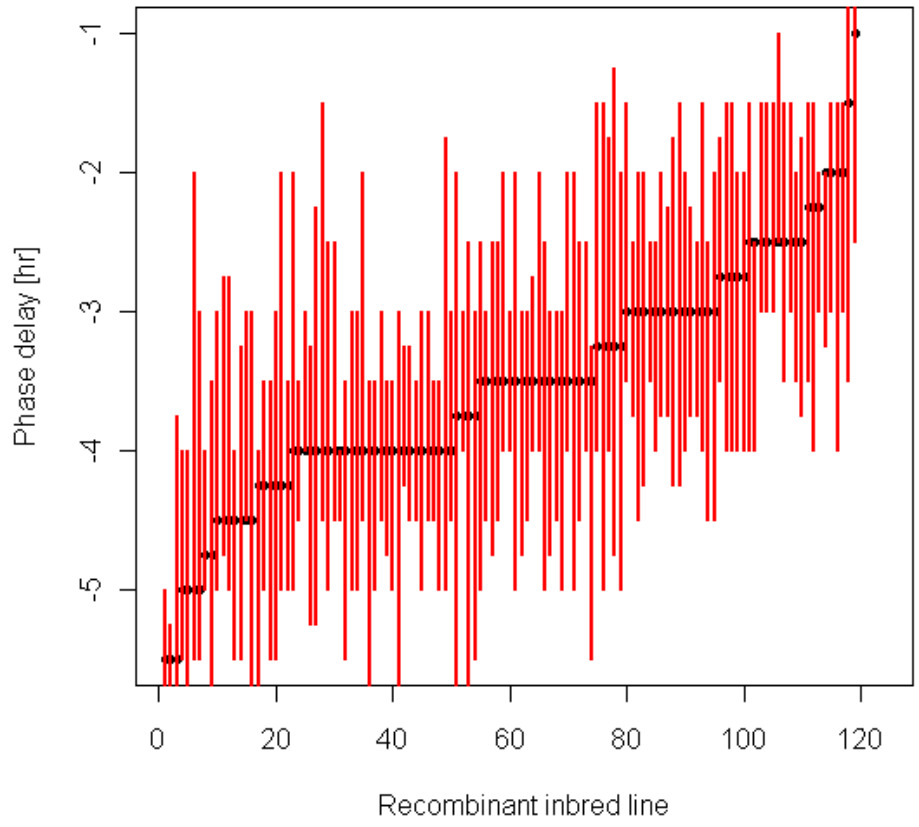

Figure 3.3: Range of light response variation in 123 RI lines

For each line, the median and 25-75 percentiles are plotted from the strong to the weakest delays.

3.3.2 QTL mapping

Composite interval mapping (CIM) was used to identify QTL underlying circadian photosensitivity in the RI lines. One significant QTL was detected with a LOD score of 2.4 and three additional suggestive QTL were indicated by multiple-interval mapping MIM (Table 3.3 and Fig 3.4). Together, these QTL explained 30% of the variation in delay response, with the major QTL (QTL2) explaining 12% of the total phenotypic variation observed for this trait. This QTL is located on the left arm of second chromosome (22C1 - 25A3) and spans a genomic region of about 2,600 kb encompassing 316 genes (Table 3.3). The QTL on chromosome X (cytological bands 10C7 -11B12) explains 7.1 %, while the third chromosome has two QTL both on the same arm (3L) located on cytological positions between 72A1 - 78D4 and 62D4 – 66D12 explaining 4.7% and 6.6% of the variation.

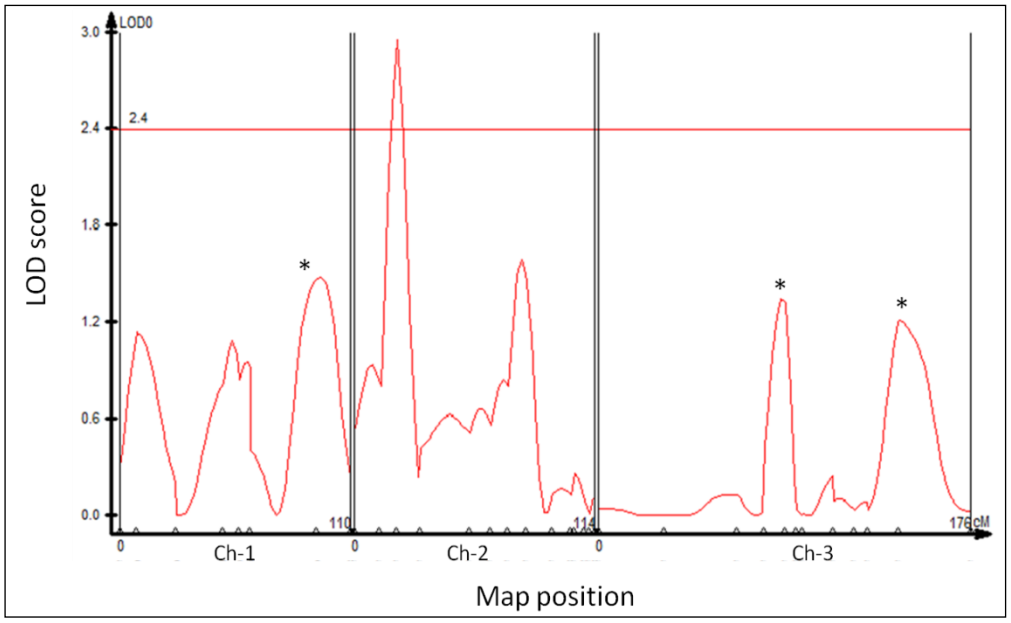

Figure 3.4: Composite interval mapping of QTL for circadian light sensitivity

Log of odds (LOD) scores and significant thresholds plotted against chromosome location for phase shift response. The red horizontal lines represents the threshold level (p=0.05) determined by 1000 permutation tests. Marker position is shown on the X-axis. Asterisks indicate additional QTL that were suggested by multiple interval mapping (MIM).

Table 3.3: QTL for delay phase shift in *Drosophila*

QTL ID	Chr	Marker	Position [cM]	Effect [Hr]	PVE (%)[1]	Interval [Mbp][2]	Candidate loci
1	X	14	98.1	-0.1945	7.1	1.4	119
2[3]	2	3	20.0	-0.2298	12.0	2	316
3	3	4	84.8	0.1803	4.7	6	723
4	3	11	141.8	-0.1786	6.6	7	803

3.3.3 Complementation tests

Out of the 10 deficiencies that were tested, two failed to complement the QTL alleles (Table 3.4) Df3133 (22A3 – 22E1) in QT2L2 and Df6411 (74D3-75B5) in QTL3. Two other deficiencies had a significant LxG interaction (Df6875 and

[1] Proportion of the phenotypic variance explained by the QTL

[2] The size of the QTL was estimated between the flanking marker on each side of the QTL

[3] The major QTL detected by CIM.

Df6082) (Fig 3.5) but the difference between the Bal genotypes was substantial and therefore could not reliably indicate failure of complementation. In addition, quantitative complementation tests were performed using loss-of-function mutations at four positional candidate genes within the QTL (Table 3.2).Two mutants tim^{0} and $cyc^{0,}$ failed to complement the QTL phenotype, while no significant interaction was found for Clk^{jrk} and $Thor^{2}$ (Fig 3.6).

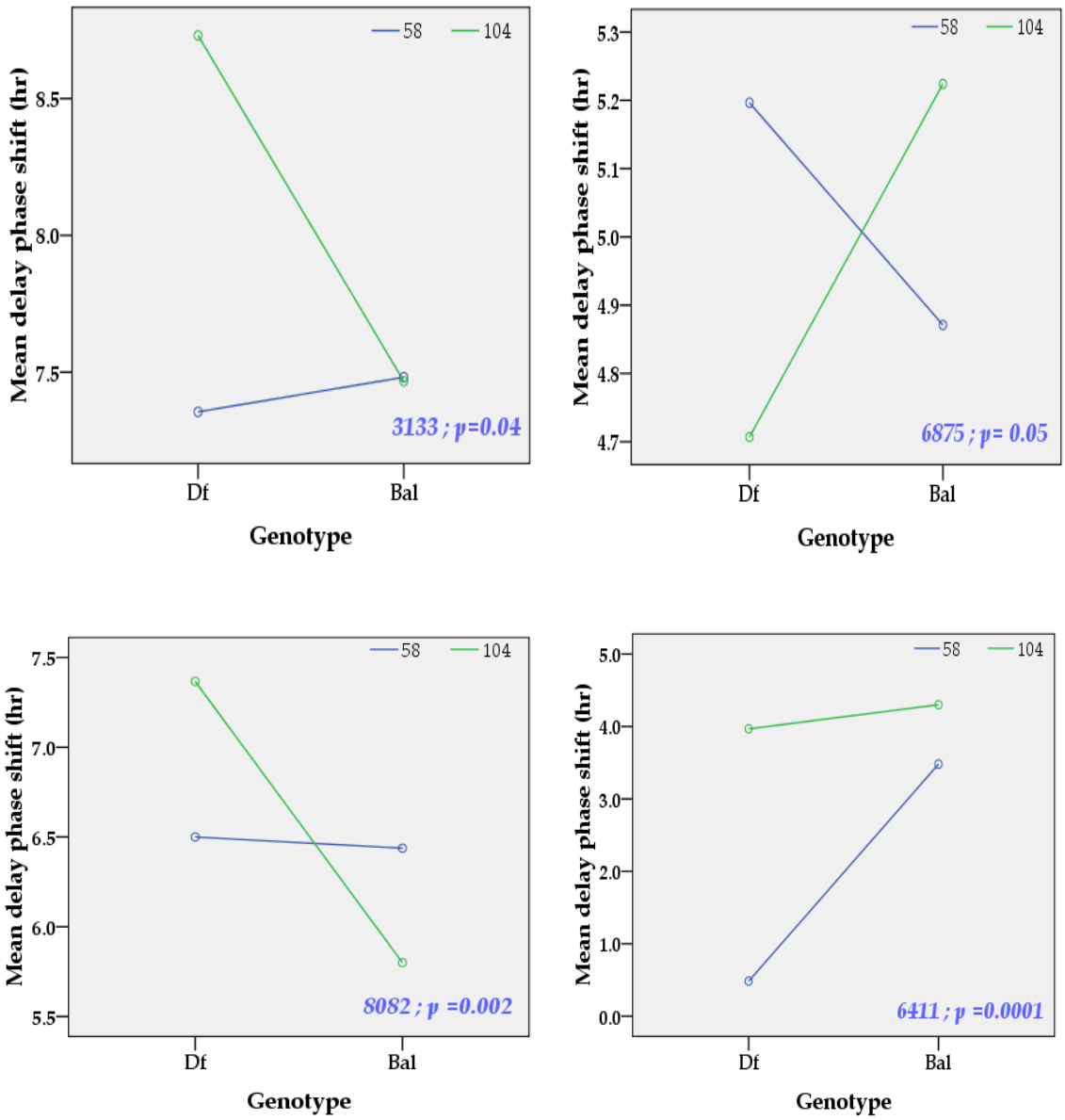

Figure 3.5: Quantitative complementation to deficiency strains

Interaction plots are shown for four deficiencies that showed a significant Genotype x Line interaction effect. Note the *p-value* and deficiency stock number (as shown in Table 3.4) on the bottom right corner of each chart.

Table 3.4: Deficiency complementation tests: two-way ANOVA

Stock ID	Deficiency Name	P value (L xG)	Cytological location	No of genes
	QTL 2			
3133	Df(2L)dp-79b, dpDA cn^1/ In(2LR)bwV1, b1 bwV1	0.04	22A3 - 22E1	111
6648	Df(2L)dppd14/ In(2LR)Gla, wgGla-1	0.40	22E4-F2;22F3-23A1	
90	Df(2L)C144, dpp^{d-ho} ed^1/ In(2LR)Gla, $^{wgGla-1}$ Bc1 $Egfr^{E1}$	0.61	23A1-23A2;23C3-23C5	
6875	Df(2L)BSC28/ SM6a, bw^{k1}	0.05	23C5-D1;23E2	29
	y1 w*; Df(2L)drm-P2, P{lacW}$Pdsw^{k10101}$/ SM6b	0.93	23F3--24A2	
6507	Df(2L)ed^1/ CyO; P{ftz/lacC}^{1}	0.38	24A2;24D4	
	QTL 3			
2993	Df(3L)st-f13, Ki^1 $^{rnroe-1}$ p^p/ TM6B, Tb^1	0.98	72C1-D1;73A3-4	
6411	Df(3L)BSC8/ TM3, Ser^1	0.0001	74D3-75A1;75B2-5	53
8082	w^{1118}; Df(3L)ED4782, P{3'.RS5+3.3'}ED4782/ TM6C, cu^1 Sb^1	0.002	75F2;76A1	18
6646	Df(3L)BSC20, st^1 ca^1/ TM6B, Tb^1	0.63	76A7-B1;76B4-5	
5126	Df(3L)XS533/ TM6B, Sb^1 Tb^1 ca^1	0.5	76B4;77B	

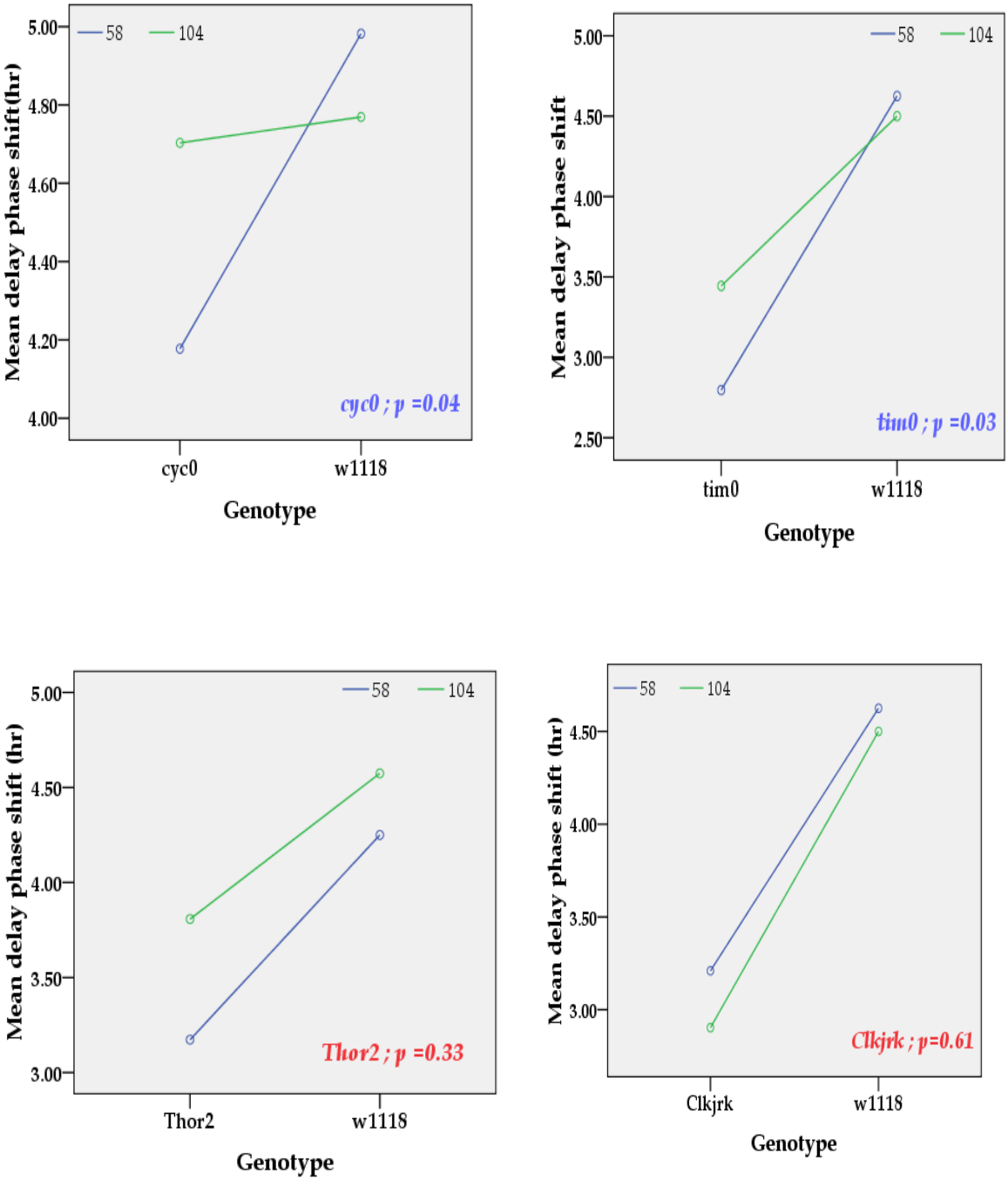

Figure 3.6: Quantitative complementation tests to null mutants: interaction plots

The gene and their *p-value* are indicated at the bottom right corner of each chart.

3.3.4 s/*ls-tim* alleles are segregating in the RI strains

The complementation tests above indicated that variation in *tim* contributes to the major QTL (QTL2). To test whether the variation in *tim* is caused by the previously published *ls-tim* polymorphism (see Introduction), I have genotyped 66 randomly selected RIL. Fig 3.7 shows that both alleles segregate in the RI strains and that *s-tim* flies responded with significantly stronger delays than *ls-tim* flies (median delays of -4.0 vs 3.3, Mann-Whitney *U =267, z=-3.52, p < 0.0001, r= -0.45*). The RI 104 flies with the stronger delay carry *s-tim* while RI 58 (less light sensitive) was *ls-tim,* this result is consistent with the known property of these *tim* natural alleles.

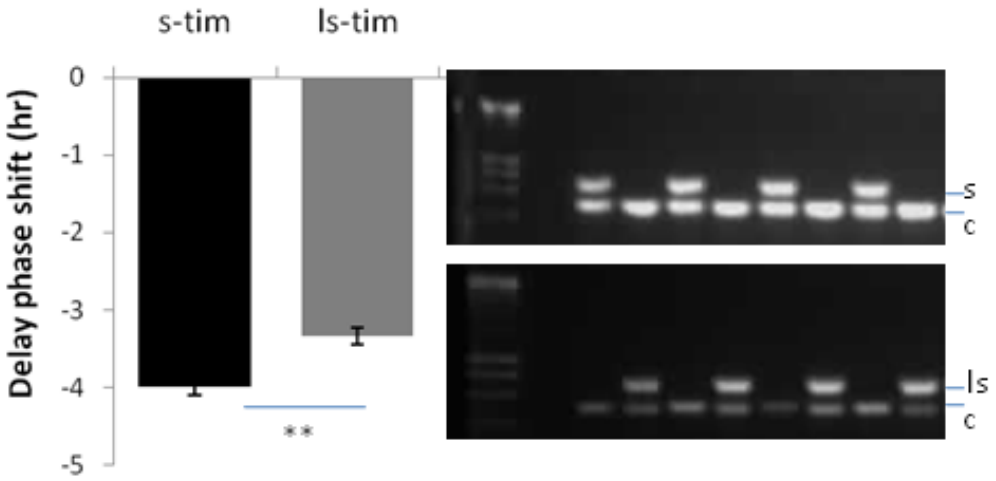

Figure 3.7: *s/ls-tim* polymorphism is present in the RI strains

Gel images show example of genotyping of 8 RI lines using allele specific primers for *s-tim* (top) and *ls-tim* (bottom). A control amplicon (c) is also shown. Strains carrying *s-tim* show significantly stronger phase delays (left panel) than *ls-tim*.

3.3.5 Microarray expression analysis

To further characterise the QTL, microarrays were used to examine gene expression of RIL58 and RIL 104 following a light pulse at ZT15. This experiment revealed extensive differential expression in both lines (Fig 3.8 and appendices 7.2 – 7.3). At the stringent level of $p < 0.001$, 185 genes were differentially expressed in RIL58 and 175 genes in RIL104. The two gene lists shared 49 genes, none of which has been previously implicated in light entrainment of the clock (Table 3.5). It is also possible that some of these genes are non-clock photic regulated as shown in (McDonald and Rosbash. 2001; Wijnen *et al*. 2006). Functional clustering of these overlapping genes shows no significant cluster but the functional terms indicate a wide range of processes (Table 3.5).

Table 3.5: Representation of overlapping genes between RIL 58 and RIL104.

See appendix 7.4 for a complete list.

FlyBase ID	Gene Symbol	Biological process term
FBgn0032839	*CG10659*	metabolic process
FBgn0038067	*CG11598*	lipid metabolic process, lipid metabolic process
FBgn0000451	*ect*	Unknown
FBgn0001942	*eIF-4a*	mitotic spindle elongation, regulation of alternative nuclear mRNA splicing, via spliceosome
FBgn0015218	*eIF-4E*	mitotic spindle elongation , regulation of cell growth, chromatin organization, translation ,
FBgn0041156	*exex*	regulation of transcription, DNA-dependent, nervous system development
FBgn0020439	*fau*	response to stress , response to oxidative stress
FBgn0025373	*Fpps*	isoprenoid biosynthetic process, germ cell migration, farnesyl diphosphate biosynthetic process
FBgn0261278	*grp*	cell cycle checkpoint , cell cycle checkpoint, cell cycle checkpoint
FBgn0040318	*HGTX*	regulation of transcription, DNA-dependent, nervous system development

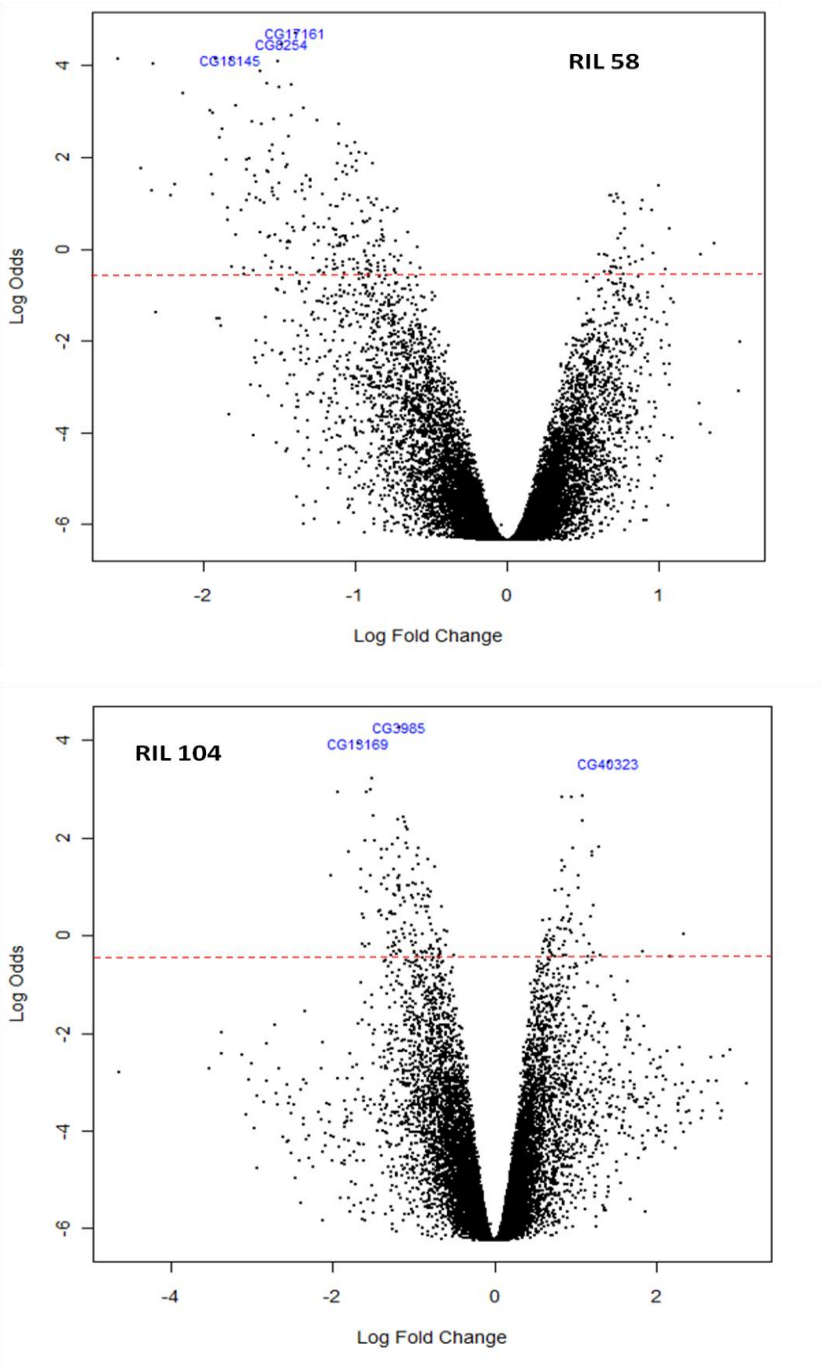

Figure 3.8: Differential expression induced by light in RI strains

Volcano plots of differential expression of RIL58 transcripts (top: 160 down-regulated and 25 up-regulated with light pulse) and RIL104 transcripts (bottom: 118 down-regulated and 56 up-regulated with light pulse). The empirical Bayes log-odds of differential expression is plotted against log [2] fold change. Positive fold change represents up-regulation of transcript in the pulsed samples compared to the controls. The red dotted line signifies p = 0.001.

Subsequent analyses addressed the contribution of natural variation in gene expression to the extensive variation in light response among the RI strains. The two-way ANOVA identified twenty-three genes with significant (treatment X line) interaction term as shown in Table 3.6.

Table 3.6: Significant QTL candidate genes from cDNA microarray data

	Genes	*pValue*	Function
QTL1			
	P24-1	0.04	transporter activity
QTL2			
	CG9879	0.01	RNA polymerase II transcription factor activity,regulation of transcription
	CG3077	0.05	protein binding; phosophoinositide binding
	Lilliputian (lilli)	0.04	transcription factor activity; DNA binding; compound eye photoreceptor development
QTL3			
	CG12713	0.04	Unknown
	CG13071	0.02	Unknown
	eukaryotic release factor 1 (eRF1)	0.05	translation termination factor activity, smoothened signalling pathway
	mTerf3	0.05	mitochondria translation
	CG13064	0.02	Unknown
	PGRP-SB1	0.02	immune response; peptidoglycan binding
	CG32159	0.05	Unknown
	CG32187	0.02	Unknown
QTL4			
	Lcp65Ag1	0.03	structural constituent of chitin-based cuticle
	Cyp4d20	0.02	electron carrier activity
	CG11349	0.04	Unknown
	CG13705	0.02	Unknown
	Cpr65Az	0.03	structural constituent of chitin-based cuticle
	CG7409	0.04	unfolded protein binding
	CG8209	0.02	Zinc ion binding
	CG7197	0.05	small GTPase mediated signal transduction
	CG6765	0.04	protein binding; Zinc ion binding
	mRpL36	0.006	structural constituent of ribosome, translation
	CG33057	0.05	2'- phosphotransferase activity

3.4 Discussion

The extensive and continuous variation in light response of the RI strains suggested that the heritability of this trait is substantial and has a polygenic architecture. To identify genomic regions underlying this variation, QTL approach was adopted. This approach has been successfully used in studying circadian phenotypes in plants (Darrah *et al*. 2006), mammals (Yoshimura *et al*. 2002), but curiously has never been attempted before in *Drosophila*.

The CIM analysis revealed a major QTL at LOD score of 2.4 and 3 additional suggestive QTL were indicated by MIM (Table 3.3). The robustness and precision of QTL location estimated by MIM has been demonstrated in several QTL studies (Kao *et al*. 1999; Latta and Gardner. 2009) and its uniqueness in using multiple marker intervals simultaneously to fit multiple putative QTL directly into the model is well documented. However, the three additional QTLs detected by MIM require further confirmation. Subsequent, quantitative complementation mapping has been used to refine QTL2 and QTL3 of which 211 candidate genes were identified within these regions. Four deficiencies failed to complement the natural alleles, narrowing the QTL to genomic regions to 22A3 -22E1 and 23C5 -23E2 for QTL 2; 74D3 – 75A1 and 75F2 – 76 A1 for QTL3 (Table 3.4).

The molecular and biological functions of these candidate genes (for which annotation was available; many genes within the QTL interval have no

known function) included a few represented functions/pathways: *Wnt (wingless* [*wg*] in fly) receptor signalling pathway, transmembrane transport, phosphatase activity, calcium modulating pathway and synapse organisation. Future experiments are required to investigate the role of these genes and their associated pathways in relation to circadian photosensitivity.

To further examine the QTL regions, several candidates circadian clock (and related) genes that are located within the QTL intervals were selected for mutation complementation tests. These genes included: *timeless*, *cycle*, *Clock*, *PAR-domain protein 1 (Pdp1)*, *retinal degeneration C (rdgC)*, *Rhodopsin 4*, *Casein kinase II beta subunit, Casein kinase I alpha* and recently implicated gene in circadian function *Thor (*Nagoshi *et al.* 2010*).* Interestingly, *Thor* is also one of the light differential-expressed genes, which is down-regulated in response to light as identified in the Affymetrix microarray screen described in chapter 4.

QTL mapping has been recently used to study various behaviours in *Drosophila* including locomotor activity (Jordan *et al*. 2007), sleep (Harbison *et al*. 2009) and aggression (Edwards and Mackay. 2009). Some of these studies were combined with global profiling by microarrays, the results confirmed that complex phenotypes are regulated by large numbers of loci. The contribution of these loci to the phenotype seems to follow an exponential distribution with few major genes showing a large effect, which often are combined with many other small effect loci (reviewed by Mackay. 2010). In the current study, the

light response appears to be controlled by a single QTL, whose peak coincides with *timeless*, a locus already known to be involved in natural variation in light-sensitivity (Tauber *et al*. 2007). The strong s-TIM/CRY binding is thought to enhance CRY degradation by JET thereby resulting in more light-sensitive flies, compared with flies carrying the long TIM isoform (Peschel *et al*. 2009; Sandrelli *et al*. 2007). Here, I have shown that the *s/ls-tim* alleles that underlie the variation and the latitudinal cline in European populations are also segregating in the RI strains (Fig 3.7). An indication that this polymorphism may also be present in North America, whether this variation follows a latitudinal cline in the new world is the subject of current research (Tauber and Kyriaocu, personal communication).

However, the evidence suggests that additional loci are also contributing to the phenotypic variation. First within the QTL2 interval, two non-overlapping deficiencies failed to complement the natural alleles indicating that this large QTL interval can be fragmented to multiple (at least two) QTL. In addition, MIM suggested 3 additional QTLs and the failure of *cyc* (which is located within QTL3 interval) mutant to complement its natural alleles in the RI lines, provided further evidence that these QTLs may indeed contribute to the variation in light sensitivity. Furthermore, the phenotypic difference due to the *s/ls-tim* alleles is less than 1 hr in the delay zone (Fig 3.7) whereas Sandrelli and coworkers (2007) compared transformant flies carrying the two alleles (i.e.

identical genetic background) and found about 3 hr difference in phase delays. In contrast, the range of phase delays exhibited by the RI strains is over 4 hr (Fig. 3.3), suggesting contribution of other loci and/or non-additive (e.g. epistatic) interactions of *tim* with allelic variation in other genes.

The substantial transcriptional variation, which was revealed by the microarray experiments, also suggested that variation in a large number of genes is associated with this phenotype (Fig 3.8). Passador-Gurgel and colleagues (2007) were first to introduce the concept of quantitative trait transcript (QTT, with analogy to QTN, {quantitative trait nucleotide}) associated with phenotypic variation. Here, the profiling of two RI strains showed that overlap between the lists (with a rather similar size of about 180 transcripts) was rather modest (49 genes, 27%), suggesting that response to light may have evolved through different mechanisms in the different RI strains. In addition, the main biological pathways represented by the differentially expressed genes in each RI strain were different. In RIL58, pathways such as G- protein couple receptor, transducer and sensory perception were highly enriched, while in RIL104 pathways such as ion channel activity, ligand-gated channel activity were over-represented. The variation between the RI strains was directly addressed by performing a two-way ANOVA, which identified genes showing significant Line x Treatment effect. Here the analysis was done with transcripts within the QTLs and 23 candidate QTT was identified. It is likely that more are

present across the whole genome but restricting the analysis to QTL regions reduced errors due to multiple testing.

QTT may reflect variation in the *cis*-regulatory region but it may also show variation in the transcription factor that drives their transcription. Hence, QTT number may overestimate the causative quantitative trait nucleotides (QTN). On the other hand, the transcriptional variation only captures a fraction of the genetic variation, as many variations may affect expression post-transcriptionally or post-translationally (*timeless* is a good example, the *ls/s tim* polymorphism is not manifested at the transcriptional level). Overall, it is reasonable to assume that more loci, perhaps with smaller effect are contributing to the variation in the Winter RI strains. Interestingly, most QTT (whose function is known) are involved in transcription at various levels and may suggest a regulatory role for these genes.

Lilliputian (lilli) is of particular interest because of its role in the Ras/MAPK pathways and eye photoreceptor development (Dickson *et al*. 1996; Tang *et al*. 2001; Wittwer *et al*. 2001). *Lilli* encodes a nuclear protein related to mammalian Fragile-X-Mental Retardation 2 (FMR2)/Acute Lymphoblastic Leukemia (AF4) family (Tang *et al*. 2001; Wittwer *et al*. 2001). The mammalian *fmr1/fmr2* has been shown to play a significant role in circadian function of the peripheral clock possibly through its defect in neuronal communication (Zhang *et al*. 2008). Similarly, null mutations of the *dfmr1* are reported to alter circadian

output with no detectable effect on the function of the central pacemaker (Inoue *et al*. 2002). Interestingly, *Fmr1* was differentially expressed in response to light stimulation (chapter 4) and when down-regulated in clock cells, there was significant reduction in the flies' response to light (Fig 4.3 chapter 4). It is therefore possible that *lilli* exerts a similar effect on the circadian clock.

In addition, *lilli* protein is a novel maternal transcriptional regulator widely expressed during development (Wittwer *et al*. 2001). It has been shown to act as a dominant suppressor of activated MAPK pathway phenotypes (Dickson *et al*. 1996). Interestingly, MAPK pathway has been reported to be activated by light, suggesting that its activation is vital for circadian light entrainment (Obrietan *et al*. 1998). MAPK signalling pathway has also been shown to mediate the function of PDF in *Drosophila* (Williams *et al*. 2001). It is possible that natural variation in *lilli* expression between these lines affects their regulation of MAPK pathway, thereby responding differently to light stimulation.

Overall, these observations suggest that strain- specific differences in transcript expression can reflect a number of different mechanisms which may underlie the extensive phenotypic variation in this population. However, it is still not clear to what extent variation in transcript levels correlates with differences in gene expression at the level of the trait and how small differences in expression that are confined to a few cells or tissues, affects the phenotype.

Chapter 4: Global profiling of gene expression associated with circadian light response in *Drosophila*

4.1 Introduction

Daily physiological and behavioural rhythms are regulated by circadian clock, which is driven by transcriptional/translational circuits (see chapter 1). Over the years, several methods such as molecular and genetic screening have been successfully used to identify the circadian clock genes (Allada *et al*. 1998; Konopka and Benzer. 1971; Williams and Sehgal. 2001). Global based approaches such as differential display identified *vri* (Blau and Young. 1999), subtractive cDNA library which uncovered about 20 *Drosophila* rhythmically expressed genes and circadian controlled gene 1 (*CCG1*) (Rouyer *et al*. 1997; Van Gelder and Krasnow. 1996). However, these methods were not robust enough, as information about most of the cycling genes identified is still not known (for review see Matsumoto. 2006).

An alternative genome-wide strategy has recently been developed, which uses high density oligonucleotide or cDNA microarray to study gene expression. Microarrays allow the simultaneous study of expression of thousands of genes. It is based on physical hybridisation of RNA or DNA targets with complementary oligonucleotides or cDNA probes (Chee *et al*. 1996). Although microarray approach has its limitations, the approach has been used successfully in plants, mammals and *Drosophila* chronobiology studies.

For instance, Harmer and colleagues (2000) identified rhythmic expression of about 6% total *Arabidopsis thaliana*'s transcripts under free-run conditions. A large cluster of these genes was implicated in clock controlled anticipation of light on and off, and transcription factors regulating cycling genes (Harmer *et al*. 2000).

Furthermore, several researchers have used microarrays to identify clock-controlled transcripts in *Drosophila'* heads. McDonald and Rosbash (2001) identified 134 cycling genes under constant dark conditions in *CS* and Clk^{jrk}. These genes are involved in diverse biological processes and are thought to be transcriptionally coregulated(McDonald and Rosbash. 2001). However, their oscillation was abolished in Clk^{jrk} mutant background, suggesting it is CLK-dependent (McDonald and Rosbash. 2001). In another study, Claridge-Chang and colleagues (2001) using *yw,cn bw,*per^0,tim^0 and Clk^{jrk} genetic background uncovered a set of 158 genes showing a robust circadian rhythm in the fly head under LD and DD conditions. Furthermore, a study by Ueda and co-workers (2002) identified 712 cycling transcripts under LD conditions in w^{1118} (laboratory strain) flies of which 115 maintained oscillation in DD. They also show that the cycling of most of these genes was abolished in Clk^{jrk} mutant background (Ueda *et al*. 2002). Not many genes overlap in these studies, which may be as result of the differences in fly strains, and different statistical analysis used (for review see Matsumoto. 2006). However, few genes have been identified as common

among the studies. For instance, 36 cycling genes were overlap between McDonald and Claridge-Chang studies and of these five are core clock genes (Kula-Eversole *et al*. 2010).

Recently, high resolution microarray studies of cycling genes was accomplished (Kula-Eversole *et al*. 2010; Nagoshi *et al*. 2010) by profiling gene expression in specific clock neurons. In these studies, researchers profiled the expression of circadian transcripts in adult and larva clock neurons confirming the oscillation of the known clock genes and the identification of novel ones. These studies shed more light on variation in clock gene expression pattern among the clock neurons and suggest that this variation to be the basis of their different roles.

There is increasing evidence that light-induced phase shifts are accompanied by changes in gene expression (Porterfield and Mintz. 2009; Rusak *et al*. 1990). Light pulse during the subjective night has been shown to alter the expression of an array of genes in various organisms (Porterfield and Mintz. 2009; Xu and Johnson. 2001). This change in expression is thought to be driven by light and in some cases by the circadian clock, resulting in phase shifts of the pacemaker rhythm (Wijnen *et al*. 2006). In mammals for instance, light is transmitted via the retinal ganglion cells to the rhythmic cells of the SCN (for review see Antle and Silver. 2005). This phototransduction mediates the release of glutamate, which binds N-methyl-D-aspartate NMDA receptors

increasing the influx of calcium in the SCN (Ding *et al*. 1997; Ebling. 1996). Subsequent activation of MAPK results in the phosphorylation of CREB, which binds the CRE elements within *per1* and *per2* promoters to activate their transcription (Akashi and Nishida. 2000; Albrecht *et al*. 1997; Field *et al*. 2000). Furthermore, light pulse during the subjective night induces the expression of a tobacco gene called *ZGT* (literally: clock and light controlled) and as the name implies *ZGT* is a clock regulated gene (Sadakane and Nakashima. 1995; Xu and Johnson. 2001).

However, little is known about the molecular changes associated with light-induced phase shift. Few studies in mammals and plants have probed how light stimulation during subjective night influences gene expression in various organs using microarray. Recently, Ben-Shlomo and Kyriacou (2010) showed that a light-pulse during the night affects the expression of genes critical for cancer and tumour progression in mouse brain. In another study, light stimulation was shown to alter global gene expressions in tomato seeds, which either inhibits or promotes seed germination (Auge *et al*. 2009). To further our understanding of the effect of light stimulation on the circadian clock, I have used Affymetirx microarrays to profile light-induced transcriptional changes in *Drosophila* heads.

4.2 Materials and methods

4.2.1 *Drosophila* Stocks

Canton S (CS), a wild-type laboratory strain was used in this study. The fly stocks were maintained on standard sugar medium as described in Chapter 2.

4.2.2 Sample collection and preparation

Male *CS* flies (1- 3 days old) were entrained and collected as described in section 2.4.1 of chapter 2. The flies were divided into two groups, one treated by 30 min light pulse at ZT 15 (experimental group) and the other without light-pulse (control). Flies were collected at ZT 16.5, an hour after light stimulation under dark conditions. Four biological replicates were snap frozen in liquid nitrogen for each condition and stored in -80^{0}c. About 1000 heads were collected independently from each frozen sample and ground with a pestle in a mortar containing liquid nitrogen. The samples were homogenised in 1 ml Tri-reagent (Invitrogen) and total RNA extracted according to the manufacturer's protocol. The total RNA samples were purified using the RNeasy® MinElute™ Cleanup kit (Qiagen). RNA concentration was determined using NanoDrop 2000 (Thermo Scientific) and sample integrity was assessed using the Agilent 2100 Bioanalyzer (Agilent Technologies, Santa Clara, CA, USA).

4.2.3 Probe preparation, hybridisation and processing

Affymetrix GeneChip one-cycle target labelling kit was used to generate cRNA from 5 μg total RNA according to the manufacturer's protocol (Affymetrix, Santa Clara, CA). The resulting biotin-labelled cRNA was fragmented and hybridised to the GeneChip *Drosophila* Genome Array 2 (Affymetrix Inc). The post-hybridisation washing, staining and detection using streptavidin-coupled fluorescent dye were done in the GeneChip Fluidics Station 400 operated according to Affymetrix's protocol. The hybridised arrays were scanned using Affymetrix GeneChip® 3000 scanner, image generation and features extraction were performed using Affymetrix GeneChip® Operating Software and saved as cell intensity (CEL) files. The experiment was performed at the University of Leicester Genome core facility, Leicester, UK.

4.2.4 Microarray data processing

The scanned image files (*.CEL) were processed using the GeneChip Robust Multi-array Average (GC-RMA) method (Wu et al. 2004) to adjust background, normalise datasets and convert multiple probe values into a single expression value for each probe-set (gene). This was done using the R package (http://www.r-project.org/) and the Graphical User Interface of the *limma* package (affylmGUI) (http://bioinf.wehi.edu.au/affylmGUI/) (Wettenhall and Simpson. 2010).

4.2.5 Microarray data analysis

Several quality control procedures were followed to ensure that the data was of high quality. Such steps included visual inspection of the chip pseudoimages generated by affylmGUI and inspection of the histograms of the raw signal intensity. The normalised data was analysed using RankProd package (Breitling *et al*. 2004) on an open-resource BioConductor project (http://bioconductor.org/) using a two-class model. RankProd is a non-parametric statistic that ranks all probe sets within each replicate by their expression level and then calculates each probe RankProd (RP) value, which depends on the number of times a particular probe set appears at the top (up-regulated) or the bottom (down-regulated) of the ranked list (Hong *et al*. 2006). This (RP) value increases if the probe set is consistently present at the top or at the bottom of the list. The program then re-orders all the probe sets based on their RP-value, taking into account all possible pair-wise comparisons and redressing for multiple hypothesis testing through permutation of the replicate labels. A percent false positive (PFP) value is calculated as an estimate of the false discovery rate for each probe set (Breitling *et al*. 2004; Storey and Tibshirani. 2003). The cut-off for significance genes was set at a false discovery rate (FDR) threshold of 10% implying that the genes selected had 10 % chance of representing a false positive signal of statistically significant differential expression.

4.2.6 Validation of microarray data by qPCR

Total RNA was extracted from 250 fly heads collected 1hr after a 30 minute light pulse at ZT 15 (experimental) and from the non- treated (control) as described in section 4.2.2. Five biological replicates were used for each condition. The RNA samples were incubated with 1µl rDNase I (2 Units/µL) and 5 µl 10X DNase I Buffer (Ambion® DNA-*free*™) in 50 µl total reaction volume at 37^0C for 10 min to digest any residual DNA in the cDNA samples. This enzymatic reaction was inactivated by 5 µl DNase Inactivation reagent (Ambion® DNA-*free*™) according to the manufacturer's instruction. cDNA was synthesised from 1 µg of the purified total RNA for each sample using 300 ng random primers (Promega) and the Stratagene AffinityScript™ Multiple Temperature Reverse kit in 20 µl reaction volume according to Stratagene's protocol. A master mix of the kit components was spiked with an exogenous *aequorin* mRNA (0.5 µl/ 20 rxn) from Jellyfish before adding to each sample.

For setting up the qPCR, cDNA samples were diluted to a total volume of 200 µl and 5 µl was used in subsequent reactions. qPCR primers were designed for the 14 selected genes from the differentially expressed gene list (Table 4.1) against their complete cDNA sequence using Primer3Plus a web-based tool (Untergasser *et al*. 2007). The following parameters were used: Tm range of 58 – 62^0C, primer length between 18 – 23 nucleotides, with optimal length set at 20 nucleotides and amplicon between 100 – 150 nucleotides.

Table 4.1: Primer information and genes analysed by qPCR

Gene name	Primer sequence	Amplicon (bp)
sugarbabe (sug)	TCATCACCTGTACGGCAAAC	141
	AGCAAAGCCATCCAGAACAC	
CG13796	TCAGATCGAGATTCGGGTTC	122
	CATTCACCTGCAAACAGTGC	
period (per)	ACTGGAACAGGCAATGGAAC	134
	TTCTCCATCTCGTCGTTGTG	
Kruppel homolog 1 (Kr-h1)	CGTCGAACTTTTCGGTTCTC	120
	GCTGCTGGGCATTAACTTTC	
Thor	CAGCAACTGCCAAATCCAAC	132
	GGGTCAATATGACCGAGAGAAC	
sine oculis (so)	ATGCCATTATAGCCCCACAC	100
	ATCCTTCCAGGAGATTGTGC	
Yolk protein 1 (Yp1)	ACATGCAGCGCTACAATCTG	148
	TGGGTCTTGGCGTTCTTAAC	
Hormone receptor-like in 38 (Hr38)	TTTAACGAGCACGTGAGCTG	131
	TTCGGTTGTGGTAGTTGCAG	
Posterior sex combs (Psc)	AAAGCTGGTCAATGGTGGAC	101
	TCGGATTCTTGGACACCTTC	
Fmr1	GGCGGAGAATGTCAAAAAGG	134
	TTACTCCGTCGAACGATGTG	
CG2051	CAATGATGCCCTGACCTTTC	137
	AATCGACGCCCAAGTAGATG	
CG3099	ACTGGACGCATTCTTTACGC	107
	ATTGGAGCGACTGATGGAAC	
Sirt6	TTCCTTCGATGAAGCCAGAC	118
	TCCGGATTTCAAGTGGAGAC	
hemipterous (hep)	CCATGTGCTTTGACAAGCTG	148
	ATGTTCGAGGGCTTCACATC	

The specificity of these primers was verified using Basic Local Alignment Search Tool (BLAST) software on NCBI web page (http://blast.ncbi.nlm.nih.gov). The optimised annealing temperature for each of the primers was determined prior to their usage in the qPCR. A sample volume of 20 µl consisting of 2 µl each of the appropriate forward and reverse

primers at stock concentration from a 5μM, 5 μl templates (diluted cDNA), 10 μl of 2 x Brilliant® II SYBR® Green QPCR Master Mix (Stratagene) and 1 μl of nuclease-free water was used. The amplification and detection of the fluorescence were measured using LightCycler ® 480 Real-Time PCR System (Roche Applied Science) according to Stratagene recommended fast two-cycling protocol. In brief, the program consisted of: 1 cycle of 95^0C for 15 min, 36 cycles of 95^0C for10 s and 62^0C for 30 s, followed by a dissociation curve. A standard curve was plotted for each of the genes using serial dilutions of cDNA and the amplification efficiency of each primer set was determined using the equation $[(10^{(-1/\text{slope})}-1)\cdot 100]$.

For each gene, five biological replicates were analysed for each condition. The cycle point (C_P) was calculated by LightCycler software version 1.2 (Roche Diagnostics, GmbH, Germany) using the second derivative maximum method. The difference in the C_P values of the control and the experimental (light pulsed) samples were used to calculate the relative expression of the gene. The relative expression values for each gene in both conditions were normalised to that of *aequorin* and statistics analysis were performed on the normalised data (control and treated) using independent *t-test.*

4.2.7 Functional analysis and gene functional classification

The bioinformatics tool **D**atabase for **A**nnotation, **V**isualisation and **I**ntegrated **D**iscovery (DAVID) web version 6.7 beta (Huang *et al*. 2009) was used to determine significant enrichment of known functional annotations and gene functional classifications in the differentially expressed gene list. The *p* values were calculated from a one-sided Fisher's exact test. At present no "gold-standard" method is available for p-value adjustment owing to the lack of independence between genes and gene ontology (GO) groups; hence the FDR test was performed in addition to the p-value tests. For the functional annotation clustering tool, the highest classification stringency setting was applied.

4.2.8 Comparison of the differentially expressed genes list with other screens

The list of differentially expressed genes from this chapter was compared with those generated from the cDNA microarray described in chapter 3. The putative candidate genes linked to circadian photosensitivity from the QTL analysis (chapter 3) were also compared with the microarray data in this chapter. Although, different fly strains were used for these experiments, the experimental conditions and treatment were the same.

4.2.9 Analysis of known circadian clock regulatory elements

In addition to each gene genomic sequence, 2 kb nucleotides immediately upstream of their transcription start site were manually searched for the presence of known circadian clock regulatory elements. These elements include: E box (CACGTG) (Hao *et al*. 1997) , CRE (TGACGTCA) (Kyriacou and Rosato. 2000) and TER box (CACGTTG) (McDonald *et al*. 2001). Note that *vri/pdp1* binding sites were not searched and no statistical test for enrichment was performed in the search.

4.2.10 Characterisation of circadian phenotypes (Light pulse, DD and LL)

Light entrainment and free-running period were examined as described in section 2.7 of chapter 2. The fly strains used were obtained from VDRC or Bloomington stock centre. UAS-IR of these genes were driven by *tim*Gal4-*dicer2* for a light pulse experiment and period analysis in both DD and LL conditions. When available, strains with EP or P-element insertions were also used.

4.2.11 Statistical analyses

Statistical analyses were performed on SPSS version 16. ANOVA with a post-hoc test (Tukey) was used to analyse the difference in light response and period among the UAS-RNAi and their controls at $p < 0.05$. In other analyses such as qPCR data, an independent *t test* was used.

4.3 Results

4.3.1 Differentially expressed genes in response to light stimulation

Of the probes spotted on the Affymetrix Drosophila Genome 2.0 Arrays, 209 were differentially expressed in response to light stimulation at a FDR threshold of 10% see Fig 4.1. The list consisted of 87 up-regulated and 122 down-regulated genes in response to light pulse (see appendix 7.5 for a complete list).

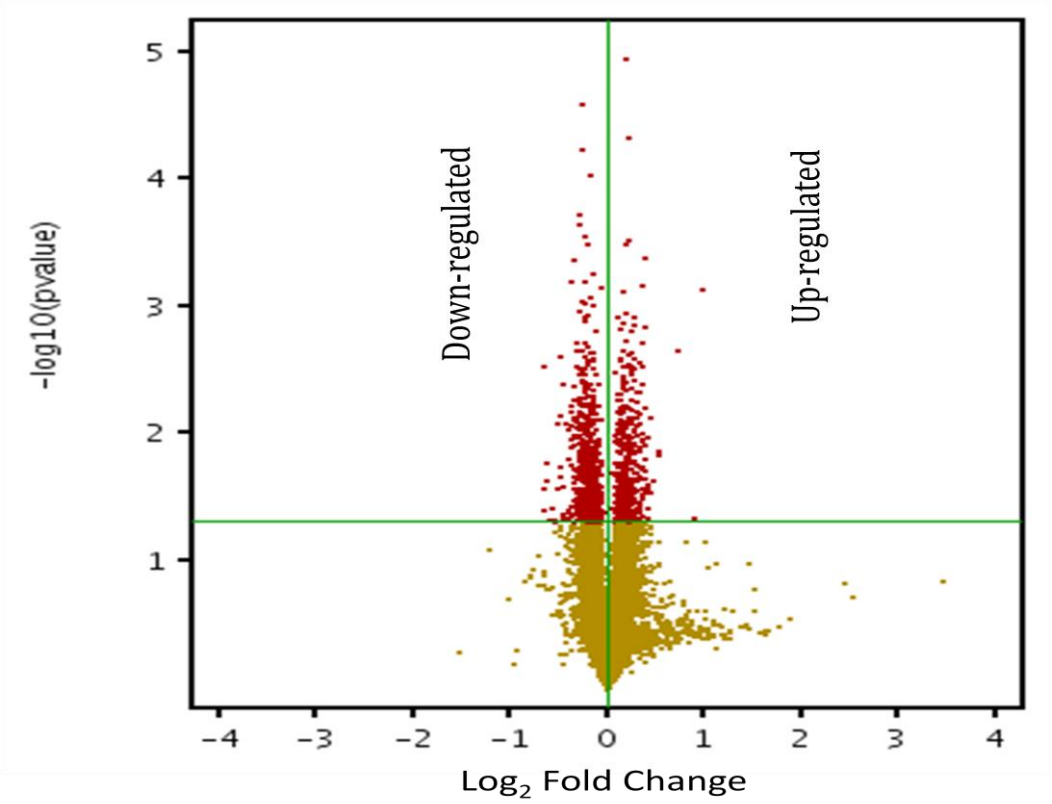

Figure 4.1: A volcano plot showing light-induced differential expression

The green horizontal line indicates threshold at p = 0.05 and the positive fold-change refers to up-regulated transcripts in light treated flies (compared to the control).

The results were validated by qPCR analysis using five biological replicates of RNA samples for each condition. The samples were processed

using the same protocol as in the microarray samples preparation. The qPCR confirmed that the transcript levels of eight out of the fourteen genes showed similar differential expression to that identified in the microarrays (Fig 4.2.).

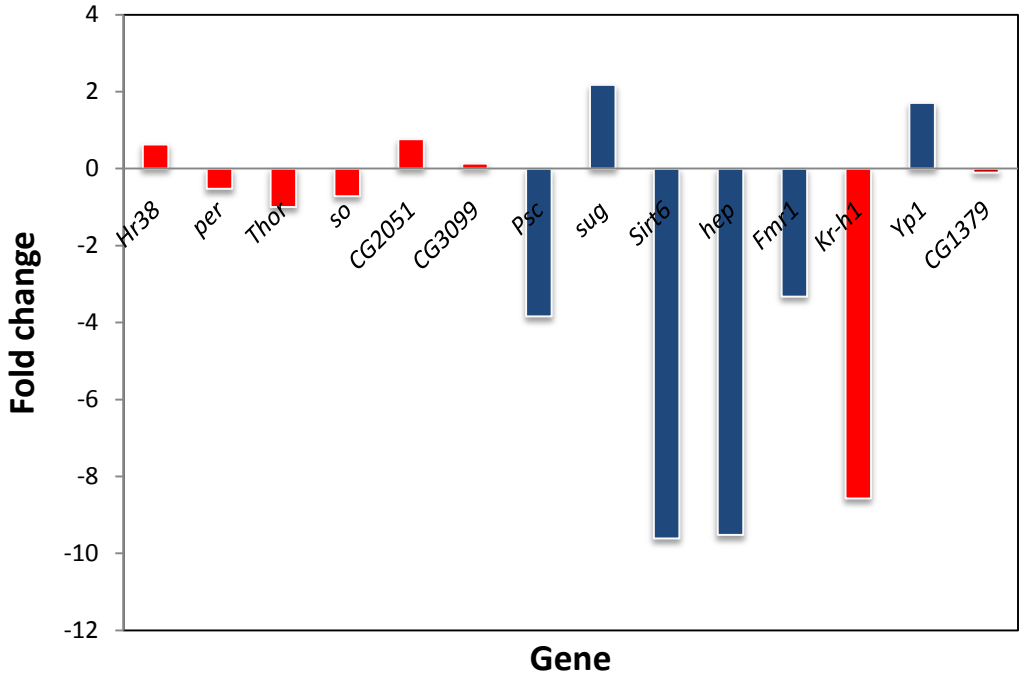

Figure 4.2: qPCR validation of the microarray result

The blue bars indicate no significant differential expression or expression in opposite direction to the trend shown by the microarrays. The red bars represent genes in the same direction as well as a significant difference in response to light pulse at $p < 0.05$ (i.e validated).

4.3.2 Functional annotation of the differentially expressed genes

The identified differentially expressed genes were interrogated by DAVID bioinformatics tools for functional analysis. The aim of these analyses was to identify the most relevant biological processes or molecular functions over-represented in the gene lists. The analysis of down-regulated genes with the DAVID functional annotation tool identified 31 terms or pathways as

significantly enriched at $p < 0.05$ (see appendix 7.6), with processes involved in ion transport showing the highest enrichment. Neurotransmitter-gated ion channel processes was identified as the next over-represented annotation term (see appendix 7.6).

One of the most statistically significant functional categories was alternative splicing, which was represented by 23 annotated genes (see appendix 7.7). This category was of a particular interest because it included genes associated with the circadian clock. From this category, six genes were selected for further studies. An additional eight genes implicated in biological processes such as light response, neuronal communication and sodium/calcium ionic balance were added see Table 4.2 for a complete list. A few of these genes such as *sif, Thor* were also identified in chapter 3 as potential circadian photosensitive candidate genes.

Table 4.2: Genes selected from the functional analyses

Note the red arrows and the green arrows indicate down-regulation and up-regulation respectively.

Gene name	chrom	direction	biological function
DopR	3R	⇩	activation of adenylate cyclase activity
CG11155	4	⇩	ion transport
Sug	2R	⇩	positive and negative regulation of transcription
Sif	3L	⇩	regulation of synapse structure and activity, synaptic transmission
Thor	2L	⇩	negative regulation of translational initiation, antibacterial humoral response
Nf1	3R	⇩	locomotor rhythm, cAMP-mediated signalling, regulation of Ras protein signal transduction
Pho	4	⇩	chromatin silencing, negative regulation of gene expression
CalX	3R	⇩	Phototransduction
nrv1	2L	⇩	potassium ion transport, sodium ion transport
modifier of mdg4	3R	⇩	regulation of apoptosis, regulation of chromatin assembly or disassembly
Hr38	2L	⇧	phagocytosis, engulfment
Fmr1	3R	⇧	circadian rhythm, brain development, neurotransmitter secretion, synaptic transmission
CG7589	3L	⇧	phagocytosis, engulfment
CG11597	3L	⇧	protein amino acid dephosophorylation

The up-regulated genes were also analysed in a similar way, using the functional annotation clustering tool on DAVID at high stringency conditions. From this analysis, four functional clusters met the statistical criteria (p <0.05), of which two clusters were related to immune and defence response. The genes in the other two clusters were mostly involved in gene regulation and

chromatin remodelling as shown in (see appendix 7.8). The specific roles of these chromatin-associated genes in the circadian clock were investigated in more detail in chapter 5. In order to test the functional role of the selected genes (Table 4.2) in the circadian rhythms, the behaviour of flies carrying null mutations, or dsRNAi knockdown transgenes was tested. The role of these genes in light entrainment was tested by light-pulse experiments, in addition to their behaviour in free-run conditions such as continuous darkness (DD) or light (LL).

4.3.3 Light pulse experiment

The expression of the selected genes was down-regulated in clock specific neurons using the binary GAL4/UAS system (Brand and Perrimon. 1993). Since the primary targets were in the clock neurons, *timGal4-dicer 2* driver was used as described in section 2.8 of chapter 2. Using ANOVA with Tukey post-hoc test, each genotype response to light was analysed (Fig 4.3). There was no significant difference between the two controls (w1118; UAS-IR and w1118; *timG4>dcr2*).

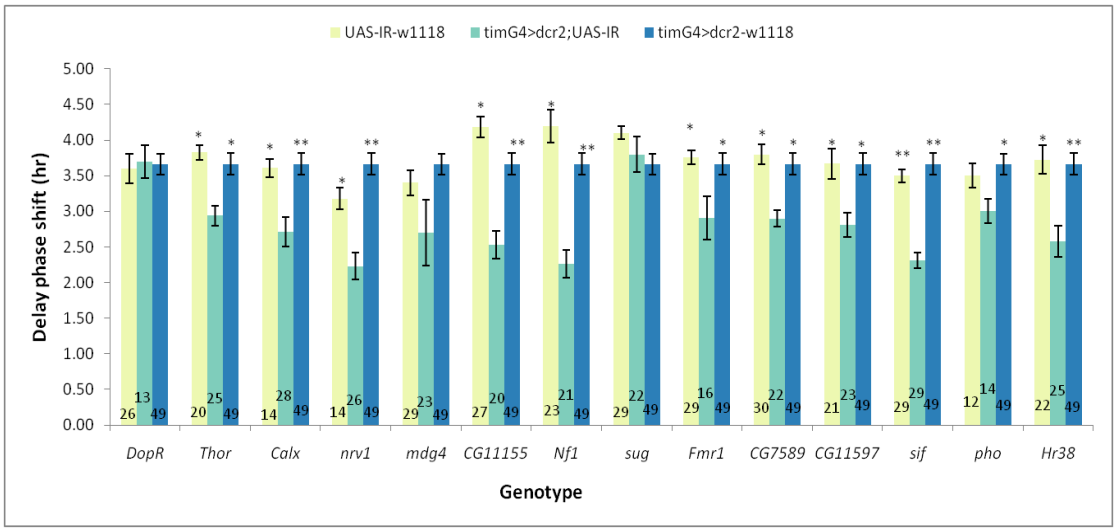

Figure 4.3: Light response of flies carrying dsRNAi transgene and their controls

The plotted error bars signify the standard error mean for each genotype. The double asterisk ** is when $p < 0.0001$, and * for $p < 0.05$ from ANOVA with post hoc analysis using Tukey test. See appendix 7.9 for more information.

In a separate line of experiments, the light response of flies with mis-expression or knockdown *Psc* transcript was compared using independent *t test* (Fig 4.4). Similar analysis was performed comparing the light response of *CG2051* over- expressed and down-regulated see Fig 4.4.

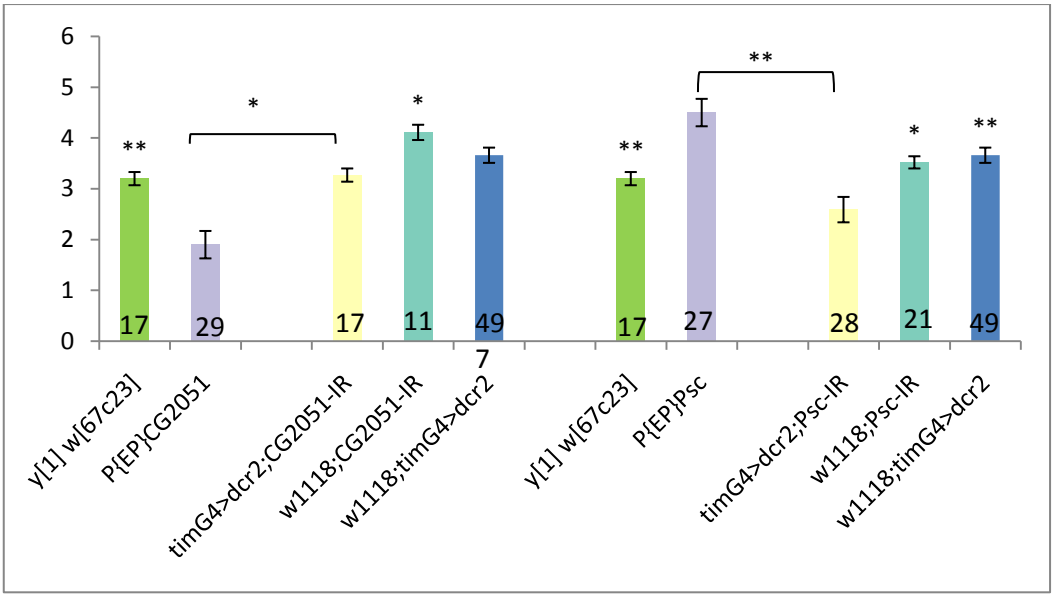

Figure 4.4: Light response of EP and UAS-IR flies: CG2051 and Psc

Note that these genes were over-expression or knockdown in clock neurons and flies light response tested. The error bars were plotted from SEM and * stands statistically significant at $p < 0.05$ between over-expressed and knockdown flies.

4.3.4 Mis-expression of the selected genes: effect on the free-running period

Genes whose mis-expression affected light response (Table 4.3) were also analysed for their free-run behaviour. The results of ANOVA with post-hoc test are presented in Fig 4.5.

Table 4.3: Candidate genes involved in light response

Gene name	Response to light pulse	Biological process
Thor	down	negative regulation of translational initiation
CalX	down	Phototransduction
nrv1	down	ion transport
CG11155	down	ion transport
Nf1	down	Ras protein signal transduction, cAMP-mediated signalling
Fmr1	up	neurotransmitter secretion, circadian rhythm
CG7589	up	ion transport; signal transduction
CG11597	up	protein amino acid dephosphorylation
Sif	down	intracellular signalling cascade, regulation of Rho protein signal transduction
Hr38	up	intracellular signalling cascade

As shown in Fig 4.5, down-regulation of *CG11155*, *sif* and *CG7589* significantly altered the free-running period of the flies. The period of these flies was significantly longer than that of their controls. The other six genes characterised show no significant difference between their periods and the controls at $p< 0.05$. See appendix 7.10 for more information.

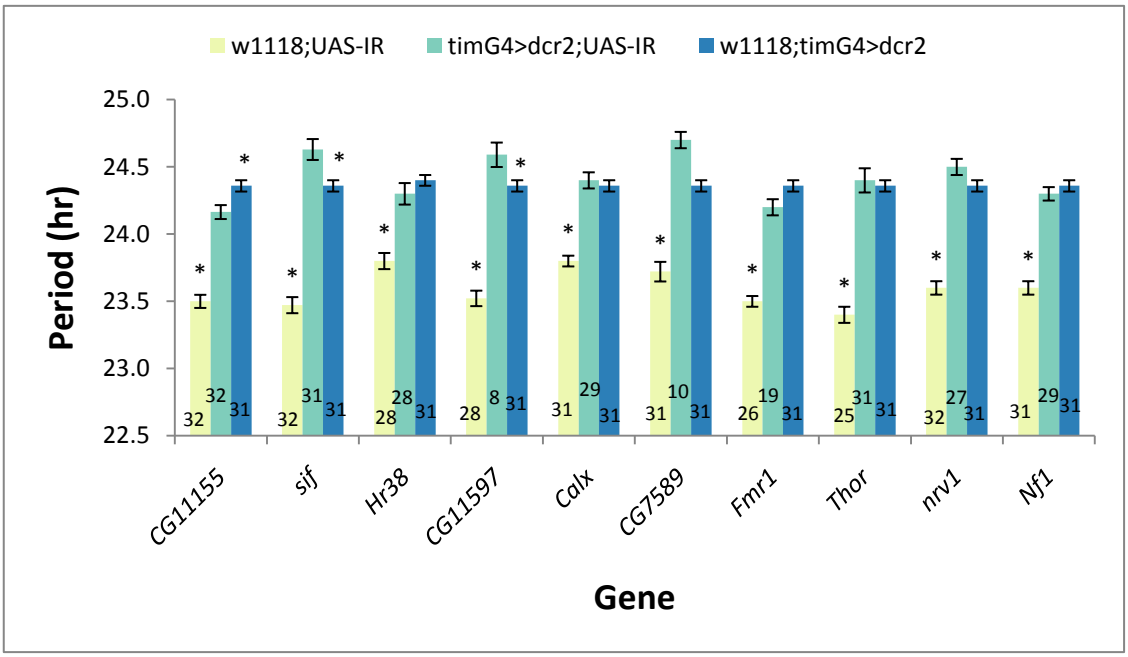

Figure 4.5: Free-run period of dsRNAi transgenic flies in DD

For more information see Table 4.6 of the appendix. Note that all the genotypes were tested simultaneously, hence the same period for the *tim*G4>dcr2; w1118 control was used for the analysis.

4.3.5 Rhythmicity in continuous light

The locomotor activity of flies with reduced expression of each of these ten genes and their respective controls was examined in continuous light (LL). Strikingly, rhythmicity of flies with knockdown of *Thor*, *nrv1*, *Nf1*, *CG11155* and *Fmr1* was substantial, ranging from 30% to 80% as shown in Fig 4.6. A further observation also confirmed that *Nf1*, *Thor* and *nrv1* on average had significantly longer period of 25.4, 25.5 and 25.1 respectively.

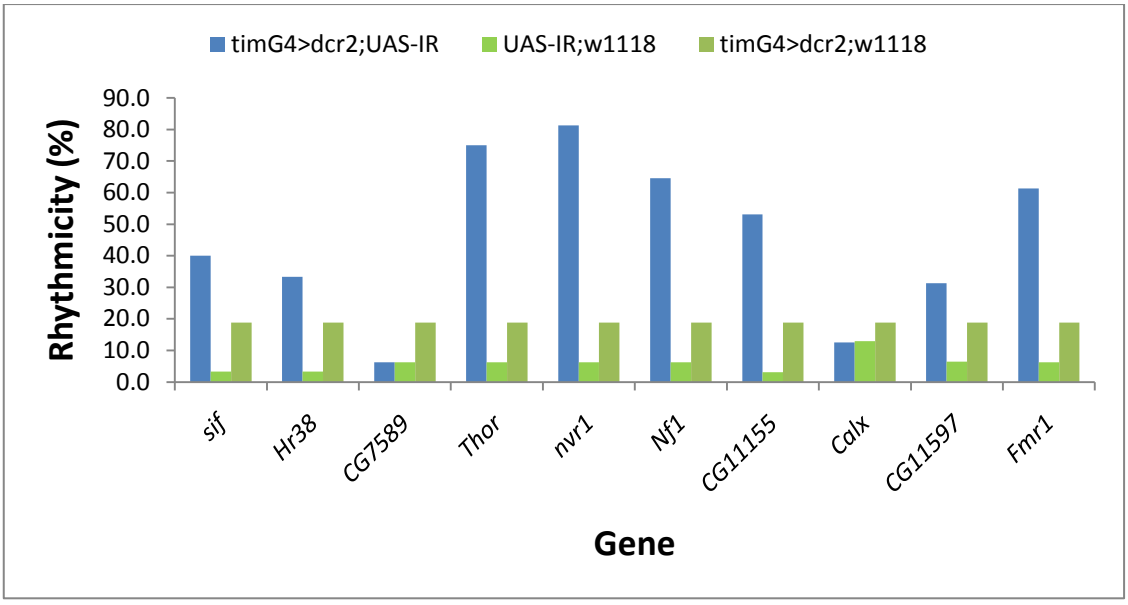

Figure 4.6: Percentage of rhythmic flies in LL

Note that each of these genes was down-regulated in clock cells using timGal4-dicer2. The number of rhythmic flies out of the total flies used for the analysis is shown in Table 4.4.

Table 4.4: Number of rhythmic flies in LL

Note that 1 in 31 represents one rhythmic fly out of thirty-one used for the analyses. The experiment was conducted using 32 flies for each genotype. Those flies not used for the analysis were dead by the end of the experiment.

Gene	w1118; UAS-IR	timG4>dcr2; UAS-IR	w1118; timG4>dcr2
sif	1 in 31	12 in 31	6 in 26
Hr38	1 in 30	10 in 30	6 in 26
CG7589	2 in 32	2 in 32	6 in 26
Thor	2 in 32	24 in 32	6 in 26
nvr1	2 in 32	26 in 32	6 in 26
Nf1	2 in 31	20 in 31	6 in 26
CG11155	1 in 32	17 in 32	6 in 26
Calx	4 in 31	4 in 32	6 in 26
CG11597	2 in 31	10 in 32	6 in 26
Fmr1	2 in 32	19 in 31	6 in 26

4.3.6 Identification of known clock regulatory elements

The analysis of the upstream sequences revealed E-box, CRE and TRE elements in few of the candidate genes. Seven of the genes have one or two of the regulatory elements and in others none was detected (Table 4.4).

Table 4.5: Summary results of manual circadian regulatory search

Gene	E box (CACGTG)	CRE (TGACGTCA)	TER box (CACGTTG)
Sif	17	1	2
Nf1	1		
Calx	5		2
nrv1		1	
Hr38	4	2	2
Fmr1	1		
CG11597	1		

4.4 Discussion

In this study, I have examined the light-induced global transcriptional changes in *Drosophila's* head using Affymetrix *Drosophila* microarrays. The main aim was to understand the biological processes associated with the circadian light response. Using stringent analysis criteria, I have identified 209 genes whose transcript levels were significantly altered in response to light pulse (see appendix 7.5) at an FDR cut-off of 10%. As shown in Table 4.4, some circadian regulatory elements known to be involved in light response or clock machinery were manually searched in the candidate genes. However, *vri/pdp1* binding sites were not searched as no clear consensus recognition sequence was found.

This result was validated using qPCR (Fig 4.2) with 57 % of the tested genes showing similar differential expression as in the microarray data. Weak concordance between qPCR and microarray data is common, owing to well documented pitfalls of these two methods (Bustin. 2002; Chuaqui *et al*. 2002). The observed difference in gene expression levels between the light treated samples and the control was subtle as seen in their low fold change values (see appendix 7.5). These low fold changes might have contributed to the discrepancy between the qPCR and microarray data in this study. There is ample evidence linking low fold change to poor correlation of microarray and qPCR data (Dallas *et al*. 2005; Morey *et al*. 2006). Another possible explanation

may be the difference in Affymetrix target sequences and the qPCR, which may result in different splice variants of the same gene being reported.

The identified 209 differentially expressed genes were further characterised using functional annotation tools available on DAVID. Examination of these genes and their biological functions, suggests the involvement of at least six biological processes in light-induced delay phase shift of rhythmic activities. These biological functions are: cAMP-mediated signalling; ion channel and transport; glutamate receptor activity; synaptic organisation and signal transduction; gene regulation and chromatin remodelling. While this chapter describes experiments carried out with the fourteen candidate genes associated with the first four biological processes, experiments for the remaining six genes (associated with chromatin remodelling) are discussed in chapter 5.

To investigate the possible function of these candidate genes in circadian clock, RNAi strategy was employed to down-regulate their expression in the clock cells. Ten out of the fourteen knockdown genes resulted in flies showing a shorter phase shift (Fig 4.3). In contrast, the over-expression of *CG2051* and *Psc* by two available enhancer promoter (EP) lines and down-regulation of their expression by dsRNAi resulted in an opposite effect on the light response (Fig 4.4).

In addition, down-regulating the expression of *sif*, and *CG7589* has an impact on the free-run period: with flies displaying a significantly longer period of locomotor activity in DD (Fig 4.5). Given the putative role of these genes in adjusting the free-run period, it is possible that they are expressed in PDF-positive cells, since these subset of neurons were shown to maintain the circadian period in DD (Grima *et al*. 2004; Stoleru *et al*. 2005). Indeed, the previous studies suggested that *sif* is expressed in the lateral neurons (Sone *et al*. 1997).

The behaviour of flies in constant light (LL) is particularly informative. Wild-type flies become arrhythmic after a day or two under LL but may remain rhythmic for weeks in constant darkness (Konopka *et al*. 1989). However, flies defective in the circadian photoreceptor CRY maintain rhythmic locomotor activity in LL with similar period to that seen in wild-type flies under DD (Emery *et al*. 2000; Stanewsky *et al*. 1998). In this thesis, knock-down of the following genes: *nrv1, Thor* and *Nf1* resulted in significantly high rhythmicity (81%, 75%, and 64% respectively) in LL (Fig 4.6). This result suggests a possible photoreception role for these genes in the circadian clock. The aberrant delay phase shift of flies with *Nf1, Thor* and *nrv1* knockdown provide further evidence for the role of these genes in photoreception.

Neurofibromin 1 (*Nf1*) encodes neurofibromin protein, which is highly conserved between humans and flies (The *et al*. 1997). This protein acts as a

tumour suppressor in humans through Ras-specific guanosine triphosphate (GTP) activity and its deficiency in humans causes neurofibromatosis type 1(NF-1) (Dasgupta *et al*. 2003; The *et al*. 1997). Studies in *Drosophila* reported that *Nf1* acts as a Ras-GTPase in vitro but there is no evidence for its in *vivo* activity (The *et al*. 1997). In addition, *Drosophila Nf1* is involved in protein kinase A (PKA)-cyclic adenosine 3', 5'-monophosphate (cAMP) signalling pathway (Dasgupta *et al*. 2003; Williams *et al*. 2001). This was evident as all the defects linked to *Nf1* mutation were effectively rescued by over-expressing cAMP dependent signalling (Williams *et al*. 2001). *Drosophila* and mouse *Nf1* positively regulates G protein stimulation and Ca^{2+} influx, thus inactivating *Nf1* would induce the Ras/MAPK pathway and down-regulate PKA-cAMP signalling (Dasgupta *et al*. 2003; Tong *et al*. 2002; Williams *et al*. 2001). Results from this study showed that by knocking down the expression of *Nf1* in clock neurons, circadian photosensitivity is reduced.

It was also reported that *Nf1* enhances the function of PDF in fly's circadian clock (Williams *et al*. 2001). Further genetic analyses suggested that *Nf1* protein acts downstream of PDF to support circadian output (Mertens *et al*. 2005; Williams *et al*. 2001). In addition, studies in *Drosophila* show that *Nf1* signalling lies upstream of CRE-mediated transcription and it acts via cAMP-dependent pathway (The *et al*. 1997; Williams *et al*. 2001). Furthermore, the interaction between *Nf1* and *CG13758* elevates calcium levels via PDF signalling

(Mertens *et al*. 2005) and mutation in *Nf1* decreases calcium influx into the cells (Dasgupta *et al*. 2003). It has been shown that inhibiting extracellular Ca^{2+} blocked light-induced phase shift (Khalsa and Block. 1988). These observations suggest *Nf1* may influence clock function by regulating Ca^{2+} movement. A membrane model of clock phase shifting was proposed involving an increase in intracellular Ca^{2+} in response to light resulting in the release of neurotransmitters (Khalsa and Block. 1988). This fits well with the results from this study, suggesting a role for *Nf1* in this process. In addition, *Nf1* may mediate the signal from CRE-genes to the clock via cAMP or MAPK pathways.

Another candidate gene of interest is *insulin-stimulated eIF-4E binding (Thor)*, a member of the 4E-binding protein involved in host immune defence and initiation of translation via binding eukaryotic initiation factor (4E) (Levitin *et al*. 2007). It is located in a close proximity to *timeless* a known circadian photo-responsive protein and its mRNA expression oscillates with high amplitude in DD (Wijnen *et al*. 2006). This oscillation was abrogated in *tim* null mutant (tim^{01}) flies, an indication that the expression was clock dependent (Wijnen *et al*. 2006).

Recently, *Thor* was reported to play a role in circadian clock function though detailed information was not provided (Nagoshi *et al*. 2010). Consistent with this report, down-regulation of *Thor* expression in fly clock neurons reduced light sensitivity as seen in the lower magnitude of the phase shift flies

(Fig 4.3). In addition, when *Thor* expression was down-regulated in *tim*-expressing cells, about 75% of the flies displayed rhythmic behaviour under LL (Fig 4.6). This observation mirrors the earlier studies of flies lacking functional CRY (Emery *et al*. 2000; Stanewsky *et al*. 1998), and further supports a possible role for *Thor* in the light input pathways.

The other key biological processes highlighted in the functional analyses were: ion channel transport; synaptic organisation; intracellular signalling cascade; and glutamate receptor activity. One common intersection of these processes is communication at cellular level, a less understood mechanism in the circadian system. Therefore, the following discussion focuses on the likely roles of these biological processes and the underlying genes in circadian clock function.

The genes *CG11155, nrv1* and *CG7589* are involved in ion transport activities and signal transmission (Tweedie *et al*. 2009). In this study, these genes were differentially expressed (see appendix 7.5) in response to light stimulation and when down-regulated in the clock neurons, photosensitivity was reduced as shown in Fig 4.3. *CG7589* is a protein coding gene located on left arm of chromosome 3 (Tweedie *et al*. 2009). When *CG7589* expression was knocked down in *tim*-expressing cells, the free-running period was lengthened (Fig 4.5).

CG11155 is a computed gene annotated in FlyBase, which encodes a protein and is located on the fourth chromosome (Tweedie *et al*. 2009). One of its predicted molecular functions is ionotropic glutamate receptor (iGluRs) activity, which mediates excitatory synaptic transmission. Glutamate has been shown as essential for circadian light response in mammals (Colwell *et al*. 1991; Ding *et al*. 1997). This may explain why down-regulating *CG11155* in this study, a putative iGluR would result in reduced circadian light sensitivity (Fig 4.3).

Another gene implicated in ion transport is *nervana 1* (*nrv1*), which encodes one of the two Na^+, K^+ -ATPase β subunit in *Drosophila* (Tweedie *et al*. 2009). Interestingly, the other subunit *nrv2* was also down-regulated in response to light in this study, though not selected for further characterisation. This enzyme is an important membrane protein largely responsible for transporting two K^+ ions inside cells in exchange for three Na^+ ions using an ATP-dependent mechanism (Górska-Andrzejak *et al*. 2009). It plays a critical role in regulating intracellular Ca^{2+} levels via the Na^+–Ca^{2+} exchange mechanism (Blaustein. 1977). In this study, down-regulating the expression of *nrv1* in the clock neurons reduced circadian light sensitivity as shown in Fig 4.3.

In addition, most of the *nrv1* down-regulated flies (81%) maintained rhythmic activity in LL when compared to their controls. This may suggest a likely role for *nrv1* in photoreception, possibly in gating Ca^{2+} channels in response to light signal. Although the spatial expression of *nrv1* was not

examined in this study, the observed circadian phenotype suggests a function in the clock neurons. This observation suggests a possible functional role for *nrv1* in other tissues than in the muscle as previously suggested by Xu and colleagues (1999). The presence of CRE within *nrv1* genomic sequence (Table 4.4), further supports its likely function in light transduction in the circadian system (Tischkau *et al*. 2003).

Sodium-calcium exchange (*CalX*), which is located on the right arm of chromosome 3 (Tweedie *et al*. 2009) was behaviourally characterised in this study. Although, *CalX* transcript does not oscillate in DD (Wijnen *et al*. 2006), search for known circadian regulatory element revealed the presence of few E-boxes and two *tim* E- box-like repeats (TER) in its genomic sequence (Table 4.4). The TER element has been shown to enhance *tim* transcription and its mutation affects dCLK- driven transcription in S2 cells (McDonald *et al*. 2001). It is possible that the *CalX* TER elements enhance the transcription of *tim* or other *dCLK*- driven transcripts in a similar way as reported by *(McDonald et al. 2001).* Thus down-regulating *CalX* expression in the clock neurons, may affect CLK-CYC control genes within the circadian system. Here, I show that circadian function (in particular light sensitivity) is disrupted when *CalX* expression level was knocked down in the clock neurons (Fig 4.3). This is consistent with earlier studies, where *CalX* mutation was shown to cause transient response to light and drastic reduction in signal amplification in *Drosophila* (Wang *et al*. 2005).

One of the known biological functions of *CalX* is phototransduction by regulating the movement of Ca^{2+} in the photoreceptors. This function coupled with that of *Nf1* and *nrv1* further support the critical role of Ca^{2+} in circadian light response.

The observations from this study seem to support the membrane model of the circadian clock first proposed by Njus and colleagues (1974). In summary, the candidate genes can be classified into four groups: (i) light responsive genes: *nrv1*, *sif*, *Thor*, *Hr38* and *CG7589* (ii) membrane potential maintenance genes: *CalX* and *nrv1* (iii) signal transduction: *CG11155*, and *Fmr1* and (iv) rhythmic output: *Nf1*. More studies are required to further understand the specific roles of these genes in clock function.

Chapter 5: Histone modifications and circadian light entrainment

5.1 Introduction

In addition to its structural function, chromatin also acts as an active regulator of gene transcription. Various modifications of histone proteins such as acetylation, methylation and phosphorylation induce local structural changes in the chromatin. This modulates the accessibility of transcription factors and their binding to DNA targets, which in turn impacts on the level of gene expression (see Box 5.1).

The first report of a possible role for histone modification in the circadian clock was made by Crosio and colleagues (2000) who found that a light pulse during the subjective night induces phosphorylation of histone H3 serine 10 residue in mouse SCN clock cells. The kinetics of this phosphorylation mirrored the expression of *per1* and further experiments suggested that the two processes are controlled by the same signalling pathway. Subsequently, it was found that in mouse liver, H3 acetylation at promoter regions of *per1*, *per2*, *cry1* and the binding of RNA polymerase II, oscillates in a circadian fashion. This oscillation synchronises with the rhythmic expression of these clock genes. Initially, p300/CBP was suspected as the relevant histone acetyltransferases (HAT), as it interacts with CLOCK-BMAL1 (Curtis *et al*.

2004). It was however, found that CLOCK itself carries HAT activity that is essential for CLOCK-BMAL1 dependent transcription (Doi *et al*. 2006).

As one may predict, circadian acetylation is coupled with anti-phase de-acetylation. Recently, *sirt1* the mammalian orthologue of the yeast *Sir2* (*silencing information regulator*) was shown to regulate the expression of clock genes through its interaction and the deacetylation of core clock genes such as *Bmal1* and *per 2*. The histone deacetylase activity (abbreviated HDAC) of *sirt1* follows a circadian rhythm and parallels the rhythmic acetylation of H3 at Lys9 and Lys14. Consistently, circadian rhythmicity is disrupted upon pharmacological inhibition of *sirt1*, or in mutant mice lacking *sirt1*. The activity of *sirt1* is NAD^+-dependent, which suggests a link between energy metabolism and the circadian clock.

Methylation of histones is another modification that contributes to circadian regulation. The mouse EZH2 (enhancer of zeste), a member of the polycomb-group, has been shown to methylate histone and also interact with CLOCK-BMAL1 (Etchegaray *et al*. 2006). This study showed that EZH2 contributes to transcriptional repression by CRY, and when knocked down (by RNAi) results in disruption of the clock.

Intriguingly, compared with the efforts to study circadian chromatin remodelling in mammals little is known about the impact of histone

modifications on the *Drosophila* clock. The microarray data presented in chapter 4 indicated that among the transcripts that responded to early night light pulse stimulus, there was a significant over-representation of genes associated with chromatin remodelling (Table 5.1) suggesting that this processes is an important component of light entrainment of the fly clock.

Table 5.1: Differentially expressed chromatin-related genes in response to light stimulation (microarray data from Chapter 4).

Gene name	Chromo	Direction	Biological function
CG2051	3R	⇧	histone acetylation; chromatin silencing at telomere
Nipped-A	2R	⇩	Signalling, transcriptional co-activator. A key component of both the SAGA and Tip60 (NuA4) chromatin-modifying complexes.
trithorax	3R	⇩	histone methylation; histone H3-K4 methylation
PSc	2R	⇧	chromatin remodelling
nejire	X	⇩	histone acetyltransferase activity, H3-K27 specific, H3-K18 specific
Sirt6	3R	⇧	Predicated histone deacetylation activity, determination of adult life span
Kr-h1	2L	⇩	transcription factor activity
Su(var)3-9	3R	⇧	negative regulation of gene expression, epigenetic

In this study, I have characterised flies in which the expression of these chromatin-associated genes was knocked-down in clock neurons or by using strains carrying null mutations of these genes. In a different set of experiments, I have used chromatin immunoprecipitation (ChIP) to test whether histone modifications are associated with the genomic regions of *per* and *tim*.

Box 5.1 Histone modification and chromatin remodelling

The nucleosome is the primary repeating unit of chromatin that consists of 147 bp DNA fragment wound in approximately 1.7 left handed superhelical turns around an octamer of the four core histones H2A, H2B, H3 and H4 (Luger and Hansen. 2005). Detailed crystal structural studies revealed that the histone octamer consists of four histone heterodimers: two molecules each of H3-H4 and H2A-H2B (White *et al*. 2001). An additional histone molecule H1 binds the internucleomal DNA (~ 20 bp) to stabilise the nucleosome and protect the linker DNA from nuclease digestion (Campos and Reinberg. 2010; Ni *et al*. 2006).

Chromatin remodelling

In order for genes to be transcribed, the chromatin structure needs to be loosened through a process referred to as chromatin remodelling (Campos and Reinberg. 2010). This process is modulated through mechanisms involving three steps: initial *trans*-acting factor; local chromatin opening at special *cis*-element and the extensive chromatin opening processes to enhance transcription (Li *et al*. 2004).

The binding of activators to DNA sites either at the promoters or enhancers extends the chromatin locally (Li *et al*. 2004). A process that facilitates the recruitment of a coactivator, which either links transcription factors to the

(Box 5.1 continued)

transcription machinery or changes chromatin structure through several enzymatic processes (Campos and Reinberg. 2010; Li *et al*. 2004). The latter function can be further categorised into two classes: the ATP-dependent chromatin-remodelling/modifying complex e.g. SWI/SNF complex and covalent modifications of histone proteins (Campos and Reinberg. 2010). The ATP-dependent-chromatin remodelling complexes use the energy of ATP hydrolysis to change the position nucleosome on the DNA causing transcription to be repressed or activated (Campos and Reinberg. 2010; Cosgrove *et al*. 2004). On the other hand, the histone-modifying complexes introduce a range of post-translational modification that can either repress or activate transcription (Campos and Reinberg. 2010; Li *et al*. 2004).

Histone modifications

Histone modifications play a vital role in different biological processes such as DNA repair, transcription regulation, and heterochromatin formation in various species (Kouzarides. 2007). Histone modifications were thought to occur only at the N-terminal tails but recent proteomics analyses implicate other histone domains including the globular domain of the core histones (Cosgrove *et al*. 2004). Remarkably, histone proteins and their target residues for modifications are evolutionary conserved in organisms, suggesting an essential role for these modifications.

(Box 5.1 continued)

Several modifications act sequentially or in combinations to influence chromatin structure and function, which have led to the idea that information is stored by multiple histone modifications that constitute a *histone code* (Strahl and Allis. 2000). At least nine distinct histone modifications have been identified and are listed in Table 5.2. For the purpose of this study, I will focus on lysine methylation, acetylation and deacetylation activity on histone 3 (H3).

Table 5.2: Histone modifications and their functions

Adapted from (Kouzarides. 2007).

	Chromatin modifications	**Residues modified**	**Functions regulated**
1	Acetylation	K-ac	Transcription, Repair, Replication, Condensation
2	Methylation (lysines)	K-me1 K-me2 K-me3	Transcription, Repair
3	Methylation (arginines)	R-me1 R-me2a R-me2s	Transcription
4	Phosphorylation	S-ph T-ph	Transcription, Repair, Condensation
5	Ubiquitylation	K-ub	Transcription, Repair
6	Sumoylation	K-su	Transcription
7	ADP ribosylation	E-ar	Transcription
8	Deimination	R > Cit	Transcription
9	Proline Isomerization	P-cis > P-trans	Transcription

K= lysine; R /ar = arginine; S = serine; T = Threonine; E = Glutamic acid; P= proline; ac = acetylation; me1 = mono-methylation; me2= di-methylation; me3 = trimethylation, ph = phosphorylation; su = sumoylation, Cit = citrulline.

(Box 5.1 continued)

Lysine methylation

Histone lysine methylation occurs when a methyl group from donor S-adenosyl-L methionine (SAM) covalently bonds to the *elipson* on lysine (Zhang and Reinberg. 2001). The lysine residue can accept up to three methyl groups resulting in mono-, di or tri-methylated lysine respectively.

Though species-specific variations occur in lysine methylation, most of histone H3 methylation occurs at lysine 4, 9, 27, 36 and 79 and on lysine 20 for H4(Kouzarides. 2007; Strahl and Allis. 2000). Histone methylation plays a critical role in chromatin organisation and marks distinct chromatin regions for biological readout.

Lysine methyltransferase

Histone lysine methyltransferases (HKMTs) catalyse the transfer of methyl groups from SAM donor to histone lysine residues. Based on domain analyses, histone lysine methyltransferases can be categorised into two protein families: SET-domain HKMTs and non-SET domain (Feng *et al*. 2002; Zhang and Reinberg. 2001).

The SET domain is an *S-adenosyl*-l-*methionine*-binding fold specific to lysine methyltransferases as well as other proteins with no known HKMT activity (Porras-Yakushi *et al*. 2006).

(Box 5.1 continued)

This domain is different from the canonical even-β-strand *S*-adenosyl-l-methionine-binding fold found in most methyltransferases (Porras-Yakushi *et al*. 2006). The SET domain was first identified in three *Drosophila* proteins: Suppressor of variegation 3-9 {Su(var)3-9}, the polycomb-group chromatin regulator Enhancer of zeste {E(z)}, and the trithorax-group chromatin regulator *trithorax* {*Trx*} (Dillon *et al*. 2005; Jenuwein *et al*. 1998). Subsequently, these genes were shown to have histone methyltransferase activitiy (Czermin *et al*. 2002; Eskeland *et al*. 2004).

Histone acetylation and histone deacetylation

Acetylated core histones are preferentially associated with transcriptionally active chromatin (Struhl. 1998). Histone acetylation is one of the well characterised covalent posttranslational modifications and involves the transfer of an acetyl group to the ε-amino group of a lysine residue by histone acetyl-transferases (HATs). This process is reversible by dedicated enzymes called histone deacetylases (HDACs), which removes the added acetyl group from the lysine. This interplay between HATs and HDACs causes dynamic transitions in chromatin structure and in switches between active (euchromatin) and inactive (heterochromatin) states.

(Box 5.1 continued)

The acetylation of histone neutralises its positive charge thereby reducing its affinity to DNA (Struhl. 1998). As a result, the chromatin structure is altered making it more accessible to transcription factor binding (Struhl. 1998). Histone acetylation is thought to translate epigenetic information by controlling gene expression patterns via changes in the chromatin structure (Lachner and Jenuwein. 2002). Although the four core histones can be acetylated, modifications in H3 and H4 mostly account for the effect on transcription.

5.2 Materials and methods

5.2.1 Drosophila stocks

All crosses were carried out at 25 ^{0}C on standard sugar medium as described in chapter 2. The mutant lines and the enhancer trap (EP) stocks listed in Table 5.3 were obtained from Bloomington *Drosophila* Stock Centre (BDSC) at Indiana University, USA. All the fly stocks for RNA interference-mediated knockdown (Table 5.3) were obtained from Vienna Drosophila RNAi Centre (VDRC) (Dietzl *et al*. 2007). The strains Canton -special (CS) (from our lab) was used as the wild-type. In the RNAi crosses, two different *tim*Gal4 drivers were used: *timGal4-dicer2* (from our lab) and *timGal4 (*from BDSC) to drive the UAS-IR constructs. *Dicer2* gene is important for the assembly of RNAi silencing complexes in *Drosophila* and over-expression of this gene greatly improves the efficacy of dsRNA mediated knockdown (Dietzl *et al*. 2007).

Table 5.3: Fly stock used in this study

Stock ID	Genotype	Source	Off target[1]
30586	*w;; UAS-Psc-IR*	VDRC	0
39378	*w;; UAS-Su(var)3-9-IR*	VDRC	0
37715	*w;; UAS-trx-IR*	VDRC	1
105115	*w;; UAS-nej-IR*	VDRC	
22483	*w;; UAS-Sirt6-IR*	VDRC	0
51282	*w;; UAS-Kr-h1-IR*	VDRC	2
52486	*w;; UAS-Nipped-A-IR*	VDRC	0
33459	*w;; UAS-CG2051-IR*	VDRC	0
169	*y[1]*	BDSC	
7126	*y^1 w^*; P{GAL4-tim.E}62*	BDSC	
	yw;timGal4-dicer2	Our lab	
807	*In(1)w[m4]*	BDSC	
6599	*y[1] w[67c23]*	BDSC	
13097	*y[1] w[67c23]; P{y[+mDint2] w[BR.E.BR]=SUPor-P}Kr h1[KG00354]/SM6a*	BDSC	
16514	*y[1]; P{y[+mDint2] w[BR.E.BR]=SUPor-P}Nipped-A[KG10162]/CyO*	BDSC	
20076	*y[1] w[67c23]; P{w[+mC] y[+mDint2]=EPgy2}Psc[EY06547]/CyO*	BDSC	
20737	*y[1] w[67c23]; P{w[+mC] y[+mDint2]=EPgy2}trx[EY12356]/TM3, Sb[1] Ser[1]*	BDSC	
22496	*y[1] w[67c23]; P{w[+mC] y[+mDint2]=EPgy2}CG2051[EY21697]*	BDSC	
6209	*In(1)w[m4]; Su(var)3-9[1]/TM3, Sb[1] Ser[1]*	BDSC	Loss-of-function

5.2.2 Histone deacetylases (HDAC) inhibition in *Drosophila*

Standard sugar fly food was prepared as described in chapter 2. The food was then divided into two equal halves, which were used for the preparation of treatment and control media. For treated media (HDAC

1 The Off-target value signifies the number of additional genes that may be targeted by the dsRNAi machinery. This applies only to the VDRC strains.

inhibition), sodium butyrate (NaB: Sigma) solution (dissolved in water) was added to the food at a final concentration of 10 mM as described by (Xing *et al*. 2007). The same volume of water (but without the drug) was added to the control media.

CS flies from the same vial were split into two groups, with one transferred into a vial with sodium butyrate (NaB) treated food, and the other into a vial with the control food. The flies were reared under the same conditions at 25^0C for a generation. The locomotor activity of adult males (1-3 day old) from each condition (NaB treated and control) was recorded and circadian parameters were tested. The activity experiments were performed as described in chapter 2 with a set of the activity tubes containing either NaB treated food or control food (non-treated). Thirty-two males, each from the NaB treated and control flies, were put in activity tubes as follows: (i) NaB treated flies into non-treated food (HDAC inhibited only at development stage) (ii) NaB treated flies into NaB treated food (HDAC inhibited continuously) (iii) control flies into NaB treated food (HDAC inhibited only at adult stage) (iv) control flies into non-treated food (control flies).

The protocol for the light pulse experiment is described in chapter 2. Independent *t-test* was performed on SPSS v16 to analysis the differences in light response and circadian period between the treated and control samples.

5.2.3 qPCR of CLK-CYC driven transcripts

Total RNA samples were prepared from five biological replicates for each condition (light-pulsed and non-treated) as described in chapter2. Transcript level was quantified by qPCR. The reagents and qPCR procedure were as described in chapter 4. Primers were designed using Primer3Plus as described in section 4.2.6 of chapter 4. Table 5.4 lists the primer sequences, in addition to primers that were previously listed (Table 4.1 of chapter 4).

Table 5.4: Primers used for clock genes qPCR

Gene name	Primer sequence	Amplicon size (bp)
timeless (tim)	CCAACAACTTGGACCAGGAG	141
	GATCTCGGTTCGCTCAAGTC	
vrille (vri)	CGAGCTGACCAAAGAGAACC	148
	GCGCTTTGTGTTACTCAGCA	
Clock (Clk)	TAGTTCCCGTGGAGGCTATG	136
	TACGTGGTCTGCACCCATAA	
cryptochrome (cry)	TCGACTAGAAGACGCCACCT	118
	GAAGCCCATGTTGTCTCCAT	
Aequorin (Aeq)	TTGACGAGATGGTCTACAAGGCATC	100
	GAAGGCTTCTACAGCATCTTTGTGTCGT	
Sirt6	TTCCTTCGATGAAGCCAGAC	118
	TCCGGATTTCAAGTGGAGAC	
Su(var)3-9	GGCCCAGCTTAAGTACAACATC	111
	AAGGATCGGATGACGATCAG	

5.2.4 Immunocytochemistry and microscopy imaging

Adult whole-brain mounts were processed and stained as described in chapter 2. The following primary antibodies were used: rat anti-TIM (gift from Isaac Edery) dilution 1:2000, rabbit anti-CRY (gift from Patrick Emery) used at

1:2000, rabbit and mouse anti-PDF (DSHB) at dilution 1:5. For the secondary antibodies: anti-mouse Alexa 488, anti-rat Alexa 594 and anti-rabbit Alexa 633 were used at 1:200 dilution (Molecular Probes). Images were captured on Olympus confocal microscopy at 20 x magnification and the same imaging setting for a study.

5.2.5 Native chromatin immunoprecipitation (nChIP)

The protocol used for this experiment was according to (Matevossian and Akbarian. 2008) and (Phalke *et al*. 2009) with a few modifications. About 250 adult fly heads were collected for each treatment (light pulsed and non-pulsed) as described in section 2.4.1 of chapter 2. The samples were ground in liquid nitrogen separately and processed simultaneously by adding 375 µl of 1 x nChIP Douncing buffer to each and the solutions were transferred into 2.0 ml tube. To each tube, 2 µl of 5U/ml micrococcal nuclease (MNase: Sigma) was added, vortexed and incubated at 37°C for 7 min. EDTA solution was added to a final concentration of 10mM to stop the MNase activity.

The content was transferred into a 15-ml falcon tube containing 4.65 ml of hypotonic lysis solution (0.1 M DTT, 0.1 M EDTA, 0.01 M PMSF, 0.1 M benzamidine), incubated on ice for 1 hour and mixed every 10 minutes. The mixture was centrifuged at 3000g for 10 min at 4°C. The supernatant was transferred into a new 15 ml falcon tube and pre-cleansed with 500 µl Protein G agarose. This mixture was incubated at room temperature (RT) for 30 min and

centrifuged at 4000 rpm for 10 min at 4°C. The supernatant was then distributed into four tubes of 1100 µl each, of which three were used for ChIP and the fourth one used as input control (containing only genomic DNA). The input control sample was stored in -80°C until further use. To the ChIP samples, 122 µl of 10 x incubation buffer (1 M EDTA at pH 8.0, 1 M Tris-Cl, 1 M NaCl) and one of the following antibodies : Abcam (anti-dimethyl H3K9, # ab1220; anti-trimethyl H3K9,# ab6002, and anti-acetyl H3K9, # ab4441) were added to each tube and mixed thoroughly. The samples were thoroughly mixed and rotated at 4°C overnight.

In a 2 ml Eppendoff tube, 1.6 ml of 1x incubation buffer was added to 245 µl protein G-agarose. The solution was separated into two 2 ml tubes and refilled up to 1.6 ml with 1 x incubation buffer. Each tube was rotated for 30 s at RT and centrifuged at 0.1g for 30 s. The supernatant was aspirated and the refilled with 1 x incubation buffer, rotated and centrifuged as described above. The supernatant from this step was then combined in a tube and 15µl of sonicated salmon sperm DNA (10mg/mL) was added. The mixture was rotated for 30 min at RT, centrifuged at 0.1g for 30 sec and the supernatant aspirated. Into each tube of ChIP samples, 200 µl of 1x incubating buffer and 90 µl of agarose beads were added and rotated at 4°C for an hour. The remaining agarose beads were refilled up to 1 ml, processed alongside the ChIP samples and served as a negative control.

The supernatant was removed from the samples (ChIP and negative control) and the beads were washed in the following order: 2× 1 mL of low salt solution (0.1% SDS, 1% Triton X-100, 2 mM EDTA, 150 mM NaCl, 20 mM Tris-Cl at pH 8.0, 1× complete protease inhibitor), 2× 1 mL of high salt solution (0.1% SDS, 1% Triton X-100, 2 mM EDTA, 500 mM NaCl, 20 mM Tris-Cl at pH 8.0), 1× complete protease inhibitor, 1× 1 mL of lithium chloride solution (0.25 M LiCl, 1% NP-40, 1% deoxycholic acid, 1 mM EDTA, 10 mM Tris-Cl at pH 8.0) rotated for 1 min at RT, and 2× 1 mL of TE solution (10 mM Tris-Cl at pH 8.0, 1 mM EDTA).

The DNA–protein complexes were eluted by adding freshly prepared 250 μL of elution buffer (100 mM sodium bicarbonate, 1% SDS) to the beads. The mixtures were rotated at room temperature for 15 min and centrifuged for 1 min at 16 g. The protein residual in both the ChIP and input samples was digested by adding: 10 μl 0.5M EDTA, 25 μl 0.8M Tris-HCl, pH 6.5, 10 mg/ml Proteinase K (1/200 sample) to each ChIP sample and lysis buffer for proteinase K digestion (1/10 of sample buffer) and 10mg/ml Proteinase K (1/200 of sample buffer) to the input samples. This was then incubated for 3 hours at 52°C. Both ChIP and input samples were purified using the phenol/chloroform as described in Chapter 2. The precipitated DNA pellets were re-suspended in water and were amplified using PCR.

5.2.6 ChIP – PCR

The DNA precipitated from the samples and the controls were amplified using PCR. Primer sequences were obtained from (Taylor and Hardin. 2008) and ordered from Sigma. The primers were designed to span E-boxes and transcriptional sites for *per* and *tim* as shown in Table 5.5. The PCR was performed as described in section 2.3 of chapter 2.

Table 5.5: Primer sequences used for ChIP- PCR

(Taylor and Hardin. 2008).

Primers	**Sequence**[1]	**size (bp)**[2]
per_CRS_F	CCAGTGCCAGTGCGAGTTC	276
per_CRS_R	GATGCCAAGTGTCAATCCAAGC	
per_E6_F	CCAGTGCCAGTGCGAGTTC	120
per_E6_R	CTGCGACTGCGGCTATCCAAATC	
per_E7_F	GGTTAACCAGCGAGTTACACAATCCTTGG	165
per_E7_R	GTTTCGACGGCCCAGAATTCAAGAAG	
per_E8_F	CAAGCCATGATTCATGAACATGAATGGCAG	150
per_E8_R	CTTCACGTTGCTCGCCAATAGTATTGT G	
tim_E1_F	GCGGCACGTTGTGATTACAC	162
tim_E1_R	ACACTGACCGAAACACCCACTC	
tim_E2_F	GGGAACTTTCGGGGCTCGTCTG	191
tim_E2_R	CGCCACCCATGTGACCATCAAG	
tim_Up1_F	GCCTGCAACCAACTGTTGATTCC	194
tim_Up1_R	GAACGACTCTGCCGTAGGCTTC	

[1] primer annealing temperature 60 ^{0}C

[2] indicates PCR product size in base pair

5.3 Results

5.3.1 Mis-expression of chromatin-associated genes

To further understand the microarray data in chapter 4, the expression levels of *CG2051*, *Kr-h1*, *Nipped-A*, *Psc*, *trx* and *Sirt6* were down-regulated via dsRNAi using the *tim*Gal4-*dicer2* driver as described in section 2.8 of chapter 2. As shown in Fig 5.1, the light response of flies carrying UAS-IR of *CG2051*, *Kr-h1*, *Nipped-A*, *Psc*, *trx* and *Sirt6* differed significantly from their respective controls. The other two genes *nej* and *Su(var)3-9* UAS-IR lines , either resulted in short-lived offspring (*nej*: died after a couple of days in DD) or were embryonic lethal in case of *Su(var)3-9* when driven by *timG4>dcr2*. Thus their cell-specific roles could not be investigated.

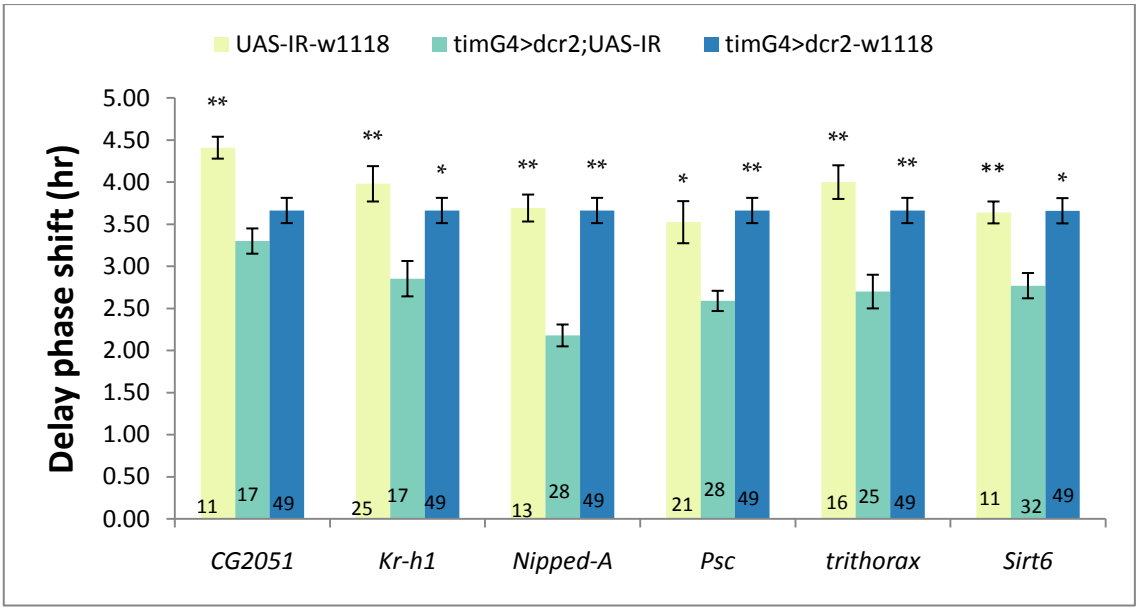

Figure 5.1: Light response in dsRNAi transgenic flies

The asterisk indicates significant difference between the treatment and the controls (UAS and Gal4). The plotted error bars signify the standard error mean for each genotype. The double asterisks ** is when $p < 0.0001$, and * for $p < 0.05$ from ANOVA with post hoc analysis using Tukey test.

To validate these results, the same light pulse experiment protocol was performed on the available candidate gene mutants either carrying *P* element or EMS induced. The results are presented in Fig 5.2; all the mutant strains were significantly different from their respective controls with the exception of *Kr-h1*^{KG00354} which showed no significant difference in light response.

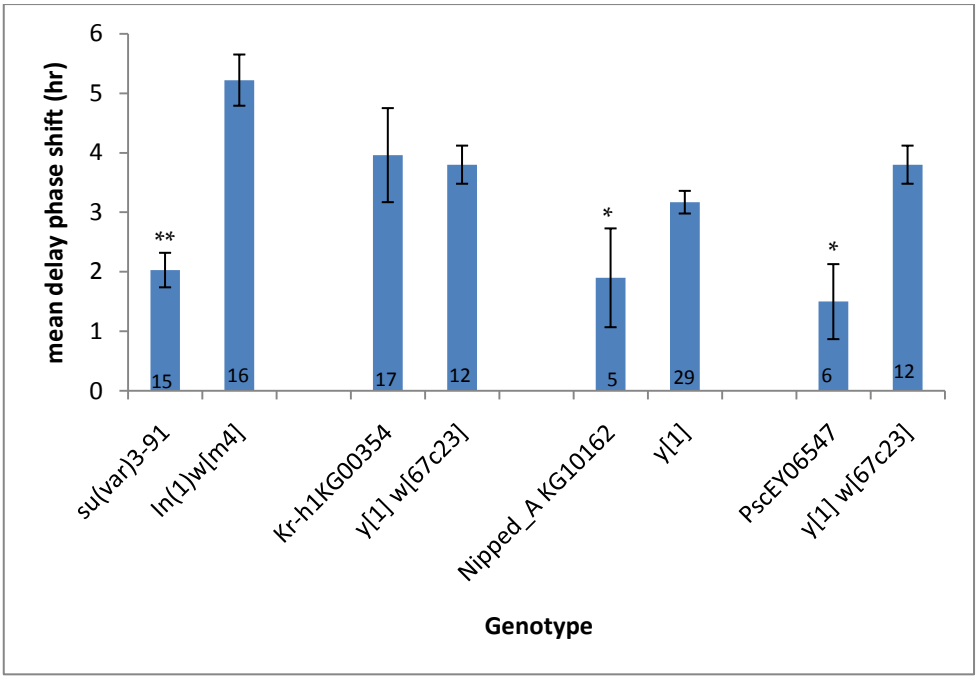

Figure 5.2: Light response in mutant flies and their background controls

The genotypes are *Su(var)3-9*^{1}, *Kr-h1*^{KG00354}, *Nipped- A* ^{KG10162}, *Psc*^{EY06547}. The error bars were based on SEM of each genotype from Independent *t test*. Note ** = $p < 0.0001$ and * = $p < 0.05$.

In two of the *P-element* lines: *Nipped A* ^{KG10162}, and *Psc*^{EY06547} most of the flies have reduced or completely lack locomotor activity (immobile) in darkness as shown in Fig 5.3 and Fig 5.4. The percentages were calculated by dividing the number of immobile or active flies with the total number of flies (excluding the dead ones) and multiplied by 100.

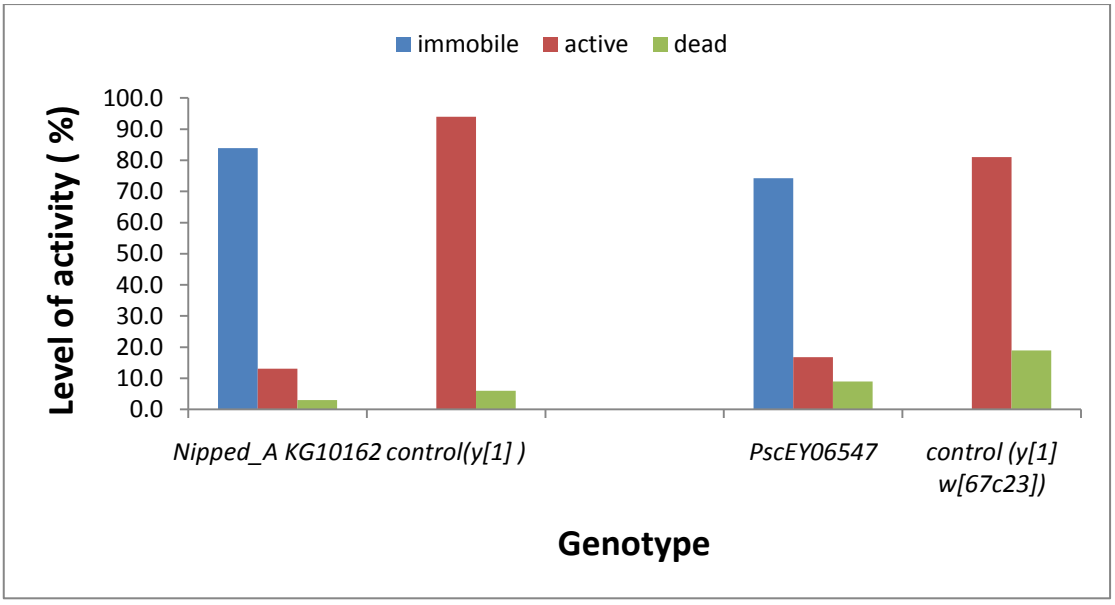

Figure 5.3: Level of activity in *Nipped_A* ^{KG10162}, *Psc*^{EY06547} and their controls in DD

Note that there were no immobile flies in the background control flies.

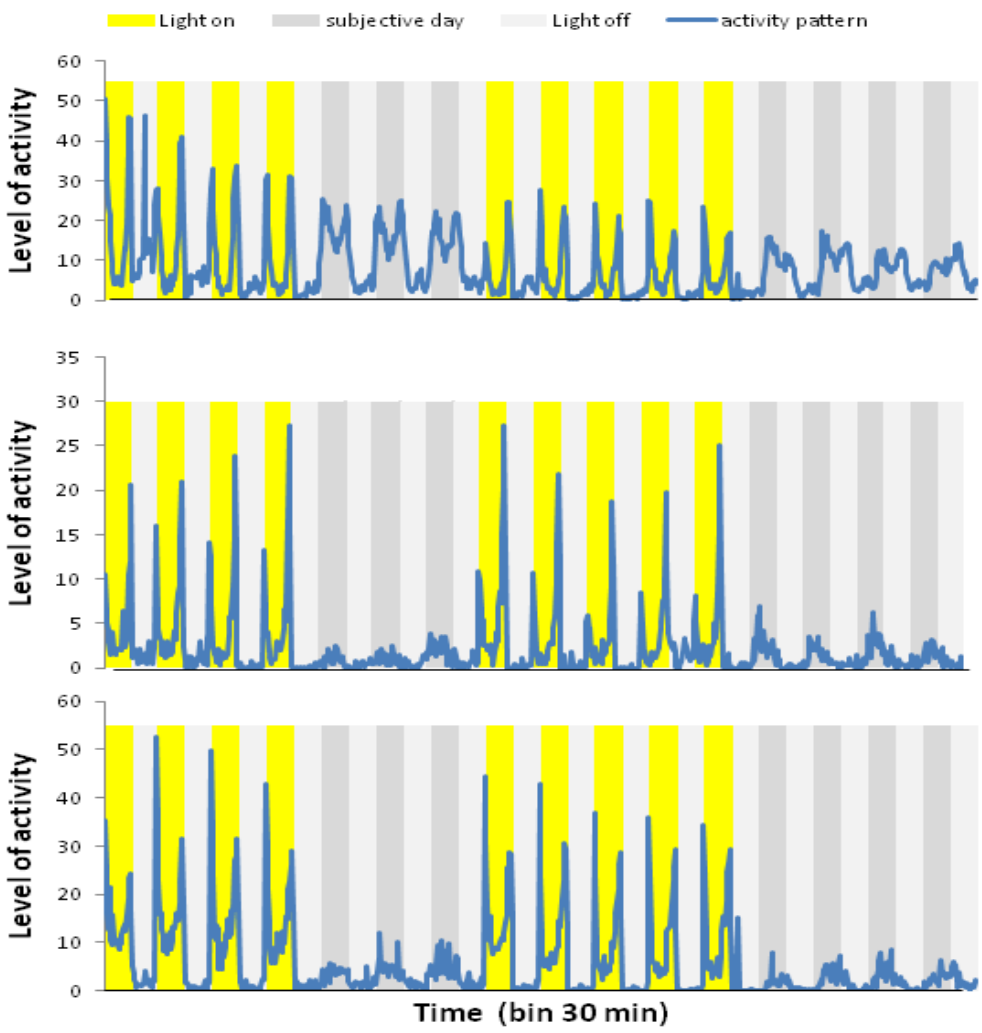

Figure 5.4: Activity profile of *Nipped_A* ^{KG10162} (middle) , *Psc*^{EY06547} (lower) and background control (upper figure) flies in DD and LD conditions

Each plot shows average data from 32 flies for each genotype.

5.3.2 Free-running period in DD

One of the hallmarks of the circadian clock is its ability to maintain rhythmic activity even in the absence of external stimuli. This section examines locomotor activity of adult flies in DD when, *CG2051*, *Psc*, *Nipped-A*, *Kr-h1* and *trx* expression were either down-regulated or over-expressed in clock cells. The results are presented in Fig 5.5 and Fig 5.6.

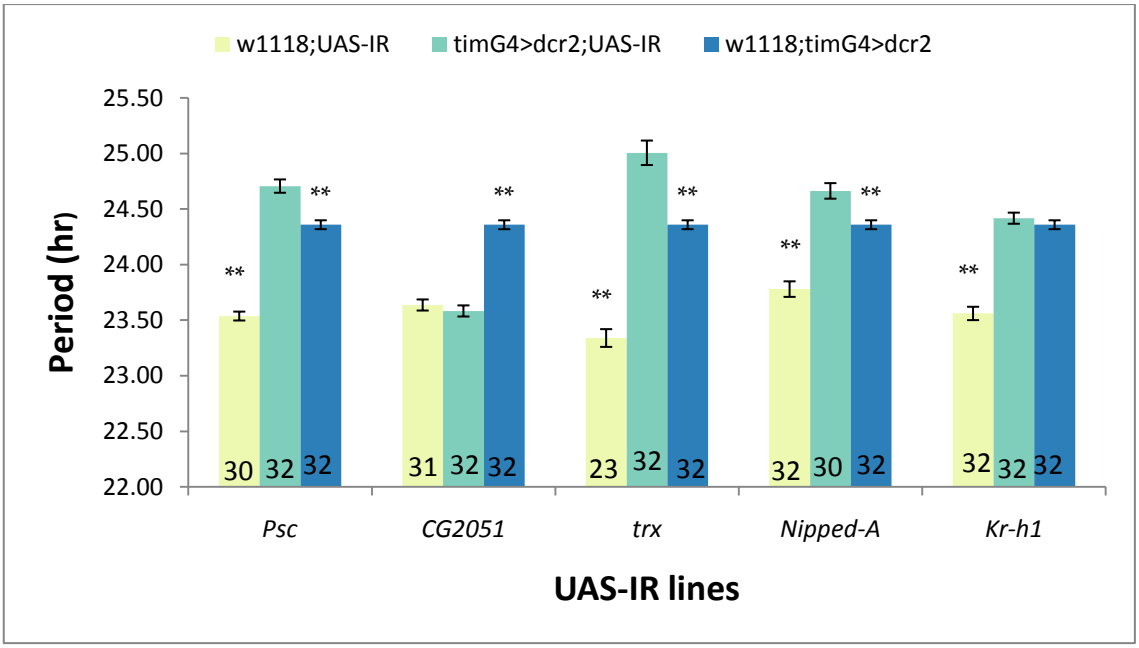

Figure 5.5: Free-running period of dsRNAi transgenic flies

The error bars represent the SEM of each genotype. The asterisk indicates significant difference between the treatment and the controls (UAS and Gal4). Note that double asterisk represents *p<0.0001* from ANOVA with post hoc analysis using Tukey test.

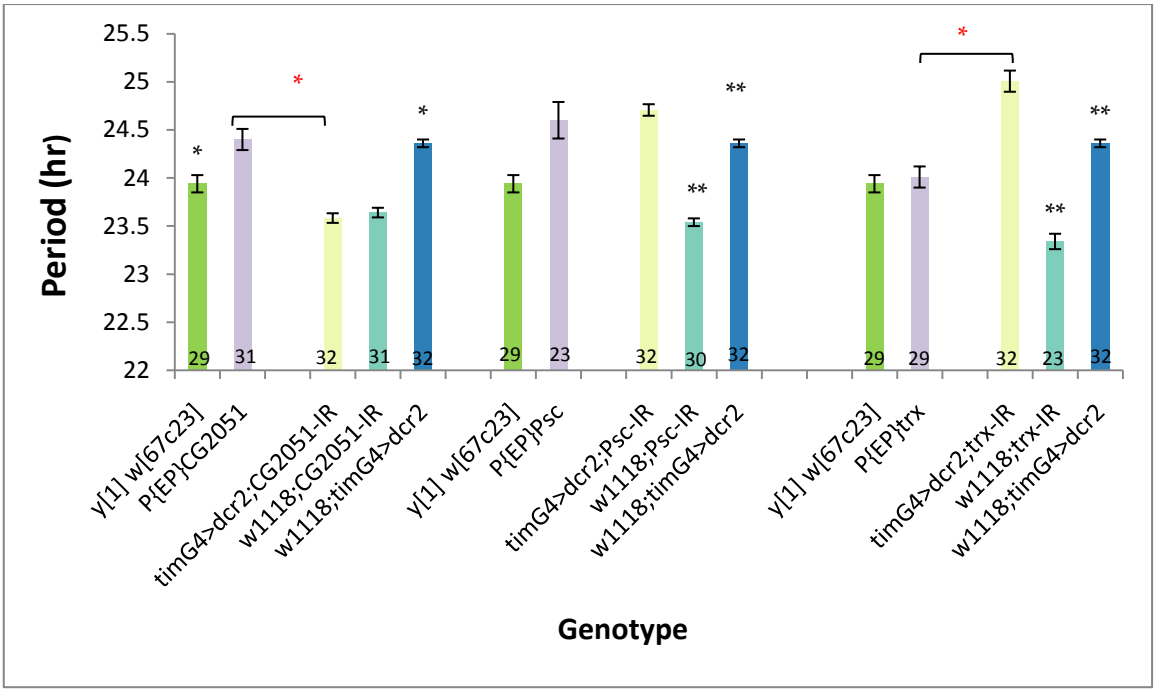

Figure 5.6: Free-running period of EP and their respective UAS-IR lines in DD

Note that expression of was driven using t*imGal4* (EP lines) and *timGal4-dicer2* (UAS-IR lines). The error bars represent the SEM of each genotype. The asterisk indicates significant difference between the EP/UAS-IR and their respective controls (y[1] w[67c23],UAS and Gal4) from independent *t-test* and ANOVA. Note that double asterisk represents *p<0.0001* from ANOVA with post hoc analysis using Tukey test. The red asterisk indicates significant difference between mis-expression and down-regulation of *trx* and *CG2051* in clock cells.

5.3.3 Locomotor activity period in continuous light (LL)

To investigate if any of these genes (Table 5.1) were directly involved in circadian photoreception, locomotor activity of adult flies was monitored in continuous light conditions at a constant temperature. This was performed in two phases: in the first phase the gene transcript levels were knocked down in the clock neurons by using *tim*Gal4-*dicer 2*, while the mutant stocks, where available, were used for the second phase. *Kr-h1* and *Nipped-A* knockdown flies displayed more than 50% rhythmic activity under LL condition, greater than

their controls. The other genotypes also displayed some degree of rhythmicity, which is greater than those seen in their control.

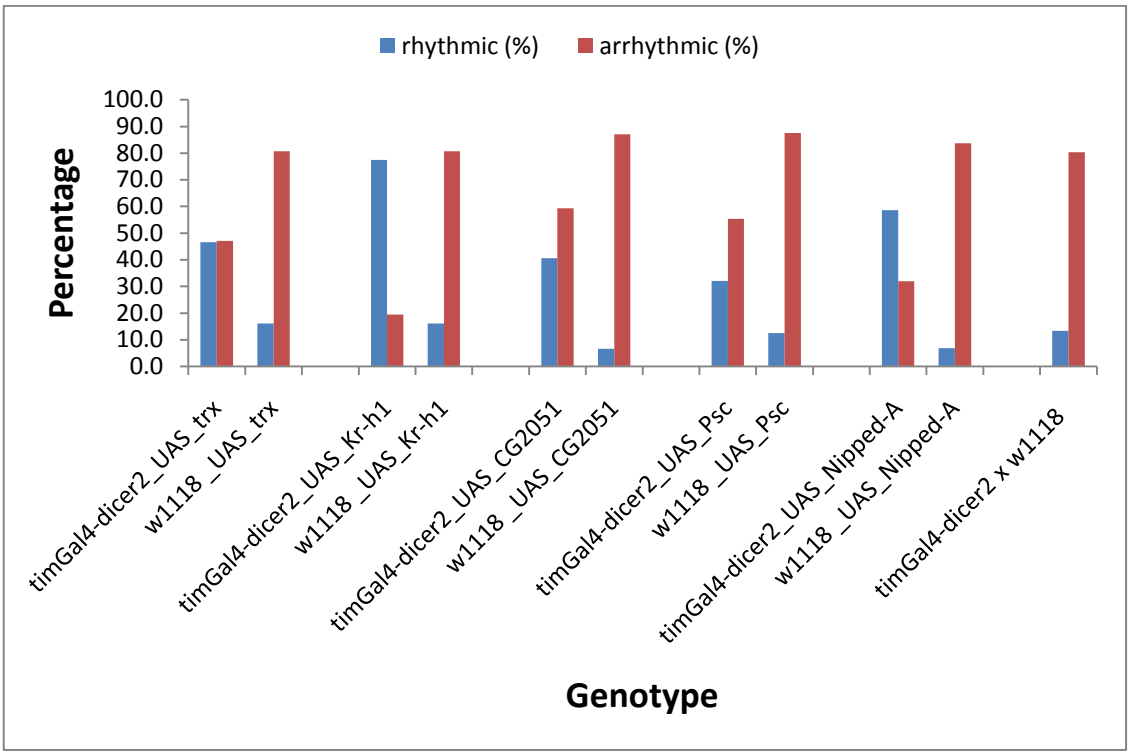

Figure 5.7: Behavioural patterns of knockdown chromatin-associated genes in LL

See Table 5.6 for detail on the number of rhythmic flies and the total number of flies used for the analyses. Note that 32 flies were used for each genotype.

Table 5.6: Number of rhythmic mutant flies in LL

Note that 5 in 31 represents five rhythmic flies out of thirty-one used for the analyses. The experiment was conducted using 32 flies for each genotype. Those flies not used for the analysis were dead by the end of the experiment.

Gene	w1118; UAS-IR	timG4>dcr2; UAS-IR	w1118; timG4>dcr2
trx	5 in 31	14 in 30	4 in 30
Kr-h1	5in 31	24 in 31	4 in 30
CG2051	2 in 30	13 in 32	4 in 30
Psc	4 in 32	9 in 28	4 in 30
Nipped-A	2 in 28	17 in 28	4 in 30

5.3.4 Locomotor activity of timG>*dcr2; UAS-nej-IR* flies in DD

The expression level of *nej* was down-regulated in clock cells using RNAi system and the circadian behaviour of the flies was characterised. In LD, the flies showed less locomotor activity (rest more during the day and low amplitude of their bimodal peaks) when compared to UAS control (Fig 5.8). The behavioural activities of *timG>dcr2; UAS-nej-IR* flies in DD and light pulse experiment could not be studied as the flies were short-lived.

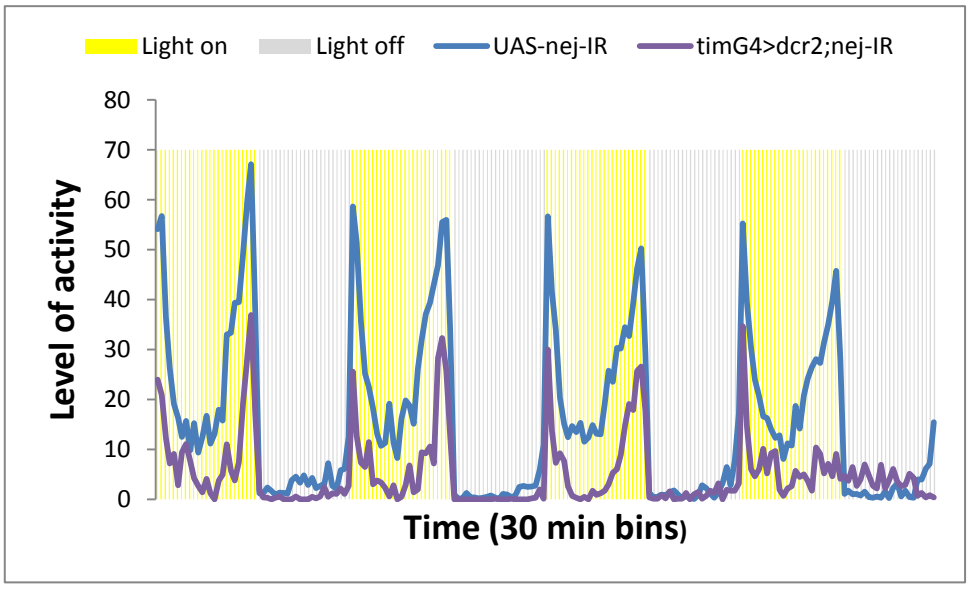

Figure 5.8: Superimposed locomotor activity of timG4>dcr2; UAS-nej-IR and UAS control flies in LD

Note the reduction in *nej* knock down flies' locomotor activity. Data was generated from 32 flies.

5.3.5 Inhibition of HDAC by sodium butyrate (NaB) attenuates light response.

To determine the role of histone deacetylation in light-induced phase shifts, NaB treated flies were stimulated by light for 30 minutes in the early

subjective night. A control experiment was performed in parallel as described in section 5.2.2. As shown in Fig 5.9, when HDAC activity was inhibited during development the flies response to light was significantly reduced. However, no significant effect in light response was seen between the control and HDAC inhibited flies during adulthood or throughout their life span.

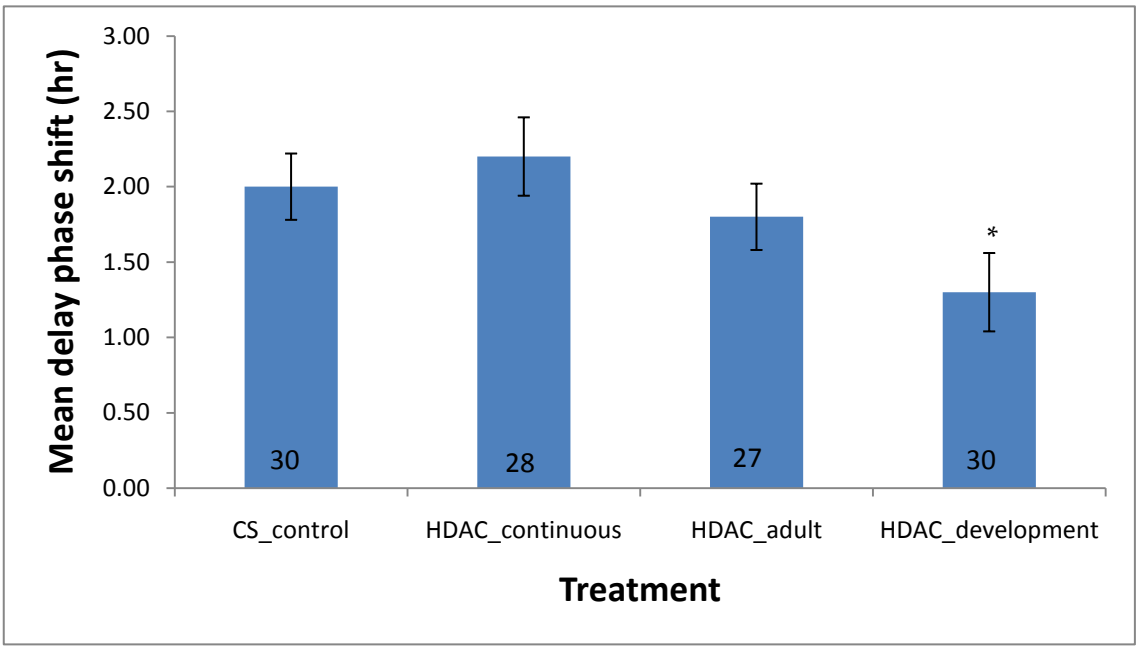

Figure 5.9: Light response of NaB-treated and control flies

The figure in the bars indicate the number of flies used and * = $p < 0.05$ from independent t test of treatment and control.

5.3.6 Free-running period of NaB-treated flies in DD

The role of HDAC in circadian clock function was investigated by studying another characteristic feature of the clock. In both the HDAC inhibited flies and the control, the free-running period in DD was determined as

described in section 2.7 of chapter 2. The results from this experiment are presented in Fig 5.10.

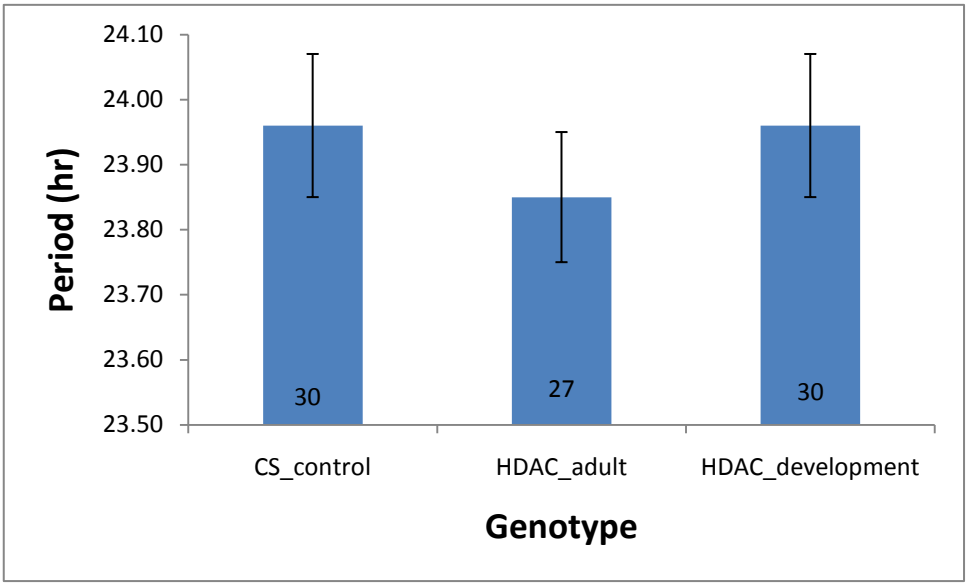

Figure 5.10: Free-running period of NaB treated and control flies

No significant difference between the treated and control from independent t test. The number of flies tested for each genotype is indicated in the bar.

5.3.7 Light on and off anticipation in NaB treated flies

A wild-type fly displays bimodal rest-activity profiles under light-dark (LD) conditions which is clock-regulated. To understand further the role of histone deacetylase in circadian clock, HDAC inhibited flies were entrained for three days in LD and left to free-run for seven days in DD. Fig 5.11 shows HDAC inhibited flies displayed a reduced or loss of morning activity peak, which was more pronounced (60%) when HDAC was inhibited during development.

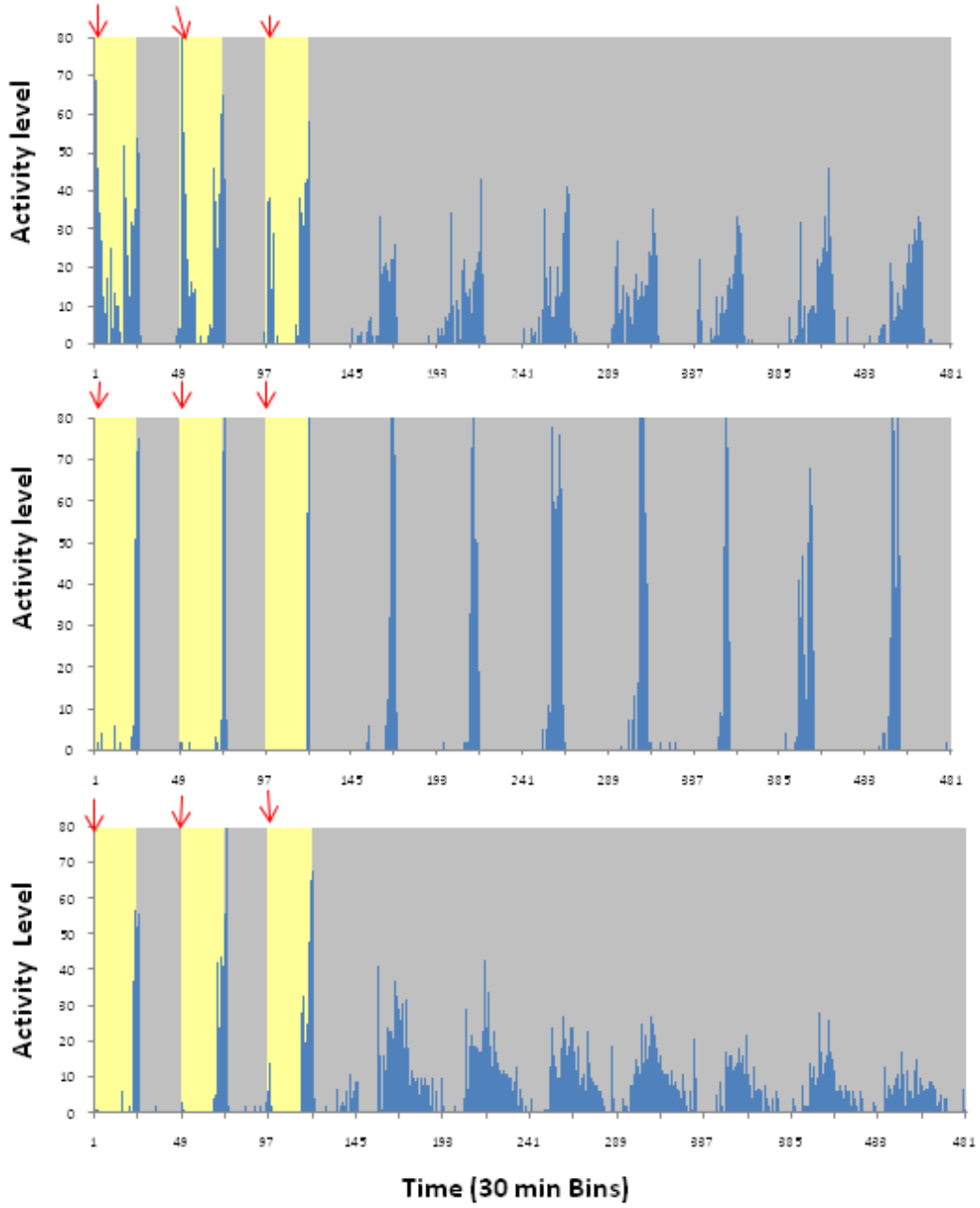

Figure 5.11: Locomotor activity of NaB-treated and control flies

The yellow bars and the grey colour indicate light phase in LD and the dark phase (in LD or DD) respectively. The red arrows show light-on and the panels: top, middle and bottom represent the control, NaB-treated flies during development and adulthood respectively.

To ascertain that the behaviour of NaB treated flies reflected clock dysfunction rather than the flies being sick, locomotor activity of HDAC and control flies was monitored in LD and their mean of activities was analysed. As presented in Fig 5.12, independent *t test* showed no significant difference in the mean activity of NaB treated and control flies in LD at $p< 0.05$.

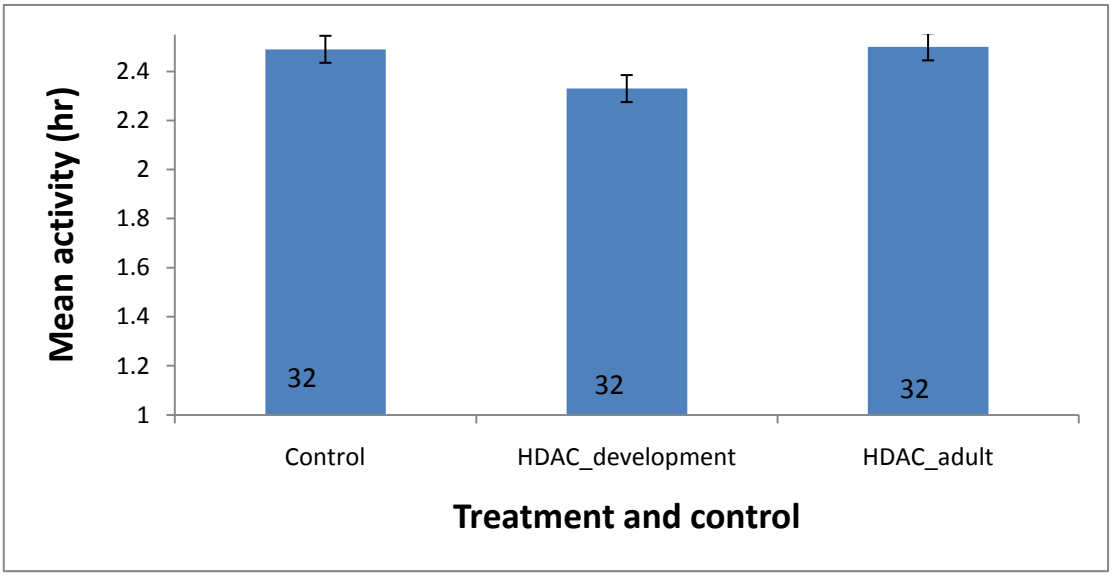

Figure 5.12: Mean activity of NaB-treated and control flies

Overall there was no significant difference (*t-test*, p =0.33) observed between the control and treated flies mean activity in LD. Note that the analyses included both flies with normal LD profile and those with missing morning peak.

5.3.8 HDAC inhibition induces changes in clock genes expression

The transcript levels of *Clk, cyc, tim, cry* and *per* in flies where the HDAC was inhibited during development were quantified at the early night by qPCR. As shown in Fig 5.13, four replicates of each of these genes showed significantly difference in expression levels in HDAC inhibited flies except *cry* which was up-regulated in HDAC inhibited flies.

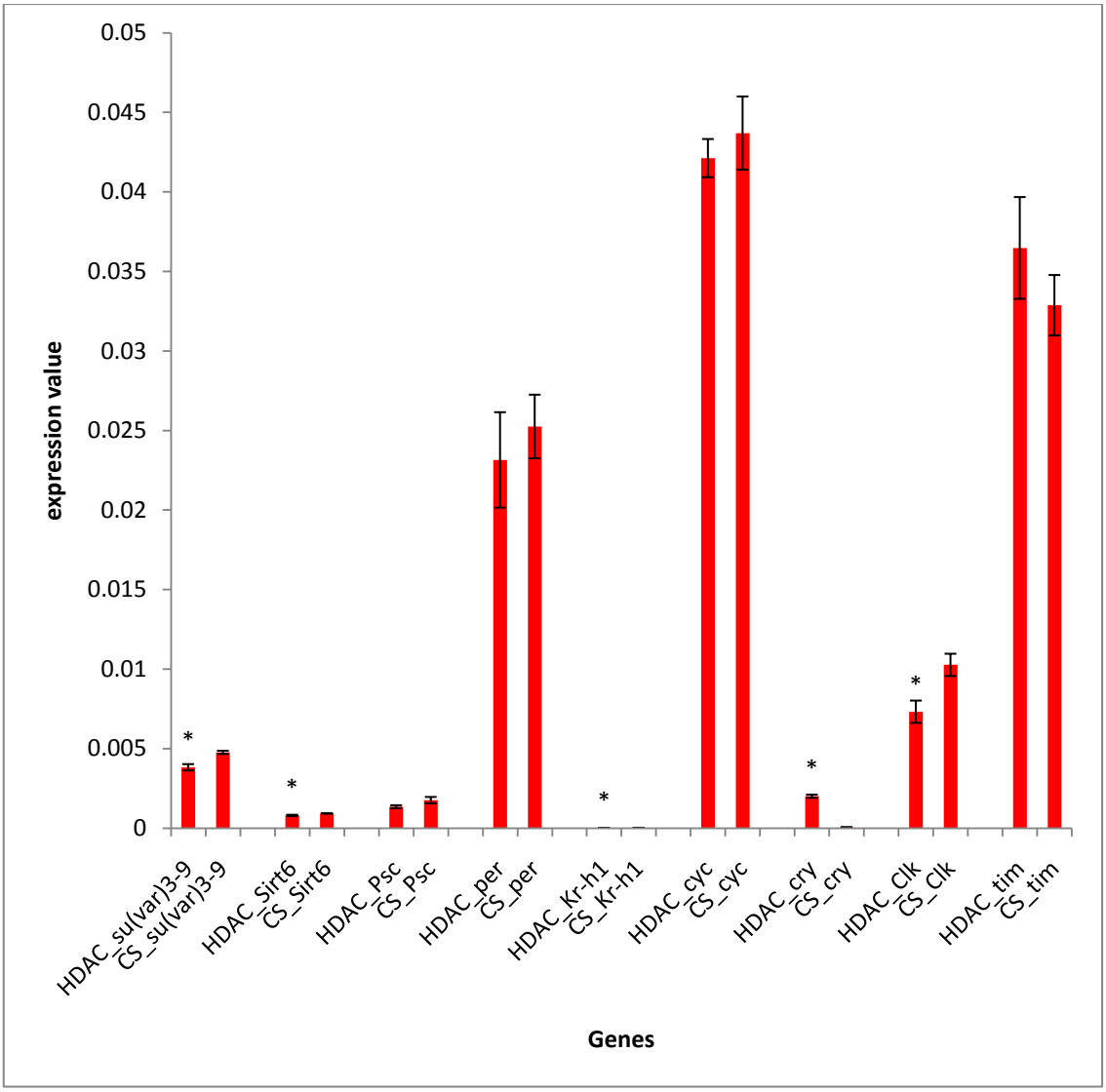

Figure 5.13: Transcription levels of clock genes in NaB treated and control flies at ZT 16.5

The transcript levels were quantified by qPCR from four replicates for each genotype.

Possible changes in dimethylation of histone H3 lysine 9 (H3K9me2) following light stimulation were tested using whole-mount ICC on adult brains (Fig. 5.14). Although the signal seems to suggest H3K9me2 modification in some of the clock cells (i.e. PDF projection to cluster of cells, which looks like DN1 and DN2), there was no clear difference in staining between light-pulsed and control flies. Intriguingly, some of the H3K9me2 staining were cytoplasmic (in mammals, this staining is usually nuclei based).

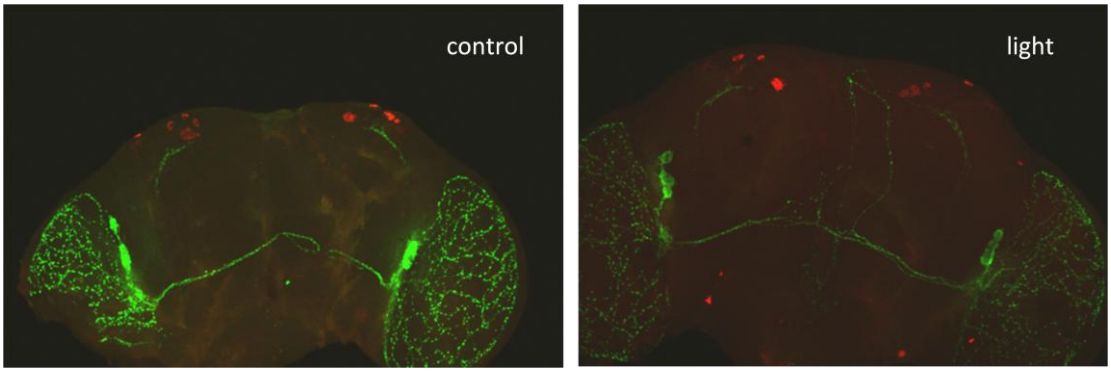

Figure 5.14: H3K9 di-methylation staining of adult brain

Two representative examples are shown: one from a fly following a light pulse (right panel) and the other from a control fly (left). See appendix 7.12 for more images. Brains were stained with ant-PDF (green) and anti-H3K9me2 (red) at 20 x magnification. Note that these images were taken on the same microscopy setting and on the same day.

ICC was also performed on whole mount brains from *Su(var)3-9*^{1} mutant and their background control flies. As previously mentioned, *Su(var)3-9* is histone lysine methyltransferases that methylates lysine 9 residue of H3 a modification associated with gene silencing. In *Su(var)3-9*-null mutants, such as *Su(var)3-9*^{1} global gene expression increases which also correlates with the reduction in the level of H3K9 methylation (Brower-Toland *et al*. 2009). As shown in Fig 5.2, *Su(var)3-9* mutant showed reduced light sensitivity. This suggests a role for H3K9 methylation in light entrainment.

Subsequent experiments were performed to study the expression levels of CRY, TIM and PDF in clock neurons of control and *Su(var)3-9* mutant flies. Images from this experiment are presented in Fig 5.15. As shown in Fig 5.15 (top panel), the expression levels of TIM within the lateral neurons and that of PDF seems reduced in the *Su(var)3-9*^{1} flies when compared with the

background control. A similar observation was seen with the immunoreactivity levels of CRY and PDF (Fig 5.15, bottom panel) in the *Su(var)3-9*^{1} flies. These observations may suggest the reduced light sensitivity in *Su(var)3-9*^{1} flies (Fig 5.2).

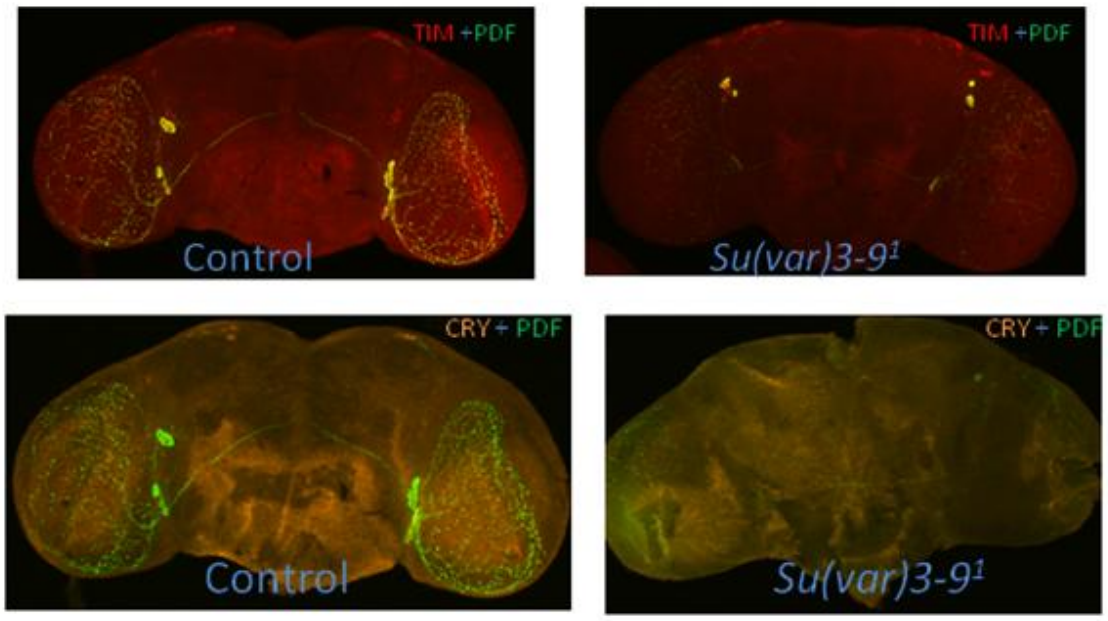

Figure 5.15: TIM, CRY and PDF expression in *Su(var)3-9*^{1} and control flies at ZT 16.5
Two representative examples are shown of TIM and CRY staining: one from a fly following a light pulse at ZT 15 (right panel) and one from a control fly (left). The ICC was performed on flies collected at ZT 16.5. See appendix 7.13 for more images. Note that the images were taken using the same microscopy setting on the same day and the yellow colour indicates co-localisation of TIM and PDF.

5.3.9 Analysis of H3K9 acetylation and dimethylation by ChIP- PCR

The pulled down DNA samples from light treated and non-treated samples using H3K9 acetylation and H3K9 dimethylation specific antibodies were amplified by ChIP-PCR (Fig 5.16). Out of the six different regions tested in *per* and *tim*, only the circadian regulatory sequence (CRS) region in *per* (per CRS

see *section* 5.2.6) showed a band from H3K9 acetylation pulled-down sample in the non-treated sample compared with light-pulsed. This is indicated with the black arrow on Fig 5.16. This band might be overspill from lane 2, the experiment needs to be replicated with more samples in order to confirm the nature of the band.

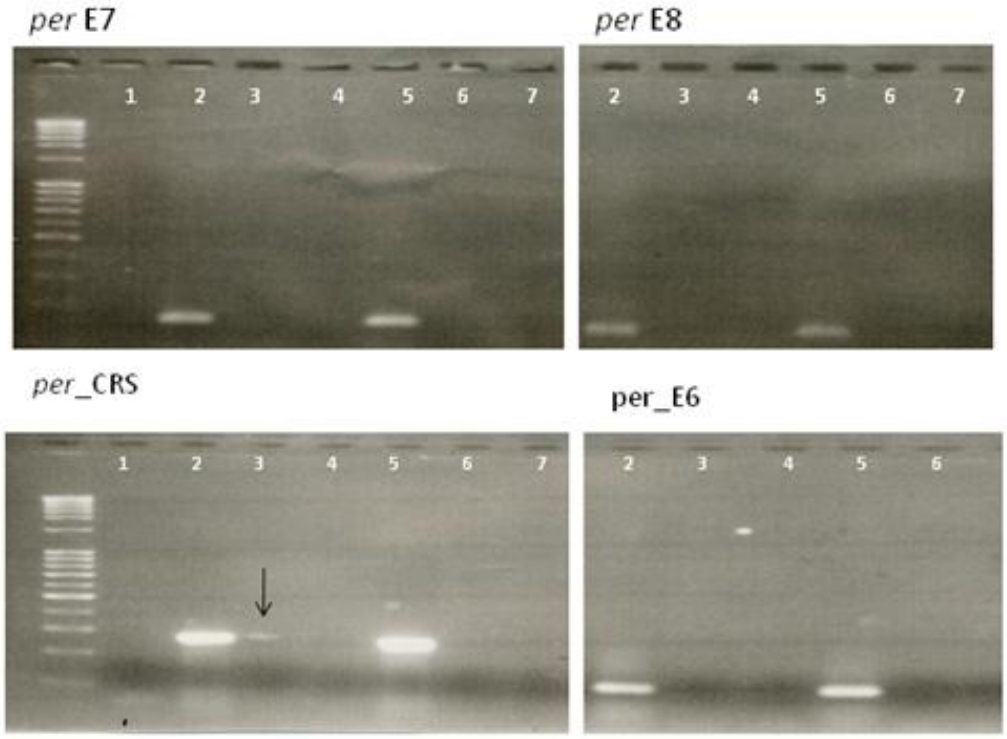

Figure 5.16: ChIP-PCR of H3K9 acetylation and dimethylation in regulatory regions of per
The black arrow indicates the suspected band of H3K9 acetylation in the control pulled-down sample. The gel loading pattern is as following: 0= DNA marker (100 bp), 1= water control, 2= non-pulsed input DNA, 3 = non-pulsed H3K9acetyl pulled DNA, 4= non-pulsed H3K9dimethyl pulled DNA, 5 = light-pulsed input DNA, 6 light-pulsed H3K9acetyl pulled DNA, 7= light-pulsed H3K9dimethyl pulled DNA.
See Table 5.5 for primers information.

5.3.10 qPCR of CLK-CYC driven transcripts

In addition to the microarray data (chapter 4), qPCR of the core known CLK-CYC driven transcripts was performed on four replicates of total RNA from each condition(light-pulsed and non-treated) flies. The aim of this experiment was to investigate the role of light stimulation on CLK-CYC mediated transcription. As shown in Fig 5.17, the expression levels of *tim*, *per*, and *vri* were down-regulated in response to light, which was consistent with the microarray data (chapter 4) for at least *per*.

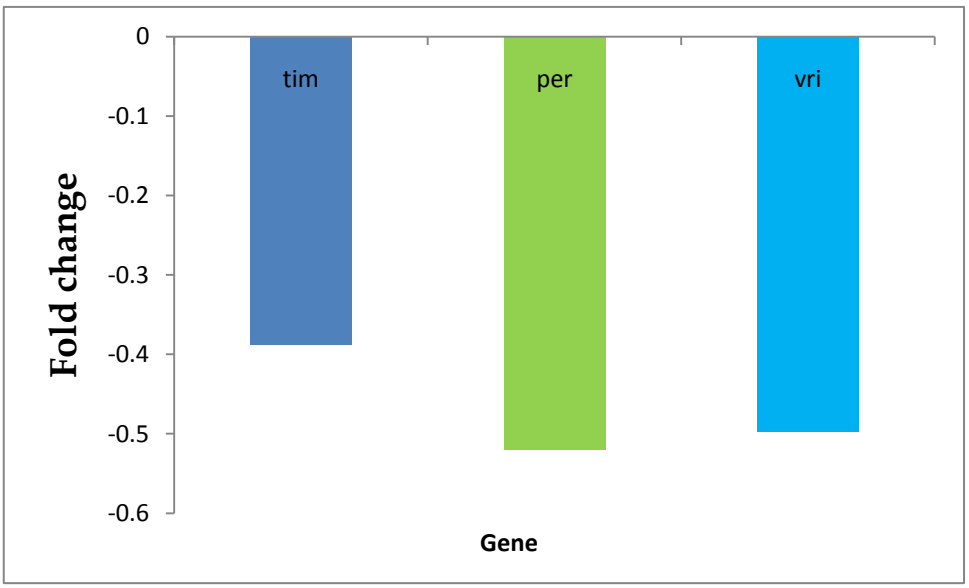

Figure 5.17: Light-induced differentially expressed CLK-CYC driven transcripts

Note that the genes expression levels were down-regulated in light stimulated flies.

5.4 Discussion

This study aimed at examining a possible role of histone modifications in circadian light entrainment, since genes associated with this function were over-represented among the light-induced differential expression transcripts (chapter 4). Most of the experiments described here were not replicated enough to allow quantitative testing of the hypotheses and should be considered as suggestive hints for future research.

The effect of light stimulation on histone modification was first observed in mouse SCN, where light pulse caused phosphorylation of ser 10 in H3, though no connection was made with the circadian feedback loops (Crosio *et al*. 2000). In this study, light stimulation was proposed to mediate histone modifications which alter chromatin structure to either allow or block binding of transcription factors that regulate circadian clock genes. The microarray data (chapter 4) alluded to suggest that light pulse seems to down-regulate genes associated with active chromatin structure (gene activation) or up-regulate those linked with compact structure (gene repression). To put it in another way, light pulse at early night seems to inhibit histone modifications such as acetylation and H3K4 methylation and activates repressive histone marks such as H3-K9 methylation and histone deacetylation.

To investigate these observations, two experimental approaches were taken: native chromatin immunoprecipitation (nChIP) and ICC. The nChIP was

used to probe for possible variation in H3-K9me2 and H3-K9acetyl modification in light -pulsed and non-treated samples at ZT 15. The result showed a suspected band in H3K9 acetylation pulled-down at *per*_CRS (~ 500 bp upstream of the *per* transcriptional start (Hao *et al*. 1999) in non-treated flies. As this experiment was not replicated, the band could be taken as overspill from the neighbouring lane.

Previous studies have shown that CLK-CYC binding to the CRS E-box of *per,* is necessary and sufficient to drive *per* expression at a high amplitude in *vivo* (Yu *et al*. 2006). In addition, Taylor and Hardin (2008) have recently shown H3K9 acetylation of *per* CRS in LD peaks at ZT 10 which coincides with the transcription activation of *per* by CLK-CYC. A similar observation has been reported in mammals, in which *per1* activation coincides with H3 acetylation (Curtis *et al*. 2004; Doi *et al*. 2006; Naruse *et al*. 2004).

In another line of experiments, ICC was performed with H3-K9me2 antibody Fig 5.14. There seems to be no apparent difference in the staining intensity and density between the samples. In addition, some of the stains appeared to be cytoplasmic, which is contrary to the expected nucleus- based activity of H3-K9me2. It is possible that the antibodies cross-react to a cytoplasm antigen, which make it difficult to draw any strong conclusion from this set of results

5.4.1 CLK-CYC transcriptional activity is facilitated by histone modifications

If the assumption that light mediates histone modifications still holds, genes regulated by CLK-CYC should be differentially expressed in response to a light pulse. To test this assumption the transcript levels of *per, tim, cry* and *vri* were quantified in a wild-type fly (CS) an hour after light pulse at ZT 15 by qPCR. As shown in Fig 5.17, the expression levels of these genes were down-regulated in response to light pulse. This result suggests that light affects the core clock genes at transcriptional level as opposed to the commonly held view that the light effect is only post-translational (Hunter-Ensor *et al*. 1996). It also indicates possible light-induced interference on CLK-CYC activity which is known to activate the expression of these genes (i.e PER-TIM balance the effect on CLK-CYC).

As reviewed in section 1.4 and 1.8 of chapter 1, the mechanism regulating the repressive activity of PER/PER-TIM and the stimulation of CLK-CYC driven expression are not fully understood. While the current molecular light entrainment mechanisms partly explain the observed down-regulation of *per*, the mechanism underlying PER or PER-TIM dependent repression of *Clk* driven transcription still remain a mystery. In addition, the model could not explain the observed down-regulation of *per*, *tim* and *vri* transcripts in response to light stimulation at early subjective night. Hence, the need for alternative

models of molecular light entrainment mechanisms that account for the role of transcripts and proteins in molecular resetting of the clock is apparent.

5.4.2 Histone acetylation mediates CLK-CYC transcriptional activity

Accumulated evidence has shown that mouse CLK possess an enzymatic HAT activity, a possible driving mechanism of its circadian clock function (Doi *et al*. 2006). dCLK contains the putative acetyl-CoA binding mofit but lacks the five extra amino acids found in the vertebrate counterparts (Doi *et al*. 2006). These extra amino acids increase mCLK sequence similarity to other HAT proteins such as yeast *Esa1,* hence its functional HAT role (Doi *et al*. 2006). On the basis of this observation dCLK lacks HAT activity but may likely bind other HAT proteins to activate gene transcription.

In *Drosophila,* one possible candidate for a HAT is *nej* - a CBP ortholog that acts as a transcription co-activator via its histone acetyltransferase activity (Das *et al*. 2009; Hung *et al*. 2007). Experimental data from recent studies indicate that NEJ physically interacts with CLK and CLK-CYC through two of its binding sites (Hung *et al*. 2007). I hypothesised that NEJ's binding to CLK-CYC enables the complex to perform HAT activity, thereby activating the expression of E-box containing clock genes. Results from chapter 4 indicated that light stimulation down-regulates *nej* expression which correlates well with down-regulation of dCLK-driven transcription (Fig 5.17).

To test this prediction, *nej* expression in the adult fly clock cells was down-regulated using *timGal4*. The assumption was: if *nej* expression is essential for functional circadian clock, reducing its expression level should affect clock parameters such as light entrainment and period. Unfortunately, neither a light pulse nor the free-running experiment could be completed on F1 progeny owing to their extreme short lifespan (less than 10 days) at 25^0C. Earlier studies have shown that loss of function of *nej* in flies leads to embryonic lethality (Hung *et al*. 2007). Despite the limited expression using *timGal4,* flies carrying UAS-*nej*-IR have reduced locomotor activity (Fig 5.8) and longevity. In addition, flies that were monitored in DD exhibit arrhythmic locomotor activity (from 3 DD data) but more data is required to establish this observation as most of the flies died shortly after the first three days. It is not clear what the cause of this lethality was but one possibility could be stress of DD as the flies seems fine in LD.

Furthermore, over-expression of *nej* has been shown to increase loss of behavioural and molecular rhythms in flies (Hung *et al*. 2007). Results from in *vivo* studies have also shown that by inhibiting the expression of *nej,* CLK-CYC dependent transcription activity was reduced (Hung *et al*. 2007). On the basis of these observations, alteration of *nej* expression likely results in dysfunction of the clock. The observation also suggests that *nej* is necessary for CLK-CYC driven transcription activity and the maintenance of the feedback loops. Hence,

reduction in its expression level in response to light pulse could explain the down-regulation of CLK-CYC driven transcription of genes such as *per.*

5.4.3 H3 Lys 4 methylation activity reduces circadian light response

Trithorax (t*rx*) another down-regulated transcript in response to light has been shown to interact with *nej* in *Drosophila* (Tie *et al*. 2009). *trx* contains a SET domain and specifically catalyses the trimethylation of H3 on lysine 4. This modification is shown to be associated with the promoter region of active genes (Barski *et al*. 2007; Smith *et al*. 2004). *trx* interaction with *nej* has been shown to prevent polycomb- mediated gene silencing by inhibiting H3 Lys 27 trimethylation (Tie *et al*. 2009). To test the role of *trx* in clock function, *trx* expression was down-regulated in *tim*-expressing cells using *timGal4-dicer2*. As shown in Fig 5.1, knockdown of *trx* expression was associated with significantly reduced light response. Furthermore, flies carrying UAS- *trx*-IR (driven by t*im*Gal4-*dicer2*) showed a significantly longer activity period in DD (Fig 5.5). In contrast, over-expression of *trx* (EP line) in clock cells significantly reduced the flies' free-running period when compared to *trx* knockdown flies (Fig 5.6). These results suggest a possible role for *trx* in the circadian clock, perhaps by forming a complex with CLK-CYC_NEJ. The interaction of TRX and NEJ in response to light stimulation may be confirmed using methods such as yeast two-hybrid, glutathione *S*-transferase (GST) pull-down assays.

5.4.4 *Nipped-A*: a putative HAT

Nipped-A is a fly homologue of yeast *Tral* and human TRRAP that acts as transcriptional co-activator in chromatin-modelling complex. *Nipped-A* expression was down-regulated in response to light pulse (chapter 4). Flies carrying *timG4>dcr2*; UAS-*Nipped-A*-IR, showed the weakest light response and significant difference from the control as seen by the magnitude of their phase shift (Fig 5.1). In addition, their free-run period in DD was significantly longer and in LL about 60% of these flies displayed rhythmic activity as compared to 15% in the controls (Fig 5.7). However, this phenotype was not seen in *Nipped-A* mutant strain, this may suggest defects in *tim* cells.

Nipped-A ^{KG10162} (*P*-element induced-mutation) although it is not known if the insertion results in loss of function but the record shows that it falls within the *Nipped-A* coding sequences and possibly affects another gene *d4(*Tweedie *et al. 2009)*. Similar to the RNAi knockdown, *Nipped-A* ^{KG10162} flies responded with reduced phase shifts (Fig 5.2). Strikingly, the locomotor activity of *Nipped-A* ^{KG10162} flies in DD was extremely reduced or completely abolished as shown in Fig 5.4. About 84 % of *Nipped-A* ^{KG10162} flies showed this phenotype in DD (note that the *P*-element insertion may affect *d4* so contribution of this gene to these phenotypes cannot be ruled out). Upon LD entrainment, the flies became active as soon as the light comes on and inactive again when light is turned off (Fig 5.4). In a recent study, *Nipped-A* down-

regulation was shown to block light-induced CRY and TIM degradation (Sathyanarayanan *et al*. 2008). The results from my study further support *Nipped-A* role in circadian light entrainment.

5.4.5 Histone deacetylation and methylation underlie PER-TIM auto-repressive activity

The mechanism in which PER or PER-TIM represses CLK-CYC driven transcription is still not fully understood though significant progress has been made. Several lines of evidence suggest a possible role of histone modifications associated with transcriptional repression such as deacetylation and methylation of H3-K9. Accumulated evidence has shown daily changes in chromatin structure that parallels CLK-CYC/BMAL1 activation cycle (Kadener *et al*. 2007). In mouse, for instance, CLK/BMAL1 binds rhythmically to E-box elements in the *albumin D element-binding protein* (*Dbp*) gene, which is in parallel with H3 K9 acetylation, H3K4 trimethylation and loosening of histone density (Ripperger and Schibler. 2006). Similarly, the promoters of *mPer1* and *mPer2* in mouse liver have been shown to display a rhythmic acetylation of H3 which correlates with their transcriptional activation (Etchegaray *et al*. 2006). Since acetylation of lysine is determined by a balance between HATs and HDACs, one can easily speculate a pivotal role for HDACs in PER/PER-TIM auto-repression.

5.4.6 H3K9 methylation may mediate PER/PER-TIM repressive activity

One of the microarray up-regulated genes was *suppressor of variegation 3-9* {*Su(var)3-9*} a known histone methyltransferase, which selectively methylates lysine 9 within the H3 tail (Bannister *et al*. 2001; Eskeland *et al*. 2004). This modification serves as a docking site for another well characterised heterochromatin-associated protein HP1, linking H3-K9 methylation with transcriptional repression (Fig 5.18) (Bannister *et al*. 2001). There is substantial evidence that DNA methylation acts downstream of H3K9 methylation (Jackson-Grusby *et al*. 2001; Mutskov and Felsenfeld. 2004) but the role of DNA methylation in circadian light entrainment is not known.

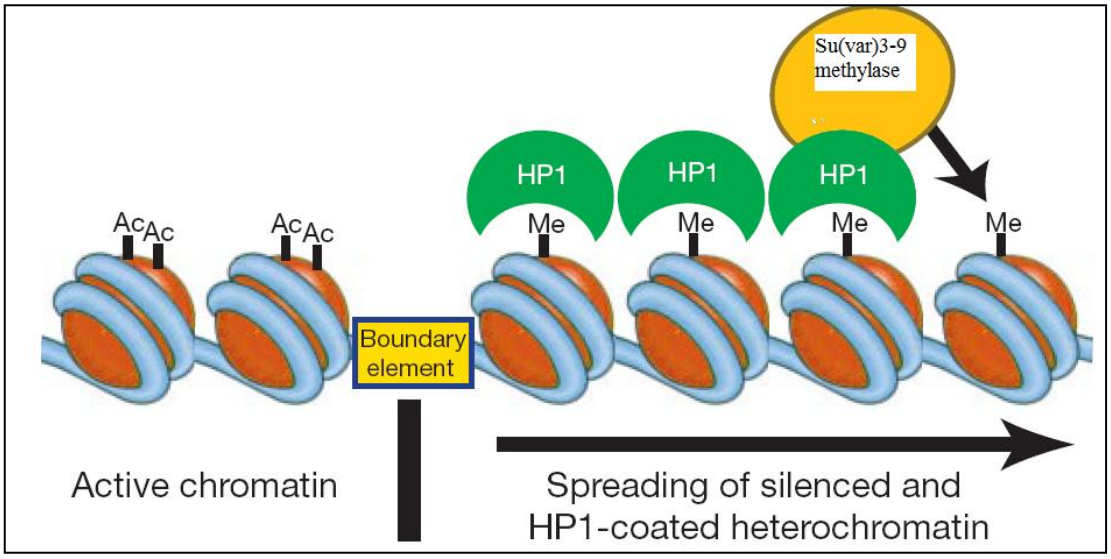

Figure 5.18: A model of *Su(var) 3-9* induced H3-K9 transcriptional silencing
Adapted from (Bannister *et al*. 2001).

Here, I tested whether H3-K9 methylation of *per* and *tim* regulatory regions may mediate PER/PER-TIM auto-repression. This probably coincides

with the translocation of PER or PER-TIM into the nucleus (Ripperger and Schibler. 2006). I examined a possible link between H3-K9 methylation and circadian clock in *Drosophila*, by testing the *Su(var) 3-9* loss-of-function(Ebert *et al*. 2004). As indicated in Fig 5.2, the light response of *su(var) 3-9*^{1} mutant flies was significantly reduced. In LL, the locomotor activity of *su(var)3-9*^{1} flies was completely arrhythmic, suggesting that this gene functions downstream of CRY in the light entrainment pathway. The expression of CRY, TIM and PDF in the mutant flies' brain was examined by ICC (although no quantitative analysis was attempted), there seems to be a reduction in the level of CRY, PDF and TIM (in LNvs) in the mutant as compared to the control flies (Fig 5.15). These results may explain the reduced light response of *Su(var) 3-9* mutants: low level of CRY may imply that less light signal reaches TIM, and the attenuated light transduction may be translated to smaller phase shifts. These observations suggest that *Su(var)3-9* plays a role in regulating CRY, TIM and PDF expression.

5.4.7 Histone deacetylases may regulate PER-TIM repressive activity

Substantial evidence suggests that HDAC complex binds mCRY1 and represses the transcription of *mPer* and *mCry* (Naruse *et al*. 2004). Also inhibition of HDAC activity by trichostatin A (TSA) activates the expression levels of m*Per1* and m*Per2* (Naruse *et al*. 2004). This leads to an increased level of H3 and H4 acetylation within m*Per1* promoter (Naruse *et al*. 2004). In *Drosophila*, neither PER nor TIM has been shown to interact with a known

HDAC. Interestingly, *Su(var)3-9* has been shown to interact with HDAC protein in *Drosophila*, which may serve as a link between PER-TIM complex and HDAC (Czermin *et al*. 2001). This interaction plays a pivotal role in *Su(var)3-9* ability to methylate acetylated histone tails(Czermin *et al*. 2001).

In examining the role of HDAC in the circadian system, both genetic and pharmacological approaches were adopted. The genetic approach involved down-regulating the expression of HDAC-associated genes (identified as differential expressed in chapter 4) and characterising their circadian phenotypes. One of these genes was *Sirt6*, which catalyses the deacetylation of H3-K9 (Kawahara *et al*. 2009). Flies carrying *tim*-Gal4>UAS-*sirt6*-IR responded less to light stimulation than their controls (Fig 5.1).

Pharmacologically, sodium butyrate was used to inhibit HDAC activity in *CS* flies at non-toxic concentration according to a previously published protocol (Xing *et al*. 2007). HDAC was inhibited at three different stages: during development, at adulthood and for the entire life span. When HDAC was inhibited during development, the flies showed a significant reduction in light response (Fig 5.9). This suggests that the drug has more effect during this stage and perhaps affects the development of photoreceptors or central clock cells. Intriguingly, there was no significant difference in light response between the control and HDAC inhibited flies (treated continuously or at adulthood). This may suggest that the potency of the drug drops as the fly develops or

compensatory phenomena arising when the inhibition was carried out throughout the development of the organism.

Although the free-running period of HDAC-inhibited flies did not differ from their controls (Fig 5.10), their locomotor activity profiles in LD did differ (Fig 5.11). The morning peak of activity was reduced or absent in many of the flies; 60% in HDAC inhibited during development and 42% of flies treated at adulthood. Analysis of the mean level of activity in these flies (including the percentage that has normal LD profile) as shown in Fig 5.12, showed no significant difference between the control and the treated flies, which suggest disruption of clock rather than flies being sick.

This reduced or absent of morning peak in LD is similar to the phenotype associated with PDF dysfunction due to a mutation in the *Pdf/ Pdfr* gene, or ablation of PDF neurons (Zhang *et al*. 2009). It is possible that HDAC activity is silencing the PDF-positive cells as this group of cells are shown to regulate morning bouts of activity in flies in LD (Grima *et al*. 2004; Stoleru *et al*. 2005). This result may also suggest a pivotal role for HDAC in intracellular communication in the circadian clock and in particular light entrainment.

HDAC activity can have a profound effect on gene expression, either driving up-regulation (Chou and Chen. 2008) or downregulation (Manabe *et al*. 2008). qPCR analysis of HDAC inhibited flies showed that the levels of *Sirt6*, a

known HDAC, were reduced (Fig 5.13). The expression of the four other genes (*Clk*, *Su(var)3-9, Kr-h1* and *cry*) were significantly different than that of the control flies (Fig 5.13). The significant up-regulation of *cry* expression in NaB treated flies, is interesting and may suggest a different regulation mechanism for *cry* expression. As previously discussed, the expression level of CRY was reduced in *Su(var)3-9* mutant flies arguing against H3K9 methylation inhibition but rather indicating a different repression mechanism. Perhaps, *cry* expression is under the influence of HDAC and when HDAC activity was inhibited, *cry* regulatory region becomes hyperacetylated hence activates its transcription.

Interestingly, the expression level of *Clk* was down-regulated when HDAC was inhibited; suggesting that transcription of *Clk* is regulated by histone deacetylase. The current model of *Clk* expression is through the binding of PER-TIM complex to CLK-CYC, this represses their own transcription and activates *Clk* expression *(Glossop et al. 2003)*. The results from this study, suggest that PER/ PER-TIM repressive activity may be mediated through histone deacetylation.

The other candidate genes which deserve discussion include *Posterior sex combs* (*Psc*), *CG2051* and *Kruppel homolog1* (*Kr-h1*). *Psc* is a component of polycomb repressive complex 1 (PRC-1), which is essential for polycomb group-mediated gene silencing. It has been shown to be sufficient for chromatin compaction, inhibition of remodelling and transcription (Francis *et al*. 2004; Lo

et al. 2009). In the current study, the light pulse up-regulates the expression level of *Psc* (see chapter 4). As shown in Fig 5.1, when *Psc* expression was down-regulated in clock neurons, the flies light response was significantly reduced. A similar effect was observed in *Psc* mutant flies (Fig 5.2). In contrast, over-expressing *Psc* in the same set of clock neurons increased light response significantly as shown in Fig 4.4 of chapter 4. In addition, down-regulating *Psc* in the clock neurons lengthens the free-running period of the flies (Fig 5.5).

Kr-h1 is a known transcription factor, whose expression level was down-regulated in response to light stimulation during the early night (chapter 4). When knocked-down in fly *tim*-expressing cells, the light response of the fly was significantly reduced (Fig 5.1). However, $Kr\text{-}h1^{KG00354}$ mutant flies showed no significant difference in their response to light (Fig 5.2). The role of this gene in circadian clock is not clear but previous studies suggested *Kr-h1* acts in neuronal development (Minakuchi *et al*. 2009; Shi *et al*. 2007).

The expression level of *CG2051* was up-regulated in response to light (chapter 4). *CG2051* possesses HAT activity based on amino acid sequence similarity to HAT1 and is thought to catalyse H4K12 and H4K5 acetylation (Allis *et al*. 2007). It is also known to be involved in histone deposition on newly synthesised DNA and in DNA repair (Allis *et al*. 2007). The results in this study, suggest that *CG2051* may be involved in circadian clock as down-regulation of this gene in the clock neurons reduced the fly's light response (Fig 5.1). Over-

expression of *CG2051* in the same set of clock neurons also drastically reduced fly's light response (Fig 4.4 of chapter 4) and longer free-running period than the knockdown flies (Fig 5.6).

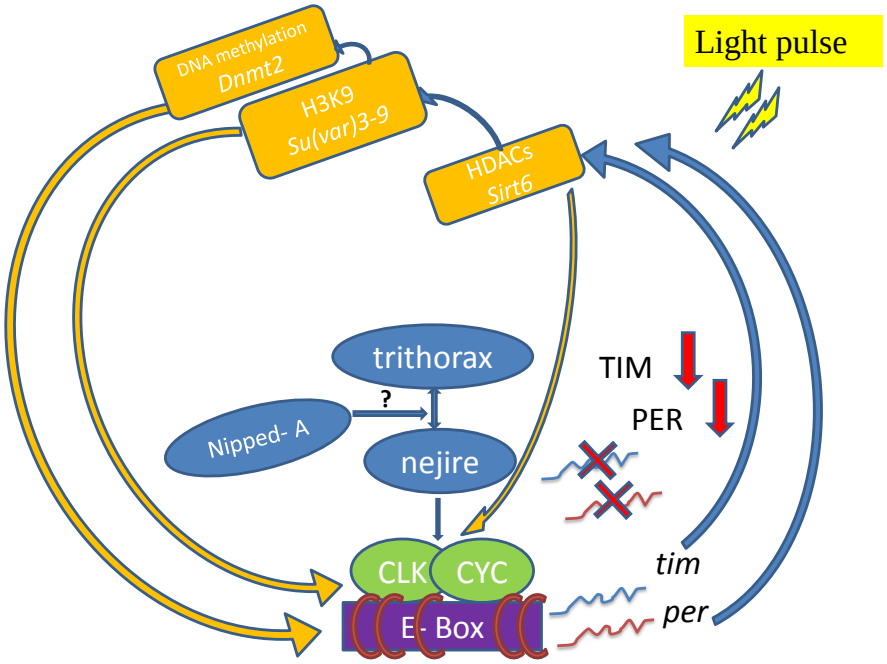

Figure 5.19: A model of circadian light response regulation by histone modifications
The blue ovals and golden rectangles represent light activated and repressed transcripts respectively. The proposal in this model is that TRX binds NEJ, the complex then binds CLK-CYC to drive the expression of E-box clock genes such as *tim, per* via acetylation but in response to light stimulation deacetylation and H3K9 methylation take over resulting in inhibition of these clock gene expression.

In summary, experiments performed in this study indicate a role for histone modifications in light entrainment of the *Drosophila* clock, and complex interactions among different histone modifications (Fig 5.19).

Chapter 6: General discussion

In this thesis, I have used QTL mapping and whole genome expression profiling to identify candidate genes and biological pathways affecting circadian light entrainment in Drosophila. During the course of this study, an important role of histone modifications in the circadian clock particularly in response to light stimulation emerged (chapter 5). The results of this study suggest a complex genetic architecture for light entrainment as several genomic regions and extensive variation in gene expression underlie this trait. This complexity may reflect the involvement and interactions of multiple mechanisms in modulating light entrainment. Figure 6.1 presents a model that summarises the findings of the current work and suggests how these multiple mechanisms may be integrated. This figure shows that light stimulation induces changes in gene expression which affect the cell ionic balance (such as calcium flux), post-translational modifications (e.g phosphorylation) and epigenetic modifications. These effects mediate light-induced phase shifts in many organisms. Interestingly, findings from both the natural population and a laboratory wild-type strain were consistent and substantiate the proposed model. Some of these observations are explained in the remaining paragraphs of this chapter.

The combination of QTL mapping and deficiency complementation mapping with expression studies proved successful in identifying candidate

genes involved in circadian photoentrainment. The major QTL (chromosome 2) was further narrowed down using deficiency complementation mapping into two smaller regions spanning 140 candidate genes. This includes genes involved in various functions such as intracellular signalling cascades (*CG34393*, *Mothers against dpp*, *cornichon-related*, *Rab-protein 5, anterior open*) and glutamate related functions (*vesicular glutamate transporter*, *Rab-protein* 5, *anterior open and Glutamate oxaloacetate transaminase 2*), which play critical roles in this model (Fig 6.1). In another set of experiments, complementation tests were performed using mutants of some of the known clock genes within the QTL regions. The results from this experiemnt suggest a possible segrgration of *tim* and *cyc* alleles in the RI lines but not of *Clk* and *Thor.* Interestingly, random genotype for *tim* alleles (*s-tim* and *ls-tim*) known to affect light response confirmed its presence in these lines. However, it is possible that other unknown *tim* alleles associating with light sensitivity exist or the presence of other gene alleles that interact with the known *tim* alleles in this population.

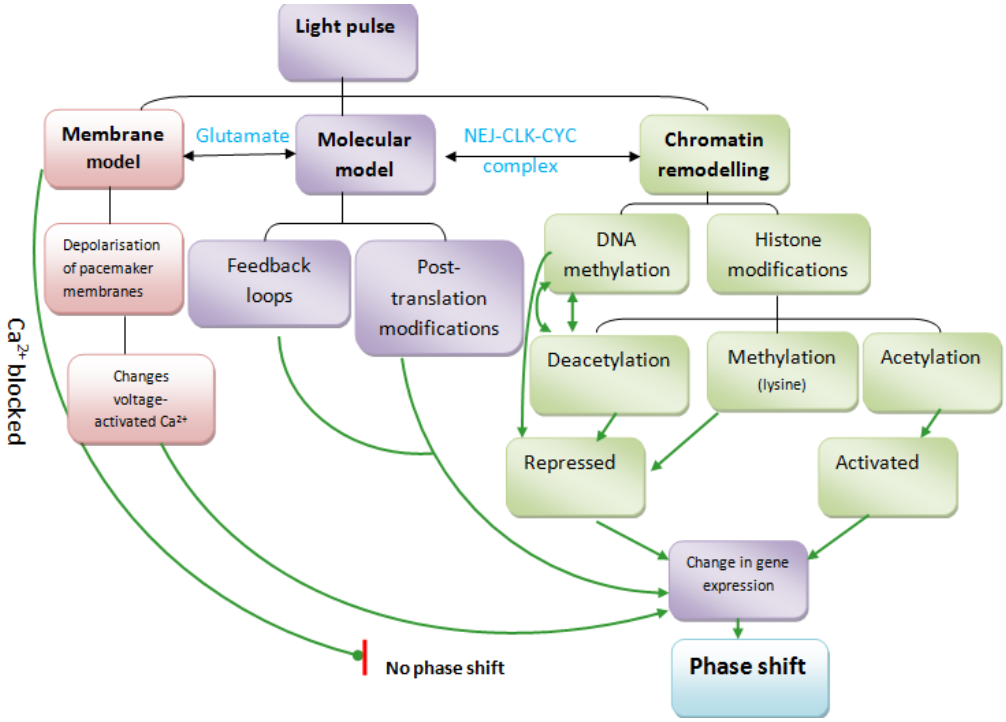

Figure 6.1: A proposed light entrainment model in Drosophila

See text in the chapter 4 and 5 for more details.

The ability of cells to detect extracellular signals and execute the appropriate response is essential for all cellular functions. Intracellular signalling cascades are activated in response to stimuli such as light, and require activating or repressing defined sets of genes. Although not all the intracellular signals are linked to the circadian clock, a few have however been implicated (Akashi and Nishida. 2000; Oh-hashi *et al*. 2002). In mammals for instance, light stimulation increases intracellular calcium levels (Khalsa and Block. 1988), which elicits immediate expression of *Per1* mRNA, suggesting the involvement of a Ca^{2+} signal-transduction pathway in resetting the clock (Balsalobre *et al*. 2000). Interestingly, a few of the genes identified by the microarray profiling in chapter 4, such as *sif* and *Hr38* are also involved in

intracellular signalling (Tweedie *et al*. 2009). When the expression of *sif* and *Hr38* were down-regulated in clock cells, the light response was significantly reduced in comparison with control flies (Fig 4.4). This may signify a role for intracellular signalling in circadian light entrainment. It is therefore possible that natural alleles of the intracellular signalling candidate genes contribute to the extensive variation in light response within this population (just as do natural variants of *timeless).*

In addition, some of these signalling pathways have also been shown to modulate the proposed light entrainment model. For instance, mitogen-activated protein (MAP) kinase /Ras pathways interact with the components of the clock membrane model regulating its calcium dynamics. The same is true of the molecular feedback model where MAPK regulates PDF signalling (Williams *et al*. 2001) and histone modifications (reviewed in Cheung *et al*. 2000; Clayton *et al*. 2000).

Another well-represented pathway relates to glutamate, which is the main neurotransmitter mediating light signal to the SCN in mammals (reviewed in Ebling. 1996). Furthermore, blocking glutamatergic transmission in the SCN was shown to inhibit light-induced phase shift (Abe *et al*. 1991). Although glutamate has not been functionally identified as a clock neurotransmitter in *Drosophila*, its presence in some of the clock neurons suggests a similar role. For instance, *vesicular glutamate transporter,* one of the

candidate genes associated with glutamate functions is expressed in larval DN1s and some subsets of DN1s and DN3s in adult (Hamasaka *et al*. 2007). This observation suggests that these neurons utilise glutamate as a neurotransmitter (Ding *et al*. 1997; Hamasaka *et al*. 2007). As indicated in the model (Fig 6.1), glutamate seems to transmit signals between the membrane (Njus *et al*. 1974) and the molecular circuit of the clock.

Accumulating evidence has shown that DN1s and DN3s communicate with the sLNvs and modulate its output (Hamasaka *et al*. 2007; Zhang *et al*. 2010). This suggests another possible means of interaction between the membrane and molecular models. Previous studies have also shown that some of these neurons contribute to LD entrainment via CRY (Veleri *et al*. 2003). However, the molecular oscillations in DN3 were still synchronised in a double $glass^{60j}$ cry^{b} mutation suggesting the presence of an unknown photoreceptor (Veleri *et al*. 2003). Since glutamate has been shown to mediate light response in SCN, it is likely to perform a similar function in DN3s. Hence, allelic variations in glutamate related genes might contribute to variation in light response within natural populations.

Another experimental strategy used in this study was to combine QTL mapping with whole genome expression profiling. The rationale behind this approach was based on the understanding that an expression difference may occur in a gene that is not itself polymorphic but contribute to the phenotypic

difference in a population (Toma *et al*. 2002). Hence a QTL mapping approach alone would neither detect the contribution of such a gene to the phenotypic variation nor identify the gene. As reported in chapter 3, extensive variation in light-induced gene expression and the represented biological pathways were observed in the 58 and 104 RI lines. Further analyses identified the expression of *lilli* and *CG9879* in response to light stimulation to be significantly different between the lines (chapter 3).

Lilli is reported to function in the Ras/MAPK pathway as well as in compound eye development (Wittwer *et al*. 2001). It has also been reported to interact with several proteins most of which are involved in signalling pathways and photoreceptor development (Sims *et al*. 2006). Some of these proteins have previously been implicated in the circadian clock such as *shaggy* and *nejire* (Hung *et al*. 2007; Martinek *et al*. 2001).

The microarray experiment (chapter 4) revealed a high number of differential genes involved in several biological processes. The enrichment of genes associated with the glutamate receptor, cellular communication, ion channel and transport and enzymatic chromatin remodelling underscores the role of intracellular signalling and chromatin modifications in the circadian light response of *Drosophila*. For instance, *Nf1* positively regulates GTPase-activity and Ca^{2+} level (Dasgupta *et al*. 2003; Williams *et al*. 2001), down-regulating *Nf1* in clock cells reduces circadian light sensitivity (see chapter 4).

In chapter 5, the role of histone modifications in circadian photoentrainment was investigated. Previous studies, mostly in mouse, have reported the involvement of histone methylation, acetylation and deacetylation in circadian molecular machinery (Doi *et al*. 2006; Etchegaray *et al*. 2006). One of the striking observations in this chapter is that light stimulation during the early night represses histone modifications associated with activation of gene expression and induces modifications linked to gene inactivation. This was consistent with a report that light induces chromatin modifications in mammalian clock cells (Crosio *et al*. 2000).

The change in expression of circadian regulated genes such as *per*, *tim* and *vri* (chapter 5 Fig 5.7) may suggest that light-induced acetylation of histones during the early night modulates the binding to E-box targets in these genes, more data are required to ascertain this observation. Recently, mammalian CLK has being shown to exhibit HAT activity and a correlation has been identified between the activation of CLK-BMAL1 –controlled clock genes and the oscillation of histone acetylation (Doi *et al*. 2006; Kadener *et al*. 2007). Although dCLK is known not to have HAT activity, it directly interacts with NEJ which has HAT activity (Hung *et al*. 2007). This interaction appears crucial for the function of the circadian clock, as down-regulation of *nej* in clock cells seems to disrupt clock oscillations (see chapter 5). Further studies such as *nej* spatial location within the clock cells and its role in histone modifications are

required to support its roles in histone acetylation and dCLK-CYC driven transcription. It would also be useful to probe the interaction of CLK-NEJ, CYC-NEJ, NEJ-TRX in response to light stimulation using assays such as yeast two-hybrid, glutathione *S*-transferase (GST) pull-down.

Furthermore, the combined activities of histone methylation and deacetylation were proposed to underlie PER-TIM auto-regulation. An intriguing possibility is that histone modification does not only regulate light entrainment but also modulates the molecular oscillation of the clock.

It may also be useful to revisit the membrane model of circadian clock first proposed by Njus and colleagues (1974) for its likely involvement in light entrainment. This model is based on feedback interactions between transmembrane ion gradients and the activities of ion transport channels. Studies in *Drosophila* strongly support this model (reviewed in Nitabach *et al*. 2005). For instance, the free-running oscillations were shown to depend on the ability of the neuronal membrane of clock cells to depolarise, thereby activating voltage-gated ionic conductance but not depending on action potential from the neuronal outputs (Nitabach *et al*. 2002; Nitabach *et al*. 2005). For example, when the influx of calcium ion was blocked in *Bulla gouldiana*, phase shift was inhibited (Khalsa and Block. 1988). This is similar to the observation in *Drosophila* where K^+ channel-mediated electrical silencing increases

arrhythmicity (Nitabach *et al*. 2002), indicating that cellular communication modulated by ion channels is essential for a functional clock.

One of the factors that confront organisms' survival and fitness is environmental conditions (reviewed in Angers *et al*. 2010). Most living organisms have devised measures to avoid unfavourable conditions. Such measures include: individual genetic variability, physiological homeostasis, and in most cases by modifying their phenotype (reviewed in Angers *et al*. 2010). Phenotypic variation may result from previously silent genetic determinants (Rutherford and Lindquist. 1998) or epigenetic variation in response to environmental stress or developmental stimuli (reviewed in Jablonka and Raz. 2009; Sollars *et al*. 2003). Epigenetic changes have been shown to contribute to environmentally-induced phenotypic variation by modifying gene or gene pathway expression (reviewed in McGowan *et al*. 2008). For instance, the differences in disease susceptibility among monozygotic twins (MZ) have been linked to epigenetic changes. These changes are thought to accumulate from exposure to different environmental conditions over their lifetime and become more distinct in older MZ (Fraga *et al*. 2005).

For instance, a mutation at the *Colourless non-ripening* (*Cnr*) gene in tomato results in the mature fruits being colourless (Manning *et al*. 2006). It was shown that cytosines at the promoter region of *Cnr* individuals were extensively methylated whereas they were largely unmethylated in the wild-

type (Manning *et al*. 2006). The A^{vy} allele at the *agouti* locus in mouse exhibits a variable degree of expression that is linked to the level of methylation of a transposable element inserted upstream of the *agouti* gene (reviewed in Angers *et al*. 2010; Morgan *et al*. 1999). When the transposable element is hypomethylated across cells, A^{vy} is ectopically expressed, resulting in more yellow coat colour and when hypermethylated, the expression and coat colour are normal (reviewed in Angers *et al*. 2010).

Mounting evidence indicates that epigenetic changes are sensitive to environmental factors such as light (Charron *et al*. 2009; Crosio *et al*. 2000), maternal behaviour, diet (reviewed in McGowan *et al*. 2008) and are heritable (reviewed in Jablonka and Raz. 2009). Light was also shown to induce histone modifications, indicating that light-induced epigenetic modifications can contribute to light response (Charron *et al*. 2009; Crosio *et al*. 2000). In addition to the conventional genetic sources of variation, other heritable forms may contribute to the extensive variation in light response within this population. It is therefore possible that epigenetic induced variation occurs in the parental lines that were used to generate the RI lines, which may be inherited by some of these RI lines. Further experiments such as profiling various histone modifications and DNA methylation in the parental lines and the RI and correlating this with their light response may shed some light on this hypothesis.

The results described in the current study may be consolidated by a number of experiments. For example, finer complementation tests could be performed if smaller deficiency regions were available. Also by reversing the crossing scheme (mating virgin female from RIL with male of the deficiency lines) the subtle effect seen in light response such as 6875, 8082 of Fig 3.5 may be avoided. As the X-chromosomal background would be the same in the F1 progeny phenotyped for light response. This study would also benefit from availability of more null mutant strains of the positional candidate genes within the QTL. In addition, increasing the number of molecular markers might contribute to a higher resolution of QTL and ease the process of its fine-mapping. Furthermore, this study will also benefit from the ongoing effort to mutate all fly genes such as the Berkeley *Drosophila* Genome Project (BDGP) gene disruption project and *Drosophila* Genetic Reference Panel project.

Furthermore, results from the complementation test to Clk^{jrk} may be more informative if the deficiency line *pb1-x1/TM6B* which uncovered *Clk* was also used. It is possible that the failure of Clk^{jrk} to complement light response was due to Clk^{jrk} semi-dominant behavioural effect (Allada *et al*. 1998). Since a single copy of Clk^{jrk} protein is known to lengthen activity period for an hour (Allada *et al*. 1998), which may also affect the phase shift in this flies and masked the role of any *Clk* segregating alleles in the RI lines.

Although, the genome-wide microarrays used in this study were useful in exploring transcriptional changes in the fly head, high resolution microarray such as cell-type specific (Nagoshi *et al*. 2010) will enhance future efforts to profile clock specific transcripts. It would be useful to analyse the efficacy of the RNAi-mediated knockdown in this study by qPCR or western blotting in the cases of available antibodies. Also the inclusion of a positive control such as *UAS-cry-IR* or *UAS-jet-IR* in the experiments would be informative. Further studies will be required to explore the roles of identified candidate genes, experiments at the protein and neural level will illuminate the current findings. The thesis has provided a few answers but has also created considerably more questions.

7: Appendices

Appendices to chapter 3

Appendix 7.1: Delay phase shift of 123 Recombinant Inbred lines

Recombinant Inbred lines	Mean delay phase shift (hr)
2	-3.58
10	-4.70
12	-5.00
14	-2.71
16	-4.19
19	-3.42
21	-3.82
22	-3.25
25	-4.18
27	-3.28
29	-3.85
47	-3.53
58	-3.79
63	-2.65
66	-2.75
71	-4.25
80	-3.03
81	-3.82
95	-3.47
101	-3.64
102	-4.26
104	-4.33
112	-2.16
113	-2.35
117	-2.60
123	-3.64
124	-1.86
135	-2.68
136	-4.08
139	-3.25
140	-4.91
147	-2.88
153	-3.92

Recombinant Inbred lines	Mean delay phase shift (hr)
156	-2.39
163	-3.29
166	-5.33
168	-3.63
169	-2.13
173	-3.97
174	-4.14
175	-3.06
179	-3.62
185	-4.36
191	-3.05
195	-4.42
200	-5.50
201	-4.81
202	-3.04
204	-3.68
205	-4.64
213	-4.08
214	-3.00
217	-4.29
218	-3.03
223	-3.69
224	-2.82
229	-3.81
234	-3.17
235	-2.64
238	-4.50
240	-3.94
241	-3.54
245	-4.32
246	-2.98
248	-2.84
251	-4.54

Recombinant Inbred lines	Mean delay phase shift (hr)
260	-3.78
263	-4.20
267	-2.69
271	-3.23
277	-4.30
278	-3.38
280	-3.06
281	-3.90
288	-3.55
296	-4.25
308	-3.06
317	-3.09
318	-3.73
323	-4.03
325	-3.35
328	-2.59
329	-2.43
335	-4.39
338	-2.93
342	-3.58
347	-2.88
348	-4.00
349	-2.94
354	-3.20
359	-3.43
371	-3.79
372	-2.63
374	-3.67
376	-3.83
383	-2.27
389	-3.74
392	-4.97
394	-3.06
397	-3.98
399	-3.14
408	-4.11
413	-3.66
414	-2.98
417	-4.41
419	-4.05
443	-4.44
445	-3.07
448	-3.30

Recombinant Inbred lines	Mean delay phase shift (hr)
449	-2.86
460	-3.63
461	-3.29
467	-3.26
476	-4.17
483	-3.15
484	-2.76
489	-3.39
492	-4.15
496	-3.03
498	-2.89
500	-3.82
519	-4.33
524	-4.71

Appendix 7.2: Light-induced differentially expressed transcripts in RIL 58

Note the positive and negative log fold change indicate up-regulation and down-regulation in light stimulation respectively

FlyBase ID	Annotation ID	Gene symbol	Log Fold Change	p.Value
FBgn0032685	*CG10211*	*CG10211*	-1.00	8.77E-05
FBgn0020765	*CG10297*	*Acp65Aa*	-0.92	0.000214
FBgn0005617	*CG10385*	*msl-1*	-1.58	0.000525
FBgn0020638	*CG10530*	*Lcp65Ag1*	-1.19	0.000861
FBgn0003057	*CG10598*	*CG10598*	-1.71	8.74E-05
FBgn0032839	*CG10659*	*CG10659*	-0.82	0.000283
FBgn0261914	*CG1086*	*Glut1*	-0.82	0.000499
FBgn0038769	*CG10889*	*CG10889*	-1.54	3.19E-05
FBgn0027788	*CG11194*	*Hey*	0.89	0.000864
FBgn0011674	*CG11312*	*insc*	-0.70	0.000795
FBgn0037419	*CG1154*	*Osi12*	-1.95	0.000123
FBgn0038067	*CG11598*	*CG11598*	-1.21	0.000194
FBgn0026564	*CG1162*	*CG1162*	-0.90	0.000347
FBgn0032964	*CG11630*	*CG11630*	-0.99	0.000223
FBgn0040340	*CG11642*	*TRAM*	-0.74	0.000289
FBgn0037563	*CG11672*	*CG11672*	-1.59	0.000801
FBgn0003373	*CG11720*	*Sgs3*	-1.66	0.000126
FBgn0037594	*CG11742*	*Or85d*	-1.79	0.000499
FBgn0031109	*CG11748*	*Obp19a*	-1.12	9.43E-05
FBgn0033371	*CG11778*	*CG11778*	-1.45	0.00059
FBgn0045866	*CG11785*	*bai*	0.96	0.000746
FBgn0033486	*CG11866*	*CG11866*	-0.88	0.000635
FBgn0002873	*CG12047*	*mud*	0.70	0.000229
FBgn0025387	*CG12184*	*CG12184*	-1.16	0.000251
FBgn0021776	*CG12249*	*mira*	-0.93	0.000789
FBgn0261287	*CG12250*	*ymp*	-0.77	0.000776
FBgn0011555	*CG12385*	*thetaTry*	-1.94	0.000192
FBgn0011554	*CG12386*	*etaTry*	-1.70	8.42E-05
FBgn0025373	*CG12389*	*Fpps*	-1.14	0.000972
FBgn0030722	*CG12395*	*CG12395*	-1.43	0.000581
FBgn0261789	*CG1249*	*SmD2*	0.80	0.000827
FBgn0030886	*CG12672*	*CG12672*	-1.65	0.00021
FBgn0033136	*CG12838*	*Tsp42Eo*	1.00	0.000157
FBgn0033572	*CG12943*	*CG12943*	-0.94	0.00074
FBgn0034031	*CG12963*	*CG12963*	-1.04	0.000199

FlyBase ID	Annotation ID	Gene symbol	Log Fold Change	p.Value
FBgn0033706	*CG13167*	*Vha36-2*	-1.30	0.00014
FBgn0033704	*CG13169*	*CG13169*	-1.63	9.37E-06
FBgn0032609	*CG13280*	*CG13280*	-0.81	0.00089
FBgn0040318	*CG13475*	*HGTX*	-1.50	1.43E-05
FBgn0034692	*CG13502*	*CG13502*	-1.01	5.76E-05
FBgn0260860	*CG1359*	*Bet5*	-0.86	0.000216
FBgn0042199	*CG13713*	*CG13713*	-1.44	0.000566
FBgn0040376	*CG13759*	*CG13759*	-1.85	0.00035
FBgn0035323	*CG13807*	*CG13807*	-1.08	0.000927
FBgn0034475	*CG13874*	*Obp56h*	-1.06	0.000515
FBgn0035138	*CG13884*	*CG13884*	0.89	0.000636
FBgn0036343	*CG14115*	*CG14115*	-2.42	0.000107
FBgn0036331	*CG14117*	*CG14117*	-1.51	7.21E-06
FBgn0036931	*CG14183*	*CG14183*	0.69	0.000199
FBgn0039467	*CG14253*	*CG14253*	-0.81	0.000524
FBgn0038079	*CG14394*	*CG14394*	-1.15	0.000432
FBgn0030571	*CG14414*	*CG14414*	-0.91	0.000961
FBgn0039617	*CG14521*	*CG14521*	0.80	0.000813
FBgn0040892	*CG14634*	*CG14634*	-1.60	0.000236
FBgn0035497	*CG14995*	*CG14995*	-0.94	0.000715
FBgn0085419	*CG15069*	*Rgk2*	-2.34	7.83E-06
FBgn0034381	*CG15088*	*CG15088*	-1.54	0.000201
FBgn0040842	*CG15212*	*CG15212*	-0.88	0.000792
FBgn0032502	*CG15639*	*CG15639*	-0.99	0.000948
FBgn0030338	*CG15741*	*CG15741*	-1.63	0.000466
FBgn0031283	*CG15880*	*CG15880*	-1.02	0.000102
FBgn0028658	*CG16889*	*adat*	-1.06	0.000503
FBgn0039904	*CG1710*	*Hcf*	-1.28	0.000852
FBgn0035581	*CG17150*	*CG17150*	-1.24	0.000414
FBgn0261278	*CG17161*	*grp*	-1.39	3.30E-06
FBgn0036447	*CG17173*	*CG17173*	-0.59	0.000655
FBgn0040253	*CG17200*	*Ugt86Dg*	-1.29	0.000138
FBgn0261970	*CG17208*	*CG42801*	-1.33	0.000217
FBgn0031488	*CG17265*	*CG17265*	-1.44	4.91E-05
FBgn0010316	*CG1772*	*dap*	-0.82	0.000567
FBgn0039192	*CG17784*	*CG17784*	-0.92	0.000361
FBgn0028946	*CG17868*	*Or35a*	-1.27	0.000386
FBgn0004175	*CG17935*	*Mst84Dd*	-1.79	2.28E-05
FBgn0032189	*CG18145*	*Ripalpha*	-1.83	6.78E-06
FBgn0013988	*CG18255*	*Strn-Mlck*	-1.13	0.00044
FBgn0034382	*CG18609*	*CG18609*	0.74	0.000487
FBgn0039582	*CG1867*	*Or98b*	-0.85	0.000942

FlyBase ID	Annotation ID	Gene symbol	Log Fold Change	p.Value
FBgn0086611	*CG18779*	*Lcp65Ag3*	-1.55	0.000919
FBgn0028420	*CG18783*	*Kr-h1*	-1.34	0.000325
FBgn0035264	*CG2069*	*Oseg4*	-1.08	0.000195
FBgn0033292	*CG2110*	*Cyp4ad1*	-1.42	0.000422
FBgn0039777	*CG2229*	*Jon99Fii*	-1.90	5.11E-05
FBgn0031467	*CG2973*	*Cpr23B*	-2.19	0.000152
FBgn0260959	*CG30038*	*MCPH1*	-1.48	7.55E-05
FBgn0050071	*CG30071*	*CG30071*	-1.50	0.000152
FBgn0050121	*CG30121*	*CG30121*	-2.57	6.86E-06
FBgn0260476	*CG30153*	*CG30153*	-0.88	0.00064
FBgn0050464	*CG30464*	*Ir52d*	-0.99	0.000114
FBgn0050493	*CG30493*	*CG30493*	-0.74	0.000811
FBgn0051427	*CG31427*	*CG31427*	-0.94	0.000373
FBgn0051600	*CG31600*	*CG31600*	-1.07	9.91E-05
FBgn0051626	*CG31626*	*CG31626*	-1.45	9.70E-05
FBgn0083962	*CG31653*	*CG34126*	-1.12	0.000258
FBgn0051736	*CG31736*	*CG31736*	-1.06	0.000563
FBgn0051988	*CG31988*	*CG31988*	-1.57	6.97E-05
FBgn0052053	*CG32053*	*CG32053*	1.37	0.000603
FBgn0052079	*CG32079*	*CG32079*	-1.08	0.000516
FBgn0261997	*CG32186*	*CG42815*	-1.40	0.000181
FBgn0052189	*CG32189*	*CG32189*	-1.46	0.000103
FBgn0052192	*CG32192*	*CG32192*	-1.65	0.000145
FBgn0085371	*CG32422*	*CG34342*	0.72	0.000197
FBgn0052533	*CG32533*	*CG32533*	1.27	0.000778
FBgn0052595	*CG32595*	*CG32595*	-1.01	0.000854
FBgn0052690	*CG32690*	*CR32690*	0.81	0.000967
FBgn0004397	*CG3299*	*Vinc*	-0.78	0.000268
FBgn0063923	*CG33045*	*Kaz1-ORFB*	-1.55	0.000185
FBgn0053062	*CG33062*	*CG33062*	-1.54	6.02E-05
FBgn0024189	*CG33141*	*sns*	-1.04	0.000867
FBgn0050461	*CG33142*	*CG30461*	-0.92	0.000907
FBgn0085443	*CG33175*	*spri*	0.85	0.000919
FBgn0053189	*CG33189*	*CG33189*	0.95	0.000279
FBgn0053252	*CG33252*	*CG33252*	-1.68	3.44E-05
FBgn0053293	*CG33293*	*CG33293*	-0.66	0.000468
FBgn0031619	*CG3355*	*CG3355*	-1.02	0.000518
FBgn0259242	*CG3367*	*CG42340*	-1.33	0.000128
FBgn0005636	*CG3385*	*nvy*	-1.35	0.000179
FBgn0025643	*CG3588*	*CG3588*	-1.17	0.000619
FBgn0038467	*CG3590*	*CG3590*	-1.34	2.43E-05
FBgn0001974	*CG3688*	*l(2)35Bd*	-0.72	0.000276

FlyBase ID	Annotation ID	Gene symbol	Log Fold Change	p.Value
FBgn0040350	*CG3690*	*CG3690*	-1.33	0.000414
FBgn0063485	*CG3849*	*Lasp*	-0.95	0.000363
FBgn0086917	*CG40123*	*spok*	-1.75	0.000281
FBgn0058130	*CG40130*	*CG40130*	-0.84	0.000646
FBgn0058174	*CG40174*	*CG40174*	-1.08	0.000115
FBgn0015218	*CG4035*	*eIF-4E*	-1.42	1.33E-05
FBgn0040035	*CG40368*	*CG40368*	0.70	0.000885
FBgn0058383	*CG40383*	*CG40383*	-1.71	0.00011
FBgn0037815	*CG4043*	*Rrp46*	0.67	0.000201
FBgn0069973	*CG40485*	*CG40485*	0.73	0.000537
FBgn0029770	*CG4151*	*CG4151*	-1.55	8.68E-05
FBgn0010453	*CG4698*	*Wnt4*	-1.10	0.0006
FBgn0036612	*CG4998*	*CG4998*	-1.03	7.47E-05
FBgn0036437	*CG5048*	*CG5048*	-0.92	0.000904
FBgn0032234	*CG5091*	*CG5091*	-1.11	3.61E-05
FBgn0030830	*CG5172*	*CG5172*	-1.62	3.60E-05
FBgn0035955	*CG5194*	*CG5194*	-1.07	0.000611
FBgn0021764	*CG5227*	*sdk*	-1.88	4.15E-05
FBgn0030577	*CG5334*	*CG5334*	-1.58	1.29E-05
FBgn0028978	*CG5408*	*trbl*	-1.45	0.000671
FBgn0032431	*CG5435*	*CG5435*	-1.53	0.000498
FBgn0001230	*CG5436*	*Hsp68*	-1.14	0.000649
FBgn0039434	*CG5468*	*TwdlM*	-1.93	6.85E-06
FBgn0038816	*CG5483*	*Lrrk*	-0.89	0.000992
FBgn0038389	*CG5516*	*CG5516*	-1.14	0.000443
FBgn0085382	*CG5566*	*CG34353*	-2.34	0.000176
FBgn0004842	*CG5811*	*NepYr*	-1.58	0.000114
FBgn0039387	*CG5959*	*CG5959*	-0.83	0.000437
FBgn0036998	*CG5969*	*CG5969*	-0.83	0.000554
FBgn0004956	*CG5993*	*os*	-1.13	0.000495
FBgn0031918	*CG6055*	*CG6055*	-1.94	2.77E-05
FBgn0002629	*CG6099*	*m4*	0.77	0.000238
FBgn0002592	*CG6104*	*m2*	-2.14	1.66E-05
FBgn0260964	*CG6119*	*Vmat*	-1.96	2.62E-05
FBgn0020439	*CG6544*	*fau*	-1.42	2.90E-05
FBgn0000451	*CG6611*	*ect*	-0.97	7.28E-05
FBgn0261872	*CG6615*	*scaf6*	-1.11	5.81E-05
FBgn0261963	*CG6634*	*mid*	-2.22	0.000198
FBgn0036488	*CG6878*	*CG6878*	-0.99	0.000509
FBgn0038978	*CG7045*	*CG7045*	-1.06	6.32E-05
FBgn0010877	*CG7129*	*l(3)05822*	-0.72	0.000893
FBgn0032262	*CG7384*	*CG7384*	-1.55	0.000168

FlyBase ID	Annotation ID	Gene symbol	Log Fold Change	p.Value
FBgn0037577	*CG7443*	*CG7443*	-1.40	0.000462
FBgn0037143	*CG7448*	*CG7448*	-1.05	0.000122
FBgn0035812	*CG7457*	*CG7457*	0.88	0.000276
FBgn0000551	*CG7673*	*Edg78E*	-0.88	0.000249
FBgn0001308	*CG7765*	*Khc*	-0.63	0.000952
FBgn0010424	*CG7930*	*TpnC73F*	-1.10	0.000644
FBgn0033388	*CG8046*	*CG8046*	-1.26	3.26E-05
FBgn0030675	*CG8191*	*CG8191*	-1.71	0.000224
FBgn0035693	*CG8219*	*CG8219*	-1.13	0.000781
FBgn0041156	*CG8254*	*exex*	-1.49	4.47E-06
FBgn0021825	*CG8269*	*Dmn*	-0.96	0.000288
FBgn0002734	*CG8328*	*HLHmdelta*	-1.63	0.000226
FBgn0033917	*CG8503*	*CG8503*	0.66	0.000799
FBgn0033741	*CG8545*	*CG8545*	0.73	0.000211
FBgn0033748	*CG8821*	*vis*	-1.45	0.00039
FBgn0038144	*CG8870*	*CG8870*	0.77	0.000427
FBgn0014391	*CG9032*	*sun*	-1.70	0.000197
FBgn0001942	*CG9075*	*eIF-4a*	-1.29	0.000162
FBgn0033582	*CG9084*	*CG9084*	-1.06	0.00054
FBgn0034588	*CG9394*	*CG9394*	0.60	0.000783
FBgn0034438	*CG9416*	*CG9416*	-1.10	0.000521
FBgn0031483	*CG9641*	*CG9641*	0.89	0.000224
FBgn0026384	*CG9820*	*Or59a*	-0.93	7.40E-05
FBgn0031444	*CG9879*	*CG9879*	-1.85	8.67E-05

Appendix 7.3: Light-induced differentially expressed transcripts in RIL 104

Note the positive and negative log fold change indicate up-regulation and down-regulation in light stimulation respectively

FlyBase ID	Annotation ID	Gene symbol	Log Fold Change	p.value
FBgn0020765	*CG10297*	*Acp65Aa*	-1.09	5.92E-05
FBgn0020639	*CG10533*	*Lcp65Af*	-1.41	0.000225
FBgn0032839	*CG10659*	*CG10659*	-0.71	0.000767
FBgn0038769	*CG10889*	*CG10889*	-1.12	0.000325
FBgn0030400	*CG11138*	*CG11138*	0.83	0.000494
FBgn0031734	*CG11147*	*CG11147*	0.88	0.000593
FBgn0003002	*CG1133*	*opa*	-1.19	0.000949
FBgn0035483	*CG1134*	*CG1134*	-1.02	0.000559
FBgn0039749	*CG11498*	*CG11498*	0.70	0.000736
FBgn0037419	*CG1154*	*Osi12*	-1.63	0.000434
FBgn0038067	*CG11598*	*CG11598*	-1.25	0.00016
FBgn0036204	*CG11611*	*Tim13*	-0.73	0.000664
FBgn0026564	*CG1162*	*CG1162*	-0.78	0.000904
FBgn0033028	*CG11665*	*CG11665*	1.20	0.000105
FBgn0003373	*CG11720*	*Sgs3*	-1.41	0.000396
FBgn0039299	*CG11854*	*CG11854*	0.73	0.000772
FBgn0035430	*CG12009*	*CG12009*	-1.04	0.000665
FBgn0027790	*CG12023*	*GV1*	0.66	0.000869
FBgn0035147	*CG12030*	*CG12030*	1.16	0.000838
FBgn0035404	*CG12079*	*CG12079*	1.09	2.82E-05
FBgn0025387	*CG12184*	*CG12184*	-1.58	2.59E-05
FBgn0261287	*CG12250*	*ymp*	-0.75	0.000932
FBgn0086368	*CG12311*	*tw*	-1.02	0.00016
FBgn0025373	*CG12389*	*Fpps*	-1.29	0.000421
FBgn0039543	*CG12428*	*CG12428*	0.91	0.000289
FBgn0033652	*CG12443*	*ths*	-0.62	0.00061
FBgn0262350	*CG12478*	*bru-3*	0.64	0.000681
FBgn0029657	*CG12535*	*CG12535*	-1.31	0.000184
FBgn0040942	*CG12643*	*CG12643*	0.95	2.87E-05
FBgn0040932	*CG12650*	*CG12650*	-2.02	0.000182
FBgn0025864	*CG12737*	*Crag*	0.92	0.000481
FBgn0033972	*CG12797*	*Ciao1*	0.92	0.000504
FBgn0033704	*CG13169*	*CG13169*	-1.68	7.36E-06
FBgn0000406	*CG13279*	*Cyt-b5-r*	1.03	0.000184
FBgn0034509	*CG13421*	*Obp57c*	-0.86	0.000976
FBgn0040318	*CG13475*	*HGTX*	-0.97	0.000361

FlyBase ID	Annotation ID	Gene symbol	Log Fold Change	p.value
FBgn0034692	*CG13502*	*CG13502*	-0.80	0.000296
FBgn0000279	*CG1373*	*CecC*	-1.01	0.000855
FBgn0033353	*CG13749*	*CG13749*	0.82	0.000605
FBgn0041247	*CG13787*	*Gr28a*	-1.65	0.000158
FBgn0033928	*CG13941*	*Arc2*	0.83	0.000165
FBgn0016076	*CG14029*	*vri*	-0.97	0.000814
FBgn0039503	*CG14262*	*CG14262*	-0.69	0.000922
FBgn0038203	*CG14360*	*Or88a*	-1.63	0.000838
FBgn0037177	*CG14454*	*CG14454*	-0.81	0.000923
FBgn0033000	*CG14464*	*CG14464*	-0.61	0.000842
FBgn0037224	*CG14639*	*TwdlF*	-1.44	0.000405
FBgn0037307	*CG14666*	*Tim17a2*	-1.31	0.00065
FBgn0030619	*CG15029*	*CG15029*	0.68	0.000486
FBgn0030191	*CG15306*	*CG15306*	0.60	0.000495
FBgn0024288	*CG15552*	*Sox100B*	-0.98	0.000678
FBgn0035004	*CG15874*	*CG15874*	0.74	0.000256
FBgn0031283	*CG15880*	*CG15880*	-0.88	0.000288
FBgn0034498	*CG16868*	*CG16868*	-1.17	0.000352
FBgn0030254	*CG16922*	*CG16922*	-0.67	0.000974
FBgn0261278	*CG17161*	*grp*	-0.78	0.00026
FBgn0040253	*CG17200*	*Ugt86Dg*	-1.19	0.000257
FBgn0261970	*CG17208*	*CG42801*	-1.36	0.000191
FBgn0039923	*CG1793*	*MED26*	-0.89	0.000216
FBgn0000425	*CG17967*	*DebA*	-1.21	0.000731
FBgn0028530	*CG18124*	*mTTF*	1.03	0.000244
FBgn0013467	*CG18285*	*igl*	-0.75	0.000149
FBgn0025360	*CG18455*	*Optix*	-0.90	0.000312
FBgn0031426	*CG18641*	*CG18641*	-0.96	0.000425
FBgn0039674	*CG1907*	*CG1907*	0.84	0.000865
FBgn0027330	*CG1994*	*l(1)G0020*	0.67	0.000615
FBgn0020653	*CG2151*	*Trxr-1*	0.86	0.000789
FBgn0000427	*CG2175*	*Dec-01*	-0.70	0.000777
FBgn0039777	*CG2229*	*Jon99Fii*	-1.25	0.000975
FBgn0037323	*CG2663*	*CG2663*	-1.01	0.000214
FBgn0037540	*CG2702*	*Pbp95*	-0.83	0.000408
FBgn0050001	*CG30001*	*CG30001*	-1.12	0.000518
FBgn0050071	*CG30071*	*CG30071*	-1.19	0.000786
FBgn0050095	*CG30095*	*CG30095*	-1.12	5.21E-05
FBgn0050192	*CG30192*	*CG30192*	-1.94	2.52E-05
FBgn0016672	*CG3028*	*Ipp*	0.81	0.000602
FBgn0050332	*CG30332*	*CG30332*	-1.28	0.000405
FBgn0050410	*CG30410*	*CG30410*	1.02	0.000791

FlyBase ID	Annotation ID	Gene symbol	Log Fold Change	p.value
FBgn0038194	*CG3050*	*Cyp6d5*	0.60	0.000501
FBgn0051446	*CG31446*	*CG31446*	-1.19	0.00023
FBgn0044809	*CG31507*	*TotZ*	-0.59	0.000636
FBgn0028396	*CG31509*	*TotA*	-0.65	0.000365
FBgn0051563	*CG31563*	*CG31563*	-0.99	0.000611
FBgn0051600	*CG31600*	*CG31600*	-1.07	9.67E-05
FBgn0051626	*CG31626*	*CG31626*	-1.49	8.16E-05
FBgn0083962	*CG31653*	*CG34126*	-1.54	2.40E-05
FBgn0051664	*CG31664*	*CG31664*	0.86	0.00015
FBgn0032820	*CG31692*	*fbp*	1.09	0.000686
FBgn0051874	*CG31874*	*CG31874*	-1.20	7.81E-05
FBgn0051901	*CG31901*	*Mur29B*	-1.01	0.000303
FBgn0051958	*CG31958*	*CG31958*	-1.33	9.95E-05
FBgn0052175	*CG32175*	*CG32175*	-1.04	0.000286
FBgn0037538	*CG3223*	*CG3223*	0.94	0.000647
FBgn0052511	*CG32511*	*CG32511*	-1.31	0.000898
FBgn0052512	*CG32512*	*CG32512*	-1.20	0.000193
FBgn0052564	*CG32564*	*CG32564*	-1.60	8.30E-05
FBgn0085443	*CG32680*	*spri*	0.83	0.000249
FBgn0052683	*CG32683*	*CG32683*	-1.12	4.63E-05
FBgn0052741	*CG32741*	*CG32741*	-1.13	0.0003
FBgn0052984	*CG32984*	*CG32984*	-1.27	8.86E-05
FBgn0063923	*CG33045*	*Kaz1-ORFB*	-1.24	0.000861
FBgn0053062	*CG33062*	*CG33062*	-1.40	0.000121
FBgn0003659	*CG33070*	*Sxl*	-1.16	0.000987
FBgn0053116	*CG33116*	*CG33116*	-0.91	0.000986
FBgn0053147	*CG33147*	*Hs3st-A*	-0.89	0.000662
FBgn0031619	*CG3355*	*CG3355*	-1.18	0.000183
FBgn0015816	*CG3539*	*Slh*	-1.26	0.000433
FBgn0025681	*CG3558*	*CG3558*	-0.82	0.000288
FBgn0040350	*CG3690*	*CG3690*	-1.25	0.000628
FBgn0003448	*CG3956*	*sna*	-1.05	0.000231
FBgn0004575	*CG3985*	*Syn*	-1.18	4.75E-06
FBgn0058088	*CG40088*	*CG40088*	-1.40	0.000446
FBgn0086917	*CG40123*	*spok*	-1.62	0.000469
FBgn0058323	*CG40323*	*CG40323*	1.40	1.22E-05
FBgn0259996	*CG40341*	*CG40341*	0.65	0.00076
FBgn0015218	*CG4035*	*eIF-4E*	-0.98	0.000219
FBgn0058383	*CG40383*	*CG40383*	-1.27	0.000888
FBgn0261882	*CG4103*	*l(2)35Bc*	0.60	0.000918
FBgn0029770	*CG4151*	*CG4151*	-1.34	0.000249
FBgn0032138	*CG4364*	*CG4364*	1.09	5.09E-05

FlyBase ID	Annotation ID	Gene symbol	Log Fold Change	p.value
FBgn0034660	*CG4402*	*lox2*	0.92	0.000503
FBgn0010747	*CG4659*	*Srp54k*	0.79	0.000938
FBgn0010453	*CG4698*	*Wnt4*	-1.22	0.000283
FBgn0036578	*CG5018*	*CG5018*	-1.22	0.000639
FBgn0038390	*CG5083*	*Rbf2*	-1.22	0.000433
FBgn0035954	*CG5093*	*Doc3*	-1.08	0.000229
FBgn0036775	*CG5147*	*CG5147*	0.79	0.000587
FBgn0030830	*CG5172*	*CG5172*	-1.41	0.000102
FBgn0021764	*CG5227*	*sdk*	-1.54	0.000182
FBgn0040383	*CG5254*	*CG5254*	0.94	0.000429
FBgn0035950	*CG5288*	*CG5288*	0.83	2.88E-05
FBgn0038351	*CG5302*	*CG5302*	-1.15	0.000603
FBgn0030577	*CG5334*	*CG5334*	-1.51	1.83E-05
FBgn0032237	*CG5362*	*CG5362*	0.83	0.000131
FBgn0039434	*CG5468*	*TwdlM*	-1.51	4.57E-05
FBgn0036769	*CG5492*	*Tsp74F*	1.29	9.36E-05
FBgn0039564	*CG5527*	*CG5527*	1.21	0.000356
FBgn0036759	*CG5577*	*CG5577*	1.20	0.000115
FBgn0004842	*CG5811*	*NepYr*	-1.24	0.000641
FBgn0039387	*CG5959*	*CG5959*	-1.08	6.34E-05
FBgn0000064	*CG6058*	*Ald*	0.87	0.000594
FBgn0002631	*CG6096*	*HLHm5*	-1.13	0.000669
FBgn0027865	*CG6120*	*Tsp96F*	-0.82	0.000251
FBgn0038725	*CG6184*	*CG6184*	0.63	0.000754
FBgn0061515	*CG6513*	*endos*	1.06	0.000541
FBgn0020439	*CG6544*	*fau*	-1.18	0.000118
FBgn0011569	*CG6577*	*can*	-1.03	0.000793
FBgn0000451	*CG6611*	*ect*	-0.94	9.69E-05
FBgn0261872	*CG6615*	*scaf6*	-0.86	0.00037
FBgn0032305	*CG6700*	*CG6700*	-0.67	0.000745
FBgn0029722	*CG7024*	*CG7024*	-0.80	0.000861
FBgn0038978	*CG7045*	*CG7045*	-0.94	0.000143
FBgn0031942	*CG7203*	*CG7203*	2.34	0.000672
FBgn0032269	*CG7363*	*w-cup*	-1.61	0.000878
FBgn0037143	*CG7448*	*CG7448*	-0.94	0.00028
FBgn0036741	*CG7510*	*CG7510*	0.90	0.000368
FBgn0004593	*CG7599*	*Eig71Ef*	0.67	0.000943
FBgn0020235	*CG7610*	*ATPsyn-gamma*	0.67	0.000798
FBgn0000551	*CG7673*	*Edg78E*	-0.79	0.000537
FBgn0033388	*CG8046*	*CG8046*	-1.10	8.57E-05
FBgn0041156	*CG8254*	*exex*	-0.83	0.000368

FlyBase ID	Annotation ID	Gene symbol	Log Fold Change	p.value
FBgn0002734	*CG8328*	*HLHmdelta*	-1.81	0.000105
FBgn0003527	*CG8592*	*stil*	-1.25	0.000805
FBgn0026376	*CG8865*	*Rgl*	0.68	0.000862
FBgn0015381	*CG9019*	*dsf*	-1.33	0.000481
FBgn0031746	*CG9029*	*CG9029*	-1.19	0.000227
FBgn0014391	*CG9032*	*sun*	-1.65	0.000241
FBgn0001942	*CG9075*	*eIF-4a*	1.83	0.000973
FBgn0035193	*CG9192*	*CG9192*	0.85	0.000475
FBgn0032916	*CG9257*	*CG9257*	0.72	0.000714
FBgn0036876	*CG9451*	*CG9451*	0.96	9.68E-05
FBgn0030597	*CG9504*	*Eo*	-0.82	0.000125
FBgn0031444	*CG9879*	*CG9879*	-1.59	0.00026
FBgn0005411	*CG9998*	*U2af50*	0.93	0.000622

Appendix 7.4 Overlapping gene between RIL 58 and 104

FlyBase ID	Gene Symbol	Biological process term
FBgn0020765	*Acp65Aa*	unknown
FBgn0032839	*CG10659*	metabolic process
FBgn0038769	*CG10889*	unknown
FBgn0038067	*CG11598*	lipid metabolic process , lipid metabolic process
FBgn0026564	*CG1162*	unknown
FBgn0025387	*CG12184*	unknown
FBgn0033704	*CG13169*	unknown
FBgn0034692	*CG13502*	unknown
FBgn0031283	*CG15880*	unknown
FBgn0050071	*CG30071*	unknown
FBgn0051600	*CG31600*	unknown
FBgn0051626	*CG31626*	unknown
FBgn0053062	*CG33062*	unknown
FBgn0031619	*CG3355*	proteolysis , proteolysis
FBgn0083962	*CG34126*	unknown
FBgn0040350	*CG3690*	transmembrane transport
FBgn0058383	*CG40383*	unknown
FBgn0029770	*CG4151*	unknown
FBgn0261970	*CG42801*	unknown
FBgn0030830	*CG5172*	unknown
FBgn0030577	*CG5334*	unknown
FBgn0039387	*CG5959*	oxidation reduction
FBgn0038978	*CG7045*	unknown
FBgn0037143	*CG7448*	unknown
FBgn0033388	*CG8046*	glycerol-3-phosphate metabolic process , transmembrane transport , oxidation reduction
FBgn0031444	*CG9879*	regulation of transcription, transcription initiation from RNA polymerase II promoter
FBgn0000451	*ect*	unknown
FBgn0000551	*Edg78E*	unknown
FBgn0001942	*eIF-4a*	mitotic spindle elongation , regulation of alternative nuclear mRNA splicing, via spliceosome
FBgn0015218	*eIF-4E*	mitotic spindle elongation , regulation of cell growth , chromatin organization , translation ,
FBgn0041156	*exex*	regulation of transcription, DNA-dependent , nervous system development
FBgn0020439	*fau*	response to stress , response to oxidative stress
FBgn0025373	*Fpps*	isoprenoid biosynthetic process , germ cell migration , farnesyl diphosphate biosynthetic

FlyBase ID	Gene Symbol	Biological process term
		process
FBgn0261278	*grp*	cell cycle checkpoint , cell cycle checkpoint , cell cycle checkpoint
FBgn0040318	*HGTX*	regulation of transcription, DNA-dependent , nervous system development
FBgn0002734	*HLHmdelta*	negative regulation of transcription from RNA polymerase II promoter , transcription
FBgn0039777	*Jon99Fii*	unknown
FBgn0063923	*Kaz1-ORFB*	regulation of proteolysis
FBgn0004842	*NepYr*	signal transduction , G-protein coupled receptor protein signalling pathway
FBgn0037419	*Osi12*	unknown
FBgn0261872	*scaf6*	unknown
FBgn0021764	*sdk*	cell adhesion , cell adhesion , multicellular organismal development
FBgn0003373	*Sgs3*	puparial adhesion
FBgn0086917	*spok*	ecdysone biosynthetic process , molting cycle, chitin-based cuticle , oxidation reduction
FBgn0014391	*sun*	response to oxidative stress , determination of adult lifespan
FBgn0039434	*TwdlM*	unknown
FBgn0040253	*Ugt86Dg*	metabolic process
FBgn0010453	*Wnt4*	establishment of imaginal disc-derived wing hair orientation
FBgn0261287	*nuclear mRNA splicing*	unknown

Appendices to chapter 4

Appendix 7.5: List of differentially expressed genes.

Note the positive and negative log fold change indicate up-regulation and down-regulation in light stimulation respectively.

Probe Set ID	Gene name	Fold change(log)	FDR
1623265_at	*CG10513*	1.42	0.000
1623318_s_at	*Met75Ca /// Met75Cb*	4.31	0.000
1623635_at	*Turandot M*	1.19	0.000
1632719_at	*Cecropin*	1.60	0.000
1639366_at	*Hormone receptor-like in 38*	0.80	0.000
1629118_at	*PGRP-SC2*	1.14	0.001
1626530_at	*Cecropin B*	1.28	0.002
1633442_at	*Protein ejaculatory bulb II*	3.28	0.003
1639720_at	*CG6600*	0.61	0.004
1640401_at	*Protein ejaculatory bulb*	3.09	0.004
1637971_a_at	*CG8129*	0.64	0.004
1630741_s_at	*Peptidoglycan recognition protein LB*	0.74	0.004
1634366_at	*CG32185*	1.00	0.005
1638812_at	*CG11501*	0.96	0.005
1625433_at	*calcium binding protein*	1.07	0.005
1634309_at	*CG14322*	0.55	0.012
1636997_at	*CG18528*	0.53	0.012
1628768_at	*CG4676*	0.60	0.013
1638381_s_at	*CG32506 /// CG1695*	0.67	0.013
1624052_at	*CG6294*	0.56	0.016
1633326_at	*CG15356*	0.50	0.017
1623759_at	*CG13428*	1.18	0.018
1634733_at	*CG3831*	0.53	0.018
1632612_s_at	*Fragile X (Fmr1)*	0.50	0.018
1641642_at	*CG6663*	1.98	0.018
1635570_a_at	*cAMP-regulated enhancer-binding protein*	0.49	0.018
1629716_a_at	*CG13284*	0.54	0.018
1636674_at	*CG11407*	0.49	0.021
1640224_s_at	*CG13796*	0.68	0.021
1626153_at	*Enhancer of variegation 3-2*	0.48	0.024
1639323_at	*Turandot C*	0.45	0.028
1630429_s_at	*CG11889*	0.49	0.028
1626086_at	*selenocysteine*	0.55	0.029

Probe Set ID	Gene name	Fold change(log)	FDR
	methyltransferase		
1623804_a_at	*Hemipterous (hep)*	0.44	0.034
1627551_s_at	*attacin*	0.65	0.034
1631095_at	*Posterior sex combs (Psc)*	0.48	0.035
1625137_at	*CG3281*	0.42	0.035
1635322_a_at	*CG13322*	0.46	0.036
1633067_at	*CG13845*	0.48	0.036
1629789_at	*CG9649*	0.45	0.036
1638235_at	*diptericin-like protein*	0.73	0.037
1623401_a_at	*CG8092*	0.62	0.037
1630375_at	*Mec2*	0.36	0.038
1630072_a_at	*CG10097*	1.28	0.041
1636759_at	*CG8303*	0.48	0.042
1626324_at	*Cyp309a1*	0.47	0.052
1627613_at	*Metchnikowin*	0.58	0.052
1629834_at	*CG18628*	2.23	0.052
1634321_s_at	*CG2051*	0.44	0.055
1625124_at	*attacin*	0.59	0.057
1632955_at	*phosphorylase kinase gamma*	0.51	0.059
1637857_at	*Lectin24A*	0.33	0.062
1631399_a_at	*CG15771*	0.46	0.064
1638424_at	*CG10514*	0.47	0.066
1637997_at	*CG32155*	0.52	0.067
1630831_at	*CG7695*	0.48	0.067
1627287_at	*CG5966*	0.52	0.068
1624736_a_at	*CG5819*	0.40	0.069
1635531_at	*rolling stone*	0.43	0.070
1628339_a_at	*CG7920*	0.44	0.070
1624670_at	*CG7589*	0.41	0.070
1634813_at	*CG12641*	0.46	0.071
1630123_at	*CG3099*	0.46	0.072
1624505_at	*CG6113*	0.38	0.074
1629804_s_at	*CG6329*	0.38	0.078
1630458_at	*CheA7a*	0.46	0.080
1627302_at	*Flavin-containing monooxygenase 2*	0.41	0.081
1631697_at	*Drosocin*	0.52	0.081
1630622_at	*Sirt6*	0.36	0.082
1627870_at	*CG31900*	0.42	0.082
1635044_at	*heat shock protein hsp26*	0.42	0.083
1626215_at	*CG2202*	0.36	0.084
1634410_at	*CG11560*	0.34	0.089
1627608_s_at	*CG32048*	0.38	0.091
1637590_at	*CG5156*	0.42	0.093

Probe Set ID	Gene name	Fold change(log)	FDR
1628758_at	*CG1774*	0.41	0.093
1636566_at	*CG32368*	0.12	0.093
1635189_at	*Drosomycin*	0.46	0.095
1637804_at	*CG18673*	0.46	0.095
1625542_a_at	*Tropomyosin*	0.37	0.103
1626970_at	*UDP-glycosyltransferase*	0.34	0.104
1640419_at	*abl kinase*	0.37	0.104
1629208_at	*Odorant-binding protein 51a*	1.46	0.105
1639133_at	*CG1939*	0.34	0.105
1631115_at	*Odorant-binding protein 8a*	0.42	0.105
1638215_at	*CG8043*	0.45	0.105
1625598_at	*CG31326*	0.39	0.010
1624195_at	*sugarbabe*	-0.82	0.000
1638720_x_at	*CG41012*	-1.40	0.000
1627385_at	*Pheromone-binding protein-related protein 1*	-0.83	0.001
1638066_at	*Olfactory-specific E*	-0.73	0.001
1629740_at	*His1:CG33864*	-1.06	0.002
1623933_at	*Shaker*	-1.00	0.002
1631419_at	*yolk protein*	-1.23	0.002
1627351_at	*CG15335*	-0.61	0.002
1630730_at	*CG6808*	-0.68	0.002
1631120_at	*mindmelt*	-0.71	0.003
1629545_at	*yolk protein 1*	-1.63	0.003
1633305_at	*Odorant-binding protein 99a*	-0.46	0.003
1630261_a_at	*troponin T*	-0.65	0.004
1625877_s_at	*CG40084*	-0.77	0.007
1623655_at	*yolk protein*	-1.47	0.008
1630285_at	*RhoGAP100F*	-0.60	0.008
1626088_at	*CG2177*	-0.54	0.013
1625698_at	*CG6639 /// Regulator of G-protein signalling 7*	-0.96	0.014
1637828_a_at	*still life type 1 (sif)*	-0.58	0.015
1631016_at	*CG32822*	-0.54	0.016
1636297_at	*CG3173*	-0.50	0.018
1635666_at	*His2B:CG17949 /His2B:CG33910*	-0.64	0.018
1626802_a_at	*Shaker*	-0.59	0.019
1625937_at	*CG18646*	-0.54	0.019
1633337_at	*CG17386*	-0.49	0.019
1634756_at	*Dalpha4*	-0.59	0.019
1638452_at	*period clock protein (per)*	-0.50	0.021
1626087_at	*flamingo*	-0.55	0.021
1633468_x_at	*CG41012 /// CG41582*	-0.56	0.022

Probe Set ID	Gene name	Fold change(log)	FDR
1634083_at	*neurofibromatosis type 1(Nf1)*	-0.51	0.022
1637631_at	*turtle*	-0.46	0.023
1625724_at	*Phosphodiesterase 1c*	-0.53	0.023
1640614_at	*nightblind*	-0.52	0.023
1626842_a_at	*late puff gene at 82F*	-0.51	0.023
1623787_at	*CG7144*	-0.46	0.024
1625642_at	*CG11509*	-0.52	0.026
1629784_a_at	*myosin VII 28B1-B4*	-0.49	0.026
1638984_s_at	*CG17816*	-0.49	0.026
1629142_at	*dopamine D1 receptor*	-0.52	0.028
1623827_a_at	*frazzled*	-0.47	0.028
1637622_s_at	*Cyp12a4*	-0.56	0.028
1629467_at	*CG32005*	-0.57	0.029
1637051_at	*RhoGAP71E*	-0.48	0.029
1630376_at	*D-onecut*	-0.43	0.029
1623346_at	*CG2861*	-0.43	0.029
1625263_at	*Nipped_A*	-0.46	0.034
1633452_a_at	*ryanodine receptor*	-0.46	0.035
1624080_s_at	*transportin*	-0.48	0.039
1623659_at	*Odorant-binding protein 56d*	-0.49	0.039
1627752_s_at	*small conductance calcium-activated potassium channel*	-0.44	0.039
1637499_s_at	*CG5953*	-0.44	0.039
1630897_at	*indefinite*	-0.48	0.040
1624241_at	*put. sodium channel gene*	-0.45	0.040
1639217_s_at	*Brain Tumor*	-0.46	0.041
1624542_at	*CG31757*	-0.40	0.042
1634804_at	*CG15819*	-0.43	0.043
1640268_at	*Modifier67.2*	-0.42	0.044
1640271_s_at	*Plexin A*	-0.44	0.044
1629882_at	*CG6683*	-0.40	0.045
1629747_at	*CG8511*	-0.52	0.054
1634404_at	*CG4573*	-0.43	0.055
1625024_at	*zwilch*	-0.44	0.055
1623424_a_at	*Activin A receptor 45A*	-0.46	0.057
1623513_at	*Upf1*	-0.44	0.058
1633648_at	*sticks and stones*	-0.45	0.059
1622925_at	*CREB binding protein*	-0.42	0.059
1635364_at	*CG30343*	-0.41	0.060
1633913_at	*Pherokine 1*	-0.41	0.060
1622943_s_at	*CG2371*	-0.38	0.062
1624533_s_at	*Trithorax (trx)*	-0.41	0.062
1623727_at	*Cyp313a2*	-0.44	0.065
1627360_at	*tamou*	-0.36	0.066

Probe Set ID	Gene name	Fold change(log)	FDR
1640235_at	*head involution defect*	-0.38	0.068
1636478_at	*CG9596*	-0.42	0.068
1633020_at	*unkempt*	-0.42	0.071
1630231_at	*wrinkled*	-0.41	0.071
1628263_s_at	*CG15236*	-0.42	0.072
1628691_at	*CG17514*	-0.40	0.072
1633312_at	*CG6962*	-0.35	0.074
1626947_s_at	*Pleiohomeotic*	-0.39	0.075
1635639_a_at	*ecdysone inducible protein*	-0.40	0.075
1639306_s_at	*CG17090*	-0.40	0.076
1632550_at	*unc-5-like*	-0.38	0.077
1623234_s_at	*Na/Ca-exchange protein*	-0.38	0.077
1628815_at	*phospholipase Cgamma*	-0.37	0.077
1639492_at	*metabotropic glutamate receptor*	-0.47	0.078
1632644_s_at	*couch potato*	-0.39	0.079
1625215_s_at	*nervana2*	-0.38	0.079
1626841_s_at	*Crinkled*	-0.39	0.080
1629658_at	*CG33298*	-0.37	0.082
1627219_at	*AChR protein of Drosophila*	-0.29	0.085
1624838_a_at	*short neuropeptide F-1*	-0.38	0.088
1641675_at	*Medusa (so)*	-0.38	0.088
1631597_at	*forkhead box, sub-group O*	-0.39	0.088
1631481_a_at	*Krueppel-homolog alpha-isoform 1 (Kr-h1)*	-0.37	0.089
1639414_at	*Sno-oncogene*	-0.38	0.089
1633000_a_at	*N-cadherin*	-0.36	0.089
1633189_at	*CG13646*	-0.43	0.090
1635900_at	*insulin-stimulated eIF-4E binding protein (Thor)*	-0.36	0.090
1627736_at	*dActivin*	-0.36	0.090
1634669_at	*CG32333*	-0.42	0.091
1635248_at	*CG17144*	-0.37	0.091
1633286_at	*CG32372*	-0.37	0.092
1628709_at	*CG34265*	-0.34	0.092
1624699_s_at	*rhombotin*	-0.37	0.093
1629280_at	*CG12344*	-0.37	0.093
1636688_at	*Cyp4s3*	-0.38	0.096
1635684_a_at	*lethal (4) ry16*	-0.42	0.097
1623497_at	*split locus enhancer protein m3*	-0.37	0.097
1623546_at	*prodos*	-0.34	0.097
1626336_at	*Defense repressor 1*	-0.36	0.097
1633963_a_at	*Dalpha6*	-0.47	0.099

Probe Set ID	Gene name	Fold change(log)	FDR
1637240_a_at	*Autophagy-specific gene 7*	-0.39	0.100
1640364_at	*Nervana*	-0.34	0.105
1623784_at	*CG5732*	-0.37	0.105
1633143_s_at	*unknown-telomeric-protein-gene*	-0.38	0.105
1626496_at	*CG10348*	-0.30	0.106
1637151_at	*meiotic recombination 11*	-0.31	0.108
1634140_a_at	*CG11155*	-0.37	0.108
1629013_at	*CG11436*	-0.35	0.109
1636941_at	*CG9007*	-0.38	0.109
1623455_s_at	*IGF-II mRNA-binding protein*	-0.35	0.110

Appendix 7.6: Functional annotation of down-regulated genes

	Term	Count[1]	p Value[2]	Fold enrichment[3]
1	acetylcholine receptor (PIRSF002443)	4	6.56E-05	44.5
2	Neurotransmitter-gated ion-channel, conserved site (IPR018000)	5	3.89E-05	25.0
3	Neurotransmitter-gated ion-channel transmembrane region (IPR006029)	5	5.79E-05	22.7
4	Neurotransmitter-gated ion-channel (IPR006201)	5	6.96E-05	21.7
5	Neurotransmitter-gated ion-channel ligand-binding (IPR006202)	5	6.96E-05	21.7
6	postsynaptic cell membrane (SP_PIR_keywords)	6	4.62E-05	14.9
7	synapse (SP_PIR_keywords)	7	1.04E-05	13.8
8	ion channel complex (GO:0034702)	8	3.76E-06	11.7
9	postsynaptic membrane (GO:0045211)	7	2.36E-05	11.5
10	ionic channel (SP_PIR_keywords)	11	7.75E-08	10.6
11	cell junction (SP_PIR_keywords)	7	8.70E-05	9.5
12	Ion transport (SP_PIR_keywords)	13	3.84E-08	8.5
13	gated channel activity (GO:0022836)	11	8.95E-07	8.0
14	secreted (SP_PIR_keywords)	10	9.64E-05	5.4
15	ion channel activity (GO:0005216)	11	3.73E-05	5.3
16	disulfide bond (SP_PIR_keywords)	17	1.36E-07	5.2
17	substrate specific channel activity (GO:0022838)	11	4.74E-05	5.1
18	integral to plasma membrane (GO:0005887)	13	6.90E-06	5.0
19	channel activity (GO:0015267)	11	6.54E-05	4.9
20	passive transmembrane transporter activity (GO:0022803)	11	6.54E-05	4.9
21	intrinsic to plasma membrane (GO:0031226)	13	8.06E-06	4.9
22	signal (SP_PIR_keywords)	18	3.15E-07	4.6
23	alternative splicing (SP_PIR_keywords)	23	1.26E-08	4.3
24	developmental protein (SP_PIR_keywords)	18	4.26E-06	3.8

[1] number of genes represented by the term

[2] Pvalue in

[3] Fold enrichment

	Term	Count[1]	p Value[2]	Fold enrichment[3]
25	transport (SP_PIR_keywords)	15	3.91E-05	3.8
26	ion transport (GO:0006811)	15	3.41E-05	3.7
27	glycoprotein (SP_PIR_keywords)	14	9.42E-05	3.7
28	plasma membrane part (GO:0044459)	19	3.97E-06	3.4
29	phosphoprotein (SP_PIR_keywords)	22	6.33E-06	3.1
30	membrane (SP_PIR_keywords)	26	6.69E-06	2.7
31	transmembrane (SP_PIR_keywords)	22	9.79E-05	2.6

Appendix 7. 7: Clustering of genes involved in alternative splicing

Category	Term	pValue	Gene symbols
Functional cluster 1	Enrichment Score: 3.24		
SP_PIR_KEYWORDS	Ion transport	7.80E-06	*SK,Sh,cac,nrv2,Sh,Rya-r44F,GluCl*
SP_PIR_KEYWORDS	rna editing	2.37E-05	*SK, cao, Rya-r44F,GluCl*
SP_PIR_KEYWORDS	ionic channel	3.70E-05	*SK, cao,sh, Rya-r44F,GluCl*
GO:0022836	gated channel activity	2.07E-04	*SK, cao,sh, Rya-r44F,GluCl*
GO:0030001	metal ion transport	0.001	*SK, cao,sh, Rya-r44F,GluCl*
Functional cluster 2	Enrichment Score: 2.77		
SP_PIR_KEYWORDS	transmembrane	1.16E-05	*CadN,Kr-h1, GluCl,Sh,trx,cac,nrv2, mbl,Sh,Rya-r44F,mod(mdg4)*
UP_SEQ_FEATURE	topological domain: Cytoplasmic	0.003	
UP_SEQ_FEATURE	transmembrane region	0.010	
GO:0016021	integral to membrane	0.044	
Functional cluster 3	Enrichment Score: 2.24		
GO:0043167	ion binding	0.003	*CadN,stan,Kr-h 1,up, GluCl,Sh,trx,cac,nvr2, mbl,Sh,Rya-r44F,mod(mdg4)*
GO:0046872	metal ion binding	0.008	
GO:0043169	cation binding	0.009	
Functional cluster 4	Enrichment Score: 2.23		
GO:0009416	response to light stimulus	0.003	*Sh,DopR,cac,Sh,per*
GO:0009314	response to	0.004	*Sh,DopR,cac,Sh,per*

Category	Term	pValue	Gene symbols
	radiation		
GO:0009628	response to abiotic stimulus	0.022	*Sh,DopR,cac,Sh,per*
Functional cluster 5	Enrichment Score: 1.94		
GO:0006873	cellular ion homeostasis	0.007	*sh, up, Rya-r44F*
GO:0050801	ion homeostasis	0.008	*sh, up, Rya-r44F)*
Functional cluster 6	Enrichment Score: 1.78		
GO:0007268	synaptic transmission	0.015	*Sh, cac, sif, cpo*
GO:0019226	transmission of nerve impulse	0.016	*Sh,cac,sif,cpo*
GO:0007267	cell-cell signalling	0.020	*Sh,cac,sif,cpo*
Functional cluster 7	Enrichment Score: 1.75		
GO:0007619	courtship behaviour	0.012	*Sh,cac,Sh,per*
GO:0007617	mating behaviour	0.017	*Sh,cac,Sh,per*
GO:0051705	Circadian sleep/wake cycle	0.03	*Sh, per*
GO:0019098	locomotory behaviour	0.01	*Sh,cac,Sh,per,tutl*
Functional cluster 8	Enrichment Score: 1.49		
SP_PIR_KEYWORDS	signal	0.006	*CadN, DopR, stan, sNPF, GluCl*
SP_PIR_KEYWORDS	cell membrane	0.015	*CadN, DopR, stan, GluCl*
Functional cluster 9	Enrichment Score: 1.48		
SP_PIR_KEYWORDS	Transcription	0.003	*foxo, trx, pan, mod(mdg4)*
SP_PIR_KEYWORDS	Transcription regulation	0.003	*foxo, trx, pan, mod(mdg4)*
GO:0006350	transcription	0.036	*foxo, trx, pan, mod(mdg4)*

Category	Term	pValue	Gene symbols
Functional cluster 10	Enrichment Score: 1.27		
GO:0001745	compound eye morphogenesis	0.033	*foxo, CadN, stan,mbl*
GO:0048592	eye morphogenesis	0.039	*foxo,CadN, stan,mbl*
GO:0048749	compound eye development	0.054	*foxo,CadN, stan,mbl*

Appendix 7.8: Functional annotation clustering of the up-regulated genes

Category	Term	Count	pValue	Gene list
Functional cluster 1	Enrichment Score: 6.96			
SP_PIR_KEYWORDS	innate immunity	9	1.02E-09	*Dro,Drs,PebII,PGRP-LB,AttA,Mtk,PGRP-SA,TotM,TotC,Peb,CecC,AttA,CecC,AttA,CecB*
GO:0045087	innate immune response	10	1.15E-09	
SP_PIR_KEYWORDS	Immune response	9	1.86E-09	
GO:0006955	immune response	11	1.65E-08	
GO:0006952	defence response	11	2.17E-08	
SP_PIR_KEYWORDS	secreted	12	6.91E-08	
GO:0005576	extracellular region	13	7.19E-06	
SP_PIR_KEYWORDS	signal	13	1.83E-05	
UP_SEQ_FEATURE	signal peptide	12	3.39E-04	
Functional cluster 2	Enrichment Score: 6.53			
GO:0019731	antibacterial humoral response	7	4.50E-09	*Dro,Drs,PGRP-LB, AttA, CecC, DptB, AttA, CecB, Mtk*
GO:0042742	defence response to bacterium	8	7.88E-08	
SP_PIR_KEYWORDS	Antimicrobial	6	1.88E-07	
GO:0009617	response to bacterium	8	2.16E-07	
GO:0050829	defence response to Gram-negative bacterium	6	6.31E-07	

Category	Term	Count	pValue	Gene list
SP_PIR_KEYWORDS	antibiotic	5	9.08E-07	
GO:0019730	antimicrobial humoral response	7	1.68E-06	
GO:0006959	humoral immune response	7	4.60E-06	
Annotation Cluster 3	Enrichment Score: 1.45			
PIRSF014263	Drosophila hypothetical protein EG_34F3.5	3	0.02	
SM00587	CHK	3	0.05	
IPR015897	CHK kinase-like	3	0.05	
IPR004119	Protein of unknown function DUF227	3	0.05	*CG10513, CG11889, CG11891, CG10514*
Functional cluster 4	Enrichment Score: 1.28			
GO:0016458	gene silencing	5	0.01	
GO:0045814	negative regulation of gene expression, epigenetic	4	0.02	
GO:0006342	chromatin silencing	4	0.02	
GO:0016568	chromatin modification	4	0.02	
GO:0006338	chromatin remodelling	3	0.03	*Fmr1, su(var)3-9, Psc, CG2051, CG6284*

Appendix 7.9: Summary of the delay phase shift results.

Gene	timG4>dcr2;UAS-IR		UAS-IR;w (control)			timG4>dcr2;w (control 2)		
	No of flies	mean[1]	No of flies	mean	Pvalue[2]	No of flies	mean	Pvalue[3]
Thor	25	2.94	20	3.83	0.003	49	3.66	0.003
Calx	28	2.71	14	3.61	0.02	49	3.66	0.000
nrv1	26	2.23	14	3.18	0.01	49	3.66	0.000
DopR	13	3.7	26	3.6	0.87	49	3.66	0.89
Nf1	21	2.26	23	3.41	0.01	49	3.66	0.000
Fmr1	16	2.91	29	3.76	0.01	49	3.66	0.02
CG7589	22	2.9	30	3.83	0.002	49	3.66	0.001
CG11597	23	2.80	21	3.67	0.01	49	3.66	0.002
pho	14	3.0	12	3.50	0.4	49	3.66	0.05
Hr38	25	2.58	22	3.73	0.01	49	3.66	0.000
sug	22	3.8	29	4.1	0.67	49	3.66	0.75
CG11155	20	2.53	27	4.2	0.000	49	3.66	0.000
Still life	29	2.31	29	3.50	0.000	49	3.66	0.000
modifier of mdg4	23	2.7	29	3.4	0.22	49	3.66	0.02

Note this experiment was performed together, hence the same control 2 data was used.

[1] mean delay phase shift

[2] p value of timG4>dcr2;UAS-IR and UAS-IR;w1118 (ANOVA with Post-Hoc test)

[3] p value of timG4>dcr2;UAS-IR and timG4>dcr2;w1118 (ANOVA with Post-Hoc test)

Appendix 7.10: Summary free-running period (DD) of the ten selected genes

Genotype	Mean (hr)	No of flies	p Value
w^{1118};;*UAS-CG1115-IR*	23.5±0.05	32	0.0000 [a]
timG4>dcr2;UAS-CG11155-IR	24.2±0.05	32	0.02[b]
w^{1118};;*UAS-sif-IR*	23.5±0.06	32	0.0000 [a]
timG4>dcr2;UAS-sif-IR	24.6±0.08	31	0.007 [b]
w^{1118};;*UAS-Hr38-IR*	23.8±0.06	28	0.0000 [a]
timG4>dcr2;UAS-Hr38-IR	24.3±0.08	28	0.87 [b]
w^{1118};;*UAS-CG11597-IR*	23.5±0.06	29	0.0000 [a]
timG4>dcr2;UAS-CG11597-IR	24.6±0.09	8	0.23 [b]
w^{1118};;*UAS-Calx-IR*	23.8±0.04	31	0.0000 [a]
timG4>dcr2;UAS-Calx-IR	24.4±0.06	29	0.8 [b]
w^{1118};;*UAS-CG7589-IR*	23.7±0.07	31	0.0000 [a]
timG4>dcr2;UAS-CG7589-IR	24.7±0.10	10	0.03[b]
w^{1118};;*UAS-Fmr1-IR*	23.5±0.06	26	0.0000 [a]
timG4>dcr2;UAS-Fmr1-IR	24.2±0.09	19	0.2 [b]
w^{1118};;*UAS-Thor-IR*	23.4±0.05	25	0.0000 [a]
timG4>dcr2;UAS-Thor-IR	24.4±0.06	31	0.9 [b]
w^{1118};;*UAS-nrv1-IR*	23.6±0.05	32	0.0000 [a]
timG4>dcr2;UAS-nrv1-IR	24.5±0.05	27	0.2 [b]
w^{1118};;*UAS-Nf1-IR*	23.6±0.08	31	0.0000 [a]
timG4>dcr2;UAS-Nf1-IR	24.3±0.08	29	0.46 [b]
w^{1118};; *timG4>dcr2*	24.4±0.04	31	

[a]: p value of timG4>dcr2;UAS-IR and UAS-IR;w1118 (ANOVA with Post-Hoc test)

[b] p value of timG4>dcr2;UAS-IR and timG4>dcr2;w1118 (ANOVA with Post-Hoc test)

Appendices to chapter 5

Appendix 7.11: Light response of chromatin-associated genes

Genotype (UAS line)	**UAS_timGal4-dicer2**		**UAS_w1118 control**			**w1118_timGal4-dicer2 control**		
	No of flies	mean[a]	No of flies	mean	*pvalue*[b]	No of flies	mean	*pvalue*[c]
CG2051	17	3.25	11	4.11	0.000	49	3.66	0.05
Kr-h1	25	2.85	20	3.98	0.000	49	3.66	0.001
Psc	28	2.59	21	3.52	0.003	49	3.66	0.000
Trx	25	2.70	16	4.00	0.000	49	3.66	0.000
Nipped-A	28	2.18	13	3.69	0.000	49	3.66	0.000

[a]: p value of timG4>dcr2;UAS-IR and UAS-IR;w1118 (ANOVA with Post-Hoc test)

[b] p value of timG4>dcr2;UAS-IR and timG4>dcr2;w1118 (ANOVA with Post-Hoc test)

Appendix 7.12: Di-methylation of H3K9 in adult brain.

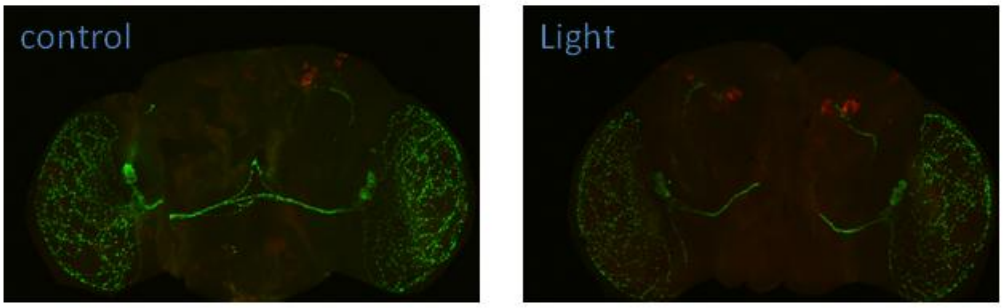

Appendix 7.13: TIM and PDF staining in *Su(var)3-9* mutant and control. The red stains TIM, the green PDF and yellow colour indicates co-localisation of TIM and PDF.

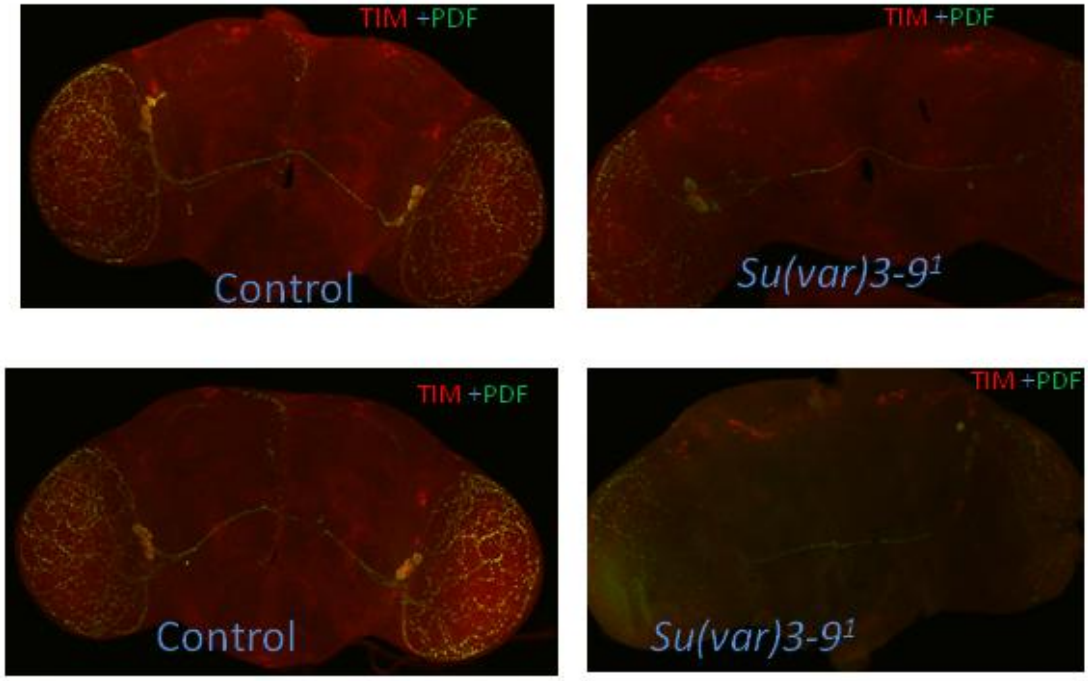

Appendix 7.14: CRY and PDF staining in *Su(var)3-9* mutant and control. The brown stains CRY and, the green PDF. Note that the sample preparations and imaging were done simultaneously under the same setting.

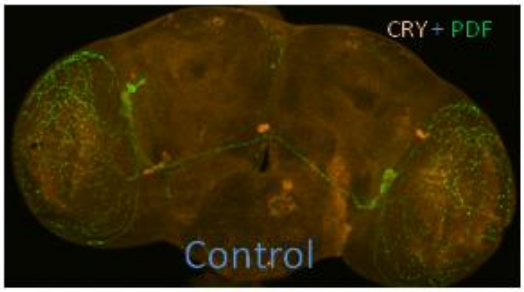

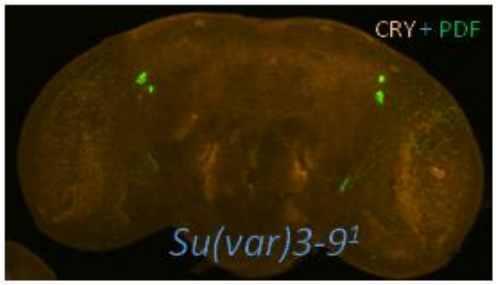

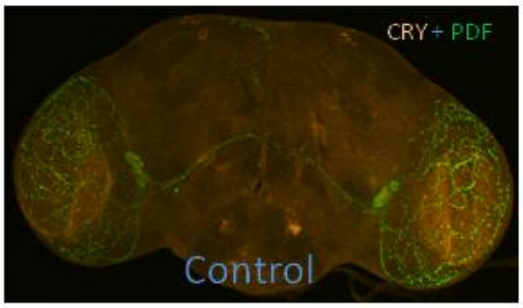

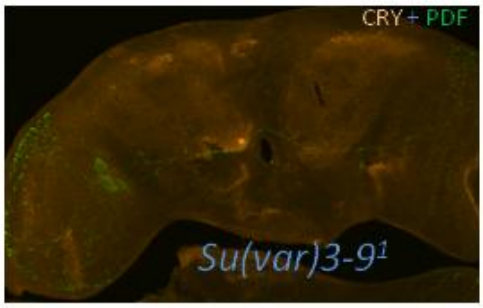

Bibliography

Abe, H., B. Rusak and H. A. Robertson, 1991 Photic induction of fos protein in the suprachiasmatic nucleus is inhibited by the NMDA receptor antagonist MK-801. Neurosci. Lett. **127:** 9-12.

Ahmad, M., and A. R. Cashmore, 1993 HY4 gene of A. thaliana encodes a protein with characteristics of a blue- light photoreceptor. Nature **366:** 162-166.

Akashi, M., and E. Nishida, 2000 Involvement of the MAP kinase cascade in resetting of the mammalian circadian clock. Genes and Development **14:** 645-649.

Albrecht, U., Z. S. Sun, G. Eichele and C. C. Lee, 1997 A differential response of two putative mammalian circadian regulators, mper1 and mper2, to light. Cell **91:** 1055-1064.

Allada, R., N. E. White, W. V. So, J. C. Hall and M. Rosbash, 1998 A mutant drosophila homolog of mammalian clock disrupts circadian rhythms and transcription of period and timeless. Cell **93:** 791-804.

Allis, C. D., S. L. Berger, J. Cote, S. Dent, T. Jenuwien *et al*, 2007 New nomenclature for chromatin-modifying enzymes. Cell **131:** 633-636.

Angers, B., E. Castonguay and R. Massicotte, 2010 Environmentally induced phenotypes and DNA methylation: How to deal with unpredictable conditions until the next generation and after. Mol. Ecol. **19:** 1283-1295.

Antle, M. C., and R. Silver, 2005 Orchestrating time: Arrangements of the brain circadian clock. Trends Neurosci. **28:** 145-151.

Ashburner, M., K. G. Golic and S. R. Hawley, 2005 *Drosophilia: A Laboratory Handbook*. Cold Spring Harbor Laboratory Press, New York.

Auge, G. A., S. Perelman, C. D. Crocco, R. A. Sánchez and J. F. Botto, 2009 Gene expression analysis of light-modulated germination in tomato seeds. New Phytol. **183:** 301-314.

Bae, K., and I. Edery, 2006 Regulating a circadian clock's period, phase and amplitude by phosphorylation: Insights from drosophila. Journal of Biochemistry **140:** 609-617.

Bae, K., C. Lee, D. Sidote, K. -. Chuang and I. Edery, 1998 Circadian regulation of a drosophila homolog of the mammalian clock gene: PER and TIM function as positive regulators. Molecular and Cellular Biology **18:** 6142-6151.

Balsalobre, A., L. Marcacci and U. Schibler, 2000 Multiple signaling pathways elicit circadian gene expression in cultured rat-1 fibroblasts. Current Biology **10:** 1291-1294.

Bannister, A. J., P. Zegerman, J. F. Partridge, E. A. Miska, J. O. Thomas *et al*, 2001 Selective recognition of methylated lysine 9 on histone H3 by the HP1 chromo domain. Nature **410:** 120-124.

Bao, S., J. Rihel, E. Bjes, J. -. Fan and J. L. Price, 2001 The drosophila double-times mutation delays the nuclear accumulation of period protein and affects the feedback regulation of period mRNA. Journal of Neuroscience **21:** 7117-7126.

Barrett, R. K., and J. S. Takahashi, 1995 Temperature compensation and temperature entrainment of the chick pineal cell circadian clock. Journal of Neuroscience **15:** 5681-5692.

Barski, A., S. Cuddapah, K. Cui, T. -. Roh, D. E. Schones *et al*, 2007 High-resolution profiling of histone methylations in the human genome. Cell **129:** 823-837.

Beaver, L. M., B. O. Gvakharia, T. S. Vollintine, D. M. Hege, R. Stanewsky *et al*, 2002 Loss of circadian clock function decreases reproductive fitness in males of drosophila melanogaster. Proceedings of the National Academy of Sciences of the United States of America **99:** 2134-2139.

Bell-Pedersen, D., V. M. Cassone, D. J. Earnest, S. S. Golden, P. E. Hardin *et al*, 2005 Circadian rhythms from multiple oscillators: Lessons from diverse organisms. Nature Reviews Genetics **6:** 544-556.

Benito, J., H. Zheng and P. E. Hardin, 2007 PDP1ε functions downstream of the circadian oscillator to mediate behavioral rhythms. The Journal of Neuroscience **27:** 2539-2547.

Ben-Shlomo, R., and C. P. Kyriacou, 2010 Light pulses administered during the circadian dark phase alter expression of cell cycle associated transcripts in mouse brain. Cancer Genet. Cytogenet. **197:** 65-70.

Bergland, A. O., A. Genissel, S. V. Nuzhdin and M. Tatar, 2008 Quantitative trait loci affecting phenotypic plasticity and the allometric relationship of ovariole number and thorax length in drosophila melanogaster. Genetics **180:** 567-582.

Blanchardon, E., B. Grima, A. Klarsfeld, E. Chélot, P. E. Hardin *et al*, 2001 Defining the role of drosophila lateral neurons in the control of circadian rhythms in motor activity and eclosion by targeted genetic ablation and PERIOD protein overexpression. Eur. J. Neurosci. **13:** 871-888.

Blau, J., and M. W. Young, 1999 Cycling vrille expression is required for a functional drosophila clock. Cell **99:** 661-671.

Blaustein, M. P., 1977 Sodium ions, calcium ions, blood pressure regulation, and hypertension: A reassessment and a hypothesis. Am. J. Physiol. **232:** C165-C173.

Brand, A. H., and N. Perrimon, 1993 Targeted gene expression as a means of altering cell fates and generating dominant phenotypes. Development **118:** 401-415.

Breitling, R., P. Armengaud, A. Amtmann and P. Herzyk, 2004 Rank products: A simple, yet powerful, new method to detect differentially regulated genes in replicated microarray experiments. FEBS Lett. **573:** 83-92.

Broman, K. W., Mapping expression in randomized rodent genomes. Nature Genetics **37:** 209 -210.

Broman, K. W., and S. Sen, 2009 *A Guide to QTL Mapping with R/qtl*. Springer, London.

Brower-Toland, B., N. C. Riddle, H. Jiang, K. L. Huisinga and S. C. R. Elgin, 2009 Multiple SET methyltransferases are required to maintain normal heterochromatin domains in the genome of drosophila melanogaster. Genetics **181:** 1303-1319.

Bunney, W. E., and B. G. Bunney, 2000 Molecular clock genes in man and lower animals: Possible implications for circadian abnormalities in depression. Neuropsychopharmacology **22:** 335-345.

Bustin, S. A., 2002 Quantification of mRNA using real-time reverse transcription PCR (RT-PCR): Trends and problems. J. Mol. Endocrinol. **29:** 23-39.

Busza, A., M. Emery-Le, M. Rosbash and P. Emery, 2004 Roles of the two drosophila CRYPTOCHROME structural domains in circadian photoreception. Science **304:** 1503-1506.

Campos, E. I., and D. Reinberg, 2010 *Histones: Annotating Chromatin*.

Cardone, L., J. Hirayama, F. Giordano, T. Tamaru, J. J. Palvimo *et al*, 2005 Cell biology: Circadian clock control by SUMOylation of BMAL1. Science **309:** 1390-1394.

Cashmore, A. R., 2003 Cryptochromes: Enabling plants and animals to determine circadian time. Cell **114:** 537-543.

Charron, J. F., H. He, A. A. Elling and X. W. Denga, 2009 Dynamic landscapes of four histone modifications during deetiolation in arabidopsis. Plant Cell **21:** 3732-3748.

Chee, M., R. Yang, E. Hubbell, A. Berno, X. C. Huang *et al*, 1996 Accessing genetic information with high-density DNA arrays. Science **274:** 610-614.

Chen, W. -., J. Majercak and I. Edery, 2006 Clock-gated photic stimulation of timeless expression at cold temperatures and seasonal adaptation in drosophila. J. Biol. Rhythms **21:** 256-271.

Cheung, P., C. D. Allis and P. Sassone-Corsi, 2000 Signaling to chromatin through historic modifications. Cell **103:** 263-271.

Chou, C. -., and C. -. Chen, 2008 HDAC inhibition upregulates the expression of angiostatic ADAMTS1. FEBS Lett. **582:** 4059-4065.

Chuaqui, R. F., R. F. Bonner, C. J. M. Best, J. W. Gillespie, M. J. Flaig *et al*, 2002 Post-analysis follow-up and validation of microarray experiments. Nat. Genet. **32:** 509-514.

Churchill, G. A., and R. W. Doerge, 1994 Empirical threshold values for quantitative trait mapping. Genetics **138:** 963-971.

Claridge-Chang, A., H. Wijnen, F. Naef, C. Boothroyd, N. Rajewsky *et al*, 2001 Circadian regulation of gene expression systems in the drosophila head. Neuron **32:** 657-671.

Clayton, A. L., S. Rose, M. J. Barratt and L. C. Mahadevan, 2000 Phosphoacetylation of histone H3 on c-fos- and c-jun-associated nucleosomes upon gene activation. EMBO J. **19:** 3714-3726.

Collins, B., E. O. Mazzoni, R. Stanewsky and J. Blau, 2006 Drosophila CRYPTOCHROME is a circadian transcriptional repressor. Current Biology **16:** 441-449.

Colwell, C. S., R. G. Foster and M. Menaker, 1991 NMDA receptor antagonists block the effects of light on circadian behavior in the mouse. Brain Res. **554:** 105-110.

Cosgrove, M. S., J. D. Boeke and C. Wolberger, 2004 Regulated nucleosome mobility and the histone code. Nature Structural and Molecular Biology **11:** 1037-1043.

Cronin, T. W., 1986 Photorecption in marine invertebrates. American Zoology **26:** 403-415.

Crosio, C., N. Cermakian, C. D. Allis and P. Sassone-Corsi, 2000 Light induces chromatin modification in cells of the mammalian circadian clock. Nat. Neurosci. **3:** 1241-1247.

Curtis, A. M., S. -. Seo, E. J. Westgate, R. D. Rudic, E. M. Smyth *et al*, 2004 Histone acetyltransferase-dependent chromatin remodeling and the vascular clock. J. Biol. Chem. **279:** 7091-7097.

Cusumano, P., A. Klarsfeld, E. Chélot, M. Picot, B. Richier *et al*, 2009 PDF-modulated visual inputs and cryptochrome define diurnal behavior in drosophila. Nature Neuroscience.

Cyran, S. A., A. M. Buchsbaum, K. L. Reddy, M. -. Lin, N. R. J. Glossop *et al*, 2003 Vrille, Pdp1, and dClock form a second feedback loop in the drosophila circadian clock. Cell **112:** 329-341.

Czermin, B., R. Melfi, D. McCabe, V. Seitz, A. Imhof *et al*, 2002 Drosophila enhancer of Zeste/ESC complexes have a histone H3 methyltransferase activity that marks chromosomal polycomb sites. Cell **111:** 185-196.

Czermin, B., G. Schotta, B. B. Hülsmann, A. Brehm, P. B. Becker *et al*, 2001 Physical and functional association of SU(VAR)3-9 and HDAC1 in drosophila. EMBO Rep. **2:** 915-919.

Daan, S., 2000 Colin pittendrigh, jurgen aschoff, and the natural entrainment of circadian systems. J. Biol. Rhythms **15:** 195-207.

Dallas, P. B., N. G. Gottardo, M. J. Firth, A. H. Beesley, K. Hoffmann *et al*, 2005 Gene expression levels assessed by oligonucleotide microarray analysis and quantitative real-time RT-PCR - how well do they correlate? BMC Genomics **6:**

Darlington, T. K., K. Wager-Smith, M. F. Ceriani, D. Staknis, N. Gekakis *et al*, 1998 Closing the circadian loop: CLOCK-induced transcription of its own inhibitors per and tim. Science **280:** 1599-1603.

Darrah, C., B. L. Taylor, K. D. Edwards, P. E. Brown, A. Hall *et al*, 2006 Analysis of phase of LUCIFERASE expression reveals novel circadian quantitative trait loci in arabidopsis. Plant Physiology **140:** 1464-1474.

Darvasi, A., A. Weinreb, V. Minke, J. I. Weller and M. Soller, 1993 Detecting marker-QTL linkage and estimating QTL gene effect and map location using a saturated genetic map. Genetics **134:** 943-951.

Das, C., M. S. Lucia, K. C. Hansen and J. K. Tyler, 2009 CBP/p300-mediated acetylation of histone H3 on lysine 56. Nature **459:** 113-117.

Dasgupta, B., L. L. Dugan and D. H. Gutmann, 2003 The neurofibromatosis 1 gene product neurofibromin regulates pituitary adenylate cyclase-activating polypeptide-mediated signaling in astrocytes. Journal of Neuroscience **23:** 8949-8954.

Dickson, B. J., A. Van Der Straten, M. Domínguez and E. Hafen, 1996 Mutations modulating raf signaling in drosophila eye development. Genetics **142:** 163-171.

Dietzl, G., D. Chen, F. Schnorrer, K. -. Su, Y. Barinova *et al*, 2007 A genome-wide transgenic RNAi library for conditional gene inactivation in drosophila. Nature **448:** 151-156.

Dillon, S. C., X. Zhang, R. C. Trievel and X. Cheng, 2005 The SET-domain protein superfamily: Protein lysine methyltransferases. Genome Biol. **6:** .

Ding, J. M., L. E. Faiman, W. J. Hurst, L. R. Kuriashkina and M. U. Gillette, 1997 Resetting the biological clock: Mediation of nocturnal CREB phosphorylation via light, glutamate, and nitric oxide. Journal of Neuroscience **17:** 667-675.

Dissel, S., V. Codd, R. Fedic, K. J. Garner, R. Costa *et al*, 2004 A constitutively active cryptochrome in *drosophila melanogaster*. Nature Neuroscience **7:** 834-840.

Dodd, A. N., N. Salathia, A. Hall, E. Kévei, R. Tóth *et al*, 2005 Cell biology: Plant circadian clocks increase photosynthesis, growth, survival, and competitive advantage. Science **309:** 630-633.

Doi, M., J. Hirayama and P. Sassone-Corsi, 2006 Circadian regulator CLOCK is a histone acetyltransferase. Cell **125:** 497-508.

Duguay, D., and N. Cermakian, 2009 The crosstalk between physiology and circadian clock proteins. Chronobiol. Int. **26:** 1479-1513.

Dunlap, J. C., 1999 Molecular bases for circadian clocks. Cell **96:** 271-290.

Ebert, A., G. Schotta, S. Lein, S. Kubicek, V. Krauss *et al*, 2004 Su(var) genes regulate the balance between euchromatin and heterochromatin in drosophila. Genes and Development **18:** 2973-2983.

Ebling, F. J. P., 1996 The role of glutamate in the photic regulation of the suprachiasmatic nucleus. Prog. Neurobiol. **50:** 109-132.

Edery, I., L. J. Zwiebel, M. E. Dembinska and M. Rosbash, 1994 Temporal phosphorylation of the drosophila period protein. Proceedings of the National Academy of Sciences of the United States of America **91:** 2260-2264.

Edwards, A. C., and T. F. C. Mackay, 2009 Quantitative trait loci for aggressive behavior in drosophila melanogaster. Genetics **182:** 889-897.

Emery, P., W. V. So, M. Kaneko, J. C. Hall and M. Rosbash, 1998 Cry, a drosophila clock and light-regulated cryptochrome, is a major contributor to circadian rhythm resetting and photosensitivity. Cell **95:** 669-679.

Emery, P., R. Stanewsky, C. Helfrich-Fӧrster, M. Emery-Le, J. C. Hall *et al*, 2000 Drosophila CRY is a deep brain circadian photoreceptor. Neuron **26:** 493-504.

Englund, A., L. Kovanen, S. T. Saarikoski, J. Haukka, A. Reunanen *et al*, 2009 NPAS2 and PER2 are linked to risk factors of the metabolic syndrome. Journal of Circadian Rhythms **7:** 1740-3391.

Eskeland, R., B. Czermin, J. Boeke, T. Bonaldi, J. T. Regula *et al*, 2004 The N-terminus of drosophila SU(VAR)3-9 mediates dimerization and regulates its methyltransferase activity. Biochemistry (N. Y.) **43:** 3740-3749.

Eskin, A., 1979 Identification and physiology of circadian pacemakers. introduction. Fed. Proc. **38:** 2570-2572.

Etchegaray, J. -., X. Yang, J. P. Debruyne, A. H. F. M. Peters, D. R. Weaver *et al*, 2006 The polycomb group protein EZH2 is required for mammalian circadian clock function. J. Biol. Chem. **281:** 21209-21215.

Falconer, D. S., and T. F. C. Mackay, 1996 *Introduction to Quantitative Genetics*. Longman, London.

Fan, Y., A. Hida, D. A. Anderson, M. Izumo and C. H. Johnson, 2007 Cycling of CRYPTOCHROME proteins is not necessary for circadian-clock function in mammalian fibroblasts. Current Biology **17:** 1091-1100.

Fang, Y., S. Sathyanarayanan and A. Sehgal, 2007 Post-translational regulation of the drosophila circadian clock requires protein phosphatase 1 (PP1). Genes and Development **21:** 1506-1518.

Feng, Q., H. Wang, H. H. Ng, H. Erdjument-Bromage, P. Tempst *et al*, 2002 Methylation of H3-lysine 79 is mediated by a new family of HMTases without a SET domain. Current Biology **12:** 1052-1058.

Field, M. D., E. S. Maywood, J. A. O'Brien, D. R. Weaver, S. M. Reppert *et al*, 2000 Analysis of clock proteins in mouse SCN demonstrates phylogenetic divergence of the circadian clockwork and resetting mechanisms. Neuron **25:** 437-447.

Fraga, M. F., E. Ballestar, M. F. Paz, S. Ropero, F. Setien *et al*, 2005 Epigenetic differences arise during the lifetime of monozygotic twins. Proc. Natl. Acad. Sci. U. S. A. **102:** 10604-10609.

Francis, N. J., R. E. Kingston and C. L. Woodcock, 2004 Chromatin compaction by a polycomb group protein complex. Science **306:** 1574-1577.

Gallego, M., and D. M. Virshup, 2007 Post-translational modifications regulate the ticking of the circadian clock. Nature Reviews Molecular Cell Biology **8:** 139-148.

Gegear, R. J., A. Casselman, S. Waddell and S. M. Reppert, 2008 Cryptochrome mediates light-dependent magnetosensitivity in drosophila. Nature **454:** 1014-1018.

Giebultowicz, J. M., R. Stanewsky, J. C. Hall and D. M. Hege, 2000 Transplanted drosophila excretory tubules maintain circadian clock cycling out of phase with the host. Current Biology **10:** 107-110.

Gloor, G. B., and W. R. Engels, 1992 Single fly DNA preps for PCR. Drosophila Information Service **71:** 148-149.

Glossop, N. R. J., L. C. Lyons and P. E. Hardin, 1999 Interlocked feedback loops within the drosophila circadian oscillator. Science **286:** 766-768.

Glossop, N. R. J., J. H. Houl, H. Zheng, F. S. Ng, S. M. Dudek *et al*, 2003 Vrille feeds back to control circadian transcription of clock in the drosophila circadian oscillator. Neuron **37:** 249-261.

Golden, S. S., C. H. Johnson and T. Kondon, 1998 The cyanobacterial circadian system: A clock apart. Current Opinion in Microbiology **1:** 669-673.

Goldsmith, T. H., 1990 The quarterly review of biology: Optimization, constraint, and history in the evolution of eyes. Q. Rev. Biol. **65:** 281-322.

Gooley, J. J., S. M. W. Rajaratnam, G. C. Brainard, R. E. Kronauer, C. A. Czeisler *et al*, 2010 Spectral responses of the human circadian system depend on the irradiance and duration of exposure to light. Science Translational Medicine **2:** .

Górska-Andrzejak, J., P. M. Salvaterra, I. A. Meinertzhagen, W. Krzeptowski, A. Görlich *et al*, 2009 Cyclical expression of Na+/K+-ATPase in the visual system of drosophila melanogaster. J. Insect Physiol. **55:** 459-468.

Green, C. B., 2004 Cryptochromes: Tail-ored for distinct functions. Current Biology **14:** R847-R849.

Grima, B., E. Chélot, R. Xia and F. Rouyer, 2004 Morning and evening peaks of activity rely on different clock neurons of the drosophila brain. Nature **431:** 869-873.

Halberg, F., 1960 Temporal coordination of physiologic function. Cold Spring Harbor Symposia on Quantitative Biology **25:** 289-310.

Halket, A. C., 1931 The flowers of silene saxifraga L.; an inquiry into the cause of their day closure and the mechanism concerned in effecting their periodic movements. Annals of Botany **45:** 15-37.

Hamasaka, Y., D. Rieger, M. -. Parmentier, Y. Grau, C. Helfrich-Förster *et al*, 2007a Glutamate and its metabotropic receptor in drosophila clock neuron circuits. J. Comp. Neurol. **505:** 32-45.

Hao, H., D. L. Allen and P. E. Hardin, 1997 A circadian enhancer mediates PER-dependent mRNA cycling in drosophila melanogaster. Molecular and Cellular Biology **17:** 3687-3693.

Hao, H., N. R. J. Glossop, L. Lyons, J. Qiu, B. Morrish *et al*, 1999 The 69 bp circadian regulatory sequence (CRS) mediates per-like developmental, spatial, and circadian expression and behavioral rescue in drosophila. Journal of Neuroscience **19:** 987-994.

Harbison, S. T., M. A. Carbone, J. F. Ayroles, E. A. Stone, R. F. Lyman *et al*, 2009 Co-regulated transcriptional networks contribute to natural genetic variation in drosophila sleep. Nat. Genet. **41:** 371-375.

Hardie, R. C., 2001 Phototransduction in drosophila melanogaster. Journal of Experimental Biology **204:** 3403-3409.

Hardie, R. C., and P. Raghu, 2001 Visual transduction in drosophila. Nature **413:** 186-193.

Hardin, P. E., 2005 The circadian timekeeping system of drosophila. Current Biology **15:** R714-R722.

Hardin, P. E., 2006 Essential and expendable features of the circadian. Current Opinion in Neurobiology **16:** 686-692.

Hardin, P. E., J. C. Hall and M. Rosbash, 1990 Feedback of the drosophila period gene product on circadian cycling of its messenger RNA levels. Nature **343:** 536-540.

Harmer, S. L., J. B. Hogenesch, M. Straume, H. -. Chang, B. Han *et al*, 2000 Orchestrated transcription of key pathways in arabidopsis by the circadian clock. Science **290:** 2110-2113.

Harms, E., S. Kivimaë, M. W. Young and L. Saez, 2004 Posttranscriptional and posttranslational regulation of clock genes. Journal of Biological Rhythms **19:** 361-373.

Headrick Zimmerman, N., and M. Menaker, 1979 The pineal gland: A pacemaker within the circadian system of the house sparrow. Proc. Natl. Acad. Sci. U. S. A. **76:** 999-1003.

Helfrich-Förster, C., and W. Engelmann, 2002 Photoreceptors for the circadian clock of the fruit fly, pp. 94-106 in , edited by V. Kumar. Springer, New York,US.

Helfrich-Förster, C., 2007 Immunohistochemistry in Drosophila: Sections and Whole Mounts.

Helfrich-Förster, C., 2003 The neuroarchitecture of the circadian clock in the brain of drosophila melanogaster. Microsc. Res. Tech. **62:** 94-102.

Helfrich-Förster, C., C. Winter, A. Hofbauer, J. C. Hall and R. Stanewsky, 2001 The circadian clock of fruit flies is blind after elimination of all known photoreceptors. Neuron **30:** 249-261.

Helfrich-Förster, C., O. T. Shafer, C. Wülbeck, E. Grieshaber, D. Rieger *et al*, 2007 Development and morphology of the clock-gene-expreasing lateral neurons of drosophila melanogaster. Journal of Comparative Neurology **500:** 47-70.

Helfrich-Förster, C., T. Edwards, K. Yasuyama, B. Wisotzki, S. Schneuwly *et al*, 2002 The extraretinal eyelet of drosophila: Development, ultrastructure, and putative circadian function. Journal of Neuroscience **22:** 9255-9266.

Hirayama, J., S. Sahar, B. Grimaldi, T. Tamaru, K. Takamatsu *et al*, 2007 CLOCK-mediated acetylation of BMAL1 controls circadian function. Nature **450:** 1086-1090.

Hofbauer, A., and E. Buchner, 1989 Does *drosophila* have seven eyes. Naturwissenchaften **76:** 335-336.

Hong, F., R. Breitling, C. W. McEntee, B. S. Wittner, J. L. Nemhauser *et al*, 2006 RankProd: A bioconductor package for detecting differentially expressed genes in meta-analysis. Bioinformatics **22:** 2825-2827.

Hrushesky, W. J. M., J. Grutsch, P. Wood, X. Yang, E. Y. Oh *et al*, 2009 Circadian clock manipulation for cancer prevention and control and the relief of cancer symptoms. Integrative Cancer Therapies **8:** 387-397.

Hu, K. G., H. Reichert and W. S. Stark, 1978 Electrophysiological characterization of drosophila ocelli. Journal of Comparative Physiology □ A **126:** 15-24.

Huang, D. W., B. T. Sherman and R. A. Lempicki, 2009 Systematic and integrative analysis of large gene lists using DAVID bioinformatics resources. Nature Protocols **4:** 44-57.

Hung, H. -., C. Maurer, S. A. Kay and F. Weber, 2007 Circadian transcription depends on limiting amounts of the transcription co-activator nejire/CBP. J. Biol. Chem. **282:** 31349-31357.

Hunter-Ensor, M., A. Ousley and A. Sehgal, 1996 Regulation of the drosophila protein timeless suggests a mechanism for resetting the circadian clock by light. Cell **84:** 677-685.

Inoue, S. B., M. Shimoda, I. Nishinokubi, M. C. Siomi, M. Okamura *et al*, 2002 A role for the drosophila fragile X-related gene in circadian output. Current Biology **12:** 1331-1335.

Ito, C., S. G. Goto, S. Shiga, K. Tomioka and H. Numata, 2008 Peripheral circadian clock for the cuticle deposition rhythm in drosophila melanogaster. Proc. Natl. Acad. Sci. U. S. A. **105:** 8446-8451.

Jablonka, E. V. A., and G. A. L. Raz, 2009 Transgenerational epigenetic inheritance: Prevalence, mechanisms, and implications for the study of heredity and evolution. Q. Rev. Biol. **84:** 131-176.

Jackson-Grusby, L., C. Beard, R. Possemato, M. Tudor, D. Fambrough *et al*, 2001 Loss of genomic methylation causes p53-dependent apoptosis and epigenetic deregulation. Nat. Genet. **27:** 31-39.

Jenuwein, T., G. Laible, R. Dorn and G. Reuter, 1998 SET domain proteins modulate chromatin domains in eu- and heterochromatin. Cellular and Molecular Life Sciences **54:** 80-93.

Johnson, C. H., 2001 Endogenous timekeepers in photosynthetic organisms. Annual Review of Physiology **63:** 695-728.

Johnson, C. H., J. A. Elliott and R. Foster, 2003 Entrainment of circadian programs. Chronobiology International **20:** 741-774.

Johnson, C. H., 1999 Forty years of PRCs--what have we learned? Chronobiology International **16:** 711-743.

Johnson, C. H., S. S. Golden and T. Kondo, 1998 Adaptive significance of circadian programs in cyanobacteria. Trends Microbiol. **6:** 407-410.

Johnsson, A., and E. Engelmann, 2008 The biological clock and its resetting by light., pp. 321-388 in *Photobiology.*, edited by L. O. Björn. Springer New York, New York,US.

Jones, C. R., S. S. Campbell, S. E. Zone, F. Cooper, A. Desano *et al*, 1999 Familial advanced sleep-phase syndrome: A short-period circadian rhythm variant in humans. Nat. Med. **5:** 1062-1065.

Jordan, K. W., M. A. Carbone, A. Yamamoto, T. J. Morgan and T. F. C. Mackay, 2007 Quantitative genomics of locomotor behavior in drosophila melanogaster. Genome Biololgy **8:** R172.

Kadener, S., D. Stoleru, M. McDonald, P. Nawathean and M. Rosbash, 2007 Clockwork orange is a transcriptional repressor and a new drosophila circadian pacemaker component. Genes and Development **21:** 1675-1686.

Kaneko, M., C. Helfrich-Förster and J. C. Hall, 1997 Spatial and temporal expression of the period and timeless genes in the developing nervous system of drosophila: Newly identified pacemaker candidates and novel features of clock gene product cycling. Journal of Neuroscience **17:** 6745-6760.

Kaneko, M., and J. C. Hall, 2000 Neuroanatomy of cells expressing clock genes in drosophila: Transgenic manipulation of the period and timeless genes to mark the perikarya of circadian pacemaker neurons and their projections. J. Comp. Neurol. **422:** 66-94.

Kao, C. -., Z. -. Zeng and R. D. Teasdale, 1999 Multiple interval mapping for quantitative trait loci. Genetics **152:** 1203-1216.

Kawahara, T. L. A., E. Michishita, A. S. Adler, M. Damian, E. Berber *et al*, 2009 SIRT6 links histone H3 lysine 9 deacetylation to NF-κB-dependent gene expression and organismal life span. Cell **136:** 62-74.

Khalsa, S. B. S., and G. D. Block, 1988 Calcium channels mediate phase shifts of the bulla circadian pacemaker. Journal of Comparative Physiology - A Sensory, Neural, and Behavioral Physiology **164:** 195-206.

Kim, T. -., B. A. Logsdon, S. Park, J. G. Mezey and K. Lee, 2007 Quantitative trait loci for the circadian clock in neurospora crassa. Genetics **177:** 2335-2347.

Kim, E. Y., and I. Edery, 2006 Balance between DBT/CKIε kinase and protein phosphatase activities regulate phosphorylation and stability of drosophila CLOCK protein. Proceedings of the National Academy of Sciences of the United States of America **103:** 6178-6183.

Klarsfeld, A., S. Malpel, C. Michard-Vanhée, M. Picot, E. Chélot *et al*, 2004 Novel features of cryptochrome-mediated photoreception in the brain circadian clock of drosophila. Journal of Neuroscience **24:** 1468-1477.

Klein, D. C., R. Y. Moore and S. M. Reppert, 1991 *Suprachiasmatic Nucleus: The Mind's Clock*. New York: Oxford University Press, USA.

Kloss, B., A. Rothenfluh, M. W. Young and L. Saez, 2001 Phosphorylation of PERIOD is influenced by cycling physical associations of DOUBLE-TIME,PERIOD, and TIMELESS in the drosophila clock. Neuron **30:** 699-706.

Kloss, B., J. L. Price, L. Saez, J. Blau, A. Rothenfluh *et al*, 1998 The drosophila clock gene double-time encodes a protein closely related to human casein kinase Iε. Cell **94:** 97-107.

Knowles, A., K. Koh, J. -. Wu, C. -. Chien, D. A. Chamovitz *et al*, 2009 The COP9 signalosome is required for light-dependent timeless degradation and drosophila clock resetting. Journal of Neuroscience **29:** 1152-1162.

Koh, K., X. Zheng and A. Sehgal, 2006 JETLAG resets the drosophila circadian clock by promoting light-induced degradation of TIMELESS. Science **312:** 1809-1812.

Konopka, R. J., and S. Benzer, 1971 Clock mutants of drosophila melanogaster. Proceedings of the National Academy of Sciences of the United States of America **68:** 2112-2116.

Konopka, R. J., C. Pittendrigh and D. Orr, 1989 Reciprocal behaviour associated with altered homeostasis and photosensitivity of drosophila clock mutants. J. Neurogenet. **6:** 1-10.

Kouzarides, T., 2007 Chromatin modifications and their function. Cell **128:** 693-705.

Krishnan, B., S. E. Dryer and P. E. Hardin, 1999 Circadian rhythms in olfactory responses of drosophila melanogaster. Nature **400:** 375-378.

Krishnan, B., J. D. Levine, M. K. S. Lynch, H. B. Dowse, P. Funes *et al*, 2001 A new role for cryptochrome in a drosophila circadian oscillator. Nature **411:** 313-317.

Kula-Eversole, E., E. Nagoshi, Y. Shang, J. Rodriguez, R. Allada *et al*, 2010 Surprising gene expression patterns within and between PDF-containing circadian neurons in drosophila. Proc. Natl. Acad. Sci. U. S. A. **107:** 13497-13502.

Kumar, S., A. Mohan and V. K. Sharma, 2005 Circadian dysfunction reduces lifespan in drosophila melanogaster. Chronobiology International **22:** 641-653.

Kuo, S. -., S. -. Chen, K. -. Yeh, M. -. Hou, Y. -. Chang *et al*, 2009 Disturbance of circadian gene expression in breast cancer. Virchows Archives **454:** 467-474.

Kyriacou, C. P., and E. Rosato, 2000 Squaring up the E-box. J. Biol. Rhythms **15:** 483-490.

Kyriacou, C. P., A. A. Peixoto, F. Sandrelli, R. Costa and E. Tauber, 2008 Clines in clock genes: Fine-tuning circadian rhythms to the environment. Trends in Genetics **24:** 124-132.

Lachner, M., and T. Jenuwein, 2002 The many faces of histone lysine methylation. Curr. Opin. Cell Biol. **14:** 286-298.

Lander, E. S., and S. Botstein, 1989 Mapping mendelian factors underlying quantitative traits using RFLP linkage maps. Genetics **121:** 185.

Lander, E. S., P. Green, J. Abrahamson, A. Barlow, M. J. Daly *et al*, 1987 MAPMAKER: An interactive computer package for constructing primary genetic linkage maps of experimental and natural populations. Genomics **1:** 174-181.

Landskron, J., K. F. Chen, E. Wolf and R. Stanewsky, 2009 A role for the PERIOD:PERIOD homodimer in the drosophila circadian clock. PLoS biology **7:**

Latta, R. G., and K. M. Gardner, 2009 Natural selection on pleiotropic quantitative trait loci affecting a life-history trade-off in avena barbata. Evolution **63:** 2153-2163.

Lee, C., K. Bae and I. Edery, 1998 The drosophila CLOCK protein undergoes daily rhythms in abundance, phosphorylation, and interactions with the PER-TIM complex. Neuron **21:** 857-867.

Lee, S. -., H. Xu, L. -. Kang, L. M. Amzel and C. Montell, 2003 Light adaptation through phosphoinositide-regulated translocation of drosophila visual arrestin. Neuron **39:** 121-132.

Levine, J. D., P. Funes, H. B. Dowse and J. C. Hall, 2002a Resetting the circadian clock by social experience in drosophila melanogaster. Science **298:** 2010-2012.

Levine, J. D., P. Funes, H. B. Dowse and J. C. Hall, 2002b Advanced analysis of a cryptochrome mutation's effects on the robustness and phase of molecular cycles in isolated peripheral tissues of drosophila. BMC neuroscience [electronic resource] **3:** 5.

Levitin, A., A. Marcil, G. Tettweiler, M. J. Laforest, U. Oberholzer *et al*, 2007 Drosophila melanogaster thor and response to candida albicans infection. Eukaryotic Cell **6:** 658-663.

Li, Y. -., X. -. Fu, D. -. Liu and C. -. Liang, 2004 Opening the chromatin for transcription. International Journal of Biochemistry and Cell Biology **36:** 1411-1423.

Lim, C., J. Lee, E. Koo and J. Choe, 2007a Targeted inhibition of Pdp1ε abolishes the circadian behavior of drosophila melanogaster. Biochem. Biophys. Res. Commun. **364:** 294-300.

Lim, C., B. Y. Chung, J. L. Pitman, J. J. McGill, S. Pradhan *et al*, 2007b Clockwork orange encodes a transcriptional repressor important for circadian-clock amplitude in drosophila. Current Biology **17:** 1082-1089.

Lin, C., and T. Todo, 2005 The cryptochromes. Genome Biology **6:**

Lin, J. -., V. L. Kilman, K. Keegan, B. Paddock, M. Emery-Le *et al*, 2002a A role for casein kinase 2α in the drosophila circadian clock. Nature **420:** 816-820.

Lin, Y., M. Han, B. Shimada, L. Wang, T. M. Gibler *et al*, 2002b Influence of the period-dependent circadian clock on diurnal, circadian, and aperiodic gene expression in drosophila melanogaster. Proc. Natl. Acad. Sci. U. S. A. **99:** 9562-9567.

Lincoln, S. E., M. J. Daly and E. S. Lander, 1993 *Constructing Genetic Linkage Maps with MAPMAKER Version 3.0: A Tutorial and Reference Manual*. Whitehead Institute for Biomedical Research, Cambridge,USA.

Lo, S. M., N. K. Ahuja and N. J. Francis, 2009 Polycomb group protein suppressor 2 of zeste is a functional homolog of posterior sex combs. Mol. Cell. Biol. **29:** 515-525.

Luger, K., and J. C. Hansen, 2005 Nucleosome and chromatin fiber dynamics. Curr. Opin. Struct. Biol. **15:** 188-196.

Lynch, M., and B. Walsh, 1998 *Genetics and Analysis of Quantitative Traits*. Sinauer Associates, Sunderland, MA.

Lyne, R., R. Smith, K. Rutherford, M. Wakeling, A. Varley *et al*, 2007 FlyMine: An integrated database for drosophila and anopheles genomics. Genome Biol. **8:** .

Mackay, T. F. C., 2010 Mutations and quantitative genetic variation: Lessons from drosophila. Philosophical Transactions of the Royal Society B: Biological Sciences **365:** 1229-1239.

Mackay, T. F. C., 2001 Quantitative trait loci in drosophila. Nature Reviews Genetics **2:** 11-20.

Manabe, H., Y. Nasu, T. Komiyama, T. Furumatsu, A. Kitamura *et al*, 2008 Inhibition of histone deacetylase down-regulates the expression of hypoxia-induced vascular endothelial growth factor by rheumatoid synovial fibroblasts. Inflammation Res. **57:** 4-10.

Mangin, B., B. Goffinet and A. Rebai, 1994 Constructing confidence intervals for QTL location. Genetics **138:** 1301-1308.

Manning, K., M. Tör, M. Poole, Y. Hong, A. J. Thompson *et al*, 2006 A naturally occurring epigenetic mutation in a gene encoding an SBP-box transcription factor inhibits tomato fruit ripening. Nat. Genet. **38:** 948-952.

Martinek, S., S. Inonog, A. S. Manoukian and M. W. Young, 2001 A role for the segment polarity gene shaggy/GSK-3 in the drosophila circadian clock. Cell **105:** 769-779.

Matevossian, A., and S. Akbarian, 2008 A chromatin assay for human brain tissue. Journal of visualized experiments : JoVE .

Matsumoto, A., 2006 Genome-wide screenings for circadian clock genes in drosophila. Sleep and Biological Rhythms **4:** 248-254.

Matsumoto, A., M. Ukai-Tadenuma, R. G. Yamada, J. Houl, K. D. Uno *et al*, 2007 A functional genomics strategy reveals clockwork orange as a transcriptional regulator in the drosophila circadian clock. Genes and Development **21:** 1687-1700.

McCabe, C., and A. Birley, 1998 Oviposition in the period genotypes of drosophila melanogaster. Chronobiology International **15:** 119-133.

McDonald, M. J., and M. Rosbash, 2001 Microarray analysis and organization of circadian gene expression in drosophila. Cell **107:** 567-578.

McDonald, M. J., M. Rosbash and P. Emery, 2001 Wild-type circadian rhythmicity is dependent on closely spaced E boxes in the drosophila timeless promoter. Mol. Cell. Biol. **21:** 1207-1217.

McGowan, P. O., M. J. Meaney and M. Szyf, 2008 Diet and the epigenetic (re)programming of phenotypic differences in behavior. Brain Res. **1237:** 12-24.

Menaker, M., and H. Underwood, 1976 Extraretinal photoreception in birds. Photophysiology **23:** 299-306.

Mertens, I., A. Vandingenen, E. C. Johnson, O. T. Shafer, W. Li *et al*, 2005 PDF receptor signaling in drosophila contributes to both circadian and geotactic behaviors. Neuron **48:** 213-219.

Meyar, P., L. Saez and M. W. Young, 2006a PER-TIM interactions in living drosophila cells: An interval timer for the circadian clock. Science **311:** 226-229.

Michael, T. P., P. A. Salomé, H. J. Yu, T. R. Spencer, E. L. Sharp *et al*, 2003 Enhanced fitness conferred by naturally occurring variation in the circadian clock. Science **302:** 1049-1053.

Miller, B. H., S. L. Olson, F. W. Turek, J. E. Levine, T. H. Horton *et al*, 2004 Circadian clock mutations disrupts estrous cyclicity and maintenance of pregnancy. Current Biology **14:** 1367-1373.

Minakuchi, C., T. Namiki and T. Shinoda, 2009 Krüppel homolog 1, an early juvenile hormone-response gene downstream of methoprene-tolerant, mediates its anti-metamorphic action in the red flour beetle tribolium castaneum. Dev. Biol. **325:** 341-350.

Montell, C., 1999 Visual Transduction in Drosophila.

Morey, J. S., J. C. Ryan and F. M. Van Dolah, 2006 Microarray validation: Factors influencing correlation between oligonucleotide microarrays and real-time PCR. Biol. Proc. Online **8:** 175-193.

Morgan, H. D., H. G. E. Sutherland, D. I. K. Martin and E. Whitelaw, 1999 Epigenetic inheritance at the agouti locus in the mouse. Nat. Genet. **23:** 314-318.

Morse, D., and P. Sassone-Corsi, 2002 Time after time: Inputs to and outputs from the mammalian circadian oscillators. Trends Neurosci. **25:** 632-637.

Moses, K., M. Elis and G. Rubin, 1989 The *glass* gene encodes a zinc-finger protein required by *drosophila* photoreceptor cells. Nature **340:** 531-536.

Mutskov, V., and G. Felsenfeld, 2004 Silencing of transgene transcription precedes methylation of promoter DNA and histone H3 lysine 9. EMBO J. **23:** 138-149.

Myers, M. P., K. Wager-Smith, A. Rothenfluh-Hilfiker and M. W. Young, 1996 Light-induced degradation of TIMELESS and entrainment of the drosophila circadian clock. Science **271:** 1736-1740.

Nagoshi, E., K. Sugino, E. Kula, E. Okazaki, T. Tachibana *et al*, 2010 Dissecting differential gene expression within the circadian neuronal circuit of drosophila. Nat. Neurosci. **13:** 60-68.

Naruse, Y., K. Oh-Hashi, N. Iijima, M. Naruse, H. Yoshioka *et al*, 2004 Circadian and light-induced transcription of clock gene Per1 depends on histone acetylation and deacetylation. Mol. Cell. Biol. **24:** 6278-6287.

Ni, J. -., L. -. Liu, D. Hess, J. Rietdorf and F. -. Sun, 2006 Drosophila ribosomal proteins are associated with linker histone H1 and suppress gene transcription. Genes and Development **20:** 1959-1973.

Nitabach, M. N., T. C. Holmes and J. Blau, 2005 Membranes, Ions, and Clocks: Testing the Njus-Sulzman-Hastings Model of the Circadian Oscillator.

Nitabach, M. N., J. Blau and T. C. Holmes, 2002 Electrical silencing of drosophila pacemaker neurons stops the free-running circadian clock. Cell **109:** 485-495.

Njus, D., F. M. Sulzman and J. W. Hastings, 1974 Membrane model for the circadian clock. Nature **248:** 116-120.

Obrietan, K., S. Impey and D. R. Storm, 1998 Light and circadian rhythmicity regulate MAP kinase activation in the suprachiasmatic nuclei. Nat. Neurosci. **1:** 693-700.

Oh-hashi, K., Y. Naruse and M. Tanaka, 2002 Intracellular calcium mobilization induces period genes via MAP kinase pathways in NIH3T3 cells. FEBS Lett. **516:** 101-105.

Ouyang, Y., C. R. Andersson, T. Kondo, S. S. Golden and C. H. Johnson, 1998 Resonating circadian clocks enhance fitness in cyanobacteria. Proceedings of the National Academy of Sciences of the United States of America **95:** 8660-8664.

Pallier, P. N., E. S. Maywood, Z. Zheng, J. E. Chesham, A. N. Inyushkin *et al*, 2007 Pharmacological imposition of sleep slows cognitive decline and reverses dysregulation of circadian gene expression in a transgenic mouse model of huntington's disease. Journal of Neuroscience **27:** 7869-7878.

Passador-Gurgel, G., W. -. Hsieh, P. Hunt, N. Deighton and G. Gibson, 2007 Quantitative trait transcripts for nicotine resistance in drosophila melanogaster. Nat. Genet. **39:** 264-268.

Peschel, N., S. Veleri and R. Stanewsky, 2006 Veela defines a molecular link between cryptochrome and timeless in the light-input pathway to drosophila's circadian clock. Proceedings of the National Academy of Sciences of the United States of America **103:** 17313-17318.

Peschel, N., K. Chen, G. Szabo and R. Stanewsky, 2009 Light-dependent interactions between the drosophila circadian clock factors cryptochrome, jetlag, and timeless. Current Biology **19:** 241-247.

Phalke, S., O. Nickel, D. Walluscheck, F. Hortig, M. C. Onorati *et al*, 2009 Retrotransposon silencing and telomere integrity in somatic cells of drosophila depends on the cytosine-5 methyltransferase DNMT2. Nat. Genet. **41:** 696-702.

Pittendrigh, C. S., 1981 Circadian systems:Entrainment, pp. 95-124 in *Handbook of Behavioral Neurobiology*, edited by J. Aschoff. Plenum Press, New York ; London.

Pittendrigh, C. S., 1960 Circadian rhythms and the circadian organization of living systems. Cold Spring Harbor Symposia on Quantitative Biology **25:** 159-184.

Pittendrigh, C. S., 1954 On temperature independence in the clock system controlling emergence time in *drosophila*. Proceedings of the National Academy of Sciences **40:** 1018-1029.

Pittendrigh, C. S., and D. H. Minis, 1964 The entrainment of circadian oscillations by light and their role as photoperiodic clocks. The American Naturalist **98:** 261-294.

Pittendrigh, C. S., V. Bruce and P. kaus, 1958 On the significance of transients in daily rhythms. Proceedings of the National Academy of Sciences of the United States of America **44:** 965-973.

Pittendrigh, C. S., 1993 Temporal organization: Reflections of a darwinian clock-watcher. Annu. Rev. Physiol. **55:** 17-54.

Pittendrigh, C. S., and T. Takamura, 1989 Latitudinal clines in the properties of a circadian pacemaker. J. Biol. Rhythms **4:** 217-235.

Pittendrigh, C. S., and D. H. Minis, 1972 Circadian systems: Longevity as a function of circadian resonance in drosophila melanogaster. Proc. Natl. Acad. Sci. U. S. A. **69:** 1537-1539.

Pittendrigh, C. S., W. T. Kyner and T. Takamura, 1991 The amplitude of circadian oscillations: Temperature dependence, latitudinal clines, and the photoperiodic time measurement. J. Biol. Rhythms **6:** 299-313.

Plautz, J. D., M. Kaneko, J. C. Hall and S. A. Kay, 1997 Independent photoreceptive circadian clocks throughout drosophila. Science **278:** 1632-1635.

Pollock, J. A., and S. Benzer, 1988 Transcript localization of four opsin genes in the three visual organs of drosophila; RH2 is ocellus specific. Nature **333:** 779-782.

Porras-Yakushi, T. R., J. P. Whitelegge and S. Clarke, 2006 A novel SET domain methyltransferase in yeast: Rkm2-dependent trimethylation of ribosomal protein L12ab at lysine 10. J. Biol. Chem. **281:** 35835-35845.

Porterfield, V. M., and E. M. Mintz, 2009 Temporal patterns of light-induced immediate-early gene expression in the suprachiasmatic nucleus. Neurosci. Lett. **463:** 70-73.

Price, J. L., J. Blau, A. Rothenfluh, M. Abodeely, B. Kloss *et al*, 1998 Double-time is a novel drosophila clock gene that regulates period protein accumulation. Cell **94:** 83-95.

Renn, S. C. P., J. H. Park, M. Rosbash, J. C. Hall and P. H. Taghert, 1999 A pdf neuropeptide gene mutation and ablation of PDF neurons each cause severe abnormalities of behavioral circadian rhythms in drosophila. Cell **99:** 791-802.

Richier, B., C. Michard-Vanhée, A. Lamouroux, C. Papin and F. Rouyer, 2008 The clockwork orange drosophila protein functions as both an activator and a repressor of clock gene expression. J. Biol. Rhythms **23:** 103-116.

Rieger, D., O. T. Shafer, K. Tomioka and C. Helfrich-Förster, 2006 Functional analysis of circadian pacemaker neurons in drosophila melanogaster. Journal of Neuroscience **26:** 2531-2543.

Rieger, D., R. Stanewsky and C. Helfrich-Förster, 2003 Cryptochrome, compound eyes, hofbauer-buchner eyelets, and ocelli play different roles in the entrainment and masking pathway of the locomotor activity rhythm in the fruit fly drosophila melanogaster. Journal of Biological Rhythms **18:** 377-391.

Ripperger, J. A., and U. Schibler, 2006 Rhythmic CLOCK-BMAL1 binding to multiple E-box motifs drives circadian dbp transcription and chromatin transitions. Nat. Genet. **38:** 369-374.

Roenneberg, T., and M. Merrow, 1999 Circadian systems and metabolism. J. Biol. Rhythms **14:** 449-459.

Roenneberg, T., and R. G. Foster, 1997 Twilight times: Light and the circadian system. Photochem. Photobiol. **66:** 549-561.

Rosato, E., and C. P. Kyriacou, 2006 Analysis of locomotor activity rhythms in drosophila. Nature Protocols **1:** 559-568.

Rosato, E., V. Codd, G. Mazzotta, A. Piccin, M. Zordan *et al*, 2001 Light-dependent interaction between drosophila CRY and the clock protein PER mediated by the carboxy terminus of CRY. Current Biology **11:** 909-917.

Rouyer, F., M. Rachidi, C. Pikielny and M. Rosbash, 1997 A new gene encoding a putative transcription factor regulated by the drosophila circadian clock. EMBO J. **16:** 3944-3954.

Ruby, N. F., D. E. Burns and H. C. Heller, 1999 Circadian rhythms in the suprachiasmatic nucleus are temperature- compensated and phase-shifted by heat pulses in vitro. Journal of Neuroscience **19:** 8630-8636.

Rusak, B., H. A. Robertson, W. Wisden and S. P. Hunt, 1990 Light pulses that shift rhythms induce gene expression in the suprachiasmatic nucleus. Science **248:** 1237-1240.

Rutherford, S. L., and S. Lindquist, 1998 Hsp90 as a capacitor for morphological evolution. Nature **396:** 336-342.

Rutila, J. E., V. Suri, M. Le, W. V. So, M. Rosbash *et al*, 1998 Cycle is a second bHLH-PAS clock protein essential for circadian rhythmicity and transcription of drosophila period and timeless. Cell **93:** 805-814.

Sadakane, Y., and H. Nakashima, 1995 Synthesis of mRNA is required for light-induced phase shifting of the circadian conidiation rhythm in neurospora crassa. Plant and Cell Physiology **36:** 473-480.

Sambrook, J., and D. W. Rusell, 2001 *Molecular Cloning- a Laboratory Manual*. Cold Spring Harbor Laboratory, USA.

Sandrelli, F., E. Tauber, M. Pegoraro, G. Mazzotta, P. Cisotto *et al*, 2007 A molecular basis for natural selection at the timeless locus in drosophila melanogaster. Science **316:** 1898-1900.

Sathyanarayanan, S., X. Zheng, R. Xiao and A. Sehgal, 2004 Posttranslational regulation of drosophila PERIOD protein by protein phosphatase 2A. Cell **116:** 603-615.

Sathyanarayanan, S., X. Zheng, S. Kumar, C. -. Chen, D. Chen *et al*, 2008 Identification of novel genes involved in light-dependent CRY degradation through a genome-wide RNAi screen. Genes and Development **22:** 1522-1533.

Saunders, D. S., S. W. Gillanders and R. D. Lewis, 1994 Light-pulse phase response curves for the locomotor activity rhythm in period mutants of drosophila melanogaster. J. Insect Physiol. **40:** 957-968.

Scully, A. L., and S. A. Kay, 2000 Time flies for drosophila. Cell **100:** 297-300.

Sehgal, A., J. Price and M. W. Young, 1992 Ontogeny of a biological clock in drosophila melanogaster. Proceedings of the National Academy of Sciences of the United States of America **89:** 1423-1427.

Sehgal, A., J. L. Price, B. Man and M. W. Young, 1994 Loss of circadian behavioral rhythms and per RNA oscillations in the drosophila mutant timeless. Science **263:** 1603-1606.

Shafer, O. T., C. Helfrich-Fӧrster, S. C. P. Renn and P. H. Taghert, 2006 Reevaluation of drosophila melanogaster's neuronal circadian pacemakers reveals new neuronal classes. J. Comp. Neurol. **498:** 180-193.

Shi, L., S. Lin, Y. Grinberg, Y. Beck, C. M. Grozinger *et al*, 2007 Roles of drosophila kruppel-homolog 1 in neuronal morphogenesis. Developmental Neurobiology **67:** 1614-1626.

Shichida, Y., and T. Matsuyama, 2009 Evolution of opsins and phototransduction. Philosophical Transactions of the Royal Society B: Biological Sciences **364:** 2881-2895.

Sims, D., B. Bursteinas, Q. Gao, M. Zvelebil and B. Baum, 2006 FLIGHT: Database and tools for the integration and cross-correlation of large-scale RNAi phenotypic datasets. Nucleic acids research. **34:** D479-483.

Smith, S. T., S. Petruk, Y. Sedkov, E. Cho, S. Tillib *et al*, 2004 Modulation of heat shock gene expression by the TAC1 chromatin-modifying complex. Nat. Cell Biol. **6:** 162-167.

Sollars, V., X. Lu, L. Xiao, X. Wang, M. D. Garfinkel *et al*, 2003 Evidence for an epigenetic mechanism by which Hsp90 acts as a capacitor for morphological evolution. Nat. Genet. **33:** 70-74.

Sone, M., M. Hoshino, E. Suzuki, S. Kuroda, K. Kaibuchi *et al*, 1997 Still life, a protein in synaptic terminals of drosophila homologous to GDP-GTP exchangers. Science **275:** 543-547.

Sookoian, S., C. Gemma, T. F. Gianotti, A. Burgueño, G. Castaño *et al*, 2008 Genetic variants of clock transcription factor are associated with individual susceptibility to obesity. The American Journal of Clinical Nutrition **87:** 1606-1615.

Stanewsky, R., 2003 Genetic analysis of the circadian system in drosophila melanogaster and mammals. Journal of Neurobiology **54:** 111-147.

Stanewsky, R., M. Kaneko, P. Emery, B. Beretta, K. Wager-Smith *et al*, 1998 The cry(b) mutation identifies cryptochrome as a circadian photoreceptor in drosophila. Cell **95:** 681-692.

Stavenga, D. G., and K. Arikawa, 2008 One rhodopsin per photoreceptor: Iro-C genes break the rule. PLoS Biology **6:** 675-677.

Stephan, F. K., and I. Zucker, 1972 Circadian rhythms in drinking behavior and locomotor activity of rats are eliminated by hypothalamic lesions. Proceedings of the National Academy of Sciences of the United States of America **69:** 1583-1586.

Stephan, F. K., J. M. Swann and C. L. Sisk, 1979 Entrainment fo circadian rhythms by feeding schedules in rats with suprachiasmatic lesions. Behavioral and Neural Biology **25:** 545-554.

Stevens, R. G., and M. S. Rea, 2001 Light in the built environment: Potential role of circadian disruption in endocrine disruption and breast cancer. Cancer Causes and Control **12:** 279-287.

Stoleru, D., Y. Peng, P. Nawathean and M. Rosbash, 2005 A resetting signal between drosophila pacemakers synchronizes morning and evening activity. Nature **438:** 238-242.

Stoleru, D., P. Nawathean, M. d. l. P. Fernández, J. S. Menet, M. F. Ceriani *et al*, 2007 The drosophila circadian network is a seasonal timer. Cell **129:** 207-219.

Storey, J. D., and R. Tibshirani, 2003 Statistical significance for genomewide studies. Proc. Natl. Acad. Sci. U. S. A. **100:** 9440-9445.

Strahl, B. D., and C. D. Allis, 2000 The language of covalent histone modifications. Nature **403:** 41-45.

Struhl, K., 1998 Histone acetylation and transcriptional regulatory mechanisms. Genes and Development **12:** 599-606.

Swarup, K., C. Alonso-Blanco, J. R. Lynn, S. D. Michaels, R. M. Amasino *et al*, 1999 Natural allelic variation identifies new genes in the arabidopsis circadian system. Plant Journal **20:** 67-77.

Taghert, P. H., and O. T. Shafer, 2006 Mechanisms of clock output in the drosophila circadian pacemaker system. Journal of Biological Rhythms **21:** 445-457.

Tang, A. H., T. P. Neufeld, G. M. Rubin and H. -. J. Müller, 2001 Transcriptional regulation of cytoskeletal functions and segmentation by a novel maternal pair-rule gene, lilliputian. Development **128:** 801-813.

Tauber, E., H. Roe, R. Costa, J. M. Hennessy and C. P. Kyriacou, 2003 Temporal mating isolation driven by a behavioral gene in drosophila. Current Biology **13:** 140-145.

Tauber, E., M. Zordan, F. Sandrelli, M. Pegoraro, N. Osterwalder *et al*, 2007 Natural selection favors a newly derived timeless allele in drosophila melanogaster. Science **316:** 1895-1898.

Taylor, P., and P. E. Hardin, 2008 Rhythmic E-box binding by CLK-CYC controls daily cycles in per and tim transcription and chromatin modifications. Molecular and Cellular Biology **28:** 4642-4652.

The, I., G. E. Hannigan, G. S. Cowley, S. Reginald, Y. Zhong *et al*, 1997 Rescue of a drosophila NF1 mutant phenotype by protein kinase A. Science **276:** 791-794.

Tie, F., R. Banerjee, C. A. Stratton, J. Prasad-Sinha, V. Stepanik *et al*, 2009 CBP-mediated acetylation of histone H3 lysine 27 antagonizes drosophila polycomb silencing. Development **136:** 3131-3141.

Tischkau, S. A., J. W. Mitchell, S. -. Tyan, G. F. Buchanan and M. U. Gillette, 2003 Ca2+/cAMP response element-binding protein (CREB)-dependent activation of Per1 is required for light-induced signaling in the suprachiasmatic nucleus circadian clock. J. Biol. Chem. **278:** 718-723.

Toma, D. P., K. P. White, J. Hirsch and R. J. Greenspan, 2002 Identification of genes involved in drosophila melanogaster geotaxis, a complex behavioral trait. Nat. Genet. **31:** 349-353.

Tomioka, K., and A. Matsumoto, 2010 A comparative view of insect circadian clock systems. Cellular and Molecular Life Sciences **67:** 1397-1406.

Tong, J., F. Hannan, Y. Zhu, A. Bernards and Y. Zhong, 2002 Neurofibromin regulates G protein-stimulated adenylyl cyclase activity. Nat. Neurosci. **5:** 95-96.

Tosini, G., and M. Menaker, 1998 The tau mutation affects temperature compensation of hamster retinal circadian oscillators. Neuroreport **9:** 1001-1005.

Tsuchiya, Y., M. Akashi and E. Nishida, 2003 Temperature compensation and temperature resetting of circadian rhythms in mammalian cultured fibroblasts. Genes to Cells **8:** 713-720.

Tweedie, S., M. Ashburner, K. Falls, P. Leyland, P. McQuilton *et al*, 2009 FlyBase: Enhancing drosophila gene ontology annotations. Nucleic Acids Res. **37:** D555-D559.

Ueda, H. R., A. Matsumoto, M. Kawamura, M. Iino, T. Tanimura *et al*, 2002 Genome-wide transcriptional orchestration of circadian rhythms in drosophila. J. Biol. Chem. **277:** 14048-14052.

Untergasser, A., H. Nijveen, X. Rao, T. Bisseling, R. Geurts *et al*, 2007 Primer3Plus, an enhanced web interface to Primer3. Nucleic Acids Res. **35:** W71-74.

Van Gelder, R. N., and M. A. Krasnow, 1996 A novel circadianly expressed drosophila melanogaster gene dependent on the period gene for its rhythmic expression. EMBO J. **15:** 1625-1631.

Veleri, S., C. Brandes, C. Helfrich-Fӧrster, J. C. Hall and R. Stanewsky, 2003 A self-sustaining, light-entrainable circadian oscillator in the drosophila brain. Current Biology **13:** 1758-1767.

Vogt, K., and K. Kirschfeld, 1984 Chemical identity of the chromophores of fly visual pigment. Naturwissenschaften **71:** 211-213.

von Saint Paul, U., and J. Aschoff, 1978 Longevity among blowflies phormia terraenovae R.D. kept in non-24-hour light-dark cycles. Journal of Comparative Physiology □ A **127:** 191-195.

Vosshall, L. B., J. L. Price, A. Sehgal, L. Saez and M. W. Young, 1994 Block in nuclear localization of period protein by a second clock mutation, timeless. Science **263:** 1606-1609.

Wang, S., C. J. Basten and Z. B. Zeng, 2007 *Windows QTL Cartographer 2.5*, Department of Statistics, North Carolina State University, Raleigh, NC.

Wang, T., H. Xu, J. Oberwinkler, Y. Gu, R. C. Hardie *et al*, 2005 Light activation, adaptation, and cell survival functions of the na +/Ca2+ exchanger CalX. Neuron **45:** 367-378.

Weber, F., 2009 Remodeling the clock: Coactivators and signal transduction in the circadian clockworks. Naturwissenschaften **96:** 321-337.

Wettenhall, J., and K. Simpson, 2010 A Graphical User Interface for Affy Analysis using the Limma Microarray Package.

White, C. L., R. K. Suto and K. Luger, 2001 Structure of the yeast nucleosome core particle reveals fundamental changes in internucleosome interactions. EMBO J. **20:** 5207-5218.

Wijnen, H., F. Naef, C. Boothroyd, A. Claridge-Chang and M. W. Young, 2006 Control of daily transcript oscillations in drosophila by light and the circadian clock. PLoS Genetics **2:** 0326-0343.

Williams, J. A., and A. Sehgal, 2001 Molecular components of the circadian system in drosophila. Annual Review of Physiology **63:** 729-755.

Williams, J. A., H. S. Su, A. Bernards, J. Field and A. Sehgal, 2001 A circadian output in drosophila mediated by neurofibromatosis-1 and Ras/MAPK. Science **293:** 2251-2256.

Winfree, A. T., 1980 *The Geometry of Biological Time*. Springer, New York.

Winfree, A. T., 1970 Integrated view of resetting a circadian clock. Journal of Theoretical Biology **28:** 327-374.

Wittwer, F., A. van der Straten, K. Keleman, B. J. Dickson and E. Hafen, 2001 Lilliputian: An AF4/FMR2-related protein that controls cell identity and cell growth. Development **128:** 791-800.

Wu, Z., R. A. Irizarry, R. Gentleman, F. Martinez-Murillo and F. Spencer, 2004 A model-based background adjustment for oligonucleotide expression arrays. Journal of the American Statistical Association **99:** 909-917.

Wyse, C. A., A. N. Coogan, C. Selman, D. G. Hazlerigg and J. R. Speakman, 2010 Association between Mammalian Lifespan and Circadian Free-Running Period: The Circadian Resonance Hypothesis Revisited.

Xing, Y., S. Shi, L. Le, C. A. Lee, L. Silver-Morse *et al*, 2007 Evidence for transgenerational transmission of epigenetic tumor susceptibility in drosophila. PLoS Genetics **3:** 1598-1606.

Xu, P., B. Sun and P. M. Salvaterra, 1999 Organization and transcriptional regulation of drosophila na+,K+-ATPase β subunit genes: Nrv1 and Nrv2. Gene **236:** 303-313.

Xu, Y., and C. H. Johnson, 2001 A clock- and light-regulated gene that links the circadian oscillator to LHCB gene expression. Plant Cell **13:** 1411-1425.

Yasuyama, K., and I. A. Meinertzhagen, 1999 Extraretinal photoreceptors at the compound eye's posterior margin in drosophila melanogaster. Journal of Comparative Neurology **412:** 193-202.

Yerushalmi, S., and R. M. Green, 2009 Evidence for the adaptive significance of circadian. Ecology Letters **12:** 970-981.

Yoshimura, T., Y. Yokota, A. Ishikawa, S. Yasuo, N. Hayashi *et al*, 2002 Mapping quantitative trait loci affecting circadian photosensitivity in retinally degenerate mice. J. Biol. Rhythms **17:** 512-519.

Young, M. W., and S. A. Kay, 2001 Time zones: A comparative genetics of circadian clocks. Nature Reviews Genetics **2:** 702-715.

Yu, W., H. Zheng, J. H. Houl, B. Dauwalder and P. E. Hardin, 2006 PER-dependent rhythms in CLK phosphorylation and E-box binding regulate circadian transcription. Genes and Development **20:** 723-733.

Zaidi, F. H., J. T. Hull, S. Peirson, K. Wulff, D. Aeschbach *et al*, 2007 Short-wavelength light sensitivity of circadian, pupillary, and visual awareness in humans lacking an outer retina. Current Biology .

Zeng, Z. -., 1994 Precision mapping of quantitative trait loci. Genetics **136:** 1457-1468.

Zeng, Z. -., C. -. Kao and C. J. Basten, 1999 Estimating the genetic architecture of quantitative traits. Genetical Research **74:** 279-289.

Zhang, J., Z. Fang, C. Jud, M. J. Vansteensel, K. Kaasik *et al*, 2008 Fragile X-related proteins regulate mammalian circadian behavioral rhythms. Am. J. Hum. Genet. **83:** 43-52.

Zhang, L., B. C. Lear, A. Seluzicki and R. Allada, 2009 The CRYPTOCHROME photoreceptor gates PDF neuropeptide signaling to set circadian network hierarchy in drosophila. Current Biology **19:** 2050-2055.

Zhang, Y., and D. Reinberg, 2001 Transcription regulation by histone methylation: Interplay between different covalent modifications of the core histone tails. Genes and Development **15:** 2343-2360.

Zhang, Y., Y. Liu, D. Bilodeau-Wentworth, P. E. Hardin and P. Emery, 2010 Light and temperature control the contribution of specific DN1 neurons to drosophila circadian behavior. Current Biology **20:** 600-605.

Zhu, H., I. Sauman, Q. Yuan, A. Casselman, M. Emery-Le *et al*, 2008 Cryptochromes define a novel circadian clock mechanism in monarch butterflies that may underlie sun compass navigation. PLoS Biology **6:** 0138-0155.

Zordan, M. A., E. Rosato, A. Piccin and R. Foster, 2001 Photic entrainment of the circadian clock: From drosophila to mammals. Seminars in Cell and Developmental Biology **12:** 317-328.